REFERENCE ONLY

UNIVERSITY OF LONDON THESIS

Degree PhD Year 2005 Name of Author EVANS, P.M.

COPYRIGHT

This is a thesis accepted for a Higher Degree of the University of London. It is an unpublished typescript and the copyright is held by the author. All persons consulting the thesis must read and abide by the Copyright Declaration below.

COPYRIGHT DECLARATION

I recognise that the copyright of the above-described thesis rests with the author and that no quotation from it or information derived from it may be published without the prior written consent of the author.

LOANS

Theses may not be lent to individuals, but the Senate House Library may lend a copy to approved libraries within the United Kingdom, for consultation solely on the premises of those libraries. Application should be made to: Inter-Library Loans, Senate House Library, Senate House, Malet Street, London WC1E 7HU.

REPRODUCTION

University of London theses may not be reproduced without explicit written permission from the Senate House Library. Enquiries should be addressed to the Theses Section of the Library. Regulations concerning reproduction vary according to the date of acceptance of the thesis and are listed below as guidelines.

A. Before 1962. Permission granted only upon the prior written consent of the author. (The Senate House Library will provide addresses where possible).

B. 1962 - 1974. In many cases the author has agreed to permit copying upon completion of a Copyright Declaration.

C. 1975 - 1988. Most theses may be copied upon completion of a Copyright Declaration.

D. 1989 onwards. Most theses may be copied.

This thesis comes within category D.

☑ This copy has been deposited in the Library of UCL

☐ This copy has been deposited in the Senate House Library, Senate House, Malet Street, London WC1E 7HU.

An Investigation Of Cellular Radiosensitivity Associated With Immunodeficiency

Paul Michael Evans, B.Sc. (Hons)

Molecular Haematology and Cancer Biology Unit
Institute of Child Health
University of London

Supervisor:

Dr. Mike Hubank

Thesis submitted for the degree of Doctor of Philosophy (Ph.D.)
at the University of London

December 2004

UMI Number: U591736

All rights reserved

INFORMATION TO ALL USERS
The quality of this reproduction is dependent upon the quality of the copy submitted.

In the unlikely event that the author did not send a complete manuscript
and there are missing pages, these will be noted. Also, if material had to be removed,
a note will indicate the deletion.

UMI U591736
Published by ProQuest LLC 2014. Copyright in the Dissertation held by the Author.
Microform Edition © ProQuest LLC.
All rights reserved. This work is protected against
unauthorized copying under Title 17, United States Code.

ProQuest LLC
789 East Eisenhower Parkway
P.O. Box 1346
Ann Arbor, MI 48106-1346

Abstract

DNA Double Strand Breaks (DSBs) are induced by ionising radiation, but also arise during normal physiological processes such as V(D)J recombination during lymphocyte development. The induction of DSBs leads to the activation of proteins involved in DNA repair, but also initiates p53 dependent pathways that can result in cell cycle arrest and/or apoptosis. Defects in this damage response network may therefore result in immunodeficiency and cellular radiosensitivity. Skin biopsies obtained from undefined immunodeficient patients were used to generate primary fibroblast lines, and a group of these demonstrated cellular radiosensitivity using fibroblast survival assays. Whilst radiation-induced lymphocyte apoptosis was found to be an unreliable measure of intrinsic radiosensitivity, the examination of fibroblast division early after irradiation determined that radiosensitive fibroblasts undergo distinct cell fates after irradiation. Further characterisation revealed that all the identified radiosensitive lines were able to initiate p53-dependent gene transcription after irradiation. Analysis suggested that one undefined line (F96) might harbour a defect in DSB repair. Sequence examination of F96 candidate genes confirmed the presence of 2 novel mutations in the Artemis DNA repair gene that were expressed from separate alleles. Cloning of the Artemis gene also allowed the discovery of a new alternative exon and many novel splice variants. Concurrently, the F96 line was found to induce abnormally high levels of p53 activation after irradiation, which was associated with a more widespread induction of p53 target genes. This indicated that after DNA damage, defects in DSB repair might combine with other genetic factors that impair cellular survival to confer a radiosensitive immunodeficient phenotype.

Acknowledgments

There are many people I am grateful to for the help and support they have provided during this PhD project. I would like to thank my supervisor Dr. Mike Hubank for his continued guidance and support. I have enjoyed working with Mike Hubank and appreciate the way he encouraged me to pursue different ideas, whilst giving support where it was needed. This has taught me the skills of independent research that will be invaluable in my future career. I am also grateful to the Medical Research Council for funding this PhD project.

I would like to thank everyone in the Molecular Haematology and Cancer Biology Unit at the Institute of Child Health for being extremely helpful and approachable during my time here. The high level of technical expertise that resides in this laboratory is a great asset, and I found this to be a valuable resource that allowed me to overcome problems in my research. I am especially grateful to staff and students in the level 1 laboratory for making this an enjoyable and productive environment in which to work. I am particularly thankful to Dr Jonathan Gilley, Dr Elaine O'Sullivan, Dr John Clohessy, Dr Thomas Hughes, Dr Lesley Smyth, Miss Jennifer Lindsay, Miss Samira Salek-Ardakani and Mr Martin Woodward for the useful discussions, technical support and friendship they have provided.

I am particularly grateful to Dr Helena Kempski for her help and guidance with the Cytogenetics section of this project. This was invaluable, both in performing the study and in the final write up. I am also thankful to Mrs Jo Sinclair for her continued help with FACS analysis, and Miss Danielle Fletcher for running the Affymetrix samples and helping with sequencing reactions. I would like to acknowledge our collaborators in the laboratory of Dr Penny Jeggo at the University of Sussex for performing the γ-H2AX analysis and for useful discussions during this project.

Completing a PhD in London can be a draining experience. I would therefore like to acknowledge my friends in London for all the encouragement they have provided over the years, especially Rosemary whose continued support has been invaluable. I would also like to thank my friends in Milton Keynes, especially Pat and Mat, for helping me to retain some sanity whilst writing. I am especially indebted to my partner Jenny, for her understanding, support and encouragement over the last year, without which this thesis may not have been completed.

I am extremely grateful to my family whose support over the course of this PhD project has been immense. I would like to acknowledge my Grandfather, Donald Lofts and Nan, Norah Evans, along with my Brother and Sister, Jon Fearn and Andrea Norman, for their continued interest and encouragement. Most of all, I would like to thank my parents David and Carole Evans whose unwavering support, both financially and emotionally, has made this thesis possible.

Table of Contents

List of Figures

List of Tables

List of Abbreviations

AA	Anacardic acid
APS	Ammonium persulfate
AT	Ataxia telangiectasia
ATLD	AT like disorder
ATM	AT mutated
ATR	ATM and Rad3-related
BASC	BRCA1-associated genome surveillance complex
BMT	Bone marrow transplant
BRCA1	Breast cancer 1 gene product
BRCA2	Breast cancer 2 gene product
BRCT	BRCA1 C-terminal domain
BrdU	Bromodeoxyuridine
BSA	Bovine serum albumin
β-CASP	Metallo-ß-lactamase-associated CPSF Artemis SNM1/PSO2 domain
Cdk	Cyclin dependent kinase
CFSE	Carboxy-fluorescein diacetate succinimidyl ester
Chk	Checkpoint kinase
CIAP	Calf intestinal alkaline phosphatase
CID	Combined immunodeficiency
CPD	Cyclobutane-pyrimidine dimer
CPSF	Cleavage and polyadenylation-specific factor
CSR	Class switch recombination
D	Diversity
DMSO	Dimethylsulphoxide
DNA-PK	DNA-dependent protein kinase
DNA-PKcs	DNA-dependent protein kinase catalytic subunit
DSB	Double strand break
DSBs	Double strand breaks
DTT	Dithiothreitol
FACS	Fluorescence activated cell sorting
FBS	Fetal bovine serum
FITC	Fluorescein isothiocyanate
GFP	Green fluorescent protein
Gy	Gray
HAT	Histone acetyl-transferase
HR	Homologous recombination
hTERT	Human telomerase catalytic subunit
H2AX	Histone 2AX
γ-H2AX	Phosphorylated H2AX
Ig	Immunoglobulin
IR	Ionising radiation
IVT	*In vitro* transcription
J	Joining
MAPKs	Mitogen activated protein kinases
Mdc1	Mediator of DNA damage checkpoint protein 1
mdm2	murine double minute 2
MES	2-[N-Morpholino] ethanesulphonic acid
NBS	Nijmegen breakage syndrome
Nbs1	Mutated in Nijmegen breakage syndrome 1

NES	Nuclear export signal
NHEJ	Non-homologous end joining
NK	Natural killer
PBL	Primary blood lymphocyte
PBS	Phosphate buffered saline
P/CAF	p300/CBP-associated HAT
PCR	Polymerase chain reaction
PE	Phycoerythrin
PFA	Paraformaldehyde
PFGE	Pulse field gel electrophoresis
PHA	Phytohemagglutin
PI	Propidium iodide
PI-3K	Phosphatidylinositol 3-kinase
PS	Phosphatidylserine
PSC	Post synaptic complex
$p53_{Arg}$	p53 with arginine at position 72
$p53_{Pro}$	p53 with proline at position 72
RAG	Recombination activating gene
RDS	Radioresistant DNA synthesis
ROS	Reactive Oxygen Species
RPA	Replication factor A
RS	Recombination signal
RSS	Recombination signal sequences
RS-SCID	Radiosensitive SCID
RT-PCR	Reverse transcription-PCR
SA-βgal	Senescence associated β-galactosidase
SAPE	Streptavidin-phycoerythrin
SCID	Severe combined immunodeficiency
SDS	Sodium dodecyl sulphate
SIPS	Stress induced premature senescence
TCR	T-cell receptor
TdT	Terminal deoxynucleotide transferase
TEMED	N,N,N′,N′-Tetramethylethylenediamine
TNF	Tumour necrosis factor
TNF-R	TNF receptor
TRAIL	TNF-related apoptosis-inducing ligand
TRAILR	TRAIL receptor
Tris	Tris(hydroxymethyl) aminomethane
TX100	Triton-X 100
UTR	Untranslated region
UV	Ultraviolet
V	Variable
V(D)J	Variable(Diversity)Joining
XRCC	X-ray cross complementing
7AAD	7-aminoactinomycin-D
53BP1	p53 Binding protein 1

Chapter 1: Introduction

The preservation of genomic integrity is crucial for cell survival since cellular functions depend on the quality of information stored within genomic DNA. DNA damage therefore poses a serious threat to living organisms. Lesions in genomic DNA can result in the introduction of permanent mutations that lead to abnormal cellular function, cell death and genomic instability. Consequently, cells have evolved complex mechanisms to recognise DNA damage, instigate cell cycle arrest and activate repair mechanisms (Jackson, 2001). Whilst this provides some protection from the deleterious effects on cell viability, in metazoans DNA damage is also a precursor of cancer (Elledge, 1996). In this situation cells must not only repair the lethal effects of DNA damage, but also guard against the accumulation of mutations that may lead to a loss of cell cycle control and threaten organism survival. This is achieved by the induction of permanent arrest or apoptosis in cells that have received a high level of damage.

1.1 Sources of DNA damage

Genomic DNA is constantly exposed to a wide array of DNA damaging agents. These can arise from endogenous sources as products of normal cellular metabolism in consequence to hydrolysis, lipid peroxidation events and the formation of small reactive oxygen species (ROS) (Cooke *et al*, 2003). Electron transport chains all posses the potential to leak electrons to oxygen resulting in superoxide formation, which is a precursor to various other ROS. These ROS then have the potential to attack DNA resulting in many forms of DNA damage including base damage (Cooke *et al*, 2003) and one of the most lethal forms of DNA damage, the double strand break (DSB) (Prise *et al*, 1989). Indeed, the process of DNA replication itself can lead to the production of DSBs when replication forks collapse (Cox, 2002) and it has been suggested that about 10 replication forks collapse in a human cell replication cycle (Haber, 1999).

Although DNA DSBs pose a major threat to genome integrity, they are sometimes generated deliberately as intermediates during normal physiological processes. Probably the best-characterised example of this in higher eukaryotes is the pathway of Variable (Diversity) Joining (V(D)J) recombination, which occurs in developing B- and T-lymphocytes to provide the basis for the antigen-binding diversity of the

immunoglobulin and T-cell receptor proteins (reviewed in Bassing *et al*, 2002a). During this process lymphocytes assemble functional antigen receptor genes by the ordered rearrangement of component variable (V), diversity (D) and joining (J) gene segments, which involves the induction and repair of DNA DSBs. DSBs also arise as intermediates during meiotic recombination (Keeney *et al*, 2001), which generates the genetic variability during sexual reproduction upon which natural selection can act.

Whilst cells must be able to cope with these endogenous sources of DNA damage, there are also many genotoxic agents that arise from exogenous sources such as UV light, ionising radiation (IR) and chemical mutagens. A plethora of different chemical mutagens can produce a wide variety of lesions in DNA, such as base damage, interstrand/intrastrand cross-links and single and double strand breaks. One of the most abundant lesions induced by Ultraviolet (UV) radiation is the cyclobutane-pyrimidine dimer (CPD), which involves the covalent linking of two adjacent pyrimidine bases within the DNA double helix. Exposure of cellular DNA to IR can also result in base damage, along with single strand breaks and double strand breaks. The latter are thought to be the primary lethal lesion induced by IR. DSBs are potent inducers of mutations and cell death. In metazoa, just one DSB can kill a cell if it leads to the inactivation of an essential gene or, more frequently, triggers apoptosis (Rich *et al*, 2000). Furthermore, there is experimental evidence for a causal link between the generation of DSBs and the induction of mutations and chromosomal translocations with tumourigenic potential (Vamvakas *et al*, 1997) (Richardson *et al*, 2000) (Ferguson *et al*, 2001) (Khanna and Jackson, 2001). It is therefore vitally important that living organisms are able to detect and repair DSBs efficiently once they arise.

1.2 The cellular response to DNA DSBs

The cellular response to DNA DSBs can be divided into three levels of organisation depending on the function of its components (figure 1-1). Initially the pathway must be activated by the presence of DNA damage and this requires putative sensor proteins that are activated by DSBs. The sensors stimulate the activation of a transducer system that amplifies and diversifies the signal by targeting a series of downstream effectors. These effectors then regulate various aspects of cellular function such as cell cycle arrest, apoptosis and the regulation of DNA repair mechanisms. The components of this damage response network need to be exquisitely sensitive and selective since they must

be triggered efficiently by low numbers of, and possibly just one, chromosomal DNA DSB, yet remain inactive under other conditions.

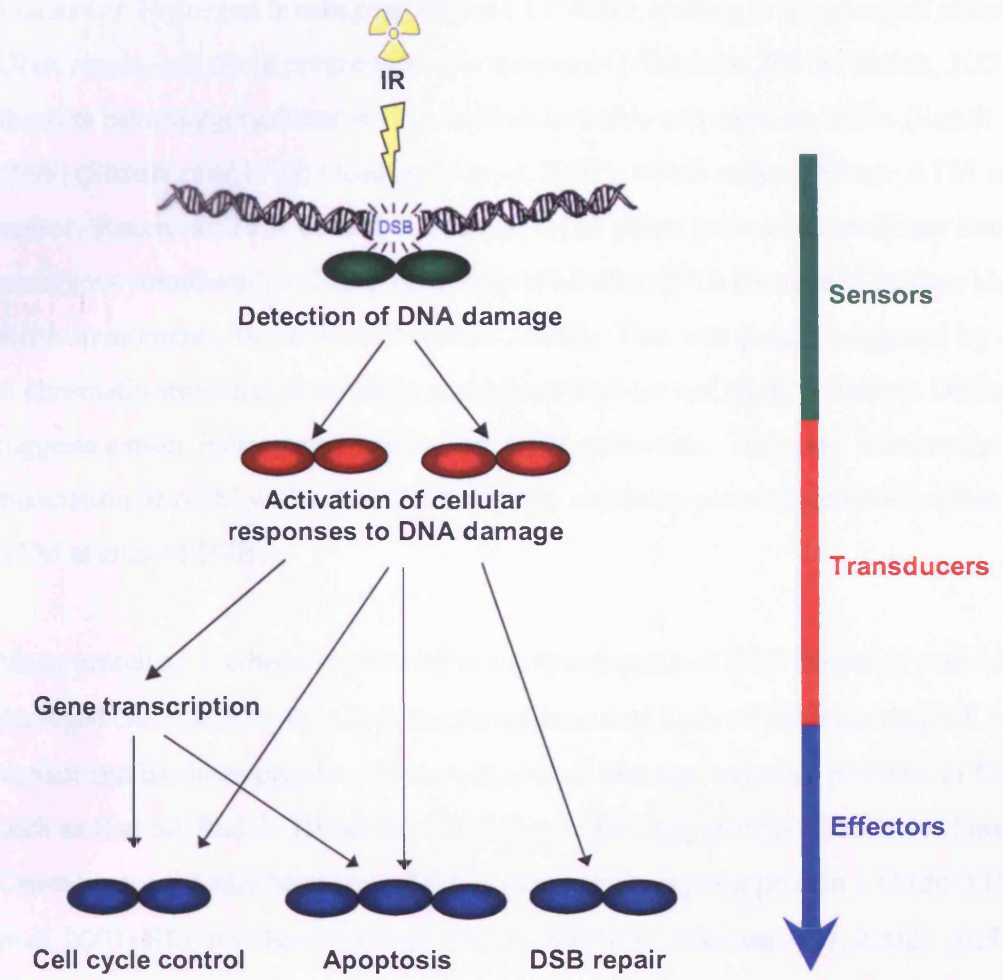

Figure 1-1: Organisation of the metazoan DNA damage response network

1.3 DSB Detection and response initiation

Although the exact mechanism of DSB detection remains unclear, many putative sensor proteins have been proposed to function in this role. ATM (AT Mutated), encoded by the gene that is mutated in individuals with the neurodegenerative syndrome Ataxia Telangiectasia (AT), is activated early after DNA damage induction and could serve as a sensor, as well as an initiator, of the ensuing cellular genotoxic response. ATM is a member of the phosphatidylinositol 3-kinase (PI-3K) superfamily that includes ATR (ATM and Rad3-related). While ATR responds to UV damage or stalled replication forks, ATM reacts primarily to DSBs induced by IR (Guo *et al*, 2000) (Hekmat-Nejad

et al, 2000) (Pandita *et al*, 2000) (Abraham *et al*, 2001). Once activated ATM phosphorylates various downstream protein targets of the damage response, including p53, the checkpoint kinase (Chk) 2, Breast cancer 1 gene product (BRCA1) and Mutated in Nijmegen breakage syndrome 1 (Nbs1), leading to a variety of effects on DNA repair, cell cycle progression and apoptosis (Abraham 2001) (Shiloh, 2001). Reports have suggested that ATM can bind to and is activated by DSBs (Smith *et al*, 1999) (Suzuki *et al* 1999) (Andegeko *et al*, 2001), which may implicate ATM as a DSB sensor. Recent data has demonstrated that ATM exists as an inactive dimer that undergoes autophosphorylation on serine-1981 after DNA damage to release kinase active monomers (Bakkenist and Kastan, 2003). This was rapidly triggered by changes in chromatin structure, even under conditions that are not likely to induce DSBs, which suggests a more indirect mechanism for ATM activation. This may involve the association of ATM with other DNA damage mediator proteins that co-localise with ATM at sites of DSBs.

Many proteins have been implicated in the recruitment of DSB response proteins to damaged chromatin. γ-H2AX is the phosphorylated form of the Histone 2AX (H2AX) variant and has been proposed to recruit several damage response proteins to DSB sites such as Rad 50, Rad 51 (Paull *et al*, 2000), p53 binding protein 1 (53BP1) (Fernandez-Capetillo *et al*, 2002) Mediator of DNA damage checkpoint protein 1 (Mdc1) (Stewart *et al*, 2003) BRCA1 (Bassing *et al*, 2002b) and Nbs1 (Celeste *et al*, 2002). γ-H2AX foci form over large chromatin domains surrounding damaged DNA (Rogakou *et al*, 1999). This phosphorylation is reported to be performed by ATM (Burma *et al*, 2001) and its PI-3K homologue DNA dependent protein kinase (DNA-PK) in a redundant, overlapping manner (Stiff *et al*, 2004a). Whilst the phosphorylation of H2AX is important for the recruitment of some damage response proteins, this event is likely to occur downstream of DSB recognition and ATM activation. Recent reports suggest that although this modification is important for the retention of damage response proteins within nuclear foci, the initial recognition of DSBs occurs in the absence of H2AX phosphorylation (Celeste *et al*, 2003).

A protein complex that is a good candidate for a DSB sensor that is able to stimulate ATM activity is the Mre11 complex, which consists of Mre11, Rad50 and Nbs1. This trimeric complex is recruited to DSB sites rapidly (Mirzoeva and Petrini, 2001), and examination at early timepoints after irradiation revealed this was unaffected by ATM

deficiency (Mirzoeva and Petrini, 2001) and caffeine treatment to inhibit ATM, ATR and DNA-PK (Mirzoeva and Petrini, 2003). Furthermore, the initial recruitment of the Mre11 complex to DSBs 8 minutes after irradiation is not affected by H2AX deficiency (Celeste *et al*, 2003). This is consistent with the lack of checkpoint deficiency observed in H2AX deficient cells (Celeste *et al*, 2002), and although Nbs1 foci formation was impaired in this study, early timepoints when DSBs are first recognised were not examined. The Mre11 complex has also been shown to be required for the activation of ATM dependent pathways (Uziel *et al*, 2003), which is consistent with its role upstream of ATM as a sensor, but Nbs1 has also been shown to be phosphorylated by ATM after irradiation (Lim *et al*, 2000). These results suggest an intriguing situation, where the DNA damage sensor is also a target for the transducing kinase.

Recent work showing that the Mre11 complex binds to ATM and increases its affinity towards substrates demonstrated that Nbs1 phosphorylation enhances this activity (Lee and Paull, 2004a). But this phosphorylation is not required for Nbs1 recruitment to damage sites, as shown by the proficient radiation-induced foci formation in Nbs1 S343A cells (Kobayashi *et al*, 2002). Similarly, early Mre11 foci are formed by a mechanism independent of ATM, ATR and DNA-PKcs (Petrini *et al*, 2003). Furthermore ATM activation and binding to sites of DNA damage requires a functional Mre11 complex (Uziel *et al*, 2003). Together these findings suggest that ATM, initially recruited to DNA damage by the Mre11 complex, phosphorylates H2AX, and this H2AX phosphorylation in turn is required for the recruitment and retention of additional Nbs1 and other damage response proteins at DSB sites. This consequently leads to an amplification of this cascade, initiating a chain reaction involving ATM and these damage response proteins (Figure 1-2).

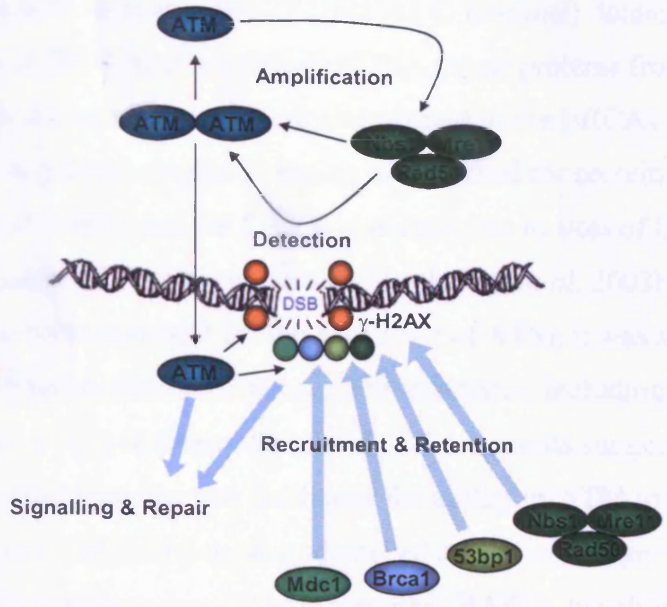

Figure 1-2: Detection of DSBs leads to the recruitment of damage response proteins into sub-nuclear foci, and the activation of ATM dependent signaling pathways. DSBs are detected by the Mre11 complex which then activates the ATM protein kinase, although this is probably not the only mechanism of ATM activation. ATM can phosphorylate Nbs1 which amplifies the signal leading to the enhanced phosphorylation of ATM substrates such as H2AX. Phosphorylated H2AX (γ-H2AX) is able to retain the Mdc1, Brca1 and 53bp1 adaptor proteins in nuclear foci along with additional Mre11 complexes, and together these are able to facilitate the phosphorylation of downstream ATM targets that function in DNA repair, cell cycle arrest and apoptosis.

Mdc1 and 53bp1 are two of the damage response proteins that are recruited to sites of DSBs after irradiation (Schultz *et al*, 2000) (Anderson *et al*, 2001) (Goldberg *et al*, 2003) (Lou *et al*, 2003a), (Stewart *et al*, 2003) and it has been suggested that similarly to the Mre11 complex these proteins may also function in the activation of ATM (Mochan *et al*, 2003). Mochan *et al* demonstrated that the suppression of Mdc1 by siRNA inhibited ATM activation and phosphorylation of various ATM substrates. Mdc1 is known to interact with Nbs1 (Goldberg *et al*, 2003) and a recent study indicated this protein may function as a H2AX-dependent interaction platform enabling a switch from transient, Mdc1 independent recruitment of Nbs1 to DSBs towards sustained, Mdc1-dependent interactions with the surrounding chromosomal microenvironment (Lukas *et al*, 2004). Also, in cells with defective Nbs1, suppression of 53bp1 was shown to further abrogate ATM activation (Mochan *et al*, 2003). The Mre11 complex may therefore require other damage response proteins for the sustained activation of ATM, and this may not be the only mechanism of DSB detection.

Mdc1 and 53bp1 both contain 2 BRCT (BRCA1 C-terminal) domains (Mochan *et al*, 2004) (Stucki *et al*, 2004) that are found in DNA repair proteins from yeast to mammals, and as the name suggests are also present in the BRCA1 protein. BRCT domains behave as phosphopeptide binding motifs ideal for protein targeting (Manke *et al*, 2003) (Yu *et al*, 2003), and BRCA1 is also recruited to sites of DSBs (Zhong *et al*, 1999) by a mechanism that is dependent on Mdc1 (Lou *et al*, 2003b). Although BRCA 1 does not appear to be essential for the activation of ATM, it was shown to be required for IR induced phosphorylation of some ATM substrates, including p53, Chk2 and Nbs1 (Foray *et al*, 2003) (Fabbro *et al*, 2004). These results suggested that BRCA1 might act as a scaffold protein that facilitates the ability of ATM to phosphorylate some downstream targets. BRCA1 has been identified as part of a larger protein complex, the BRCA1-associated genome surveillance complex (BASC), which contains ATM, the Mre11 complex and many other DNA damage response proteins (Wang *et al*, 2000). Since ATM phosphorylates BRCA1 (Cortez *et al*, 1999) (Gatei *et al*, 2000), Mdc1 (Goldberg *et al*, 2003), and 53bp1 (Mochan *et al*, 2004) this could regulate the formation of large aggregates of damage response proteins at DSB sites. These proteins may then act as adaptors to allow ATM to signal to other downstream targets in the damage response that effect DNA repair, cell cycle arrest and apoptosis.

1.4 Signal transduction and effector function: the p53 response

After the detection of DSBs the active ATM protein kinase phosphorylates transducer proteins that can signal the presence of DNA damage to the cell cycle and apoptotic machinery. The p53 tumour suppressor protein plays a key role in this part of the DNA damage response, and acts as a node or hub for the incoming stress signals it receives. ATM can directly and indirectly facilitate an accumulation and activation of the p53 tumour suppressor, the function of which largely depends on its transcriptional activator properties. ATM directly phosphorylates p53 on serine-15 (Banin *et al*, 1998) (Canman *et al*, 1998) (Khanna *et al*, 1998) (Nakagawa *et al*, 1999), which seems to enhance its transcriptional activator function (Lambert *et al*, 1998) (Dumaz and Meek, 1999). Serine-15 phosphorylation is then thought to nucleate a series of subsequent post-translational modifications on p53 that contribute to both its stabilisation and biochemical activation (as many as 17 sites in p53 undergo phosphorylation or acetylation) (Appella and Anderson, 2001).

ATM can indirectly induce phosphorylation of p53 at serine 20 through activation of Chk2 (Chehab *et al*, 2000) (Shieh *et al*, 2000), a modification that appears to increase p53 stability by interference with p53's association with its inhibitor, murine double minute 2 (mdm2) (Chehab *et al*, 1999) (Unger *et al*, 1999). mdm2 is a prime mediator of p53's degradation, serving as the E3 ligase, which mediates both the ubiquitylation and proteasome dependent degradation of p53 (Michael *et al*, 2003). Another facet to our understanding of ATM mediated induction of p53 came with the finding that ATM phosphorylates mdm2 in response to DSBs (Khosravi *et al*, 1999) (de Toledo *et al*, 2000) and that this attenuates the p53-inhibitory potential of mdm2 (Maya *et al*, 2001). Other work suggested that ATM might also inhibit mdm2 by the phosphorylation and induction of E2F1 transcription factor (Lin *et al*, 2001). This would allow the subsequent induction of ARF, a negative regulator of mdm2.

Coupled with the stabilization of p53, phosphorylation of serine-15, threonine 18 and serine-20 also stimulates the recruitment of transcription factors including p300, CBP (both transcriptional co-activators and histone acetyl-transferases [HATs]) and P/CAF (a p300/CBP-associated HAT) (Appella and Anderson, 2001). These factors not only stimulate transcription from p53-responsive promoters but also promote acetylation of a cluster of C-terminal lysine residues in p53 that are normally targets for ubiquitylation (Li *et al*, 2002b). Phosphorylation of serine 15 and serine 20 may also block export of p53 mediated by mediated by a nuclear export signal (NES) present in this region of the N-terminus (Zhang *et al*, 2001b).

1.4.1 Checkpoint Activation

A major consequence of ATM activation after DNA damage is therefore the induction of p53 dependent gene transcription. One of the first effects of p53 induction in nearly all cell types is cell cycle arrest. Cell cycle checkpoints function at a number of critical points in the cell cycle, including the G1/S and G2/M boundaries and during S-phase (Nyberg *et al*, 2002) (figure 1-3). These checkpoints are triggered by a mixture of p53 dependent and p53 independent pathways, and may initially prevent cells from conducting DNA replication or mitosis in the presence of unrepaired damage, allowing time for repair processes to complete their function. A wealth of evidence confirms that p53 is required for proper G1 arrest after DNA damage (Kastan *et al*, 1991) (Kuerbitz *et al*, 1992) (Donehower and Bradley, 1993) (Ko and Prives, 1996), and this is triggered

largely through the transactivation of $p21^{Waf1}$ by p53, which inhibits G1 cyclin dependent kinases such as Cyclin dependent kinase (Cdk) 2 and Cdk4 (El-Deiry *et al*, 1993) (Harper *et al*, 1993). This results in the maintenance of the Rb-E2F complex to consequently prevent S-phase entry (Gottlieb and Oren, 1996) (Ko and Prives, 1996) and inactivated Cdk2 accumulates and cannot phosphorylate Cdc45 to initiate replication. This p53 dependent pathway is thought to be responsible for the maintenance of G1 arrest, but another more rapid pathway involving CDC25A may induce an initial, transient arrest in G1 that lasts for only several hours and involves the inhibition of Cdk2 within 20–30 min (Bartek and Lukas, 2001). This pathway also functions in the S-phase checkpoint response and is described below.

Over 2 decades ago it was observed that irradiation of cells results in delayed progression during the S-phase of the cell cycle, and a defect in this process was noticed in cells with defective ATM function that displayed Radioresistant DNA Synthesis (RDS), a characteristic of cells derived from patients with AT and Nijmegen Breakage Syndrome (NBS) (Painter and Young, 1980). The extent of RDS in NBS cells is milder than that in cells deficient in ATM, suggesting that the S-phase checkpoint is regulated by two parallel branches that are triggered by ATM (Falck *et al*, 2002) (figure 1-3). One branch is the ATM-Chk2-CDC25A pathway and the other requires Nbs1. In the ATM-Chk2-CDC25A pathway ATM activates Chk2, which then phosphorylates the cell cycle regulator CDC25A, leading to its degradation by polyubiquitination-mediated hydrolysis, and thus maintaining the inhibitory phosphorylation on Cdk2 that is consequently unable to initiate DNA synthesis through Cdc45. This prompt cell cycle delay is independent of p53 mediated transcription and may serve the purpose of temporarily slowing down cell cycle progression to provide more time for DNA repair. The other pathway places Nbs1, BRCA1 and SMC1 in a complex where all are phosphorylated by ATM and directly or indirectly affect Cdk2 activity. Both pathways do not exclude each other, since Nbs1 may facilitate the phosphorylation of CDC25A and lead to its degradation (Falck *et al*, 2002).

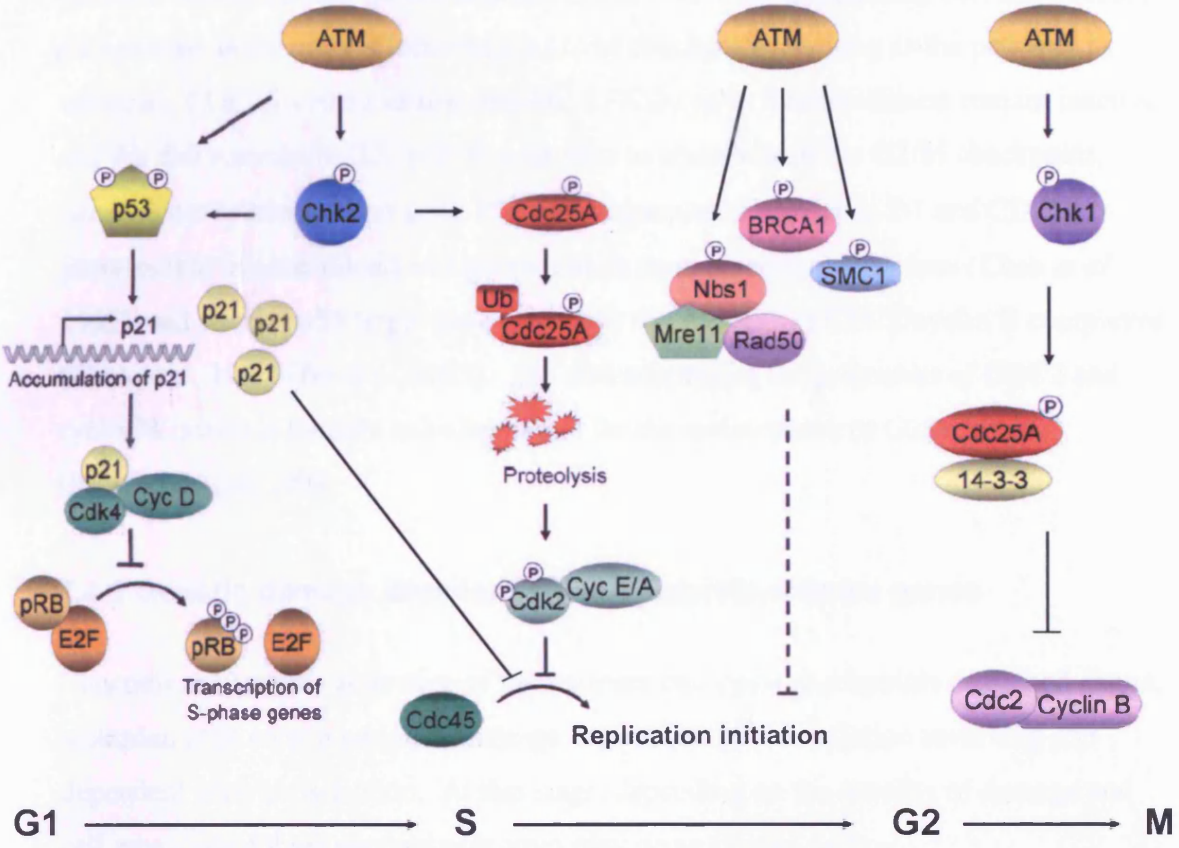

Figure 1-3: Ionising radiation induced DNA damage checkpoints in mammalian cells.

After a cell has completed DNA replication there is a second growth phase of the cell cycle (G2) before mitosis is initiated. This transition is also subject to a DNA damage checkpoint; the G2/M checkpoint. It has been reported that there are two distinct G2/M checkpoint pathways. Whereas one is ATM dependent, IR-dose independent and of rapid response, the other is a prolonged response, ATM independent and IR dose sensitive (Xu *et al*, 2002). The prolonged G2/M delay has not been thoroughly investigated. It appears to be partly the result of a loss of DNA damage induced S-phase checkpoint response and represents an accumulation of cells that were damaged during DNA replication (Xu *et al*, 2002). The rapid response pathway involves the activation of ATM, which then activates the downstream transducing kinase Chk1 (Gatei *et al*, 2003) (figure 1-3). Subsequently, Chk1 phosphorylates CDC25 family members promoting their sequestration by 14-3-3 protein(s). Originally Cdc25C was though to be the effector of the G2/M checkpoint (Peng *et al*, 1997), but it was subsequently found that mouse Cdc25C (-/-) cells have normal G2/M checkpoint (Chen

et al, 2001). In contrast, disruption of the Chk1-Cdc25A pathway abrogates ionizing radiation-induced S and G2 checkpoints (Zhao *et al*, 2002), indicating that the Cdc25A phosphatase is the main effector of the G2/M checkpoint. As long as the pathway is activated, CDC25A remains inaccessible, CDC2-cyclin B heterodimers remain inactive and the cell remains in G2. p53 also appears to contribute to the G2/M checkpoint, since its downstream target gene 14-3-3σ can sequester the cyclin B1 and CDC2 proteins that initiate mitosis and prevent them from entering the nucleus (Chan *et al*, 1999), and another p53 target gene GADD45 can destabilize CDC2/cyclin B complexes (Zhan *et al*, 1999) (Jin *et al*, 2002). p53 also suppresses the promoters of CDC2 and cyclin B, which is thought to be important for the maintenance of G2/M arrest. (Passalaris *et al*, 1999)

1.4.2 Genetic damage assessment and survival effector genes

Concomitant with the activation of the transient cell cycle checkpoints described above, metazoan cells enter a period of damage assessment after irradiation involving p53 dependent gene transcription. At this stage, depending on the severity of damage and cell type, one of three survival outcomes may occur (figure 1-4): -

1) Survival

Independent of p53 activation, ATM activates signalling pathways that enhance cell survival. ATM is required for activation of NF-κB after DNA damage (Lee *et al*, 1998b) (Piret *et al*, 1999) (Panta *et al*, 2004), and this response may induce a transcriptional program that promotes cell survival after irradiation (Stankovic *et al*, 2004). Additionally, ATM has also been shown to facilitate escape from terminal growth arrest induced by a complex genotoxin such as Chromium (VI) (Ha *et al*, 2003). Some p53 target genes have been described that enhance cell survival. The p53 induced gene Heparin-Binding EGF-like growth factor (HB-EGF) (Fang *et al*, 2001) has been shown to promote cell survival through the activation of Mitogen activated protein kinases (MAPKs) and Cyclooxygenase 2 (Cox-2) (Han *et al*, 2002). This constitutes a rare, pro-survival example of a p53 target gene, since most are involved in the induction of apoptosis or cell cycle arrest.

2) Permanent arrest

The cell may enter permanent cell cycle arrest, a senescent like state that involves prolonged expression of the p53 targets p21 and GADD45, followed by the delayed induction of another Cdk inhibitor, p16 (Robles and Adami, 1998). DNA damage of normal human fibroblasts induces terminal growth arrest, which is accompanied by phenotypic changes that bear a striking resemblance to cells that undergo replicative senescence (Di Leonardo *et al*, 1994) (Robles and Adami, 1998) and is now termed Stress induced premature senescence (SIPS) (Toussaint *et al*, 2000). This effectively removes highly damaged cells from the replicative population and therefore functions as a protective mechanism against the propagation of genomic instability in multicellular organisms (Linke *et al*, 1997).

3) Apoptosis

In other cell types such as lymphocytes DNA damage may induce apoptosis and unlike permanent cell cycle arrest, which seems to involve just a few genes, this appears to result from the co-ordinated induction of a wide variety of apoptotic p53 target genes (Vousden and Lu, 2002) (Sax *et al*, 2002). These genes contribute to induction of both the mitochondrial and death-receptor pathways of apoptosis. For example many of these proapoptotic gene products such as Bax, Puma, Noxa and p53AIP1 localise to the mitochondria and promote the loss of mitochondrial membrane potential and cytochrome c release, resulting in the formation of the apoptosome complex with Apaf1 and caspase 9 (Oda *et al*, 2000), (Nakano and Vousden, 2001), (Yu *et al*, 2001), (Matsuda *et al*, 2002). ROS produced by PIGs (p53-induced genes) can also cause damage to the mitochondria and initiate apoptosis (Polyak *et al*, 1997). In contrast, the proapoptotic gene products such as Fas, TNF-related apoptosis-inducing ligand receptor (TRAILR)/DR5 and PIDD are components of the death receptor-mediated cell death pathway (Owen-Schaub *et al*, 1995) (Lin *et al*, 2000) (Takimoto and El-Deiry, 2000) (Wu *et al*, 2000). In this instance caspase 8 is activated at the cell membrane following the clustering of death receptors that occurs following their occupation by factors such as TRAIL or the Fas ligand. The activation of the caspase family of cysteine proteases in both the mitochondrial and death receptor pathways then results in cleavage of cellular substrates and production of the apoptotic phenotype. Another p53 induced gene, HTRA2, is a serine protease that cleaves CIAP, a mammalian homologue of Drosophila Inhibitor of Apoptosis Proteins (IAPs), during p53 induced apoptosis to

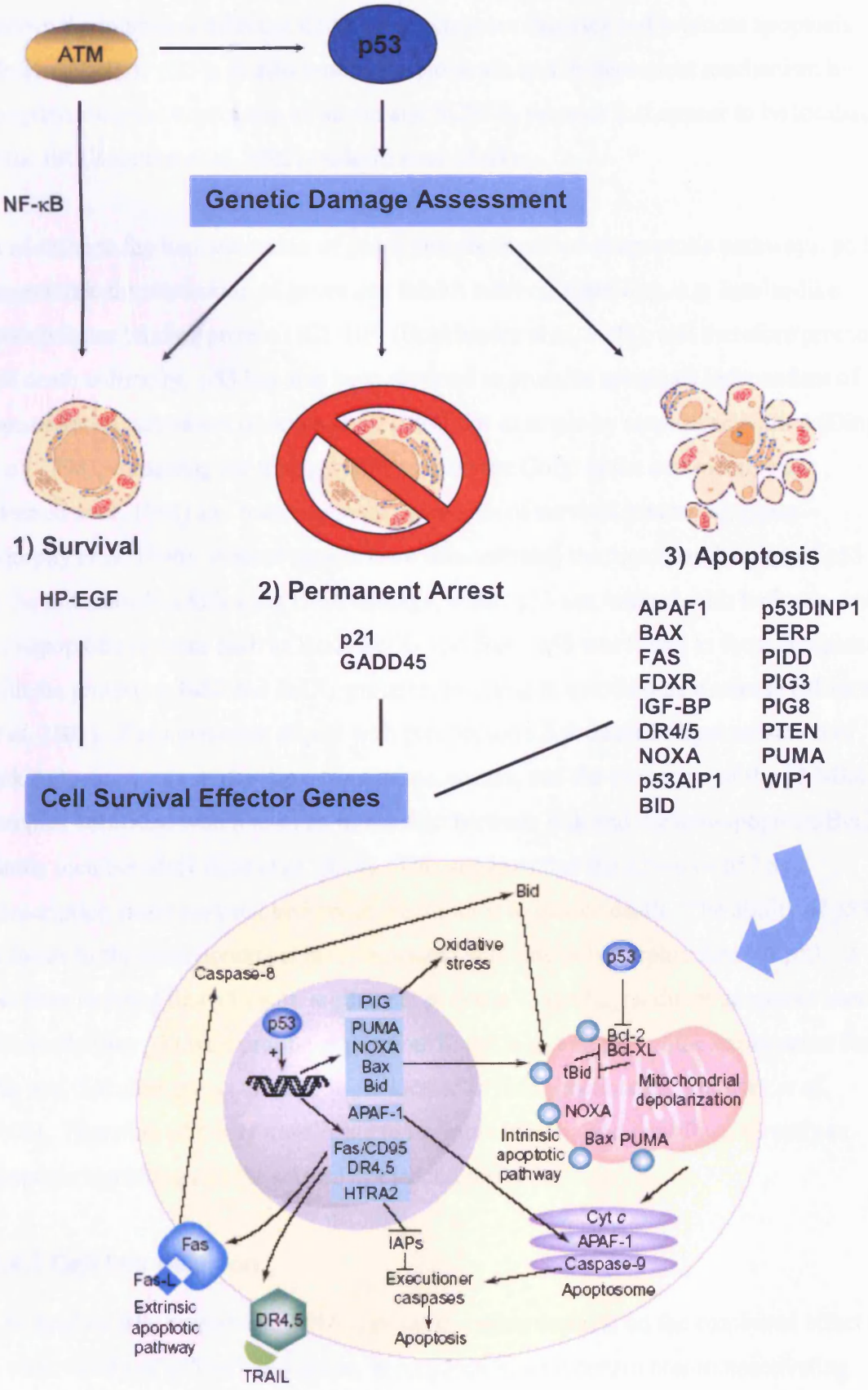

Figure 1-4. p53 genetic damage assessment, survival effector genes and mechanisms of p53 induced apoptosis. (Modified from Hofseth *et al*, 2004)

remove the inhibitory effect of CIAP on executioner caspases and promote apoptosis (Jin *et al*, 2003). p53 may also induce apoptosis via an ER-dependent mechanism by transactivating the expression of Scotin and SCN3B, proteins that appear to be localised to the ER (Bourdon *et al*, 2002) (Adachi *et al*, 2004).

In addition to the transactivation of genes directly involved in apoptotic pathways, p53 can activate the expression of genes that inhibit survival signalling, e.g. Insulin-like growth factor binding protein (IGF-BP) (Buckbinder *et al*, 1995), and therefore promote cell death indirectly. p53 has also been reported to promote apoptosis independent of transcriptional activation (Caelles *et al*, 1994), for example by caspase activation (Ding *et al*, 1998), enhancing the transport of Fas from the Golgi to the cell membrane (Bennett *et al*, 1998) and transcriptional repression of survival promoting genes (Murphy *et al*, 1996). Recent reports have demonstrated the direct localisation of p53 to the mitochondria following DNA damage, where p53 can interact with both pro- and anti-apoptotic proteins such as Bcl2, $BclX_L$ and Bak. p53 was found to form complexes with the protective Bcl2 and $BclX_L$ proteins, resulting in cytochrome c release (Mihara *et al*, 2003). The interaction of p53 with proapoptotic Bak caused oligomerisation of Bak and release of cytochrome c from mitochondria, and the formation of the p53-Bak complex coincided with loss of an interaction between Bak and the anti-apoptotic Bcl2-family member Mcl1 (Leu *et al*, 2004). This suggests that the action of p53 as a transcription factor may not be a requirement for it to induce death. The ability of p53 to locate to the mitochondria is also associated with one polymorphic form of p53. It has been reported that p53 with arginine at position 72 ($p53_{Arg}$) induces apoptosis more efficiently than p53 with proline at position 72 ($p53_{Pro}$), and part of the explanation for this was that more $p53_{Arg}$ than $p53_{Pro}$ is located in the mitochondria (Dumont *et al*, 2003). Therefore p53 may translocate to the mitochondria and contribute directly to apoptotic signalling and the release of cytochrome c.

1.4.3 Cell fate decision

The final cellular response to DNA damage therefore depends on the combined effect of a wide variety of p53-induced genes, in conjunction with certain non-transactivating properties of p53 and independent pro-survival signalling through ATM. In cells capable of p53-dependent apoptosis, low levels of DNA damage generally induce cell cycle arrest whereas high levels of p53 are required for apoptosis (Chen *et al*, 1996). Some evidence suggests this could be due to the presence of high- and low-affinity p53

binding sites in the promoters of cell cycle arrest and apoptotic genes (Szak *et al*, 2001) (Kaeser ad Iggo, 2002). Therefore, increased levels or activity of p53, governed by the type and/or intensity of the signal, can lead to the onset of apoptosis once a certain threshold level is achieved. A model for the differential control for p53-dependent gene transcription was proposed by a recent study that involves the composition of transcription initiation complexes at the core promoters of p53 responsive genes (Espinosa *et al*, 2003). Basal levels of p53, binding to cognate sites upstream of the core promoter region, mediate assembly of a poised RNA Polymerase II initiation complex on the core promoters of genes involved in the growth arrest response (including p21 and GADD45). Following DNA damage, the paused polII complex is permitted to engage the elongation phase of transcription. This preloading of the transcriptional machinery lowers the threshold for p53 activation, and therefore small increases in p53 activity give rise to a rapid induction of target gene expression. Conversely, for proapoptotic genes there is a significantly lower level of bound initiation complex compared to growth arrest genes prior to a stress stimulus. In this instance, after a stress stimulus the induction of gene expression requires a higher level of p53 activation and proceeds with much slower kinetics. A failure to terminate the p53 response, for example due to the persistence of DNA DSBs, may therefore provide time for the accumulation of sufficient levels of the appropriate apoptotic gene products to initiate an apoptotic response (figure 1-5).

The threshold for p53-mediated apoptosis may be set at different levels in different cell types, since this response has been shown to vary between tissues. For example, thymocytes and splenocytes undergo p53-dependent apoptosis in vivo in response to ionising radiation, whereas fibroblasts arrest in a p53-dependent manner. These different cell types may therefore exhibit low and high thresholds, respectively, for the onset of apoptosis. The currently accepted model for the choice between arrest and apoptosis is based principally on the idea that p53 is able to differentially transactivate promoters of growth arrest and apoptosis genes depending on the cellular context. This is reflected in our personal observation that lymphoid human cancer cell lines that undergo apoptosis following irradiation induce PUMA, while primary fibroblasts that are resistant to apoptosis do not. Built into this idea are many factors that influence the extent to which p53 can favour a given class of promoters, including the presence of pro-apoptotic proteins that govern promoter selectivity, and the concerted action of apoptosis-related pathways that shift the balance of p53 induction in favour of

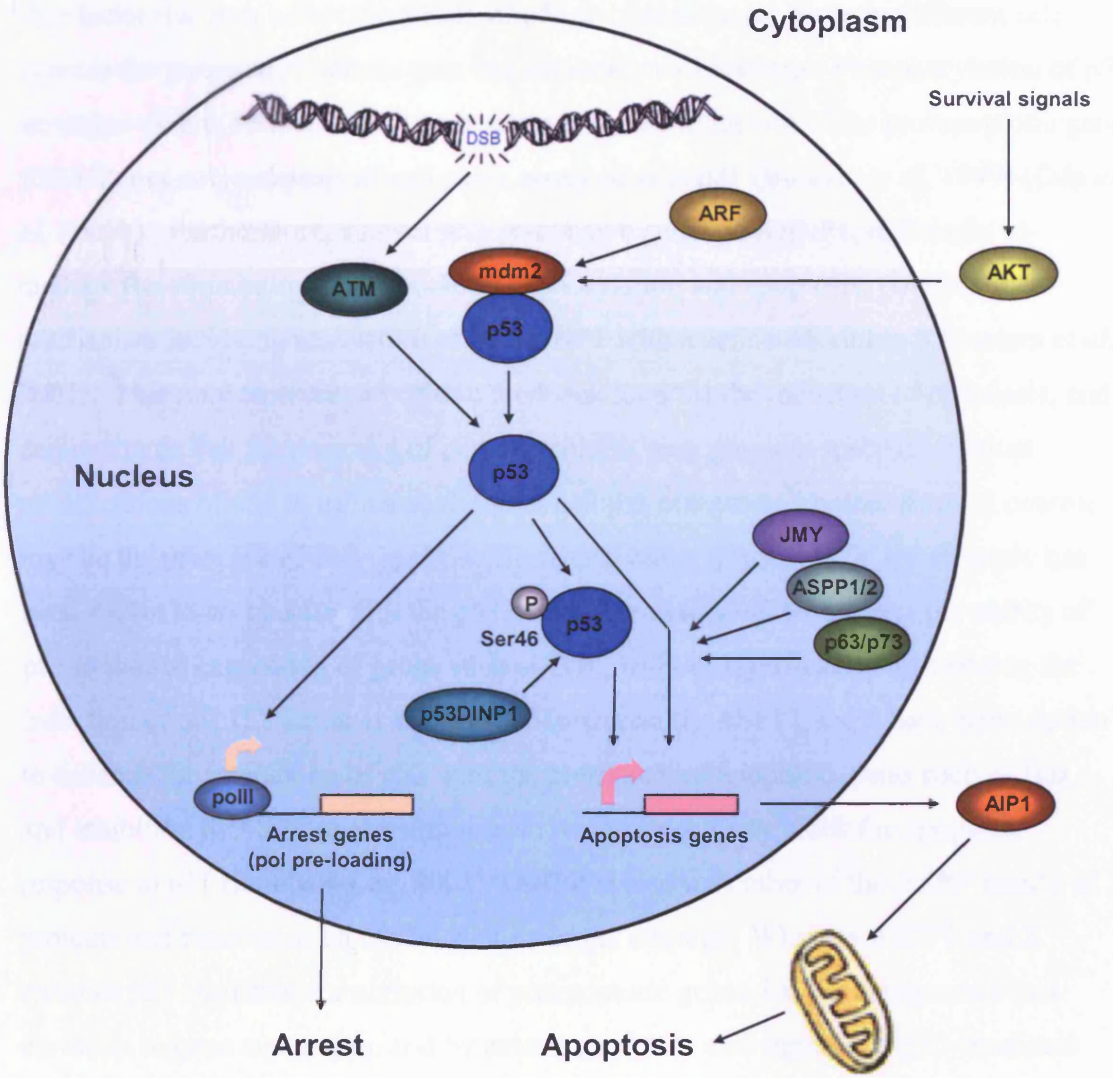

Figure 1-5: Factors that may influence the choice between p53 dependent growth arrest or apoptosis. (modified from Meek *et al*, 2004)

cell death, either by influencing the cellular environment or by impinging directly on the ability of stress signals to induce a p53 response (Gudkov and Komarova, 2003) (Vousden and Lu, 2002).

One factor that may affect the ability of p53 to bind to target genes in different cell types is the presence of certain post-translational modifications. Phosphorylation of p53 on serine-46 has been shown to be important for the induction of the pro-apoptotic gene p53AIP, but not mediators of cell cycle arrest such as p21 (Bulavin *et al*, 1999) (Oda *et al*, 2000b). Furthermore, a novel p53-responsive gene, p53DINP1, is thought to mediate the stimulation of serine-46 phosphorylation and apoptosis, possibly by a mechanism involving interaction of p53DINP1 with a serine-46 kinase (Okamura *et al*, 2001). This may represent a positive feedback loop for the induction of apoptosis, and demonstrates that the presence of certain proteins may promote specific covalent modifications of p53 to influence the final cellular outcome. Another form of control may be the presence of cell-type specific co-activators of p53. JMY for example has been shown to co-operate with the p53 binding protein p300 to enhance the ability of p53 to induce expression of genes such as Bax, without significantly influencing the induction of p21 (Shikama *et al*, 1999). More recently ASPP1 and 2 have been shown to enhance the interaction of p53 with the promoters of apoptotic genes such as Bax, and inhibition of ASPP expression was shown to selectively block the apoptotic response to p53 (Samuels-Lev, 2001). iASPP is also a member of the ASPP family of proteins and behaves as an inhibitor of its larger siblings. Whereas ASPP1 and 2 enhance p53-mediated transcription of proapoptotic genes, iASPP antagonises this elevation in gene expression, and by extension iASPP also suppresses p53-mediated death (Bergamaschi *et al*, 2003). Other p53 family members may also contribute to this level of control, since p63 and p73 were shown to be required for p53-dependent apoptosis (Flores *et al*, 2002). The presence of certain co-factors may therefore prime a cell to respond to p53 activation in a particular fashion once a specific threshold of DNA damage is achieved (figure 1-5).

Factors that influence the p53-mdm2 loop are likely to play a significant role in setting the threshold for p53 activation and consequently apoptosis. mdm2 is the target of the AKT protein kinase that mediates many survival signals that are transduced through the PI3-kinase pathway (Mayo *et al*, 2001) (Ogawara *et al*, 2002). AKT mediated phosphorylation of mdm2 has been reported to stimulate nuclear import of mdm2 and

mdm2 mediated p53 degradation. Removal of survival signaling blocks this phosphorylation of mdm2, and the basal level of p53 is increased, effectively lowering the threshold needed to initiate p53 induction in response to other factors. Under these circumstances p53 induction becomes acutely sensitive to DNA damaging agents in a manner that favours apoptosis (Gottlieb *et al*, 2002). Conversely, mutation of the PTEN tumour suppressor gene, whose product inhibits survival signals propagated by AKT, can lead to a constitutively high level of mdm2 activity in tumour cells, which increases the threshold required for p53-mediated apoptosis (Mayo *et al*, 2002). ARF, the protein inhibitor of mdm2 that is induced by hyper-proliferative signals, may also contribute to regulating the threshold level for p53 induction, since murine fibroblasts lacking this protein show a weakened induction of p53 and consequently p21 in response to DNA damage (de Stanchina *et al*, 1998) (Khan *et al*, 2000). ARF has also been shown to be a component of the DNA damage response in primary human fibroblasts (Khan *et al*, 2004). ARF may therefore contribute to setting the threshold for p53 induction through its interaction with mdm2 in a manner that may reflect the proliferative status of the cell.

1.5 Double Strand Break (DSB) Repair

Concurrent with the activation of the p53 response to DNA damage, the presence of DNA DSBs leads to the activation of proteins that function to repair this potentially lethal lesion. Two major pathways exist for the repair of DSBs, Non-homologous end joining (NHEJ) and Homologous recombination (HR) (Valerie and Povirk, 2003). Homologous recombination requires that the cell be diploid for the region that requires repair and in vertebrate organisms is restricted to late S and G2 phases of the cell cycle (Johnson and Jasin, 2000) (Takata *et al*, 1998). The NHEJ pathway of DSB repair is active throughout the cell cycle, including late S and G2 (Takata *et al*, 1998). Hence NHEJ is thought to repair the majority of DSBs in mammalian cells.

1.5.1 Homologous Recombination (HR)

HR involves the use of a homologous, undamaged partner molecule, for example a sister chromatid, and is therefore relatively error free. The DNA transactions of HR can be divided into three basic steps: 1) pre-synapsis, preparation of a recombination proficient DNA end; 2) synapsis, formation of a joint molecule between the

recombination proficient DNA end and a double-stranded homologous template; 3) post-synapsis and resolution, repair of DNA strands and separation of the recombined DNA molecules (figure 1-6).

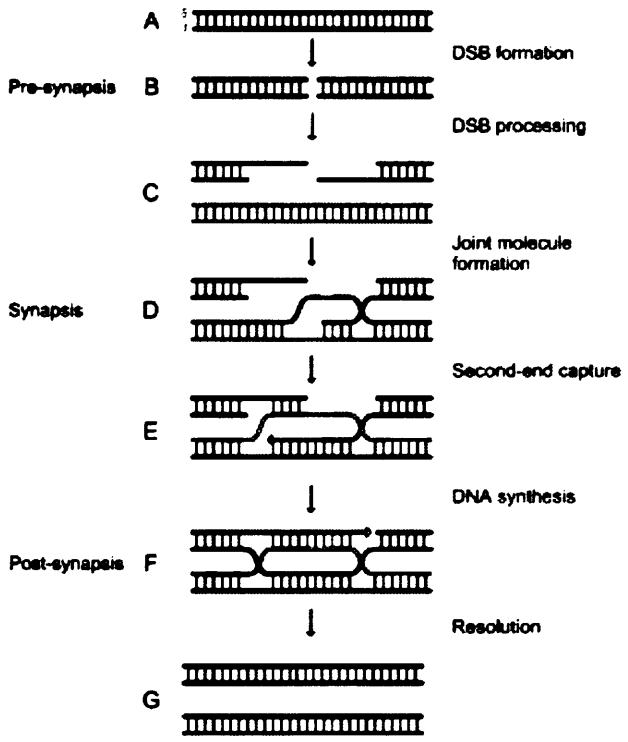

Figure 1-6: Schematic representation of Homologous Recombination (HR) repair of a DSB. Duplex DNAs are indicated by ladders with the rungs representing base pairs. Pre-synapsis consists of stages A-C. The damaged DNA molecule is nucleolytically processed to result in 3′ single-stranded tails. The white duplex DNA molecule represents a homologous DNA molecule such as a sister chromatid. Synapsis, comprised of stages D and E, involves the formation of a joint molecule between the processed broken DNA and the intact homologous template using the strand invasion and exchange properties of the Rad51 protein. Post-synapsis, stages E-G. Base pairs between the joint molecule and second DNA end are established, DNA is re-synthesised, and Holiday junctions are resolved by structure specific endonucleases. (Modified from Wyman *et al*, 2004)

The first event to occur in HR repair is the nucleolytic resection of the DNA DSB in the 5′ to 3′ direction during pre-synapsis. The efficiency of this reaction relies upon, and probably involves, the Mre11 complex (comprised of Mre11, Nbs1 and Rad50). Even though *in vitro* this complex has 3′ to 5′ exonuclease activity, the kinetics of the appearance of recombinogenic single-stranded DNA with a 3′ end is significantly lower in Mre11 mutant yeast cells (Lee *et al*, 1998a). Nbs1 was also shown to be required for

HR in higher vertebrate cells, and the rare recombinants observed suggested the Mre11 complex might be required to process recombination intermediates (Tauchi *et al*, 2002).

After the resection of the DSB, the ensuing 3′ single stranded tails are then bound by Rad51 to promote synapsing and strand invasion. This process is influenced by a range of other proteins, including replication protein A (RPA), Rad52 and Rad54. The RPA protein binds to the 3′ single stranded overhang and prevents secondary structures from forming that might inhibit downstream repair events (Bauman *et al*, 1997) (Sugiyama *et al*, 1997). A side effect of RPA binding to the overhang that needs to be overcome is that it hinders Rad51 from interacting with the single-stranded DNA (Sung *et al*, 1997). There is evidence that the Rad52 protein, which is able to bind both single and double stranded ends of DNA, overcomes this inhibitory effect, possibly by direct interaction with Rad51 (Benson *et al*, 1998) (New *et al*, 1998) (Parsons *et al*, 2000) (Sung *et al*, 1997). Notably, Rad52 has been shown to preferentially bind to DSBs, leading to the model whereby competition between Rad52 and the NHEJ protein Ku for DNA ends determines which of the two DSB repair pathways is employed (Van Dyck *et al*, 1999). Therefore it is plausible that Rad52 binds to resected DNA ends, whilst RPA binds along the 3′ single stranded overhangs. Once these initial interactions are complete, Rad52 then recruits and facilitates Rad51 binding to the overhang. Five Rad51 paralogs, X-ray cross complementing (XRCC) 2, XRCC3, Rad51B, Rad51C and Rad51D found in vertebrates, that dimerise to form distinct complexes, have also been proposed as mediators of presynaptic filament assembly, and are likely to have a role in the delivery of Rad51 to recombination substrates (Sung *et al*, 2003). In addition, the results of diverse *in vitro* assays can support roles for Rad54 at all three stages of HR, including presynaptic filament assembly.

The Rad51 nucleoprotein filament then interacts with an undamaged DNA molecule and, when a homologous region has been located, Rad51 catalises strand-exchange events in which the damaged molecule invades the other DNA duplex, displacing one strand as a D-loop (figure 1-6, stage D). Rad54 appears to be crucial for this step. Although Rad 51 has only a modest ability to make a D-loop, addition of a catalytic amount of Rad54 renders D-loop formation highly robust (Symington *et al*, 2002) (Krejci *et al*, 2003) (Petukhova *et al*, 1998). Rad54 uses the free energy from ATP hydrolysis to fuel its translocation along duplex DNA, leading to the transient opening of DNA strands (Van Komen *et al*, 2000). It is thought this facilitates the location of

homologous sequences and the extension of heteroduplex DNA in the joint molecule. At this point the 3′ terminus of the damaged DNA molecule is extended by a DNA polymerase that copies information from the undamaged partner, and the ends are ligated by DNA ligase I.

Table 1-1: Proteins implicated in the different stages of HR

Stage of HR	Process mediated	Proteins
Pre-synapsis (A-C)	Endprocessing	Mre11 complex
	Negotiating single stranded DNA	RPA
	Recombinase loading	Rad52, Rad51 paralogs, Rad54
Synapsis (D, E)	Joint molecule formation by strand invasion	Rad51, Rad54
Post-synapsis (F, G)	Branch migration	Rad54
	Resolution of crossed DNA ends	Not defined

Repair of DSBs by homologous recombination is not complete until the product DNA molecules are separated. Because DNA structures with crossed strands (Holliday junctions) are an unavoidable consequence of homologous recombination (figure 1-6 D-F) they need to be resolved by structure-specific endonucleases. In the prokaryote *E. coli* the RuvA and RuvB proteins are involved in branch migration whereas the RuvC protein performs the resolution of Holliday junctions (reviewed in West, 1996). These proteins are also capable of performing branch migration and resolution *in vitro* (Eggleston *et al*, 1997). More recently, a mammalian protein complex was identified, which is able to perform both branch migration and resolution of Holliday junctions in a manner that is homologous to the RuvABC system of *E. coli* (Constantinou *et al*, 2001). Further work is required to establish the identities of the components of this complex, and to investigate whether it is required for HR.

Strong links have been established between HR and the breast cancer susceptibility proteins, BRCA1 and BRCA2 in mammalian cells. Cells that are deficient for either BRCA1 or BRCA2 have compromised HR suggesting a role for these proteins in this repair process (Moynahan *et al*, 1999) (Snouwaert *et al*, 1999) (Moynahan *et al*, 2001) (Xia *et al*, 2001). The function of BRCA1 and BRCA2 might be mediated via interactions with Mre11-Rad50-Nbs1 and Rad51 proteins. BRCA1 interacts directly with Rad50 and is found in the same foci as the Mre11 complex following treatment

with ionising radiation, and both BRCA1 and BRCA2 associate with Rad51 in vivo (Chen *et al*, 1998) (Scully *et al*, 1997) (Zhong *et al*, 1999). Indeed, it has been shown that, through its BRCT motifs, BRCA2 directly interacts with Rad51 thereby affecting both the nuclear localisation and DNA binding properties of Rad51 (Davies *et al*, 2001) and permitting Rad51 to form foci at sites of DNA damage within the cell (Scully *et al*, 2000) (Chen *et al*, 1999a) (Yuan *et al*, 1999) BRCA1 and BRCA2 may therefore function in HR as protein scaffolds to co-ordinate the HR machinery, or as modulators of chromatin structure (Bochar *et al*, 2000)

There is evidence that proteins that are involved in the signaling of DNA damage might regulate HR by means of Rad51. For example, work in the chicken DT40 system has shown genetically that ATM functions, at least in part, by affecting the HR pathway (Morrison *et al*, 2000). One mechanism by which this regulation might take place is through the protein kinase c-Abl. In response to ionising radiation, ATM interacts with, and activates c-Abl (Baskaran *et al*, 1997) (Shafman *et al*, 1997). Once activated, c-Abl phosphorylates Rad51, a modification that enhances Rad51-Rad52 interaction (Chen *et al*, 1999b). The Rad51 and Rad52 interaction following treatment with ionising radiation is impaired in both ATM and c-Abl deficient cells, and in human cells the ATM, c-Abl and Rad51 can be co-immunoprecipitated (Chen *et al*, 1999b). These findings suggest that following DNA damage by ionising radiation, the ATM protein activates c-Abl, which in turn, facilitates Rad51-Rad52 interaction by phosphorylating Rad51. In addition ATM directly phosphorylates Nbs1 (Lim *et al*, 2000) and BRCA1 (Cortez *et al*, 1999) (Gatei *et al*, 2000) in response to DSBs, modifications that may be important for the regulation of HR, and the phosphorylation of H2AX by ATM (Burma *et al*, 2001) is thought to modulate chromatin structure to allow access of both the HR and NHEJ repair complexes.

1.5.2 Non Homologous End Joining (NHEJ)

As mentioned above NHEJ is the predominant repair pathway for DNA DSBs in higher eukaryotes. Since the chemical configuration of both pathologic and physiologic DNA DSBs is highly diverse, this key vertebrate repair pathway needs to be able to handle the varied chemical nature of these lesions. This is achieved because the proteins and enzymes involved in NHEJ recognise DNA ends based on their structure rather than on their sequence. This theme is illustrated throughout the mechanistic steps of NHEJ (figure 1-7).

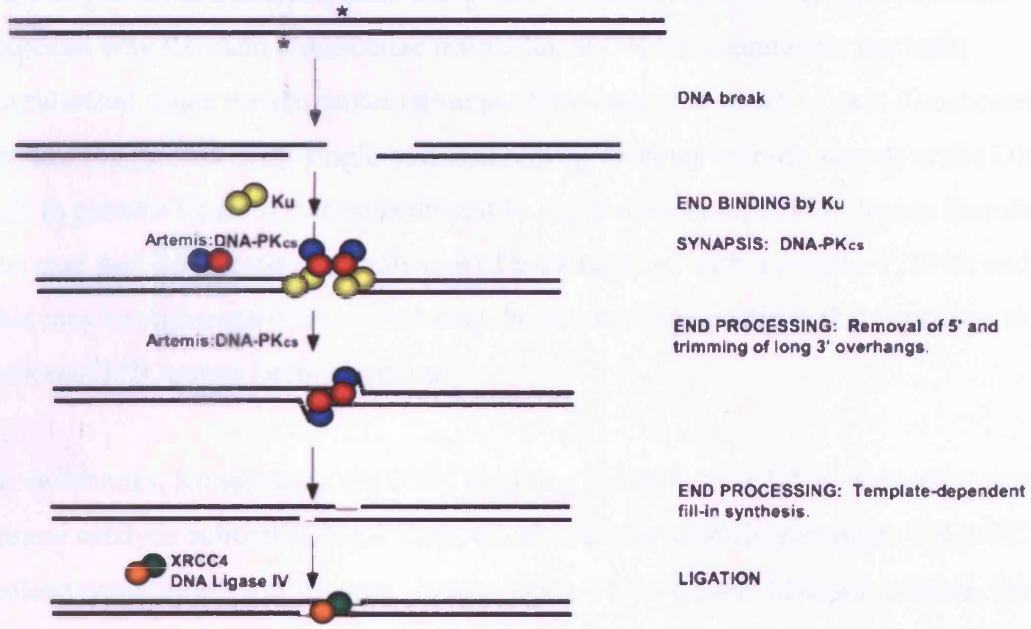

Figure 1-7: Non Homologous End Joining (NHEJ), the predominant DSB repair pathway in vertebrate cells. DSB ends are first recognised by the Ku heterodimer, which then recruits the DNA-PK-Artemis complex. To allow subsequent repair steps to proceed the two ends must be held in close proximity. This step is referred to as synapsis and evidence suggests this is performed by two DNA-PKcs molecules. For complex (incompatible) DNA ends, as would be generated by ionising radiation, there is often need for nucleolytic processing. This is carried out by the Artemis-DNAPKcs complex, and the β-lactamase domain of Artemis is essential for this nuclease activity. End processing may also involve the filling in of gaps by polymerases. Ligation is the final step in NHEJ, and is performed by the XRCC4-ligase IV complex. A simpler pathway that involves only Ku and the XRCC4-LigaseIV complex may occur at blunt or compatible ends that do not require a nuclease or polymerase. (Modified from Lieber *et al*, 2004)

The first stage in NHEJ repair is therefore recognition of the DNA break. Although the identity of the initial sensor protein that functions to activate ATM at DSB sites in the signaling response is only just beginning to emerge, the initial sensor for NHEJ repair has been known for some time. The Ku protein is central to NHEJ in organisms from yeast to man, and binds to the two DNA ends of a DSB. Ku is a heterodimer of two subunits called Ku70 (~69 kDa in man) and Ku80 (~83 kDa in man, also called Ku86) (Critchlow and Jackson, 1998) (Lieber, 1999) (Smith and Jackson, 1999). It has been established that Ku binds to DNA in a non-sequence-dependent manner that relies on DNA DSBs (Dynan *et al*, 1998). Once loaded onto a DNA terminus, Ku can diffuse to internal positions (de Vries *et al*, 1989) (Yaneva *et al*, 1997). The crystal structure for Ku reveals a form that is ideally suited to its function and biochemical properties (Walker *et al*, 2001). A 20 Å hole through the center of Ku seems to permit it to thread

onto any DNA end in a sequence independent manner, and this toroidal structure explains why Ku cannot dissociate from a linear DNA molecule that has been circularized, since the Ku protein dose not have an end at which to exit. Functional studies suggest that long single-stranded arms projecting off both strands at the DNA end (a pseudo-Y) are not an impediment to Ku (Falzon *et al*, 1993). It may therefore be the case that Ku threads onto only one of the strands of such a pseudo-Y DNA end, and this may be understandable considering the action of the nuclease that functions to process DSB termini before ligation.

In vertebrates, Ku serves as the DNA targeting subunit of the DNA-dependent protein kinase catalytic subunit (DNA-PKcs), which together with Ku forms the DNA-PK holoenzyme (Smith and Jackson, 1999). DNA-PKcs is a 469 kDa polypeptide, the c-terminal region of which has homology to the catalytic domains of proteins of the PI-3 kinase family, such as the ATM protein kinase described earlier (Hartley *et al*, 1995). It is believed that Ku first binds to the DNA end, translocates inwards by one helical turn, and then recruits DNA-PKcs and stabilises its binding to DNA. Once bound to DNA ends, DNA-PKcs itself can tether the broken DNA ends together in a synaptic complex containing two DNA-PKcs molecules (Cary *et al*, 1997) (DeFazio *et al*, 2002). Therefore, one function of DNA-PK in DSB repair may be to bridge the broken ends to facilitate rejoining. The other function of DNA-PK is to recruit, and, perhaps, activate proteins involved in DNA-end processing and ligation. This is likely to involve the kinase activity of DNA-PK, which appears to be activated by an interaction with a single stranded region derived from a DSB that may arise from 'breathing' of the DNA end (Hammarsten *et al*, 2000) (Martensson *et al*, 2002).

Pathological and physiological DSBs usually result in incompatible ends, therefore rejoining typically requires nuclease activity to remove several nucleotides prior to rejoining. This is believed to be performed by the Artemis protein (Moshous *et al*, 2001), which is a target for phosphorylation by DNA-PK (Ma *et al*, 2002). Within eukaryotic cells, some fraction of Artemis and DNA-PKcs molecules are bound to each other in a very stable complex, and therefore Artemis is presumably localised to DSB sites along with DNA-PKcs. Artemis has nuclease activity that is limited to 5′ exonuclease activity in the absence of DNA-PKcs. However, once bound to a DNA end, DNA-PKcs phosphorylates itself and Artemis (Ma *et al*, 2002), and one of these targets (or perhaps both) permits the Artemis-DNA-PK complex to function as an

endonuclease, allowing it to cleave both 5′ and 3′ overhangs of any length (Ma *et al*, 2002). Since mutations of Artemis in its β-lactamase fold abolish endonuclease activity, this region may be at least partly responsible for the nuclease activity. The Artemis-DNA-PKcs complex is also very efficient at opening DNA hairpins, which is extremely important in the context of V(D)J recombination during lymphocyte development. Blunt or compatible DNA ends, such as the signal ends generated during V(D)J recombination, may not require nuclease processing and could therefore be repaired independently of Artemis-DNA-PK. Given that pathologic sources of DSBs (such as ionising radiation) are thought to induce multiple local sites of oxidative damage to bases and sugar moieties (Nikjoo *et al*, 2001), it is assumed that the nuclease activity of Artemis-DNA-PK is required for the repair of a significant amount these lesions. Consistent with this model, recent work has confirmed that Artemis deficient cells are unable to repair a subset of radiation-induced DSBs, and this defect is enhanced by agents that induce relatively high levels of complex DSBs (Riballo *et al*, 2004). Furthermore, ATM was shown to phosphorylate Artemis and function in a common DSB repair pathway, which may explain the elevated level of residual DSBs observed in AT cells after irradiation (Cornforth and Bedford, 1985) (Foray *et al*, 1997). H2AX, 53BP1 and the Mre11 complex were also required for this ATM dependent rejoining (Riballo *et al*, 2004) suggesting these proteins may have important adaptor functions in certain NHEJ events.

Recent work has suggested that certain polymerases may function at this stage of NHEJ to allow gaps to be filled in where microhomologies exist between the two DNA ends. However, NHEJ mechanistic schemes that do not require a polymerase for at least some NHEJ events could be proposed. For example, the Artemis-DNA-PK nuclease activity could simply resect the two DNA ends until they were compatible as blunt ends or with one- or two-nucleotide compatible overhangs. One study in mammalian cells has shown that when Ku and the XRCC4-Ligase IV complex, which performs the final ligation step of NHEJ (Li *et al*, 1995) (Critchlow *et al*, 1997) (Grawunder *et al*, 1997), are bound at a DNA end, then polymerase μ is recruited (Mahajan *et al*, 2002). Although the polymerase μ knockout mouse and cells from it are not sensitive to IR (Bertocci *et al*, 2002), slightly shortened coding ends at the kappa light chain junctions were observed in lymphocytes suggesting somewhat abnormal V(D)J recombination (Bertocci *et al*, 2003). Immunodepletion of polymerase λ from human crude extracts has been used in support of the possibility that this polymerase is also involved in NHEJ

(Lee *et al*, 2004b). Recently, NHEJ reactions reconstituted *in vitro* have shown that polymerases μ and λ can bind Ku and function in certain NHEJ events (Ma *et al*, 2004). Some NHEJ reactions are therefore likely to use a polymerase prior to ligation where appropriate, but this does not to appear to be essential for NHEJ per se.

Once the DSB has been processed into a form suitable for rejoining, Artemis-DNA-PKcs may dissociate from the Ku-DNA complex to permit the ligation step of NHEJ by the XRCC4-Ligase IV complex. This rearrangement process may involve autophosphorylation of DNA-PKcs, since there is evidence that this modification regulates its binding to DNA, and this activity is required for DSB rejoining (Chan *et al*, 1996) (Merkle *et al*, 2002) (Ding *et al*, 2003) (Block *et al*, 2004) (Reddy *et al*, 2004). Recently, Mdc1was implicated in NHEJ since it was shown to regulate DNA-PK autophosphorylation activity (Lou *et al*, 2004). DNA-PK also phosphorylates XRCC4 *in vitro* and IR induced phosphorylation of XRCC4 is dependent on DNA-PKcs *in vivo* (Leber *et al*, 1998) (Matsumoto *et al*, 2000), although it is not clear what significance this modification has since it does not seem to be required for efficient rejoining (Mizuta *et al*, 1997) (Grawunder *et al*, 1998) (Leber *et al*, 1998). Although the XRCC4-Ligase IV complex does not seem to form a stable complex with DNA, it does so with a Ku-DNA complex (Chen *et al*, 2000). The Ku protein has been shown to load the XRCC4-Ligase IV complex onto DNA ends and stimulate DNA end ligation (Ramsden and Gellert, 1998) (Nick McElhinny *et al*, 2000). Endogenously the XRCC4-Ligase IV complex exists in a pre-adenylated form. Recruitment of the XRCC4-Ligase IV complex causes inward translocation of Ku, allowing the AMP moiety of the ligase-adenylate complex to transiently attach to the DNA end promoting ligation (Kysela *et al*, 2003). The XRCC4 protein appears to function by stabilising and enhancing the activity of Ligase IV (Grawunder *et al*, 1997) (Grawunder *et al*, 1998), and evidence exists in lower eukaryotes that XRCC4 may also help target Ligase IV to DSB sites (Teo *et al*, 2000). Recently the high molecular weight protein AHNAK, that is under-expressed in many radiosensitive neuroblastoma cell lines, was shown to interact with the XRCC4-Ligase IV complex and stimulate DNA end joining (Stiff *et al*, 2004b). AHNAK was also able to link two DNA molecules, suggesting that this protein may have a role in the synapsis of DNA ends during the ligation phase of NHEJ.

1.5.3 Regulation of DSB repair

Whereas HR is restricted to the certain phases of the cell cycle and may be regulated by cellular signalling mechanisms (described above), the NHEJ system is ideally configured to be the constitutive pathway of DSB repair. If the density of Ku protein in a typical nucleus is calculated and a random distribution is assumed, then the average distance between two Ku molecules is only 4-6 times the Ku diameter (Lieber *et al*, 2003). Any Ku molecule is therefore only 4-6 diameters from any potential DSB, so early DSB detection by Ku is unlikely to be a rate-limiting step, especially given the high affinity of Ku for DNA ends. Elimination of Ku has been reported to result in increased HR, which suggested that there was competition between these two pathways (Adachi *et al*, 2001) (Fukushima *et al*, 2001) (Pierce *et al*, 2001). In this situation defects in the XRCC4-Ligase IV complex should not stimulate HR since Ku would still be able to recruit DSBs for NHEJ, but HR was found to be increased in mammalian cells with mutations in XRCC4 (Delacote *et al*, 2002). This has led to the proposal that NHEJ is the initial pathway that is attempted and, if this fails, HR might take over. This process would be restricted to the late S- or G2-phases of the cell cycle, when HR is active.

1.5.4 V(D)J recombination and DSB repair

In vertebrates the adaptive immune system depends on the generation of a vast repertoire of soluble and membrane bound antigen receptors expressed in B lymphocytes and T lymphocytes respectively. The variable regions of immunoglobulin (Ig) and T-cell receptor (TCR) chains directly bind foreign antigen, and are encoded by a modest number of gene segments. During early B and T lymphocyte development immunological diversity is achieved through a series of programmed DNA rearrangements, termed V(D)J recombination, where germline variable (V), diversity (D) and joining (J) gene segments are rearranged to code for a highly diverse repertoire of Ig and TCR variable regions (reviewed in Bassing *et al*, 2002a). TCR β and δ chain and Ig heavy chain (IgH) variable region exons are assembled from V, D and J segments, while TCR α and γ chains and Ig light chain variable region exons are assembled from just V and J segments. This developmental process involves the programmed induction of DSBs between V, D and J (coding) sequences and flanking recombination signal sequences (RSS) by the recombination activating gene (RAG) 1 and RAG2 proteins. RAG proteins are expressed only in lymphoid progenitors and the

cell cycle expression profile of RAG2 serves to restrict introduction of RAG generated DSBs to the G1 phase of the cell cycle (Lee *et al*, 1999). The RAG generated ends are then joined in a new configuration by the NHEJ DSB repair proteins to complete V(D)J recombination.

The molecular steps through which RAG introduces DSBs between coding and RSS have been extensively characterised in vitro (reviewed in Fugmann *et al*, 2000) (Gellert *et al*, 2002). The DNA cleavage phase begins when the RAG-1, RAG-2 and HMG1 proteins form a complex that binds at the RSS (depicted as triangles, figure 1-8) adjacent to each V, D or J element (depicted as rectangles). The RAG complex nicks the DNA at each of the RSS. RSS are composed of highly conserved heptamers and nonamers separated by either 12 or 23 bp spacers. One nicked 12-signal (next to a V segment, for example, at the kappa light chain gene locus) and one nicked 23-signal (next to a J segment at the J segment of the kappa light chain locus) are brought into synapsis by the RAG complex (figure 1-8). In a subsequent reaction step, RAG then catalyses a trans-esterification reaction in which the coding strand 3′OH attacks the opposite coding strand to form sealed DNA hairpin coding ends and recombination signal (RS) ends in the form of blunt, 5′ phosphorylated DSBs (McBlane *et al*, 1995) (van Gent *et al*, 1995).

The four RAG liberated DNA ends remain associated with RAG in a stable postcleavage synaptic complex (PSC), and RAG, in the context of this complex, appears be important for directing the joining phase of the reaction (Qiu *et al*, 2001) (Yarnell Schultz *et al*, 2001) (Tsai *et al*, 2002). At this stage the RAG proteins may be involved in recruiting NHEJ factors and in holding the broken ends in close proximity. The Ku protein is presumed to bind some or all of the four DNA ends, perhaps thereby displacing the RAG complex to allow DNA repair proteins to gain access, since retention of signal sequences within the signal complex has been shown to prevent their joining by the XRCC4-Ligase IV complex (Jones and Gellert, 2001). The Artemis-DNA-PKcs complex, recruited to the coding ends by Ku, opens the hairpinned V, D or J ends (Ma *et al*, 2002). The Artemis-DNA-PK complex then acts as an endonuclease (and perhaps Artemis acts as an exonuclease) to trim the V, D or J ends to variable extents, thereby contributing to junctional diversity (Ma *et al*, 2002). A template dependent polymerase, such as polymerase μ, may then fill in the gaps. At this stage terminal deoxynucleotide transferase (TdT), which is expressed in B- and T- cell

lymphoid progenitors, is recruited to coding ends in a process that probably involves Ku (Purugganan *et al*, 2001) (Sandor *et al*, 2004). TdT is then responsible for template-independent DNA synthesis, which markedly contributes to the junctional diversity at the coding end. Finally, the XRCC4-Ligase IV complex carries out the ligation of the two ends (Figure 1-8).

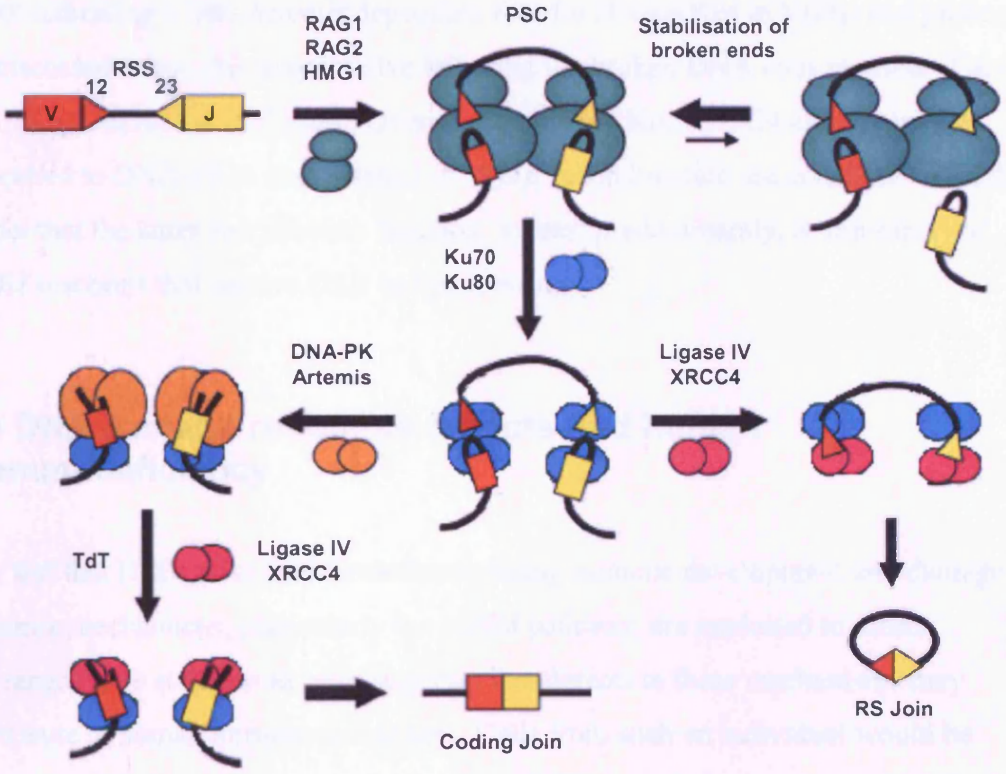

Figure 1-8: Mechanism of the V(D)J recombination reaction. RAG1, RAG2, and HMG1 form a complex that binds recombination signal sequences (RSS). The RAG complex creates a nick adjacent to the coding end side of each RSS, and the two nicked species are brought into synapsis. The RAG complex then catalyses a trans-esterification reaction to create hairpinned coding ends at the end of the V, D or J ends. Ku binds to the coding ends and recruits Artemis-DNA-PKcs which opens the hairpins. TdT then conducts template-independent DNA synthesis to increase coding join diversity. Ku also binds to signal ends, and the XRCC4-Ligase 4 complex is recruited to complete the end joining reaction for both coding and signal ends. (Modified from Bassing and Alt, 2004)

The signal ends are also rejoined by the XRCC4-Ligase IV complex (Bassing *et al*, 2002a), and whereas Ku is absolutely required for this, possibly to recruit the ligase complex, DNA-PKcs-Artemis is dispensable for this reaction. Thus, while DNA-PKcs mice are essentially completely defective for ability to join coding ends, they are relatively unimpaired in their ability to generate signal joins (Gao *et al*, 1998) (Taccioli *et al*, 1998). This may be because blunt ends do not require nucleolytic processing and,

hence, Ku and XRCC4-Ligase IV may be sufficient. Consistent with this model, Artemis deficient mice and humans display a similar molecular phenotype to DNA-PKcs mutants, being blocked for coding joint formation, but showing normal signal joining (Moshous *et al*, 2001) (Rooney *et al*, 2002). However, while Artemis appears to have no role in signal end joining, DNA-PKcs deficiency does have variable effects on this reaction, particularly with respect to fidelity (Bogue *et al*, 1998) (Fukumura *et al*, 2000) indicating a non-Artemis dependent role for DNA-PKcs in V(D)J end joining. As discussed above this may involve tethering the broken DNA ends together (Cary *et al*, 1997) (DeFazio *et al*, 2002). Overall, the roles of Ku, XRCC4 and Ligase IV compared to DNA-PKcs and Artemis in V(D)J recombination are consistent with the model that the latter two proteins function, at least predominantly, in the subset of NHEJ reactions that require DSB end processing.

1.6 DNA damage response defects and human immunodeficiency

The fact that DSBs arise as intermediates during immune development and damage response mechanisms, particularly the NHEJ pathway, are exploited to effect rearrangements at the break sites suggests that defects in these mechanisms may contribute to human immunodeficiency. Cells from such an individual would be sensitive to IR since the repair of exogenous DSBs would also be compromised. Indeed, immunodeficient patients that display cellular radiosensitivity have been described with mutations in proteins that function in the NHEJ pathway of DSB repair. As expected, cells from these patients were also impaired in their ability to perform V(D)J recombination. Other DNA damage response defects do not necessarily impinge on the ability to conduct V(D)J recombination (Table 1-2). Ataxia telangiectasia (AT), resulting from mutations in the ATM transducing kinase, is an autosomal recessive disorder characterised by diverse clinical symptoms including immunodeficiency. Whilst AT patients are proficient in V(D)J recombination, cells from these patients are severely radiosensitive and have defects in checkpoint activation. Similar to AT, Nijmegen Breakage Syndrome (NBS) and AT like disorder (ATLD), resulting from defects in the Mre11 complex, are also disorders that do not directly affect V(D)J recombination, but result in clinical immunodeficiency and cellular radiosensitivity associated with checkpoint defects. In addition to the described defects in NHEJ and DSB signaling, other individuals have been described that do not appear to fall into

either category. Despite being immunodeficient and radiosensitive, these patients display normal levels of V(D)J recombination and activate checkpoints efficiently. These patients may have defects that affect the DNA damage assessment process, where an inappropriate cell survival outcome, such as permanent arrest or apoptosis, results from only a modest level of damage (Table 1-2).

Table 1-2: Proposed DNA DSB response defects that result in immunodeficiency

Human Disorder	Mutant protein	Immune phenotype	Defective DSB Response	Cellular phenotype
AT	ATM	Variable immunodeficiency	DSB signalling & repair	Checkpoint and repair defects
NBS	Nbs1	Variable immunodeficiency	DSB signalling & repair	Checkpoint and repair defects
ATLD	Mre11	Mild variable immunodeficiency		
LIG4 syndrome	Ligase IV	Pancytopenia	NHEJ repair	Repair defect, checkpoints normal
Artemis defect	Artemis	SCID		
Not classified	Survival effector	Pancytopenia	Survival assessment	Increased senescence, apoptosis. Normal repair

1.6.1 Ataxia Telangiectasia (AT)

Ataxia telangiectasia (AT) was one of the first recognised disorders in which immunodeficiency was associated with an abnormal response to DNA damage (Taylor *et al*, 1975). AT is characterized by diverse clinical features including immunodeficiency, progressive cerebellar ataxia, oculocutaneous telangiectasies, clinical radiosensitivity, chromosome instability and elevated risk of lymphoid malignancy (Jorgensen *et al*, 1996) (Taylor *et al*, 1996). The immunodeficiency associated with AT involves cellular and humoral impairment, but clinical manifestations are extremely variable ranging from normal to profoundly reduced responses to bacterial antigens (Shiloh *et al*, 1997). Sinopulmonary infection is common and lymphopaenia has been described. Low or absent IgA, IgE or IgG subclasses are also commonly observed suggesting an impairment of B cell maturation.

The mutations found in ATM patients are frequently truncations resulting in inactivation of protein function (Savitsky *et al*, 1995). The wide range of clinical

characteristics associated with AT is reflected at the cellular level with a pleiotropic phenotype (Jorgensen *et al*, 1996) (Taylor *et al*, 1996) (Rotman and Shiloh, 1998). AT cells display severe γ-radiation sensitivity associated with defects in cell cycle checkpoint control including an inability to arrest at the G1/S and S-phase checkpoints and, for cells in G2 at the time of irradiation, an impaired G2/M arrest (Beamish and Lavin, 1994) (Houldsworth and Lavin, 1980) (Kastan *et al*, 1992) (Painter *et al*, 1980). Furthermore AT cells fail to stabilise p53 after radiation exposure (Khanna *et al*, 1995) (Lu and Lane, 1993) an event that is required for efficient G1/S arrest. The severe radiosensitivity observed in AT cell lines had thus been attributed to the failure to arrest the cell cycle in the face of high levels of DNA damage, but the fact that p53 defective cells lines, which are also unable to arrest at the G1 checkpoint, are radioresistant rather than radiosensitive suggests that absence of this checkpoint, at least, does not confer radiosensitivity (Slichenmyer *et al*, 1993). Radiosensitivity has also been observed in non-dividing AT cells (Thacker *et al*, 1994) which indicates that defective checkpoints are not solely responsible for this radiosensitive phenotype.

There is increasing evidence that AT cells also harbor a significant defect in DSB repair and this contributes to the radiosensitive phenotype. It has long been known that although the initial rate at which arrested AT cells repair radiation induced-DSBs is normal, they retain a higher level of residual breaks than control cells (Cornforth and Bedford, 1985) (Foray *et al*, 1997). This finding was confirmed by monitoring the removal of γ-H2AX foci, a marker of DSBs, and at prolonged repair times the defect in AT cells was more pronounced than that of Ligase IV mutant cells (Kuhne *et al*, 2004) (Riballo *et al*, 2004). This suggests that, similar to Artemis, ATM is required for the repair of a subset of DSBs. Other work has shown that ATM is important for the control of HR DSB repair (Morrison *et al*, 2000), and a recent study using glioma cells indicates that this regulation occurs throughout the cell cycle (Golding *et al*, 2004). Defects in HR may therefore contribute to the inherent chromosomal instability associated with AT.

AT cells are able to carry out V(D)J recombination using a cell based assay (Hsieh *et al*, 1993). Nevertheless, AT patients show frequent translocations that involve the V(D)J loci (Shiloh *et al*, 1997). One explanation for this may be that although the efficiency of DSB rejoining is only marginally affected, the fidelity of repair is significantly compromised. Consistent with this are findings that AT cells are impaired in the

fidelity of DSB rejoining (Cox *et al*, 1986) (North *et al*, 1990). This function may be coupled to the recently described role of ATM in the routine surveillance of intermediates of V(D)J recombination (Perkins *et al*, 2002), which may help to suppress potentially oncogenic translocations when repair fails. It has also been suggested ATM may be required to halt the cell cycle in G1 until V(D)J recombination is complete (Rotman and Shiloh, 1998). Therefore, although the heterogeneous immunodeficiency observed in AT does not appear to result from a specific defect in V(D)J recombination, ATM may have an ill defined regulatory role that could influence DSB repair to some extent.

1.6.2 AT-Like Disorder (ATLD) and Nijmegen Breakage Syndrome (NBS)

AT-Like Disorder (ATLD) and Nijmegen Breakage Syndrome (NBS) are conditions resulting from defects in the Mre11 complex, caused by mutations in the Mre11 and Nbs1 proteins respectively. The clinical features of patients with ATLD are very comparable to those of AT, with the clearest similarity being the progressive cerebellar ataxia shown in both cases. In contrast to AT, however, ATLD patients show no telangiectasia, and the slower progression of the disorder gives the overall appearance of a milder condition than AT (Taylor *et al*, 2004). These similarities suggest that the Mre11 complex and ATM function in the same pathway, but NBS patients have very different clinical features involving pronounced developmental delay in contrast to the progressive neurological impairment seen in AT and ATLD (Shiloh *et al*, 1997) (Stewart *et al*, 1999). Both ATLD and NBS patients show a measurable immunodeficiency, although NBS is more comparable to AT in this respect, displaying humoral and cellular abnormalities associated with a more severe immunodeficient phenotype than observed in ATLD (Jeggo and Concannon, 2001).

An explanation for the different clinical symptoms observed in NBS compared to ATLD may be the result of the mutational change in the respective proteins, or could be that the components of the Mre11 complex have some distinct functions. The roles of the individual Mre11 complex proteins is difficult to decipher since the mutations in NBS and ATLD cells result in global effects on the Mre11 complex. However, a recent study using Mre11/Rad50 that is able to locate to the nucleus in the absence of Nbs1 (nuclear localisation of the Mre11 complex is thought to be one of the main functions of Nbs1) has suggested some distinct roles for Mre11 complex components. Whereas only

Mre11 and Rad50 were required for ATM activation early after low doses of irradiation, the entire Mre11 complex is required for certain ATM-dependent phosphorylation events later after irradiation (Cerosaletti *et al*, 2004). At the cellular level both disorders exhibit hypersensitivity to ionising radiation, measured chromosomally and by cell survival (Stewart *et al*, 1999) (Varon *et al*, 1998). Radiation-induced autophosphorylation of ATM, which is a measure of ATM activation, is impaired in both cases (Delia *et al*, 2004) (Horejsi *et al*, 2004), possibly reflecting mutations that affect the entire Mre11 complex. The downstream radiation-induced phosphorylation of p53 has been reported as both normal (Jongmans *et al*, 1997) (Stewart *et al*, 1999) (Lim *et al*, 2000) and defective (Delia *et al*, 2004), but theses discrepancies may be due to different dosing regimes. After higher levels of irradiation other DSB responsive pathways may compensate for the underlying defects. Indeed, a dose dependent G1/S checkpoint defect has been defined in NBS cells after low doses of radiation (Girard *et al*, 2002), and ATLD cells have also been associated with an abrogated G1 arrest (Delia *et al*, 2004). Cells from patients with both disorders are certainly defective in S-phase checkpoint arrest, and display RDS (Painter and Young, 1980) (Stewart *et al*, 1999) although this is not as severe as that observed in AT cells, because of a parallel ATM-dependent, Nbs1-independent S-phase checkpoint pathway (Falck *et al*, 2002).

Comparable to AT cells, the radiosensitivity of NBS cells does not consistently correlate with checkpoint deficiencies, and may involve a defect in DSB repair. An immortalized NBS fibroblast line (347BR) with near normal checkpoints demonstrated severe sensitivity to radiation (Girard *et al*, 2000), and this line displayed an elevated level of residual breaks similar to that observed in AT cells. This repair defect does not affect the overall rate of DSB repair in human cells (Kraakman-van der Zwet, *et al* 1999), but may impair the resolution of a subset of DSBs (Riballo *et al*, 2004). Since the Mre11 complex is required for efficient HR repair (Yamaguchi-Iwai, *et al*, 1999), a defect in this pathway may contribute to the repair deficiency of this line. NBS cells are proficient in V(D)J recombination (Yeo *et al*, 2000), suggesting the Mre11 complex is not essential for V(D)J recombination associated DSB repair. This may not be the case for other immune specific processes involving NHEJ repair. Class Switch Recombination (CSR) is a process whereby B-lymphocytes replace the immunoglobulin Cμ constant region with the constant region of another immunoglobulin, and involves the NHEJ pathway of DSB repair. Whereas CSR involves Ku (Manis *et al*, 1998), DNA-PKcs does not appear to be essential (Bosma *et al*, 2002). The immunodeficiency

observed in NBS patients has recently been linked to a defect CSR (van Engelen *et al*, 2001), and a recent study suggests a similar deficit exists in ATLD patients (Lahdesmaki *et al*, 2004). Since ATM has also been implicated in CSR (Pan *et al*, 2002) (Lahdesmaki *et al*, 2004), ATM and the Mre11 complex may be involved in NHEJ during CSR, a process that is independent of DNA-PKcs. Defective CSR may therefore contribute to the immunodeficient phenotypes of AT, ATLD and NBS.

1.6.3 LIG4 syndrome

Mutations in the Ligase IV DSB repair gene have been reported in five patients. One patient, designated 180BR, was clinically normal but developed leukaemia at age 14 and dramatically over-responded to subsequent chemotherapy (Riballo *et al*, 1999). The remaining patients all displayed pancytopenia as well as additional features that include microcephaly and developmental delay (O'Driscoll *et al*, 2001). The patients also show facial features that have been described as "bird-like", "Seckel-like" or more simply "characteristic facial features" (O'Driscoll *et al*, 2004), and 2 of the patients displayed telangiectasies, a clinical feature that overlaps with AT.

Given that Ligase IV is essential for V(D)J recombination, a T-B- Severe Combined Immunodeficient (SCID) phenotype may be expected in patients with Ligase IV defects, but these patients display a milder form of pancytopenia reminiscent of NBS. Mice with inactivating mutations in Ligase IV are embryonic lethal (Barnes *et al*, 1998) (Frank *et al*, 2000). Thus, the mutations identified in Ligase IV patients are anticipated to be hypomorphic, generating expressed proteins that retain some residual function. Indeed, the mutations identified were either missense mutations or small truncations. The published Ligase IV mutations include a R278H substitution in the catalytic site and a G469E missense as well as two nonsense mutations (R580X and R814X) (Riballo *et al*, 1999) (O'Driscoll *et al*, 2001). These mutations lead to C-terminus truncation of the protein in the region containing the two BRCT motifs, previously shown to be required for the proper interaction with XRCC4 (Grawunder *et al*, 1998) (Sibanda *et al*, 2001). The severity of clinical features may reflect the impact of the mutational change on protein function. Consistent with this concept, in vitro expressed Ligase IV harbouring the R278H mutation, identified in the clinically normal patient 180BR, retains a higher level of residual activity relative to proteins harbouring other mutational changes identified in the more severe patients (O'Driscoll *et al*, 2004). Another patient

with the R278H mutation had more severe clinical features, and this was attributed to the presence of 2 additional linked polymorphisms that when combined with the otherwise mild R278H mutation, reduced Ligase IV activity to a level observed in the more severely affected patients displaying immunodeficiency (Girard *et al*, 2004). Analysis of V(D)J recombination in cells from Ligase IV patients showed that while the frequency of rejoining was only marginally reduced, the fidelity of rejoining was dramatically impaired (O'Driscoll *et al*, 2001). This partially functional V(D)J recombination pathway may therefore be sufficiently 'leaky' to allow a limited amount of immune development to occur in these patients. The effect of the 180BR mutation is apparently mild enough to allow relatively normal lymphocyte development, but the deficit in joining fidelity could have predisposed this patient to the development of leukaemia.

In contrast to the leaky immune phenotype observed in Ligase IV syndrome, cells from these patients, including 180BR, show dramatic radiosensitivity and a DSB repair defect that is not substantially different from that observed in fully inactivated rodent cell lines. This may be explained if the residual activity of the mutant Ligase IV proteins is sufficient to handle the small number of breaks that arise during V(D)J recombination but is insufficient to repair the much larger number of breaks arising from exposure to IR. This defect in DSB repair does not impinge on checkpoint signaling pathways, since Ligase IV defective lines were shown to have normal G1/S, S- and G2/M checkpoint function (O'Driscoll *et al*, 2001). Thus the radiosensitivity of Ligase IV defective cells is attributed to impaired NHEJ.

1.6.4 Defects in Artemis

Amongst T-B- SCID patients identified are some who have very significant defects in coding joint formation but little or no impairment in the ability to join signal ends (Moshous *et al*, 2000). Immunophenotyping of bone marrow samples from 2 patients showed the absence of complete V_H-J_H gene rearrangements and consequently a complete B-cell differentiation arrest at the pre-B-cell receptor checkpoint (Noordzij *et al*, 2003). Cells from these patients also display radiosensitivity (Nicolas *et al*, 1998), and this condition is therefore referred to as Radiosensitive (RS)-SCID. A similar T-B- SCID condition (referred to as SCIDA) occurs with a very high incidence in inbred populations of Athabascan-speaking Native Americans, including Navajos and

Apaches, and the V(D)J recombination defect in SCIDA and RS-SCID was found to be identical (Moshous *et al*, 2000). This phenotype is comparable to that described for cell lines defective in DNA-PKcs, raising this as a potential candidate gene. Linkage analysis from affected families, however, mapped the gene to a location distinct from DNA-PKcs on chromosome 10 (Li *et al*, 1998) (Moshous *et al*, 2000). Based on this localisation, the Artemis gene, the defect of which is responsible for RS-SCID, was identified and cloned through *in silico* gene search (Moshous *et al*, 2001). Functional complementation studies and mutation analysis then confirmed that Artemis was indeed responsible for RS-SCID and SCIDA (Moshous *et al*, 2001) (Li *et al*, 2002a)

Most of the Artemis mutations identified in RS-SCID patients seem to represent null alleles, which result from genomic deletions covering several of the 5′ exons or involve the production of severely truncated proteins (Moshous *et al*, 2001). These truncations are caused by genomic deletions or insertions, nonsense mutations in the coding region, or mutations in splice sites. The founder mutation identified in Athabascan-speaking Native Americans is a nonsense mutation predicted to result in prematurely truncated protein (Li *et al*, 2002a). Another founder mutation identified in Japanese families results in deletion of exon 3 (Kobayashi *et al*, 2003). All of these mutations affect the NH2 half of Artemis encompassing the metallo-β-lactamase homology domain, which is thought to define the core catalytic region of the protein (Poinsignon *et al*, 2004). In addition four missense mutations that affect this region have been described; S32C (Le Deist *et al*, 2004), G118V, G135E (Noordzij *et al*, 2003), and D165N (Ma *et al*, 2002). Overall these results indicate that Artemis is not essential for viability, unlike Ligase IV and XRCC4. Indeed, Artemis KO mice are viable and present the same phenotype of RS-SCID (Rooney *et al*, 2002).

Significantly, four patients with hypomorphic mutations in Artemis have been identified (Moshous *et al*, 2003). All of them presented with partial T and B lymphocyte immunodeficiency, low serum IgG, absent IgA and developed recurrent pulmonary and respiratory infections soon after birth. These patients exhibited truncations of Artemis within the last exon, thereby leaving the metallo-β-lactamase domain intact, and this appeared to confer residual V(D)J recombination activity (Moshous *et al*, 2003). Hence, some B and T lymphocytes could be generated. Interestingly, these patients have an elevated frequency of EBV positive B cell lymphomas, which is highly reminiscent of the emergence of pro-B-cell lymphomas described in NHEJ deficient

mice when crossed onto a $p53^{-/-}$ background (Difilippantonio *et al*, 2000) (Ferguson *et al*, 2000) (Zhu *et al*, 2002). Artemis deficiency may therefore confer elevated cancer predisposition, raising the possibility that Artemis is a genome caretaker. In this context it is noteworthy that fibroblasts derived from Artemis deficient mice also display elevated chromosome instability (Rooney *et al*, 2002).

Although Artemis has been found to open the DNA hairpin structures that arise as intermediates during V(D)J recombination (Ma *et al*, 2002), (which explains the immunodeficiency observed in RS-SCID patients), the role of Artemis in the repair of radiation induced DSBs is less well defined. DNA hairpins are not generated by exposure to γ-radiation or treatment with radiomimetic drugs, such as bleomycin. The increased radiosensitivity of Artemis-deficient cells may be explained if Artemis was required for the processing of other types of DNA end structures present at radiation induced DNA breaks. This function could include the specific 5′ and 3′ single stranded overhang nuclease activity of Artemis in the presence of DNA-PKcs (Ma *et al*, 2002), which could produce blunt ends, removing any associated base damage in the process, ready for ligation by the XRCC4-Ligase IV complex. The model whereby Artemis is required for the repair of a subset of radiation-induced DSBs has been reinforced by the observation that although Artemis deficient cells demonstrate a normal initial rate of DSB repair, an elevated level of residual breaks is demonstrated (Riballo *et al*, 2004). The repair of simple breaks may therefore proceed unimpaired through ligation by the XRCC4-Ligase IV complex conferring a normal initial rate of repair, but complex breaks that require processing persist and hinder survival. This model is consistent with the unaffected formation of signal ends during V(D)J recombination (Nicolas *et al*, 1998), and one may argue that Artemis is dispensable for the DNA repair of 5′ phosphorylated blunt DNA termini.

1.6.5 Uncharacterised immunodeficiency – damage assessment defects

There are a significant number of undefined immunodeficient patients where defects in genes likely to be involved in damage response mechanisms are associated with some form of immunodeficiency, albeit frequently ill defined. Such examples include a patient defective in DNA ligase I (Barnes *et al*, 1992), a patient that appears to have a defect in an as yet unidentified component of the NHEJ repair machinery (Dai *et al*, 2003), and some uncharacterised examples that may not involve a deficiency in DNA

repair. Severe immunodeficiency associated with lymphopaenia that was progressive with age was described in two siblings, one of which (designated F96) was examined in more detail (Peake *et al*, 1999). Although, unlike other combined immunodeficiencies, the T cells that were present seemed to be functionally normal, they displayed increased levels of spontaneous apoptosis *in vitro*. This prompted the investigators to examine factors know to promote apoptosis in lymphocytes, such as decreased expression of the anti-apoptotic protein Bcl2 and abnormal death receptor signaling, but these pathways appeared to be functionally normal.

It then became apparent that the underlying defect did not only affect lymphocyte survival, but had more widespread implications. Examination of the patient's fibroblasts demonstrated that although these cells did not show an increased susceptibility to apoptosis, they did display elevated sensitivity to γ-radiation. This suggested that there may be defects in the response to DNA DSBs, but no deficiencies in DSB repair or the induction of cell cycle checkpoints (at least one feature of which is displayed by the characterised radiosensitive immunodeficient disorders described above) could be identified in this patient's fibroblasts. This prompted the investigators to postulate this fibroblast line represented a new radiation-sensitive phenotype, in which radiation sensitivity is not associated with a cell cycle checkpoint defect nor a V(D)J recombination defect, and is not a chromosome breakage disorder.

The mutation in this patient seems to lie in a gene that influences both radiosensitivity and a mechanism that commits to apoptosis. A defect in the DNA damage assessment process involving p53 may not necessarily affect a cell's ability to repair damage or initiate cell cycle checkpoints, but may still result in an inappropriate cell survival outcome. Lymphocytes, which are highly sensitive to DNA damage induced apoptosis, may be particularly influenced by this defect. This could confer an immunodeficient phenotype through the impaired survival of developing lymphocytes. Since fibroblasts are notoriously resistant to apoptosis (Dikomey *et al*, 1998) (Chung *et al*, 1998) (Kawabe *et al*, 2001) (Zhang *et al*, 2001a), the radiosensitivity observed in these cells may be conferred through a distinct mechanism. Thus, in both cell lineages there could be a commitment to an inappropriate cell survival outcome, and depending on cell type this may be apoptosis or another less well-defined mechanism such as permanent cell cycle arrest. Some undefined immunodeficient patients may therefore have similar

defects in the survival assessment process after DNA damage, and further investigation is required characterise these potential disorders.

1.7 Statement of the problem and project strategy

The examination of cells from patients with radiosensitive immunodeficiency has proved to be a valuable method of research in learning more about the DNA damage response and the factors that affect cell survival after irradiation. This work has improved our understanding of the processes that function to promote genomic stability and restrain the accumulation of mutations, cellular characteristics that are pivotal in the suppression of malignant transformation. A subset of undefined immunodeficient patients may have novel defects in the DNA damage response network similar to those described above and we sought to investigate this possibility. Patients were selected that displayed varying degrees of pancytopenia of unknown origin, which should include patients with potential DNA repair and/or survival assessment defects. Cellular radiosensitivity is generally determined with fibroblasts irradiated *in vitro* using a colony forming assay (Arlett *et al*, 1988) (Peake *et al*, 1999) (O'Driscoll *et al*, 2001) (Dai *et al*, 2003) (Kobayashi *et al*, 2003) (Noordzij *et al*, 2003). Fibroblast lines generated from patient skin biopsies were examined in this way in order to identify patients with potential radiosensitive disorders.

The generation of primary fibroblast lines and subsequent colony forming assays is a procedure that can take several months to complete from the initial receipt of the skin biopsy. In an attempt to identify radiosensitive patients more rapidly, we also aimed to develop novel assays for cellular radiosensitivity that might speed up this process. Lymphocytes are easily isolated from whole blood, a tissue more readily obtained from patients than skin biopsies, and these cells display radiation-induced apoptosis after a matter of days (Camplejohn *et al*, 1995) (Hertveldt *et al*, 1997). We therefore investigated whether this endpoint could be used as a measure of intrinsic radiosensitivity, and where possible compared this to fibroblast radiosensitivity results. Another limitation of fibroblast colony forming assays is that they give no insight into the mechanisms that may be responsible for a radiosensitive phenotype. We were interested in developing novel methodology that could examine the fate of cells that survive the initial genotoxic insult, but do not return to cycle to form colonies. We therefore investigated fibroblast division within the first week of irradiation in normal

and radiosensitive lines. Using this technique we further characterised the radiosensitive phenotype to delineate how damaged cells may be removed from the proliferative population, and if particular defects in the DNA damage response are associated with certain cell fates.

Undefined radiosensitive lines may have defects in the repair of DNA damage and/or the survival assessment process. We further investigated these crucial aspects of the damage response to determine if such deficiencies were apparent in the selected radiosensitive lines. Examination of chromosome damage and DNA repair after irradiation, in parallel with the analysis of p53 dependent processes, concentrated our search for the underlying defects, which could then be related to the cell fate observed after irradiation. The approach taken in this study was to investigate undefined immunodeficient patients for potential radiosensitive disorders, and develop new methodologies to achieve this whilst learning more about the processes concerned. Through the characterisation of radiosensitive lines we hoped to gain insight into the mechanisms involved in cellular radiosensitivity, identify the mutant genes responsible and study the wider implications of certain defects on the cellular response to DNA damage.

Chapter 2: Materials and methods

2.1 Patient selection criteria

Patients with low T and B lymphocyte function of unknown origin and variable Natural Killer (NK) cell counts were selected by medical staff at Great Ormond Street Hospital. The decision to further investigate patients for radiosensitivity was based on expert clinical and scientific judgment provided by the medical staff at Great Ormond Street Hospital and the academic staff at the Institute of Child Health. This involved the assessment of clinical parameters to decide whether the observed immunodeficiency was likely to result from a radiosensitive disorder based on previous experience described in the literature. This was intended to identify patients with either DNA repair or survival defects.

2.2 Generation of fibroblast cell lines and culture

Primary fibroblast lines were generated from skin biopsies from the patients. These were sent to the unit in the fibroblast culture medium described below. On arrival, each biopsy was placed in a 6 cm tissue culture dish with 1ml of fibroblast culture medium. As much of the fat and dermal layer was removed as possible using a scalpel, and if large enough the biopsy was cut in half to allow one piece to be cryo-preserved. The remaining tissue was cut into small fragments (1mm/2mm square) with a scalpel using a downward cutting action to prevent shearing of the tissue. 5 ml of fibroblast culture medium was added to 2 x 25 cm^2 tissue culture flasks making sure the surface area was completely wet, and the small pieces of skin were transferred to the top half of the flask in a slanted position so that the explants were free of the medium. Flasks were left in this slanted position for approximately 48 hours in a humidified 5 % CO_2 atmosphere at 37 °C to allow the skin fragments to adhere. The flasks were then gently lowered to allow the medium to cover the explants, and left until there was a 1 cm diameter of cells around some pieces. Cells were then trypsinised, expanded and cryo-preserved.

In addition to the undefined primary fibroblast lines examined, this project utilised a series control and known mutant primary fibroblast lines for comparison (table 2-1).

Table 2-1: Control and known mutant fibroblast lines used for comparison

Primary line	1BR	48BR	249BR	A-T1BR	CJ179	180BR
Defect	Control	Control	Control	ATM	Artemis	Ligase IV

Fibroblast lines were cultured in Minimal Essential Medium (Gibco Invitrogen) supplemented with 15% Fetal Bovine Serum (FBS) (Sigma), 0.2% sodium bicarbonate (Gibco Invitrogen), 2mM L-glutamine (Gibco Invitrogen), 100 U ml^{-1} penicillin G sodium and 100 $\mu g\ ml^{-1}$ streptomycin sulphate using standard methods (Arlett *et al*, 1983). Fibroblasts were routinely cultured in 75 cm^2 tissue culture flasks and incubated in a humidified atmosphere at 37°C, 5 % CO_2. Cells were split using 1 x trypsin-EDTA (Gibco Invitrogen) and washed in 1 x PBS (Gibco Invitrogen).

2.3 Fibroblast radiosensitivity survival assays

Fibroblasts below passage 15 in the exponentially growing phase were trypsinised, washed in PBS and counted using a haemocytometer followed by serial dilution. Cells were then subsequently irradiated with a ^{137}Cs γ-ray source at a dose rate of 0.09 Gy sec^{-1} and plated into 6 cm tissue culture dishes as described in table 2-2 in quadruplicate. In control and patient lines that displayed mild radiosensitivity doses up to 6 Gy were initially employed to extend the dose response curve, further reduce survival and possibly aid in classification. During this time we found doses up to 4 Gy were sufficient to classify radiosensitivity and this dose range was therefore used routinely to screen undefined patients for cellular radiosensitivity. Due to the poor plating efficiency of GOS5 cells, the number of cells plated for each dose was doubled when using this line in order to obtain a reasonable amount of colonies on the mock-irradiated plates.

Table 2-2: Plating numbers for the radiosensitivity survival assay

Dose (Gy)	Number of cells plated per 6cm dish
0	200
1	400
2	800
4	1600
6	1600

The cells were then incubated at 37 °C, 5 % CO_2 until colonies were visible to the naked eye (14-21 days). 2.5 ml 1 % Methylene Blue (Sigma) staining solution was then added carefully to the culture medium of each plate. After 30 minutes the staining solution was poured off and the plates were placed upside down and dried overnight. The following day the plates were carefully washed in H_2O before visible colonies were counted. The colonies counted were well defined and contained more than 50 cells. Smaller, ill defined colonies were also observed that are likely to represent cells that ceased to divide after a certain number of divisions. This endpoint was regarded as a form of clonogenic death, therefore these colonies were not included in the count of surviving colonies. The plates with the mock-irradiated cells were used as a standard to derive plating efficiency. The cell survival was then calculated and plotted on log graphs.

2.4 Case reports of 10 undefined immunodeficient patients with cellular radiosensitivity

The case reports of 10 undefined immunodeficient patients that demonstrated cellular radiosensitivity using the fibroblast survival assay are shown below.

Table 2-3: Phenotype of 10 radiosensitive patients' lymphocytes (Data from clinical reports)

Patient	Lymphocytes x10^9 cells/litre	Phenotype of lymphocytes %				
		CD3+	CD19+	CD16/56+	CD4+	CD8+
F96	1.1	54	32	58	14	38
GOS1	3.74	86	5	4	50	37
GOS3	5.32	99	0.5	0.5	75	26
GOS4	0.62	40	29	19	27	9
GOS5	1.07	70	8	10	45	21
GOS10	0.25	0.5	0.7	85	0.5	0
GOS14	0.77	54	25	20	41	12
GOS17*	0.5	72	11	20	13	59
GOS21*	1.4	78	15	6	39	39
GOS23	0.62	39	18	37	19	10
Normal Range (Child)	2-6	50-80	10-20	1-30	35-65	15-35
Normal Range (Adult)	1-3	50-80	5-20	5-30	35-65	15-35

* These patients were adults

Case reports

F96

This patient was previously described (Peake *et al*, 1999). Briefly, a 4 year old boy was found to have Combined Immunodeficiency (CID) with recurrent infections. He was lymphopaenic (1.1 $x10^9$ cells/litre) and hypogammaglobulinaemic [IgG, 4.1 g/l (NR for age, 5.3-10.1); IgA, <0.2 g/l (NR, 0.34-0.78); IgM, 0.85 g/l (NR, 0.54-1.06)] with no specific antibody responses. Lymphocyte cultures exposed to 1 Gy γ-radiation showed 30 lesions/50cells (0.6 per cell) compared with 16 lesions/40cells in control cells (0.4 per cell).

GOS1

This patient was a 1-year-old female that presented with CID, repeated severe Varicella Zoster Virus (VZV) infection and later developed Hodgkin's lymphoma. There was no specific response to purified protein derivative of tuberculin and Haemophilus influenzae type b (Hib) vaccine. She was hypogammaglobulinaemic [IgG 2.87 g/l (NR, 3.1-13.8); IgA 0.27 g/l (NR, 0.3-1.2); IgM 0.43 g/l (NR, 0.5-2.2)] and T-cell mitogenic responses to phytohemagglutin (PHA) were poor. Lymphocyte numbers were normal (3.74 $x10^9$ cells/litre).

GOS3

This male infant was 2 months old at the time of this study. He had normal levels of T-lymphocytes with CD4 and CD8 cells in appropriate proportions. B-lymphocytes and NK cells were absent. He was Hypogammaglobulinaemic [IgA 0.39 g/l (NR, 0.7-2.5); IgM 0.43 (NR, 0.5-1.8)] and T-cell mitogenic responses to PHA were normal.

GOS4

This patient was a 5-month-old female who presented with severe lymphopaenia (0.62 $x10^9$ cells/litre). T-cell responses to PHA were absent and immunoglobulin levels were normal or just below the normal range [IgG 1.46 g/l (NR, 3.1-13.8); IgA 0.24 g/l (NR, 0.7-2.5); IgM 0.57 g/l (NR, 0.5-1.8)].

GOS5

This patient was a 10-year-old boy that was diagnosed with CID. He was lymphopaenic (0.95 $x10^9$ cells/litre) and had a poor vaccine response. Immunoglobulin levels were

not lower than normal but suggested IgA dysregulation [IgG 9.16 g/l (NR, 3.1-13.8); IgA 5.88 g/l (NR, 0.7-2.5); IgM 0.53 g/l (NR, 0.5-1.8)]. T cell mitogenic responses to PHA were poor. The patient subsequently had a bad response to chemotherapy used for pre-Bone Marrow Transplant (BMT) conditioning.

GOS10

This patient was a 4-month-old boy from a consanguineous family who presented with a severe T-B-NK+ immunodeficiency. He was hypogammaglobulinaemic [IgA 0.06 g/l (NR, 0.7-2.5); IgM 0.05 (NR, 0.5-1.8)] and there were insufficient numbers of T-cells to perform a PHA activation assay. This patient was subsequently found to have a homozygous Y589X mutation in the RAG1 protein.

GOS14

This patient was a 9-year-old girl that presented with CID and cryptosporidium. She was severely lymphopaenic (0.45 $x10^9$ cells/litre), with a particular deficiency in Cytotoxic T Lymphocytes (CTLs) (table 4-2). There was no specific response to vaccine. She was hypogammaglobulinaemic with a particular deficit in IgM [IgA 0.54 g/l (NR, 0.7-2.5); IgM 0.06 (NR, 0.5-1.8)]. T cell mitogenic responses to PHA were variable.

GOS17

This patient was a dysmorphic 43-year-old male with lymphopaenia [0.5 $x10^9$ cells/litre (NR 1-3)]. He had normal levels of immunoglobulin and suffered from extensive warts.

GOS21

This patient was a dysmorphic 20 year old male with extensive warts. Although absolute numbers of lymphocytes were normal, there was a low ratio of CD4/CD8 cells. Immunoglobulin levels were normal.

GOS23

This patient was a 7-year-old girl diagnosed with CID. She was severely lymphopaenic (0.62 $x10^9$ cells/litre) with low T-cell numbers and exhibited developmental delay. She was severely hypogammaglobulinaemic [IgA 0.06 g/l (NR, 0.5-2.7); IgM 0.08 g/l (NR, 0.5-1.8)] and T-cell mitogenic responses to PHA were poor. Metaphase analysis of chromosomes demonstrated an elevated level of random chromosome breakage.

Similarities amongst radiosensitive patients

Most of the patients that were found to be radiosensitive had combined immunodeficiency with poor responses to vaccine. Lymphopaenia was present in all patients that demonstrated intermediate levels of sensitivity (F96, GOS5 and GOS23), and four mildly sensitive patients (GOS4, GOS10, GOS14 and GOS17). Since patient GOS10 was subsequently found to have a homozygous Y589X mutation in the RAG1 protein, and this is not expected to confer a radiosensitive phenotype, the patients that demonstrated borderline-mild radiosensitivity may in fact represent the lower end of the normal range. A severe lack of immunoglobulin levels or function coupled with lymphopaenia (but normal NK cell levels) may therefore be a good biological marker of patients with radiosensitive immune disorders, but may also select patients with RAG disorders.

2.5 Lymphocyte Apoptosis

Primary blood lymphocytes (PBLs) were isolated from heparinised blood by density gradient centrifugation using Lymphoprep (Nycomed Pharma, Oslo, Norway). Where possible a control blood sample from a healthy volunteer under 30 years of age was transported with the patient's blood. An equal volume of Phosphate buffered saline (PBS) was first added to fresh heparinised blood and mixed well. 2 ml of lymphoprep (Nycomed) per 10 ml of blood/PBS mixture was then slowly layered underneath the blood/PBS mixture by placing the tip of the pipette containing the lymphoprep at the bottom of the sample tube. The sample was then centrifuged at 2000 rpm with no brake. The white cell layer containing the PBLs was then removed by pipetting, and the cells were added to 8 – 10 ml of RPMI medium (Gibco Invitrogen) supplemented with 5 % FBS (Sigma). The cells were then washed and resuspended in 1 ml of RPMI, 5 % FBS. Cells were counted, diluted to 1 x 10^6 cells/ml and cumulatively treated with a ^{137}Cs γ-ray at a dose rate of 0.09 Gy sec^{-1} until each of the required doses was reached, then a 1 ml aliquot of cells was removed and transferred to a 24 well tissue culture plate. Cells were then incubated at 37 °C, 5 % CO_2 for 24 hours, after which 100 µl of each dose was transferred to FACS tubes in triplicate and cells were washed with 1 ml of ice cold PBS. Lymphocytes were stained for apoptosis using the Annexin V-Fluorescein isothiocyanate (FITC) apoptosis detection kit (Pharmingen) by first resuspending in 100

µl of binding buffer. 5 µl of Annexin V-FITC antibody solution and 5 µl of 1 mg ml^{-1} 7-aminoactinomycin-D (7AAD) (Sigma) was then added to each sample, gently mixed and incubated for 15 minutes at room temperature in the dark. A further 400 µl of 1 x binding buffer was then added to each tube, and cells were analysed for apoptosis (AnnexinV positive) by flow cytometry immediately on a Coulter EPICS XL Analyser using 10,000 events/sample, unless otherwise stated.

2.6 CFSE cell division analysis

2.6.1 Early and late division experiments

Carboxy-fluorescein diacetate succinimidyl ester (CFSE) (Molecular Probes, Leiden, Netherlands) was dissolved in dimethylsulphoxide (DMSO) at a concentration of 5 mM as a stock solution and kept at -20°C until further use. Fibroblasts to be assayed were seeded at a density of 5 x 10^4 in 10 cm tissue culture plates and incubated overnight to allow them to adhere. Duplicate plates were prepared for each dose and time point. Cells were washed once with 5 ml Opti-MEM (Gibco Invitrogen), CFSE stock was diluted 1/1000 in Opti-MEM (5 µM final concentration) and 5 ml of this was added to label each cell culture. Cells were incubated with CFSE for 10 min at 37°C, 5 % CO_2, washed twice with 5 ml Opti-MEM, followed by the addition of fibroblast culture medium. Cells were then irradiated with a ^{137}Cs γ-ray source at a dose rate of 0.09 Gy sec^{-1} and incubated at 37°C, 5 % CO_2 for the appropriate time. FACS analysis was then performed counting 15,000 events per sample.

For each experiment 1 plate was used as a 0 day labelling control. These cells were trypsinised immediately after labelling, fixed in 1 % paraformaldehyde (PFA) and stored at 4 °C until the day FACS analysis was performed. These cells were then used to set the zero division level in order to account for any differences in labelling that may have occurred between each cell line and experiment. In early division experiments 5 x 10^4 cells per sample were labelled as described above and then treated with 0, 1, 2, or 4Gy γ-radiation on day 0. FACS analysis was then performed on these cultures after a 6 day incubation at 37°C, 5 % CO_2. For late division experiments, 5 x 10^4 cells per sample were treated with 0, 1, 2, 4 or 6 Gy γ-radiation on day zero and incubated for 5 days at 37 °C, 5 % CO_2. Labelling was then performed as described above and cultures

were incubated for a further five days at 37 °C, 5 % CO_2. During this period if the unirradiated or low dose cultures approached confluence, they were split either 1:4 or 1:8 to keep them at a sub-confluent density that is optimal for cell division. FACS analysis was then performed on day 10 after irradiation.

2.6.2 CFSE cell sorting

5 x 10^4 1BR or F96 cells were seeded into ten 10 cm tissue culture plates and left overnight to adhere. The following day 8 plates from each line were exposed to 4Gy γ-radiation and the remaining 2 were mock irradiated. After a 5 day incubation, the cells were labelled with CFSE and one plate was harvested and fixed in 1 % PFA to serve as a 0 day labelling control. The remaining 9 plates were incubated for a further 5 days (10 days after irradiation) similar to the late division experiments previously described. These cells were than harvested for cell sorting. The 0 day labelling control was used to set the highest level of CFSE fluorescence, and the mock irradiated sample represented cells that had divided normally in this time frame. Cells from the 8 irradiated plates were pooled together and sorted into high, medium and low CFSE fluorescence populations according to the gates shown in figure 4-12 using a Coulter EPICS ALTRA cell sorter. Approximately 5 x 10^4 – 1.5 x 10^5 cells were sorted for each population. Cells were then plated out in fresh growth medium and left overnight to adhere. Cell morphology and senescence associated β-galactosidase (SA-βgal) activity was examined. Photographs were taken using a Nikon-F70 camera in conjunction with a Nikon TMS-F microscope at 100x magnification.

2.6.3 Senescence Associated β-Galactosidase (SA-βgal) staining of CFSE labeled cells

Cells were washed once with PBS and fixed in tissue cultures plates with 3 % formaldehyde. Fixed cells were then washed 3 times with PBS and incubated at 37 °C overnight with SA-βgal staining solution (40 mM Citric Acid, 12 mM Sodium Phosphate, 5 mM $K_3Fe(CN)_6$, 5 mM $K_4Fe(CN)_6$, 150 mM NaCl, 2 mM $MgCl_2$, 1mg ml^{-1} 5-bromo-4-chloro-3-indolyl-beta-D-galactopyranoside (X-gal)).

2.6.4 Apoptosis detection with CFSE labeled cells

Late CFSE division experiments were performed as described above. Before FACS analysis cells were stained with AnnexinV-Phycoerythrin (PE) and 7AAD using the

AnnexinV-PE Apoptosis Detection Kit (Pharmingen) according to the manufacturer's instructions. Briefly, cells were washed twice with cold PBS and resuspended in 100 µl of binding buffer. 5 µl of Annexin V-PE and 5 µl of 1 mg ml^{-1} 7AAD was then added to each sample, followed by a 15-minute incubation at room temperature in the dark. 400 µl of binding buffer was then added and the amount of apoptosis at different CFSE fluorescence levels was examined by FACS. Unstained cells and cells stained with Annexin-PE and 7AAD alone served as controls.

2.7 BrdU cell cycle analysis

Cells were seeded into 6 cm tissue culture plates at least 24 hrs prior to irradiation at densities to prevent contact inhibition. Cultures were then either mock irradiated or exposed to a ^{137}Cs γ-ray source at a dose rate of 0.09 Gy sec^{-1} to give a total dose of 4 Gy. 12 hrs after irradiation cultures were pulse-labeled with 10 µM bromodeoxyuridine (BrdU) (Pharmingen) for 30 min, harvested by trypsinisation, and resuspended in 0.6 ml PBS. The cells were then added drop wise to 10 ml of ice-cold 70 % ethanol and incubated on ice for at least 1 hr. The fixed cells were then centrifuged at 2150 rpm for 7 min, resuspended in 1 ml chilled 0.1M HCl, 0.5 % Triton-X 100 (TX100) and incubated on ice for 10 min in order to extract histone proteins. Following the addition of 5 ml H_2O, cells were centrifuged at 1200 rpm for 10 min, and resuspended in 1.5 ml H_2O. At this stage samples were transferred to 1.5 ml eppendorf tubes, and incubated for 10 min at 100 °C to denature cellular DNA. Cells were then incubated on ice for 3 min, centrifuged at 13,000 rpm for 3 mins and washed once in 1 ml PBS, 0.5 % TX100. Cells were resuspended in 100 µl of 5µg ml^{-1} Anti-BrdU-fluorescein solution (Roche) diluted in PBS, 0.1 % Bovine serum albumin (BSA), 0.1 % TX100 and incubated for 30 min at room temperature in the dark. Cells were then washed once with PBS, and resuspended in 500 µl PBS. 27 µl RNase A (10 mg ml^{-1}) and 20 µl propidium iodide (PI) solution (50 µg ml^{-1}) was then added to each sample followed by a 30 min incubation at room temperature in the dark. Subsequently FACS analysis was performed. Cellular debris and fixation artifacts were gated out and the fraction of cells in S-phase (BrdU positive) was quantified.

2.8 Preparation of RNA and northern analysis

Total RNA was prepared from irradiated or unirradiated cells for use on northern blots and the preparation of cDNA. Cells were lysed *in situ* using Trizol reagent (Invitrogen) following the protocol supplied by the manufacturer. For northern blots mRNA was then isolated from total RNA with Oligotex beads (Qiagen) according to the manufacturer's instructions and quantified using the Agilent Bioanalyser system. RNase free H_2O (Qiagen) was used for all RNA work. Northern blots were performed using a modified version of the GeneScreen protocol (NEN Life Science Products). Briefly, 2-5 µg of mRNA was resuspended in 1 x MOPS (40 mM Morpholinopropanesulfonic acid, 10 mM Sodium acetate-$3H_2O$, 1 mM ethylenediaminetetraacetic acid (EDTA)-Na_2-$2H_2O$, pH 7.2), 3.5 µl Formaldehyde (Sigma) and 10 µl Formamide (Amresco). The volume was adjusted to 20 µl using RNase free H_2O. The secondary structure of the mRNA was denatured by heating to 65 °C for 15 minutes, followed by chilling on ice whilst loading dye was added to each sample. The mRNA samples were then separated on a 1.2 % agarose gel containing 10 % Formaldehyde using 90 V for 2 hours. The gel was then soaked in ddH_2O for 3 x 10 minutes and transferred overnight to GeneScreen membrane in 10 x SSC. The membrane was then washed briefly in 2 x SSC to remove residual agarose, UV auto-crosslinked and baked at 80 °C for 2 hours.

2.9 Probing northern blots

The membrane was incubated for 1 hour in a rotating hybridisation bottle filled with 5 ml pre-hybridisation solution (For 200 ml pre-hybridisation mix 20 g Dextran Sulphate (Sigma), 40 ml 20 x SSC, 20 ml 50 x Denhardts Solution (Sigma) 130 ml ddH_2O and 10 ml 10 % SSC were mixed) containing 100 µg ml^{-1} denatured sheared salmon sperm DNA (Sigma).

A p21 probe was generated by reverse transcription-polymerase chain reaction (RT-PCR) using cDNA prepared from irradiated 1BR fibroblasts as a template. Primers p21-U and p21-L were designed to generate a 598 bp fragment from the 3′ non-coding region of p21 mRNA using an annealing temperature of 65 °C.
Sequence of p21 PCR primers: -

p21-U: **5'-GCTACTTCCTCCTCCCCACTTG-3'**

p21-L: **5'-TCCCTTCCCCTTCCAGTCCATTG-3'**

The p21 PCR product was run on an ethidium bromide stained 1 % agarose gel, gel purified and run on another ethidium bromide stained 1 % agarose gel to assess the concentration of the probe template.

Labelling of probe templates was carried out by mixing 25-50 ng probe template DNA with ddH_2O to a final volume of 10 µl. The sample was denatured by heating to 95 °C for 6 minutes and then immediately placed on ice. On ice 5 µl 20 ng μl^{-1} random primers (6-mers to 9-mers in ddH_2O), 5 µl 5 x 9LB reaction buffer (10 ml 9LB buffer is prepared by mixing 4.55 ml ddH_2O, 50 µl β-mercaptoethanol (Sigma), 100 µl each of 100 mM dATP, 100 mM dGTP and 100 mM d TTP and 5 ml 0.5 M Na phosphate buffer, pH 7.4. 200 ml 0.5 M Na phosphate buffer, pH 7.4 was prepared by mixing 22.6 ml 1 M NaH_2PO_4, 77.4 ml 1M Na_2HPO_4 and 100 µl H_2O), 1 µl of 0.5 M $MgCl_2$/10 µg μl^{-1} BSA solution, 3 µl α^{32}P-dCTP (>3000 Ci mM^{-1} ICN), and 1 µl 5 U μl^{-1} Klenow fragment (Promega). The reaction was subsequently incubated at 37 °C for 30 minutes. Following primer extension 80 µl TE – 0.1 % sodium dodecyl sulphate (SDS) was added and the sample transferred to a spin column containing sephadex G-50 (Pharmacia) and centrifuged into a fresh eppendorf tube containing 33 µl 1M NaOH. To the denatured, labelled probe template was then added 135 µl 2M Tris (Tris(hydroxymethyl) aminomethane), pH8. The probe was then transferred to the hybridisation bottle and incubated in a rotating hybridisation oven at 65°C overnight.

The following morning, the pre-hybridisation mix with the probe template was discarded and the membrane washed in 2 x SSC, 0.1 % SDS for 5 minutes at room temperature. The membrane was then washed twice in 2 x SSC, 0.1 % SDS at 55 °C for 10- 15 minutes. The membrane was then wrapped in saran wrap and monitored with the probe of a Gieger counter. If the monitor detected large amounts of background emitted from the membrane, as identified by strong signals in places where the probe was not expected to hybridise, e.g. the edges of the membrane, additional washes were performed using 2 x SSC, 0.1 % SDS until the background emission had washed off. The membrane was then wrapped in saran wrap, placed in a cassette and exposed to photographic film (Kodak) at –70 °C. Following exposure the film was developed and the autorad examined for signal.

2.10 Chromosome break analysis

For chromosome break analysis cells were grown in 75 cm^2 tissue culture flasks with 15 ml of fibroblast growth medium. Cells in the exponentially growing phase were mock irradiated or irradiated with a ^{137}Cs γ-ray source at a dose rate of 0.09 Gy sec^{-1} to give a final dose of 3 Gy. After an incubation period of 8 hrs, 150 µl of Colcemid solution (10 µg ml^{-1}, Gibco BRL) was added to each tissue culture flask and incubated overnight. Cells arrested at metaphase were harvested by partial trypsinisation for 2 min at room temperature, taking care to collect any floating cells present in the growth medium or PBS during washing steps. Cells were then resuspended in 5 ml preheated (37 °C) 1 % sodium citrate and incubated at 37 °C for 15 minutes to allow adequate cell swelling. Samples were then centrifuged at 1200 rpm for 5 min and carefully resuspended in 10 ml of fix solution (3 : 1, methanol : acetic acid). To minimise clumping the first 1 ml of fix was added as the centrifuge tube was flicked, and the sample was subsequently vortexed. This process was repeated for addition of the first 3 ml of fix, and the last 7 ml was added together. Cells were then washed 3 times in 5 ml of fix solution and resuspended in 1 ml of fix solution. Using a Pasteur pipette, fixed cells were then dropped onto clean glass slides held at arms length. Slides were allowed to dry, stained with giemsa for 10 min, washed twice and propped up to dry. After the application of cover slips, metaphase spreads were visualised by light microscopy at 1000x magnification using a Zeiss Axioskop microscope (Photometrics, Tucson, Ariz) and the number of unrepaired chromosome and chromatid breaks were counted per metaphase. Chromosome breaks were defined as acentric chromosome fragments and chromatid breaks were defined as chromatid gaps (larger than a chromatid width) or fragments. We also noted the number of dicentric chromosomes observed. Metaphase spreads were prepared from at least 2 separate experiments for each primary line.

2.11 Candidate repair gene sequencing

Total RNA, extracted from control and patient fibroblasts, was used to synthesise cDNA using random hexamer primers and SUPERSCRIPT II reverse transcriptase according to the manufacturer's instructions (Invitrogen). PCR of cDNA with Pfx polymerase (Invitrogen) was performed with sense (U) and antisense (L) primers for the coding sequence of the gene in question. All primers were designed with DNASTAR

PrimerSelect and MacVector software using sequences retrieved on the NCBI database at:

www.ncbi.nlm.nih.gov/entrez/query.fcgi?db=Nucleotide

Details of primers and cycling conditions are listed below: -

XRCC4

These primers target XRCC4 transcript variant 3 (NM 022550), which includes the 3' portion of non-coding exon 1 that is missing in the other two known variants (1 and 2). The protein-coding region of transcript 3 is the same as that of variant 1.

Primers

Ux: 5'-GGAAGTAGAGTCACGGAGAGGT-3'

Lx: 5'-TGCCAGTGTCATCATCAAATCGTA-3'

Amplified fragment size, 1283bp

PCR reaction

These primers were used in a 50 µl PCR reaction consisting of 5 µl 10 x Pfx amplification buffer (Invitrogen), 5 µl 10 x Pfx enhancer solution (Invitrogen), 1.5 µl 10 mM dNTPs, 1 µl 50 mM $MgSO_4$, 1 µl UX (100 pmol μl^{-1}), 1 µl LX (100 pmol μl^{-1}), 34 µl ddH_2O, 0.5 µl Pfx (Invitrogen) and 1µl cDNA.

Cycling conditions

94 °C for 2 min

94 °C for 15 sec

Annealing temp 61 °C for 30 sec } 35 cycles

68 °C for 1 min 30 sec

68 °C for 10 min

Hold at 4 °C

Ligase IV

PCR of the coding region was performed using two separate reactions. The amplified fragments overlapped within the coding region, and extended into the 5′ untranslated region (UTR) (5′ fragment) or the 3′ UTR (3′ fragment).

5′ fragment

Primers

UB: **5′-ATGGCTGCCTCACAAACTTC-3′**

LB: **5′-GGGGCTTCTCTGCTACTGC-3′**

Amplified fragment size, 1473bp

PCR reaction and cycling conditions

As with XRCC4, except for *annealing temp* of 53 °C

3′ fragment

Primers

UA: **5′-ACGGGGTGGAATGATGTCTC-3′**

LA: **5′-CTTGGCTTTGGGCTATTGTCT-3′**

Amplified fragment size, 1496bp

PCR reaction and cycling conditions

As with XRCC4, except for *annealing temp* of 53 °C

Artemis

PCR of the coding region was performed using two separate reactions. The amplified fragments overlapped within the coding region, and extended into the 5′ UTR (5′ fragment) or the 3′ UTR (3′ fragment).

5′ fragment

Primers

UA: **5′-GATCGGCGGCGCTATGAGTT-3′**

LA1: **5′-GGTGAACTGTTCTAGCTCTC-3′**

Amplified fragment size, 1160bp

PCR reaction and cycling conditions

As with XRCC4, except for *annealing temp* of 54°C

3′ fragment

Primers

UA2: 5′-CCTCCTACAGTGAGATTAAA-3′

LA: 5′-TGTCATCTCTGTGCAGGTT-3′

Amplified fragment size, 1177bp

PCR reaction and cycling conditions

As with XRCC4, except for *annealing temp* of 51°C

Each fragment was amplified three times in separate PCR reactions, and the resulting products were sequenced in both directions. This was intended to generate adequate sequence data for analysis that could account for errors that may occur during the PCR reaction.

Double-stranded PCR products were gel purified and sequenced using ABI BigDye Terminator Cycle Sequencing Kit V1.1 (Applied Biosystems, Foster City, CA). Sequencing reactions contained 6 µl Big Dye terminator, 2.4-3.2 pmol sequencing primer and 30 – 90 ng of purified PCR product, with the reaction made up to 15 µl with PCR-grade water. Cycling conditions were as follows; 96 °C for 1 minute, followed by 25 cycles of 96 °C for 10 seconds, 50 ° C for 5 seconds, 60 °C for 4 minutes and then hold at 4 °C. DNA was then precipitated by adding 50 µl absolute ethanol and 3 µl 3 M Sodium Acetate pH4.6 and incubating at –20 °C for 30-45 minutes. Precipitated DNA was then washed twice with 70 % ethanol and stored as a dry pellet at –20 °C until analysis. The oligonucleotides employed in the initial PCR reactions were used in combination with the following sense (U) and anti-sense (L) primers in order to fully sequence the amplified products (depicted in section 6.2): -

XRCC4 sequencing primers

U1: 5′-TCTCATTCAGACTTGGTTCC-3′

U2: 5′-AAAGGAGACAGCGAATGC-3′

L1: 5′-TGCTCCTGACAACAATGC-3′

L2: 5′-GTCTCCTTTTTCTACTTGGTGC-3′

Ligase IV sequencing primers

5′ fragment

U2: 5′-GATGGAAAAGATGCCCTC-3′
U3: 5′-GAAAAAGTCTGTAGGCAACTGC-3′
U4: 5′-CAGACAAAAGAGGTGAAGGG-3′
L1: 5′-AGTTCCAGTGGGTGTTCTG-3′
L2: 5′-GGGTAAGAGAACCTTCAGTAGG-3′

3′ fragment

U6: 5′-AGTGGAACAGATAGCCAGCC-3′
U7: 5′-ATGAGGGGACAAGGTTAGC-3′
L4: 5′-TCTTCATCTTTGGGGCAG-3′
L5: 5′-TTCTTCAGGAGTCTGCTCG-3′

Artemis sequencing primers

5′ fragment

U2: 5′-AGGAGACTTCAGATTGGCG-3′
U3: 5′-TGGTTTGGAGAAAGGAGC-3′
L4: 5′-TGCTGATTATGTGGAGTGG-3′
L5: 5′-TCTTCCTTCTCTCCTGATGC-3′

3′ fragment

U4: 5′-TGAGACAAACCCCAGGATG-3′
U5: 5′-CCCGAGGAAAAAAGTTTGC-3′
L2: 5′-GGAGTAAGTATCCTTTGGGC-3′
L3: 5′-TCTCAGTTTTTCAGGCTGC-3′

Extension products were run on an Applied Biosystems Prism 377 automatic sequencer and the resulting data was analysed using EditView (ABI) and DNASTAR software.

2.12 Artemis cloning

2.12.1 Cloning of the 5′ half of F96 Artemis

The sequence data produced from the 5′ fragment of Artemis isolated from the radiosensitive F96 line suggested the presence of mutations, but this was difficult to confirm because of the poor quality of sequence data produced in this region. Since the 5′ region of Artemis has previously been reported to undergo many alternative splicing events in other radiosensitive cells (Li *et al*, 2001), we decided to clone and sequence the 5′ fragment of F96 Artemis. This was performed using the pZErO cloning system (Invitrogen), which allows the efficient cloning of blunt ended PCR products.

2 of the 5′ fragments of F96 Artemis generated in separate PCR amplifications in section 2.10 were used in ligation reactions with pZErO, which had been previously cut with EcoRV and gel purified. This was performed at a ratio of 10:1 (insert:vector), and each reaction contained 1 µl of pZErO (10ng μl^{-1}), 1 µl 10 x ligase buffer (NEB), 0.5 µl gel purified F96 5′ Artemis fragment (70 ng μl^{-1}) and 6.5 µl ddH_2O. A vector only negative control was also prepared that contained everything except the F96 Artemis insert. 1 µl of 400 U μl^{-1} T4 DNA ligase (NEB) was then added to each ligation mix and the reactions were incubated at 16 °C for 1 hour. The ligations were then transformed into chemically competent DH5α *E.coli* (Invitrogen). The transformations were carried out by mixing 2 µl of each ligation with 50 µl of competent DH5α *E.coli*, and incubating the mixtures on ice for 20 minutes. The transformation mix was then heated to 42 °C for 90 seconds and then chilled on ice for 2 minutes. In order to allow time for expression of the Zeocin resistance gene present in pZErO, 350 µl of L-Broth (10 g Bacto Tryptone (Becton Dickenson), 7 g Bacto Yeast extract (BD), 10 g NaCl, in 1 litre) was added to each transformation, which was then incubated in a shaking incubator (37 °C, 225 rpm) for 1 hour. The transformations were then plated on low salt LB agar plates (1 % tryptone, 0.5 % yeast extract, 0.5 % NaCl, 1.5 % agar, pH 7.5) containing Zeocin (50 µg ml^{-1}) and incubated overnight at 37 °C. Using sterile pipette tips 3 clones from each transformation were picked and cultured overnight in 5 ml low salt L-Broth supplemented with 50 µg ml^{-1} Zeocin and miniprepped using the Qiaprep Miniprep protocol (Qiagen). To test for the presence of Artemis inserts, miniprep DNA was digested with EcoR1 and Xho1 restriction endonucleases that cut either side of the

insert, with EcoR1 also cutting once within the wild type Artemis sequence. This should produce 3 bands of 2775, 861 and 332 bp when the digests are run on an ethidium bromide stained 0.8 % agarose gel, and potential Artemis clones were sequenced using T7 and SP6 primers with ABI Dyedeoxy Terminator Cycle Sequencing apparatus (Applied Biosystems, Foster City, CA).

2.12.2 Cloning of full length Artemis into the gateway system

By cloning the 5′ half of Artemis isolated from F96 cells we discovered the presence of alternatively spliced variants together with the full length transcript. Sequencing results also indicated the presence of potential mutations in the F96 Artemis gene that appeared to be mutually exclusive and therefore present on separate alleles. In order to fully characterise the variety of alternatively spliced transcripts expressed in human fibroblasts and confirm the presence of mutations in the F96 Artemis gene, full length Artemis from wild type and F96 cells was cloned into the gateway cloning system (Invitrogen). Full length Artemis coding sequence was first obtained by PCR using cDNA as a template with primers ArtF1 and ArtR1.

ArtF1: 5′-CACCATGAGTTCTTTCGAGGG-3′
ArtR1: 5′-CCAGGTATCTAAGAGTGAGC-3′

Primer ArtF1 consisted of the ATG translation initiation codon followed by the first 14 bases of the Artemis coding sequence. 5′ to the ATG start codon we inserted a **CACC** motif in order to allow efficient directional cloning into a TOPO gateway expression vector (Invitrogen). The primer ArtR1 was designed to modify the translation stop codon of Artemis to code for tryptophan, and this was achieved by incorporating a **CCA** codon at the 5′ end of this anti-sense primer that will modify the TAA stop codon to TGG in the amplified product. This would allow the Artemis coding sequence to be cloned in frame with a C-terminal protein tag, which could be useful in any later expression studies since there was not a reliable Artemis antibody available at the time of this study. These primers were used in a 50 µl PCR reaction consisting of 5 µl 10 x Pfx amplification buffer (Invitrogen), 5 µl 10 x Pfx enhancer solution (Invitrogen), 1.5 µl 10 mM dNTPs, 1 µl 50 mM $MgSO_4$, 1 µl ArtF1 (100 pmol μl^{-1}), 1 µl ArtR1 (100 pmol μl^{-1}), 34 µl ddH_2O, 0.5 µl Pfx and 1µl cDNA. The following cycling conditions were found to be optimal for this amplification reaction.

Cycling conditions

	94 °C for 2 min	
	94 °C for 15 sec	35 cycles
Annealing temp	50 °C for 30 sec	
	68 °C for 2 min 15 sec	
	68 °C for 10 min	
	Hold at 4 °C	

After amplification the PCR reaction was loaded onto an ethidium stained 1 % agarose gel and the 2083 bp Artemis product was visualised, then gel-purified using the Qiagen spin column protocol (Qiagen).

The full length coding sequence of Artemis amplified from either control (1BR) or F96 cDNA was cloned into the pcDNA3.2/V5/GW/D-TOPO vector (Invitrogen) according to the manufacturer's instructions. Briefly, 20 ng of Artemis insert was combined with 1 µl TOPO salt solution (Invitrogen), 1 µl of pcDNA3.2/V5/GW/D-TOPO and made up to 5 µl with ddH_2O. A vector only control reaction was also prepared, which consisted of everything except the Artemis insert. The reactions were mixed gently and incubated at room temperature for 30 minutes. 2 µl of each cloning reaction was then transformed into One Shot TOP10 competent cells (Invitrogen) using the protocol described in section 2.11.1, plated on LB agar plates (1 % tryptone, 0.5 % yeast extract, 1 % NaCl, 1.5 % agar, pH 7) containing Ampicillin (100 µg ml^{-1}) and incubated overnight at 37 °C. For both the 1BR and F96 transformations, 26 clones were picked using sterile pipette tips, cultured overnight in 5 ml L-Broth supplemented with 100 µg ml^{-1} Ampicillin and miniprepped using the Qiaprep Miniprep protocol (Qiagen). To test for the presence of Artemis inserts, miniprep DNA was digested with EcoRV and HindIII restriction endonucleases that both cut once within the full length Artemis coding sequence. This approach also allowed us to identify the presence of certain previously described alternative transcripts (Li *et al*, 2002), since together these enzymes are predicted to generate distinct fragments for some variants. Digestion of full length, SCIDA-V1 and SCIDA-V2 Artemis transcripts releases a 1280 bp fragment from the recombinant plasmid. SCIDA-V3 and SCIDA-V4 both release a 1224 bp fragment, and digestion of the latter also liberates a 119 bp fragment due to the presence of an additional HindIII site. These subtle differences were apparent after careful

examination on an ethidium stained 0.8 % agarose gel. Cloned SCIDA-V5 and SCIDA-V6 were both predicted to generate fragments of 1280bp and 30bp, and consistent with sequencing results we did not observe this signature in any of the clones examined. 25 1BR clones and 23 F96 clones that demonstrated the presence of an Artemis insert after restriction digestion were then sequenced using T7 (forward) and TK (reverse) primers. The additional sequencing primers U2, U3, U4, U5, L2, L3, L4, and L5 described in section 2.10 were then used to generate comprehensive sequence data for the full-length 1BR, F96 ΔGTT207-209 and F96 G377A transcripts.

2.12.3 Artemis recombination reactions using the Gateway cloning system

We had cloned full-length wild type and F96 mutant Artemis coding sequences into the pcDNA3.2/V5/GW/D-TOPO gateway vector that allows expression of V5 tagged Artemis in mammalian cells. At this point we were also interested in expressing Artemis using a system that produces green fluorescent protein (GFP)-tagged recombinant protein. The gateway cloning system enables the rapid and highly efficient transfer of DNA sequences into multiple vector systems while maintaining orientation and reading frame using the bacteriophage lambda site-specific recombination process. We therefore utilised this system to transfer the Artemis coding sequence from the pcDNA3.2/V5/GW/D-TOPO vector to the pDEST47 (Invitrogen) destination vector that incorporates a C-terminal GFP tag. In order to achieve this, 2 successive gateway recombination reactions were required. The first recombines the Artemis gene (Art) cloned into pcDNA3.2/V5/GW/D-TOPO with a gateway donor vector (pDONR221) in a BP clonase reaction to produce an entry clone (pENTR221-Art) (Figure 2-1). This entry clone can then be used in an LR recombination reaction with a destination vector (pDEST47) to produce an expression clone (pEXP47-Art). This process was completed for the full length wild type, F96 ΔGTT207-209 and F96 G377A Artemis alleles.

BP recombination reaction

BP recombination reactions were performed according to the manufacturer's instructions. Briefly, 500 ng (~100 fmol) of pcDNA3.2/V5/GW vector containing the Artemis gene was used in a BP recombination reaction consisting of 2 μl pDONR221 (150 ng μl^{-1}, ~100 fmol), 4 μl 5X BP Clonase Reaction Buffer, 4 μl BP Clonase enzyme mix, and made up to 20 μl with TE buffer (10 mM Tris, 1 mM EDTA, pH 8.0). This reaction was incubated at room temperature for at least 2 hours. 2 μl Proteinase K

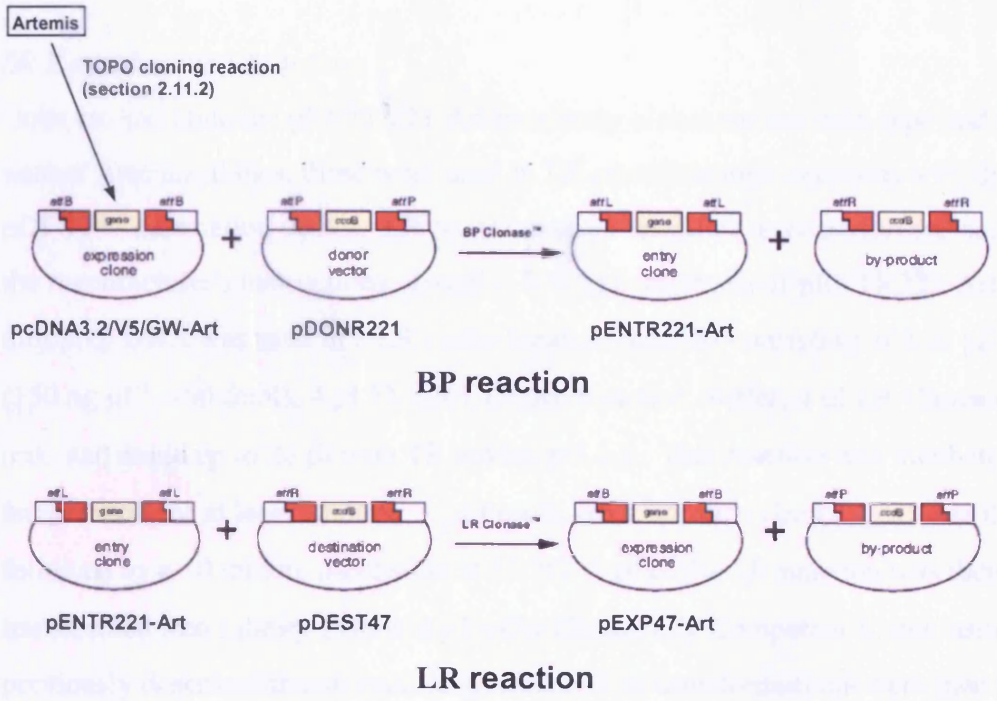

Figure 2-1: Strategy for the transferral of Artemis from the pcDNA3.2/V5/GW cloning vector to the destination vector pDEST47 using gateway recombination reactions. The Artemis genes cloned into pcDNA3.2/V5/GW were first transferred to the donor vector pDONR221 in a BP clonase reaction to produce pENTR221-Art entry clones. The pENTR221-Art entry clones were then recombined with the destination vector pDEST47 in LR reactions to produce pEXP47-Art expression clones, which code for GFP-tagged Artemis recombinant proteins.

solution (Invitrogen) was then added followed by a 10 minute incubation at 37 °C. 1 µl of the BP reaction was then transformed into Library Efficiency DH5α Chemically Competent *E. coli* using the previously described transformation protocol. The transformations were then plated on agar plates containing Kanamycin (50 µg ml^{-1}) and incubated overnight to select for pENTR221-Art vectors, which have a Kanamycin resistance gene but have also recombined with the Artemis insert to lose the toxic *ccd*B gene. The following day 3 colonies from each transformation were picked and grown using sterile pipette tips, cultured overnight in 5 ml L-Broth supplemented with 50 µg ml^{-1} Kanamycin and miniprepped using the Qiaprep Miniprep protocol (Qiagen). Test digests were performed with EcoRV that should cut once within the Artemis coding region and once within the pDONR221 sequence to produce bands of 1930 and 2729 bp after ethidium bromide-stained agarose gel electrophoresis. Glycerol stocks of DH5α *E. coli* clones containing the pENTR221-Artemis entry clone were prepared my mixing 850 µl of exponentially growing culture in Kanamycin containing L-Broth with 150 µl of glycerol and freezing at –80 °C.

LR Recombination Reactions

Once we had obtained pENTR221-Artemis entry clones for the wild type and F96 mutant Artemis alleles, these were used in LR recombination reactions with the pDEST47 destination vector. LR recombination reactions were performed according to the manufacturer's instructions. Briefly, 200 ng (~60 fmol) of pENTR221-Artemis miniprep DNA was used in a LR recombination reaction consisting of 2 μl pDEST47 (150 ng μl^{-1}, ~60 fmol), 4 μl 5X LR Clonase Reaction Buffer, 4 μl LR Clonase enzyme mix, and made up to 20 μl with TE buffer, pH 8.0. This reaction was incubated at room temperature for at least 2 hours. 2 μl Proteinase K solution (Invitrogen) was then added followed by a 10 minute incubation at 37 °C. 1 μl of the LR reaction was then transformed into Library Efficiency DH5α Chemically Competent *E. coli* using the previously described transformation protocol. The transformations were then plated on agar plates containing Ampicillin (100 μg ml^{-1}) and incubated overnight to select for pEXP47-Artemis vectors, which have an Ampicillin resistance gene but have also recombined with the Artemis insert to lose the toxic *ccd*B gene. The following day 3 colonies from each transformation were picked and grown using sterile pipette tips, cultured overnight in 5 ml L-Broth supplemented with 100 μg ml^{-1} Ampicillin and miniprepped using the Qiaprep Miniprep protocol (Qiagen). Test digests were performed with HindIII that should cut once within the Artemis coding region and twice within the pDONR221 sequence to produce bands of 696, 1617 and 5931 bp after ethidium bromide-stained agarose gel electrophoresis. Glycerol stocks of DH5α *E. coli* clones containing the pEXP47-Artemis expression clone were prepared my mixing 850 μl of exponentially growing culture in Ampicillin containing L-Broth with 150 μl of glycerol and freezing at –80 °C.

To obtain large amounts of DNA for use in transfections, pEXP47-Artemis DH5α *E. coli* clones were grown up in 300 ml Ampicillin (100 μg ul^{-1}) containing L-Broth for 16 hours, the culture was then split in half and 2 HiSpeed Plasmid Maxipreps (Qiagen) were performed. Plasmid DNA was eluted in 500 μl TE buffer and recombined to give 1000 μl of high concentration (≥1 μg μl^{-1}) pEXP47-Artemis plasmid DNA. This was also performed for the pcDNA3.2/V5-Artemis expression clone.

2.13 Expression of Artemis recombinant protein in cell lines

2.13.1 Transfection of 293T and HCT116 cells

We were unable to express recombinant Artemis protein in human fibroblasts using integrin mediated transfection (Estruch *et al*, 2001) despite achieving a transfection efficiency of ~50 % using a GFP only vector (pGFP). This suggested that human fibroblasts are sensitive to high levels of Artemis protein. We therefore transfected Artemis into the 293T and HCT116 cell lines, which are known to express recombinant proteins more readily.

293T cells were grown in DMEM (Gibco Invitrogen), 10 % FCS, 2 mM L-glutamine (Gibco Invitrogen), 100 U ml^{-1} penicillin G sodium and 100 μg ml^{-1} streptomycin sulphate (Gibco Invitrogen). HCT116 cells were grown in McCoys 5A medium (Gibco Invitrogen) 10 % FCS, 2mM L-glutamine (Gibco Invitrogen), 100 U ml^{-1} penicillin G sodium and 100 μg ml^{-1} streptomycin sulphate (Gibco Invitrogen). This protocol was used to transfect cells at 80 % confluence in a 6 well plate, but was scaled up accordingly to transfect larger amounts of cells. In one 5 ml universal tube 1 μg of plasmid DNA (0.5 μg of each construct for co-transfection) was diluted to 100 μl with Opti-MEM (Invitrogen). In another 5 ml universal, 5 μl Lipofectamine (1mg ml^{-1}, for 293T cells) or Lipofectamine 2000 (1mg ml^{-1}, for HCT116 cells) was diluted to 100 μl with Opti-MEM. The diluted DNA was then added drop wise to the diluted Lipofectamine reagent, and incubated for 20 minutes at room temperature to allow the formation of lipid-DNA complexes. The cells were then washed once with Opti-MEM, and 800 μl of Opti-MEM was replaced in each well. The DNA complexes (200 μl) were then added drop wise to each well and the cells were incubated at 37 °C, 5 % CO_2 for 4 hours, after which 500 μl of growth medium was added and the cells were incubated overnight. The next morning fresh medium was replaced in each well, and the cells returned to incubation. Depending on the particular experiment the transfected cells were then treated accordingly 24 hours after the initial addition of DNA-lipid complexes. Expression levels of V5 tagged protein were ascertained by western blot. The levels and localization of GFP tagged protein were visualised using a Zeiss Axiovent S100 fluorescent microscope at 400x magnification and/or FACS analysis.

2.13.2 Cell sorting of Artemis-GFP positive HCT116 cells

Four 10 cm tissue culture plates containing HCT116 cells at 80 % confluence were transfected with wild type Artemis-GFP or co transfected with G126D and ΔL70 Artemis-GFP expression constructs. 24 hours later 2 plates from each transfection were exposed to 1Gy γ-radiation, while the remainder was mock irradiated. After a further 4 hour incubation cells were sorted on a Coulter EPICS ALTRA sorter into GFP positive and negative populations. Approximately 5 x 10^5 cells were sorted for each population and cell lysate was immediately prepared for analysis of p53 status by western blot.

2.14 Protein methodology

2.14.1 Protein lysates

To prepare protein lysate cells were trypsinised, washed once in PBS, resuspended in 1 ml PBS and transferred to a 1.5 ml eppendorf tube. Each sample was then centrifuged at 1800 rpm for 5 minutes in a microfuge and resuspended in 50-100 μl of cell lysis buffer (125 mM Tris/HCl, 32 mM dithiothreitol (DTT), 2 % SDS, 1 complete mini protease inhibitor cocktail tablet (Roche), in 10 ml total solution). The lysate was then placed in a heating block at 100 °C for 10 minutes, and centrifuged at top speed (13200 rpm) in a microfuge for 10 minutes. The supernatant containing total cellular protein was transferred to a fresh eppendorf tube and stored at –80 °C until required.

2.14.2 Estimation of protein concentration

The protein concentration in each sample was measured using the BCA Protein Assay Kit (Pierce) according to the manufacturer's instructions. This method is based on the absorbance of protein samples at 562 nm. A standard curve using known concentrations of BSA was first completed (figure 2-2), and this allowed us to calculate the concentration of total cellular protein in our samples using the relationship Absorbance x 0.0012^{-1} = Protein concentration (μg ml^{-1}). Protein samples to be assayed were first diluted 1:100 with water, and this dilution factor was taken into account when calculating protein concentration.

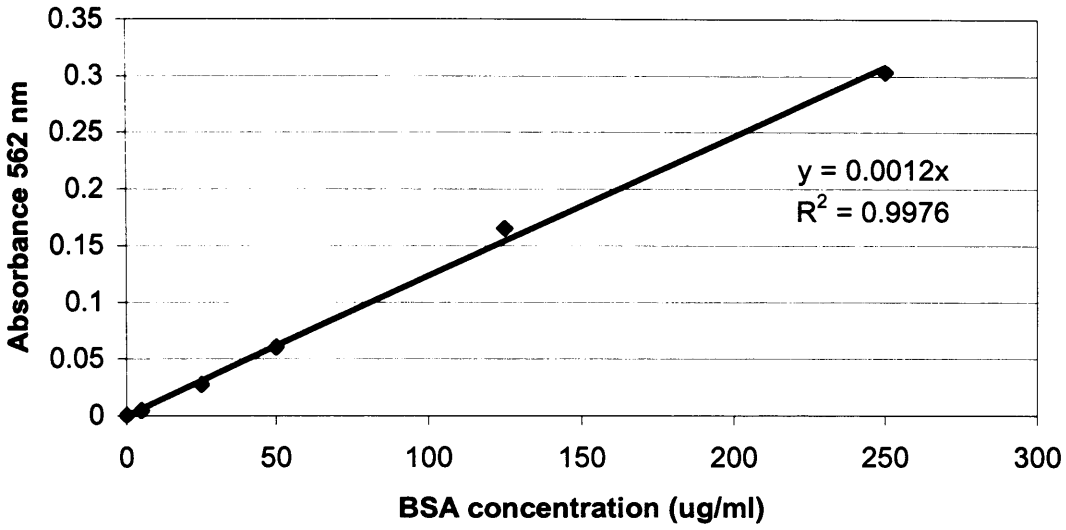

Figure 2-2: Standard curve for measurement of protein concentration using the BCA Protein Assay Kit. The absorbance of known concentrations of BSA allowed the relationship Absorbance = Protein concentration ($\mu g\ ml^{-1}$) x 0.0012^{-1} to be calculated from the line of best fit, $R^2 = 0.9976$.

2.14.3 Western blotting

20-40 µg of protein was diluted to 10 µl with lysis buffer and mixed with 5 µl of 3X Red Reducing SDS Loading Buffer (NEB). The samples, along with 15 µl of Broad Range Prestained Protein Marker (NEB), were then denatured by heating to 100 °C for 5 minutes, and centrifuged at top speed (13000 rpm) in a microfuge for 3 minutes.

For examination of p53 and Artemis proteins the samples were loaded onto a large 10 % SDS-PAGE gel prepared in a Hoefer Sturdier SE400 vertical unit (Amersham Pharmacia Biotech). The gel was made by first preparing the 10 % resolving gel by mixing 15.8 ml H_2O, 13.3 ml ProtoGel 30 % w/v Acrylamide (National diagnostics), 10 ml 1.5 M Tris pH 8.8, 400 µl 10 % SDS, 400 µl freshly made 10 % Ammonium Persulfate (APS) and 16 µl N,N,N',N'-Tetramethylethylenediamine (TEMED). The stacking gel was then prepared by mixing 1.7 ml H_2O with 1.7 ml ProtoGel 30 % w/v Acrylamide, 1.25 ml 1 M Tris pH 6.8, 100 µl 10 % SDS, 100 µl freshly made 10 % APS and 10 µl TEMED. The gel was run in 1 x running buffer (3.03 g Tris base, 14.4 g Glycine, 10 ml 10 % SDS, made up to 1 litre with H_2O) overnight at 50 V ensuring adequate resolution of the 47.5, 62 and 83 kDa markers. The gel was then transferred overnight onto a Hybond-C extra nitrocellulose membrane (Amersham) in 1 x transfer buffer (Transfer buffer was prepared by mixing 3.03 g Tris base, 14.4 g glycine with 1

litre of H_2O, adding 400 ml methanol, then making the solution up to 2 litres with H_2O) at 300 mA.

For examination of p21, samples were loaded onto 12 % SDS-PAGE gels prepared using BioRad MiniGel apparatus. A 12 % gel comprised of 6.6 ml H_2O, 8 ml ProtoGel 30 % w/v Acrylamide (National diagnostics), 5 ml 1.5 M Tris pH 8.8, 200 µl 10 % SDS, 200 µl freshly made 10 % Ammonium Persulfate (APS) and 8 µl TEMED. The stacking gel and running buffer was the same as described above. These gels were run at 80 V for approximately 2 hours until the loading dye reached the bottom of the gel. The gel was then transferred in 1 x transfer buffer at 60 V for 1 hour 30 minutes.

After the transfer was complete the sandwich was dismantled and protein transfer examined using Ponceau S solution (Sigma). The membrane was then blocked in TBS-T (To make 1 litre TBS-T mix 12.5 ml 1M Tris pH 7.6, 30 ml 5M NaCl, 1 ml Tween-20 and make up to 1 litre with H_2O) with 5 % marvel (milk powder) on a rocking platform either for 1 hour at room temperature or overnight at 4 °C. The membrane was then washed once in a large volume of TBS-T, and incubated with primary antibody diluted 1:1000 in TBS-T with 0.5 % marvel on a rocking platform, either for 1 hour at room temperature or overnight at 4 °C. The primary antibody was then removed by washing twice in a large volume of TBS-T, 10 minutes each time. The washing solution was then discarded and replaced by secondary antibody (Santa Cruz), which was diluted 1:2500 in TBS-T with 0.5 % marvel and incubated on a rocking platform for 1 hour. The secondary antibody was then discarded and the membrane was washed 3 times in large volumes of TBS-T, 15 minutes each time. The signal on the membrane was visualised using ECL reagents (Amersham) according to the manufacturer's instructions, and autoradiographic film was exposed to the membrane for various periods of time depending on this intensity of the bands. Where applicable, bands were quantified using a BioRad Densitometer.

Primary antibodies used were as follows: -

- Anti-V5 mouse monoclonal (Invitrogen)
- Phospho-p53 (Ser15) rabbit polyclonal (Cell Signaling Technology)
- p53 (FL-393) goat polyclonal (Santa Cruz)
- p21 (C-19) rabbit polyclonal (Santa Cruz)

2.14.4 Phosphatase treatment of cell lysate

200 µg of total cellular protein isolated using standard lysis buffer was diluted to 100 µl with 50 mM Tris, 1mM $MgCl_2$. 10 µl of Calf intestinal alkaline phosphatase (CIAP) (1 unit μl^{-1}, Promega) was then added to each sample and incubated at 37 °C for 30 minutes. To stop the reaction 50 µl of 3X Red Reducing SDS Loading Buffer (NEB) was added to each sample, and 30 µl (40 µg) was loaded onto a standard 10 % SDS-PAGE gel. The remainder was frozen at -80 °C until required.

2.14.5 Inhibition of p53 protein acetylation using Anacardic Acid

Anacardic acid (AA) (Calbiochem) is a non-competitive inhibitor of the p300 and P/CAF acetyltransferases that are known to target p53. This compound was dissolved in DMSO at a concentration of 10 mg ml^{-1} and stored as a stock solution at –20°C. For both the 1BR and F96 lines, 6 cell cultures were grown in 3.5 cm tissue culture plates to 80 % confluence. 6 µl of DMSO or 6 µl of AA (10 mg ml^{-1}) was then added to 2 plates from each line and incubated for 12 hours prior to irradiation. 2 hours prior to irradiation 6 µl AA solution was then added to the 2 remaining plates of each line. 1 plate from each treatment regime (12 hrs DMSO, 12 hrs AA and 2 hrs AA) was then exposed to 1 Gy γ-radiation while the other was mock irradiated, and all were incubated for a further 4 hours. Total cellular protein was then isolated and p53 status investigated by western blot as previously described.

2.15 Sequencing of p53

A 1426 bp fragment encompassing the entire coding region of p53 was amplified from cDNA using primers P5F and P7F described below: -

Primers

P5F: 5'-TCCGGGGACACTTTGCGTTC-3'

P7R: 5'-AGCCCCGGGACAAGCAA-3'

Amplified fragment size, 1426 bp

PCR reaction

These primers were used in a 50 µl PCR reaction consisting of 5 µl 10 x Pfx amplification buffer (Invitrogen), 1.5 µl 10 mM dNTPs, 1 µl 50 mM $MgSO_4$, 1 µl P5F (100 pmol μl^{-1}), 1 µl P7R (100 pmol μl^{-1}), 38.5 µl ddH_2O, 1 µl Pfx (Invitrogen) and 1µl cDNA.

Cycling conditions

	94 °C for 2 min	
	94 °C for 15 sec	35 cycles
Annealing temp	57 °C for 30 sec	
	68 °C for 2 min	
	68 °C for 10 min	
	Hold at 4 °C	

The double-stranded PCR product was gel purified and sequenced using ABI Dyedeoxy Terminator Cycle Sequencing apparatus with a Prism 377 automatic sequencer (Applied Biosystems, Foster City, CA). For each line the p53 fragment was amplified three times in separate PCR reactions, and the resulting products were sequenced in both directions. The oligonucleotides employed in the initial PCR reaction were used in combination with the following forward (F) and reverse (R) primers in order to fully sequence the amplified products (depicted in figure 7-3): -

p53 sequencing primers

P6F: 5'-CTCCTGGCCCCTGTCATCTT-3'
P7F: 5'-AGTGTGGTGGTGCCCTATGA-3'
P5R: 5'-ATGTGCTGTGACTGCTTGTAG-3'

2.16 Affymetrix GeneChip analysis

The F96 line displayed enhanced levels of p53 phosphorylation after DNA damage, and this appears to result in the abnormally high induction of the Cdk inhibitor p21, a p53 target gene. We were interested in further investigating radiation-induced gene expression in the F96 line to determine whether this enhanced response was restricted to the induction of p21, or if other damage response genes were induced at similarly high levels in these mutant cells. This was achieved using Affymetrix GeneChip analysis, which allows the researcher to simultaneously monitor the activities of thousands of genes and compare this between experimental samples.

Affymetrix GeneChips are fixed oligonucleotide arrays with complementary probes for each gene in specific locations on the chip. Each feature on a chip consists of millions of copies of a 25mer oligonucleotide, and each gene is represented by 11-16 pairs of such oligos, designed to non-conserved regions at the 3′ end of the gene (often in the 3′ untranslated regions). Each pair of oligos consists of a perfect match (PM) to the probe sequence and a mismatch (MM) oligo that differs in only one position (13 of 25), and acts as a cross hybridisation control. High quality total RNA prepared from the test sample is first reverse transcribed into cDNA using a primer that incorporates a T7 promoter at its 5′ end, which then serves as a template for an *in vitro* transcription (IVT) labeling reaction that produces many copies of complementary RNA (cRNA) that has incorporated biotinylated nucleotides. Biotin labeled cRNA is then fragmented, hybridized to the GeneChip and stained with a fluorescent marker directed against the biotin tag. The relative levels of gene expression are determined by analysing fluorescence intensities at particular locations (figure 2-3).

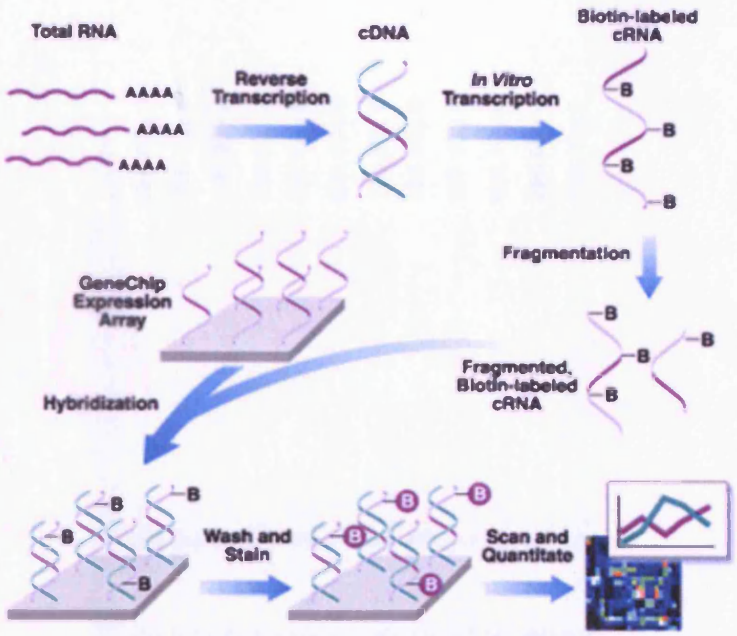

Figure 2-3: Standard eukaryotic gene expression assay using Affymetrix GeneChips. The basic concept behind the use of GeneChip arrays for gene expression. Labelled cRNA targets derived from the mRNA of an experimental sample are hybridised to nucleic acid probes attached to the solid support. By monitoring the amount of label associated with each DNA location, it is possible to infer the abundance of each mRNA species represented. Taken from the Affymetrix website, www.affymetrix.com.

2.16.1 Preparation of target cRNA

Analysis of total RNA quality and concentration

Total RNA was isolated from 1BR and F96 cells 4 hours after exposure to either 0 or 1Gy γ-radiation using Trizol reagent (Invitrogen) according to the manufacturer's instructions. This procedure was completed 3 times in separate experiments, which generated triplicate RNA samples for each cell line before and after irradiation. The quality and concentration of each Total RNA sample was then assessed using an Agilent 2100 Bioanalyser (figure 2-4).

Double Stranded cDNA Synthesis

cDNA synthesis was performed with the Microarray cDNA Synthesis Kit (Roche). For each sample 8 µg of total RNA was mixed with 2 µl of T7-Oligo(dT) Primer (200 pmol) and made up to 21.5 µl with RNase free H_2O.

T7-Oligo(dT) Primer:

5'-GGCCAGTGAATTGTAATTGTAATACGACTCACTATAGGGAGGCGG-$(dT)_{24}$-3'

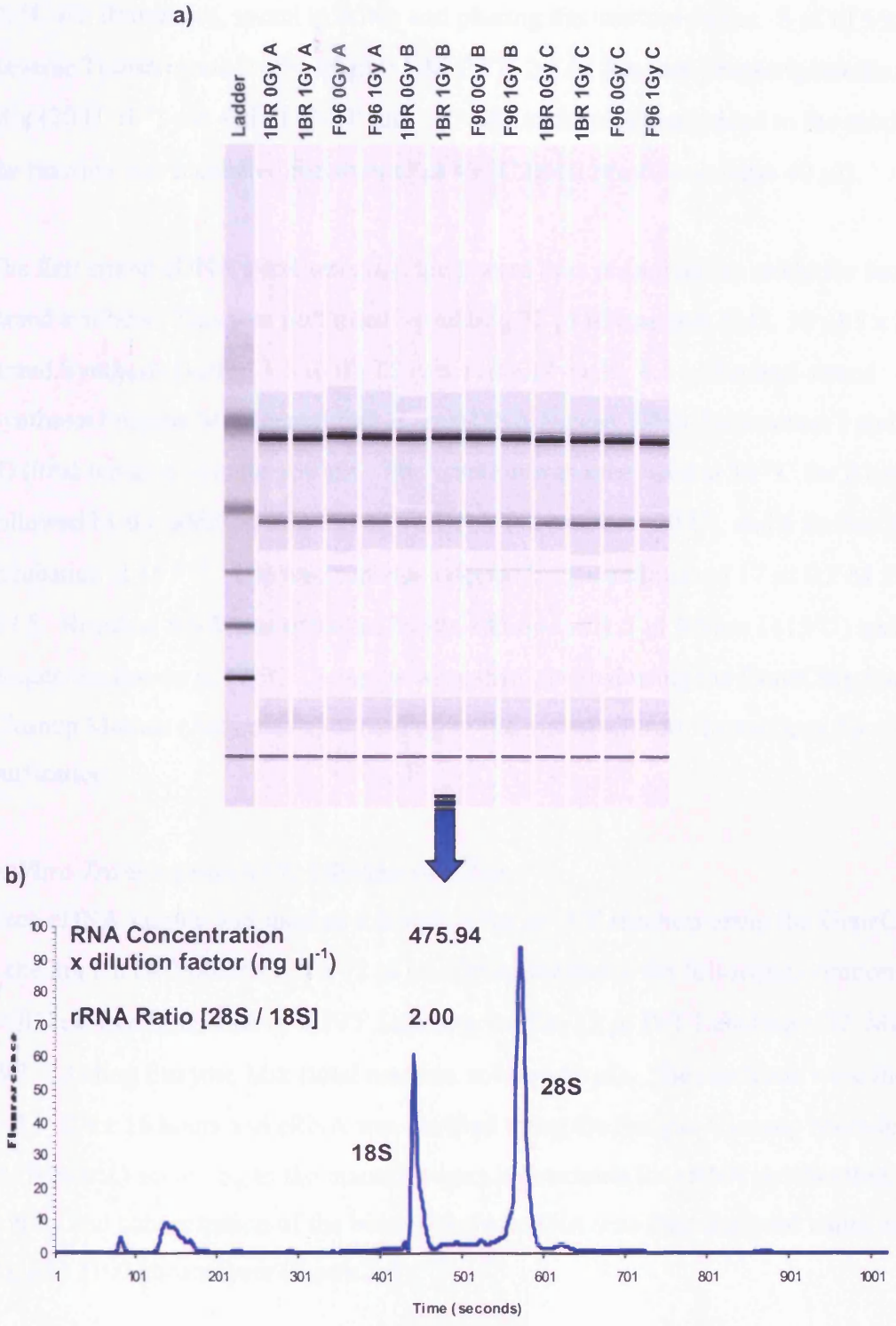

Figure 2-4: Analysis of total RNA quality and concentration using an Agilent 2100 Bioanalyser. a) Agilent 2100 Bioanalyser gel image of all 12 total RNA samples isolated from primary fibroblasts to be analysed by gene chip analysis. A, B and C refers RNA obtained from 3 separate expriments. b) Electropherogram (from Agilent 2100 Bioanalyser) of a representitve total RNA sample (1BR 1Gy B, lane 6). For a high quality RNA sample, two well defined peaks corresponding to the 18S and 28S ribosomal RNAs should be observed, with ratios approaching 2:1 for the 28S:18S bands.

The T7-Oligo(dT) Primer was hybridised to poly-A RNA by incubating the mixture at 70 °C for 10 minutes, spinning down and placing the mixture on ice. 8 µl of 5 x Reverse Transcriptase Buffer, 4 µl 0.1 M DTT, 2.5 µl Reverse Transcriptase Enzyme Mix (20 U μl^{-1}) and 4µl of dNTP mix (10 mM each) was then added to the mixture and the reaction was incubated for an hour at 42 °C (total reaction volume 40 µl).

The first strand cDNA sysnthesis reactions were then placed on ice ready for second strand syntheis. This was perfomed by adding 72 µl RNase free H_2O, 30 µl 5 x Second-strand Synthesis Buffer, 1.5 µl dNTP mix (10 mM each), 6.5 µl Second-strand Synthesis Enzyme Mix (containing *E. coli* DNA Ligase, DNA Polymerase I and RNase H) (total reaction volume 150 µl). The reaction was incubated at 16 °C for 2 hours, followed by the addition of 20 µl of T4 DNA Polymerase (20 U), and a further 5 minute incubation at 16 ° C. The reaction was stopped by the addition of 17 µl 0.2 M EDTA pH 8. Residual RNA was removed by the addition of 1.5 µl RNase I (15 U) and a 30 minute incubation at 37 °C. Samples were then purified using the GeneChip Sample Cleanup Module (Affymetrix) according to the manufacturers instructions for cDNA purfication.

In Vitro Transcription (IVT) labeling reaction

Each cDNA sample was used as a template for an IVT reaction using the GeneChip IVT Labeling Kit (Affymetrix). To 12 µl of cDNA, we added the following components; 8 µl RNase free H_2O, 4 µl 10 x IVT Labeling Buffer, 12 µl IVT Labeling NTP Mix, 4 µl IVT Labeling Enzyme Mix (total reaction volume 40 µl). The reactions were incubated at 37 °C for 16 hours and cRNA was purified using the Sample Cleanup Module (Affymetrix) according to the manufacturers instructions for cRNA purification. The quality and concentration of the biotin-labeled cRNA was then analysed using an Agilent 2100 Bioanalyser (figure 2-5)

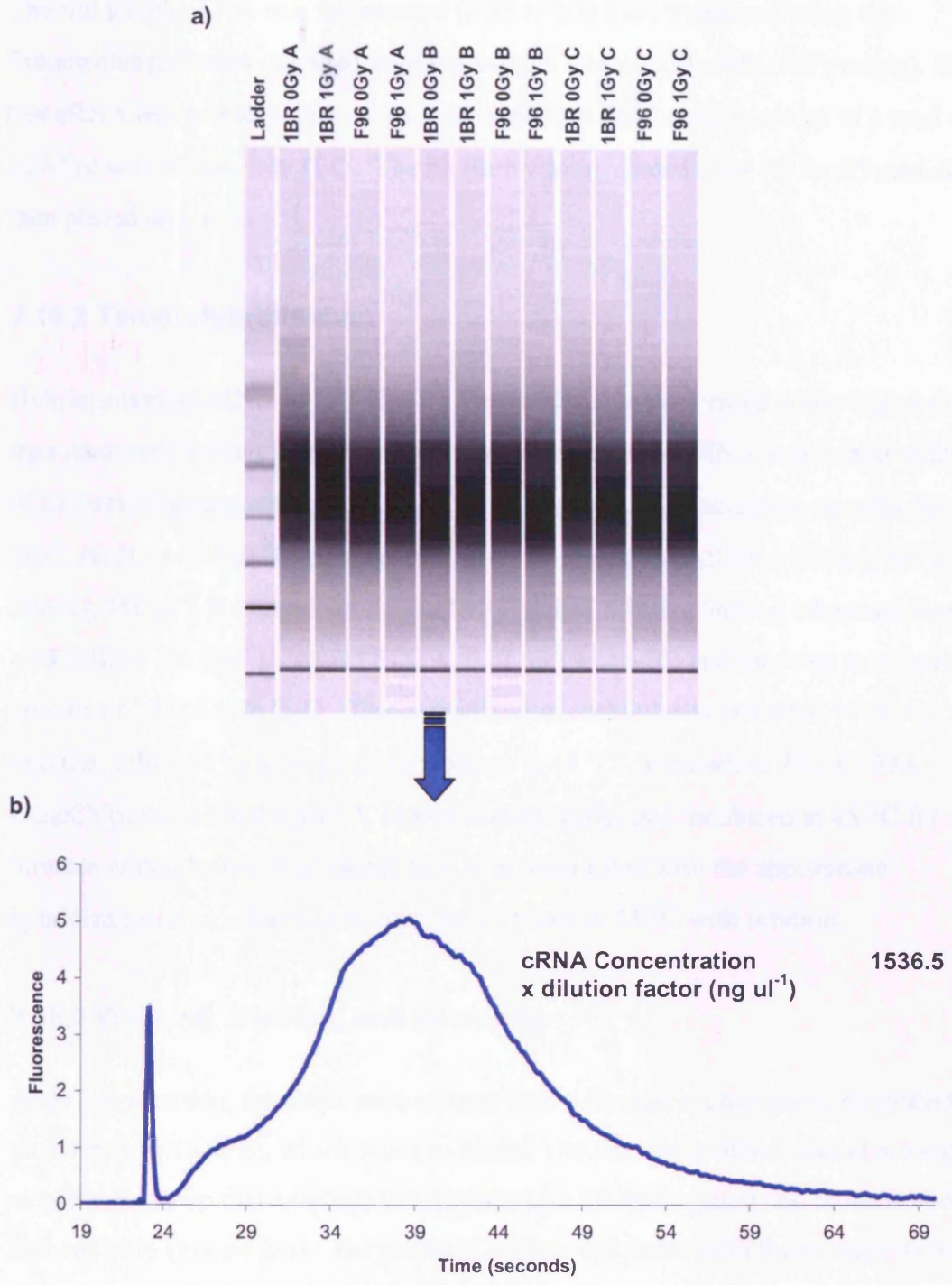

Figure 2-5: Analysis of cRNA samples after *in vitro* transcription using an Agilent 2100 Bioanalyser. a) Agilent 2100 Bioanalyser gel image of the 12 labeled cRNA samples generated by *in vitro* transcription to be used for GeneChip analysis. B) Electropherogram (from Agilent 2100 Bioanalyser) of a representitve cRNA sample (1BR 0Gy B, lane 6).

Fragmentation of RNA

The full length cRNA was fragmented to 35 to 200 base fragments using the Fragmentation Buffer supplied with the Sample Cleanup Module (Affymetrix). 20 µg of test cRNA was mixed with 8 µl 5 x Fragmentation Buffer and made up to a total volume of 40 µl with RNase free H_2O. The mixture was incubated at 94 °C for 35 minutes and then placed on ice.

2.16.2 Target Hybridisation

Hybridisation of cRNA to HG-U133A GeneChips was performed according to the manufacturer's instructions. Briefly, 15 µg of fragmented cRNA was mixed with 5 µl of Control Oligonucleotide B2, 15 µl 20 X Eukaryotic Hybridisation controls (*bioB, bioC, bioD, cre*), 3 µl Herring Sperm DNA (10 mg ml^{-1}), 3 µl BSA (50 mg ml^{-1}), 30 µl DMSO, 150 µl 2 X Hybridisation Buffer (100 mM 2-[Morpholino] ethanesulphonic acid (MES), 1M [Na^+], 20 mM EDTA, 0.01 % Tween-20) and made up to a final volume of 300 µl with H_2O. This hybridization cocktail was heated to 99 °C for 5 minutes, followed by a 5-minute incubation at 45 °C. Meanwhile, HG-U133A GeneChips were filled with 1 X Hybridisation Buffer and incubated at 45 °C for 10 minutes with rotation. The GeneChips were then filled with the appropriate hybridization cocktail and incubated for 16 hours at 45 °C with rotation.

2.16.3 Washing, Staining and Scanning

After hybridisation, the chips were stained with a fluorescent molecule, streptavidin-phycoerythrin (SAPE), which binds to biotin. The staining protocol includes a signal amplification step that employs anti-Streptavidin antibody (goat) and biotinylated goat IgG antibody (Figure 2-6). The series of washes and stains with these reagents binds the biotin and provides an amplified flour that will emit light when the chip is scanned with a confocal laser. SAPE mix was prepared by mixing 600 µl 2 X Stain Buffer (100 mM MES, 1 M [Na^+], 0.05 % Tween-20), 48 µl BSA (50 mg ml^{-1}), 12 µl SAPE (1mg ml^{-1}), 540 µl H_2O.

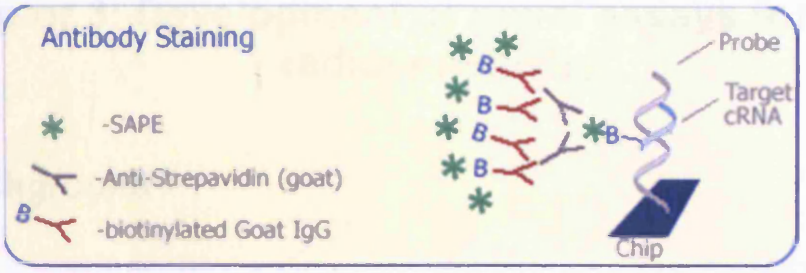

Figure 2-6: Fluorescent staining of the hybridised GeneChip arrays incorporates a signal amplification step involving SAPE, Anti-Streptavidin (goat) and biotinylated Goat IgG.

Biotin antibody solution mix was prepared by mixing 300 µl 2 X Stain Buffer, 24 µl BSA (50 mg ml^{-1}), 6 µl 10 mg ml^{-1} Goat IgG (10 mg ml^{-1}), 3.6 µl biotinylated antibody (0.5 mg ml^{-1}) and 266.4 µl H_20. The hybridised GeneChip arrays were washed and stained using a Fluidics Station 400 operated by Microarray Suite 5 (Affymetrix). The fluidics station was set to run the Affymetrix wash and stain script EukGE-WS2v4 (table 2-4)

	EukGE-WS2v4*
Post Hyb Wash #1	10 cycles of 2 mixes/cycle with Wash Buffer A at 25°C
Post Hyb Wash #2	4 cycles of 15 mixes/cycle with Wash Buffer B at 50°C
Stain	Stain the probe array for 10 minutes in SAPE solution at 25°C
Post Stain Wash	10 cycles of 4 mixes/cycle with Wash Buffer A at 25°C
2nd Stain	Stain the probe array for 10 minutes in antibody solution at 25°C
3rd Stain	Stain the probe array for 10 minutes in SAPE solution at 25°C
Final Wash	15 cycles of 4 mixes/cycle with Wash Buffer A at 30°C. The holding temperature is 25°C

- Wash Buffer A = non-stringent wash buffer
- Wash Buffer B = stringent wash buffer

Wash Buffer A

Non-Stringent Wash Buffer 1000 ml

300 ml 20 X SSPE

(3M NaCl, 0.2M NaH_2PO_4, 0.02M EDTA)

1.0 ml 10 % Tween-20

699 ml H_20

Wash Buffer B

Stringent Wash Buffer 1000 ml

83.3 ml 12 X MES Stock Buffer

5.2 ml 5 M NaCl

1.0 ml 10 % Tween-20

910.5 ml H_2O

Table 2-4: Fluidics protocol EukGE-WSv4 and wash buffers used for antibody amplification of eukaryotic targets

The stained microarrays were then scanned with an Affymetrix GeneChip Scanner 3000 controlled by Microarray Suite 5. The Microarray Suite 5 (MAS5) statistical algorithm was used to calculate signal intensities and make significance calls for the resulting data, which was exported to GeneSpring 6.0 for comparative analysis.

Chapter 3: Development of novel assays for cellular radiosensitivity

3.1 Background

One of the main aims of this project was to develop new methods of assessing and investigating cellular radiosensitivity. Fibroblast survival assays have been widely used to identify patients with radiosensitive disorders (Arlett *et al*, 1988) (Cavazzana-Calvo *et al*, 1993) (Nicolas *et al* 1996) (Nicolas *et al* 1998) (Peake *et al*, 1999) (Riballo *et al*, 1999) (O'Driscoll *et al*, 2001) (Dai *et al*, 2003) (Kobayashi *et al*, 2003) (Noordzij *et al*, 2003) but once a skin biopsy is received it takes approximately 2 months before a primary line is generated and the survival assays completed. We therefore investigated whether radiation induced lymphocyte apoptosis, an endpoint that can be measured after a matter of days, could be used as a more rapid screen for cellular radiosensitivity. Lymphocytes are also easily separated from whole blood, a tissue that is more readily obtained from patients than skin biopsies. This assay could therefore improve the speed and ease with which we identified radiosensitive patients.

Radiation induced lymphocyte apoptosis is an end point that can be accurately measured using Annexin V staining and subsequent FACS analysis (Hertveldt *et al*, 1997), but the relative fraction of primary human fibroblasts that initiate apoptosis in response to radiation has been reported as very low or nearly null (Chung *et al*, 1998) (Dikomey *et al*, 1998) (Kawabe *et al*, 2001) (Zhang *et al*, 2001a). In contrast, there is increasing evidence that after irradiation a substantial fraction of human cells, in particular primary fibroblasts, are inactivated by a permanent growth arrest (Little *et al*, 1985) (Di Leonardo *et al*, 1994) (Yount *et al*, 1996) (Linke *et al*, 1997) (Williams *et al*, 1997) (Boyle *et al*, 1999) (Azzam *et al*, 2000). Since survival assays focus on colony formation after 2-3 weeks, they give no insight into the fate of cells that survive the initial genotoxic insult, but ultimately fail to proliferate and form colonies. We therefore developed a novel assay to look at the proliferation of fibroblast cultures within days of irradiation. This was performed using CFSE cell division analysis, and allowed us to identify important differences between control and radiosensitive cells in relation to cell fate after irradiation.

3.2 Lymphocyte apoptosis as a measure of cellular radiosensitivity

14 patients were investigated for abnormal responses to DNA damage using the Annexin V-FITC lymphocyte apoptosis assay. Where possible, blood was obtained from a healthy adult donor (below 30 years) in parallel with patient blood, and both samples were transported together to the Institute of Child Health (ICH).

3.2.1 FACS analysis

The sample was first evaluated with respect to cell size and granularity, allowing the elimination of any debris during data acquisition (figure 3-1a-b). The gated lymphocytes were then analysed for Annexin V and 7AAD fluorescence using 10,000 events/sample, unless otherwise stated (figure 3-1c-d). Annexin V binds to phosphatidylserine (PS) residues that translocate from the inner leaflet of the plasma membrane to the outer leaflet in the early stages of apoptosis. This exposes PS to the external environment and allows the percentage of cells undergoing apoptosis to be quantified. Lymphocytes were also counterstained with 7AAD, which is a DNA binding dye and identifies necrosis and the later stages of apoptosis, when the plasma membrane becomes highly permeable.

Radiation induced apoptosis was first investigated in a control sample in order to select the criterion to be used for data analysis. We decided to use a 24 hour incubation period from a preliminary time course experiment (data not shown) of 24, 48 and 72 hours because radiation induced apoptosis was well defined, and there was minimum death resulting from cell culture conditions. After 3 Gy of γ-radiation the percentage of Annexin V positive cells (green dots) increased by approximately 10 %, and the percentage of 7AAD positive cells (blue dots) increased by approximately 4 %. This increase in Annexin V and 7AAD staining corresponds to cells that have entered the early (figure 3-1d, arrow 1) and late (figure 3-1d, arrow 2) stages of apoptosis respectively, in response to γ-irradiation. Total Annexin-V positive cells (figure 3-1c-d, green and blue dots) was used as a measure of radiation-induced apoptosis since this displayed the most consistent dose response relationship (data not shown). An increase in apoptosis of approximately 15 % was observed in total Annexin-V positive cells after 3 Gy γ-radiation at 24 hours (figure 3-1e-f).

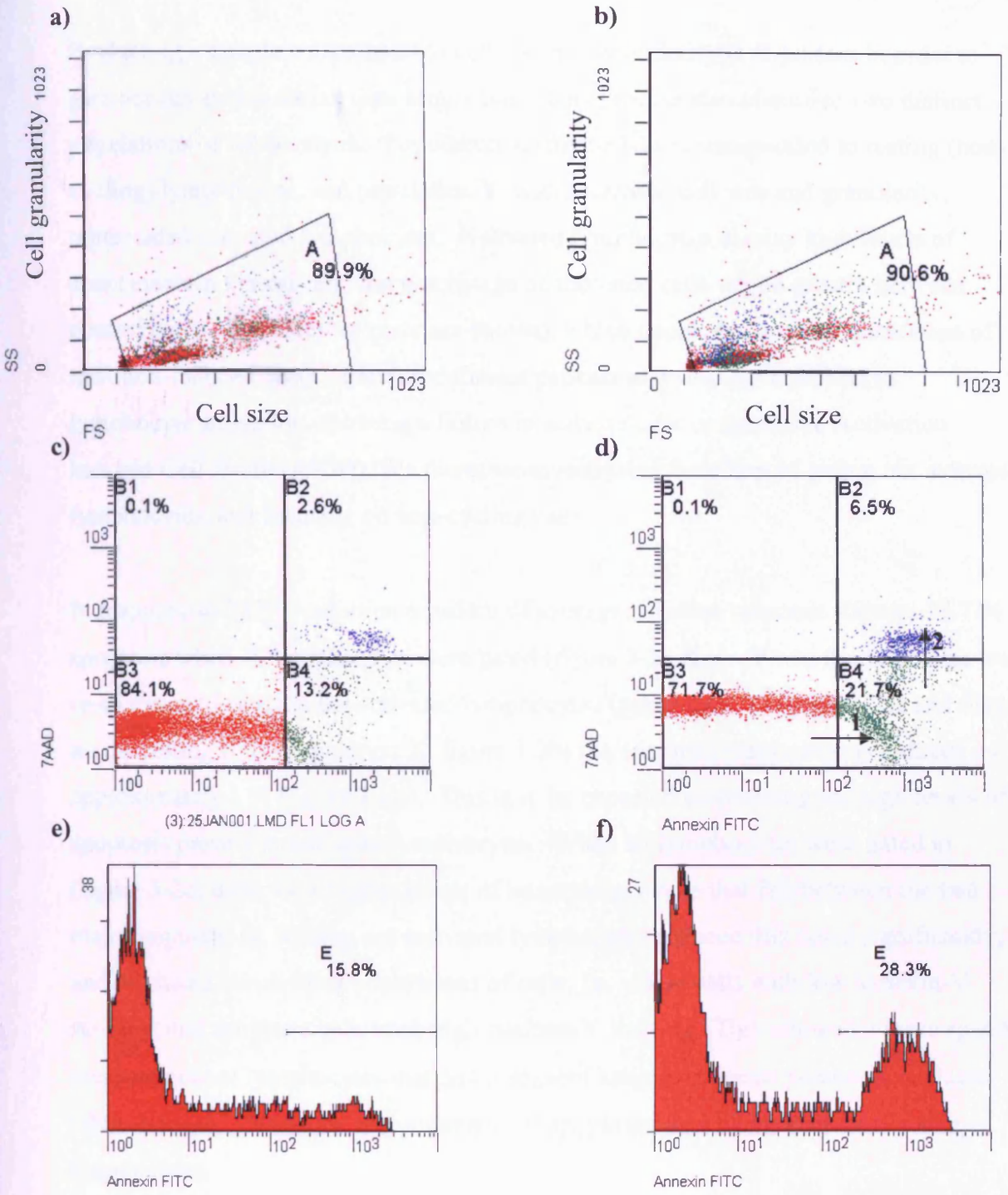

Figure 3-1: Selection of criterion for data analysis from a control of average radiation response. (a-b) Dot plots of cell size versus cell granularity 24 h after (a) 0- and (b) 3-Gy γ-radiation. The cells in the gated areas are lymphocytes. (c-d) Dot plots of Annexin V staining versus 7AAD staining showing lymphocytes (selected from the previous gated areas) 24 h after (c) 0- and (d) 3-Gy γ-radiation. Red dots are unstained cells, green are both annexin V positive and 7AAD negative and blue are both Annexin V and 7AAD positive. Their percentage is given. (e-f) Histograms of annexin V staining of lymphocytes 24 h after (e) 0- and (f) 3-Gy γ-radiation. The percentage of cells stained with annexin V is given (these data are from a control donor of average radiation response)

Evaluating a sample with respect to cell size and granularity is important in order to gate out any debris during data acquisition. This process also identified two distinct populations of lymphocytes. Population X (figure 3-2a) corresponded to resting (non-cycling) lymphocytes, and population Y, with increased cell size and granularity, represented activated lymphocytes. Activated lymphocytes display high levels of spontaneous apoptosis and the percentage of activated cells varied greatly between control and patient samples (data not shown), which could obscure any correlation of radiation-induced death. Immunodeficient patients may also have defects in lymphocyte activation, showing a failure to activate cells or excessive Activation Induced Cell Death (AICD). We therefore investigated the effect of gating out activated lymphocytes, and focusing on non-cycling cells.

In response to 3 Gy γ-radiation a patient of average radiation response showed 37.7 % apoptosis when all lymphocytes were gated (figure 3-2a & c). When the same data was re-analysed to gate out the activated lymphocytes (population Y, figure 3-2a) and focus on the resting cells (population X, figure 3-2b) the apoptotic response was reduced by approximately 5 % (figure 3-2d). This may be expected considering the high levels of apoptosis present in activated lymphocytes. When all lymphocytes were gated in (figure 3-2c) there were higher levels of intermediary cells that fell between the two major populations. Gating out activated lymphocytes reduced this noise significantly, and produced two distinct populations of cells, i.e. viable cells with low annexin-V staining, and apoptotic cells with high annexin-V staining. This allowed a more specific measurement of lymphocytes that had instigated apoptosis due to γ-radiation induced DNA damage. Therefore, measurements of apoptosis were taken from only resting lymphocytes.

3.2.2 Radiation induced PBL apoptosis

We performed the lymphocyte apoptosis assay on 14 control and 18 patient samples. PBLs isolated from whole blood were treated with increasing doses of radiation from 0 to 3 Gy, and incubated for 24 hours. Levels of apoptosis increased with radiation. In order to establish a measure of radiosensitivity, we evaluated levels of spontaneous apoptosis, what constitutes a control response, and what criteria define a difference from this control response. Where possible we compared patient lymphocyte apoptosis results to those obtained using the fibroblast survival assay.

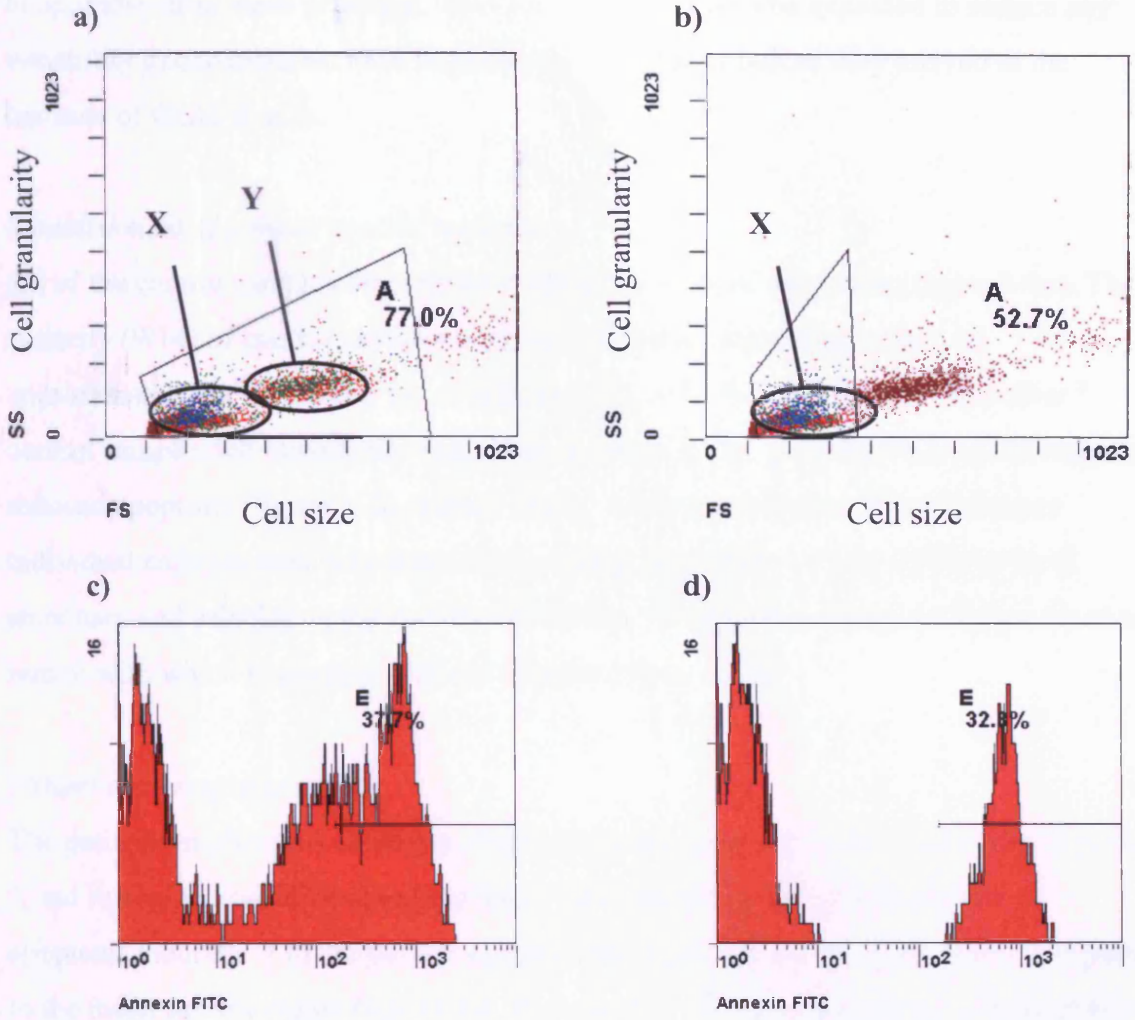

Figure 3-2: Effect of gating out activated lymphocytes for a patient of average radiation response. (a-b) Dot plots of cell size versus cell granularity 24 h after 3-Gy γ-radiation. (a) All lymphocytes gated (Population X (resting) and Y (activated)). (b) Resting cells gated (Population X). (c-d) Histograms of annexin-V staining of lymphocytes 24 h after 3-Gy γ-radiation (selected from the previous gated areas). (c) All lymphocytes gated (Population X (resting) and Y (activated)). (d) Resting cells gated (Population X). The percentage of cells stained with annexin-V is given (these data are from a patient of average radiation response). Note the clearer peak separation when resting cells are gated.

Spontaneous Apoptosis

The spontaneous (0 Gy) levels of apoptosis appeared to be highly variable between patient samples, ranging from below 5 % to approximately 30 % (figure 3-3). This range was reduced in control samples, from below 5 % to approximately 15 %. This high degree of variability between patient samples did not appear to be indicative of radiation sensitivity. Therefore, in order to identify differences in radiation-induced

apoptosis, we modified this raw data by first subtracting the spontaneous (0 Gy) levels of apoptosis from each response. This process would also be expected to reduce any variability due to differences in handling of the samples before they arrived at the Institute of Child Health.

Establishment of a mean control response

All of the control samples demonstrated radiation induced apoptosis (figure 3-4a). The majority (9/14) of control samples exhibited radiation induced apoptosis of approximately 10 - 18 % at 3 Gy of radiation (figure 3-4a. solid lines). The other 5 control samples fell outside this range and appeared to have abnormal levels of radiation induced apoptosis (figure 3-4a, dashed lines). Differences in sensitivity between individual controls were accounted for by taking an average of all (14) the control responses and calculating the standard deviation. This gave a normal radiation response region with which to compare patient samples (figure 3-4b).

Patient dose response curves

The patient lymphocytes all demonstrated increased apoptosis after irradiation (figure 3-5, red lines), and could be classified into 3 categories according to the extent of apoptosis induced. 7 of the patient samples exhibited high levels of apoptosis compared to the mean control region (figure 3-5, high group). These responses were comparable to those observed for the abnormally high control responses (figure 3-4a). 9 of the patient samples fell in the mean control range and were therefore classified as normal (figure 3-5, medium group). 2 of the patient samples demonstrated low radiation induced apoptosis compared to the mean control region (figure 3-5, low group). These responses were comparable to the abnormally low control responses (figure 3-4a)

Figure 3-3: Spontaneous (0 Gy) levels of apoptosis for control and patient samples

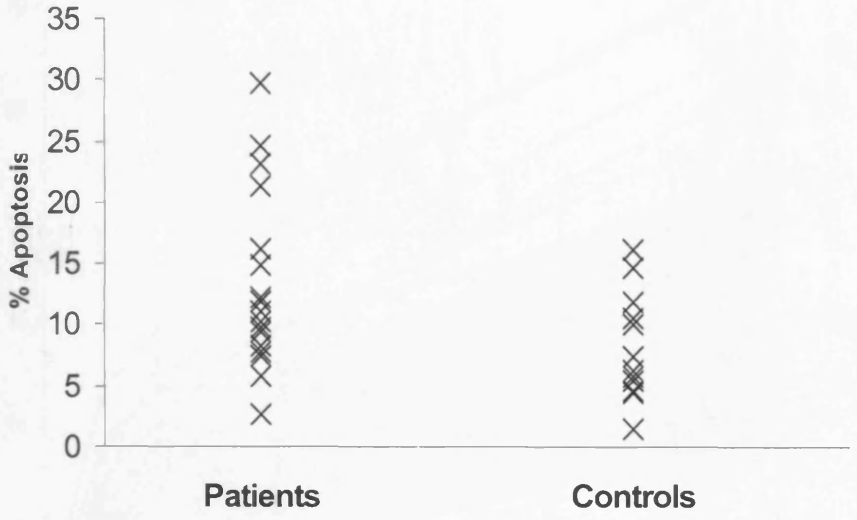

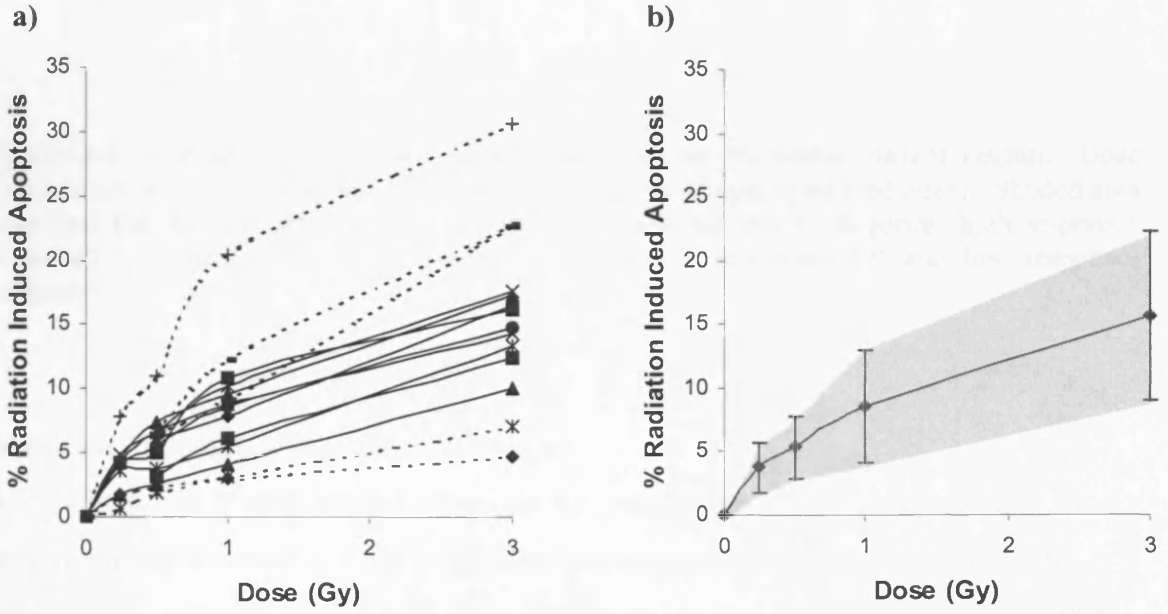

Figure 3-4: Establishment of a mean control response. (a) Radiation induced apoptosis of control lymphocytes. The majority (9/14) of control samples demonstrated radiation induced apoptosis of approximately 10 – 18 % at 3 Gy (solid lines). 5 control samples deviated from this and appeared to have abnormal levels of radiation induced apoptosis (dashed lines). (b) Mean of the 14 control responses. Grey shaded area represents one standard deviation from the mean.

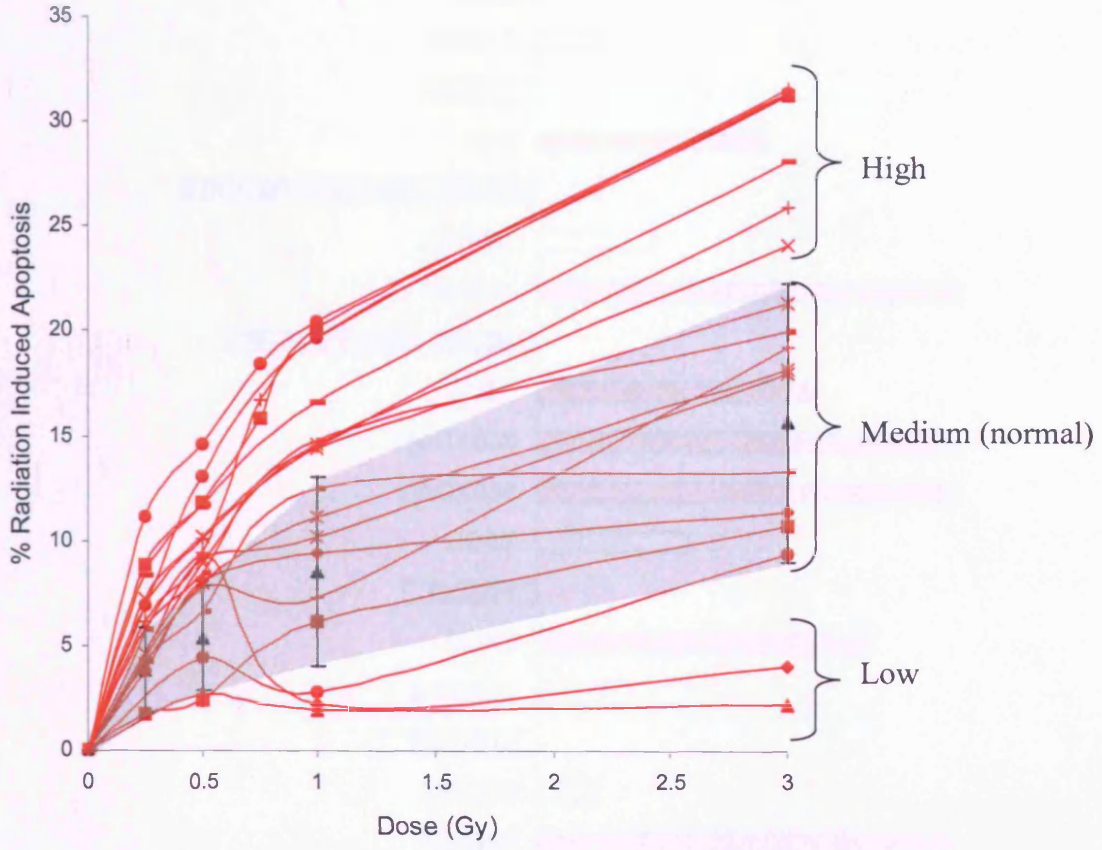

Figure 3-5: Patient dose response curves compared to the mean control region. Dose response curves of radiation induced apoptosis for patient lymphocytes (red lines). Shaded area represents the normal control region. Patient responses fell into 3 categories; high responses compared to control (7), medium responses comparable to control (9) and low responses compared to control (2).

Individual Patient Radiation Sensitivity

After subtraction of spontaneous apoptosis the lymphocyte apoptotic response of 18 patient samples exposed to 3 Gy γ-radiation was expressed as the percentage of the mean control response (figure 3-6). 4 of these samples represented repeat experiments. Patients NG1 and 455BR displayed an abnormally low induction of apoptosis in response to radiation compared to control (figure 3-6, grey bars). This may represent a defect in these patients' lymphocytes that prevents them from mounting a normal physiological response to radiation induced DNA damage. Patients NG2, GOS13, GOS14, GOS7, GOS11 and GOS12 (2 experiments) all show apoptotic responses to radiation within the control region (figure 3-6, clear bars). 2 patients displayed an elevated apoptotic response in the first experiment (figure 3-6, 1)GOS5 and 1)SMM1), but a normal response in the repeat (figure 3-6, 2)GOS5 and 2)SMM1).

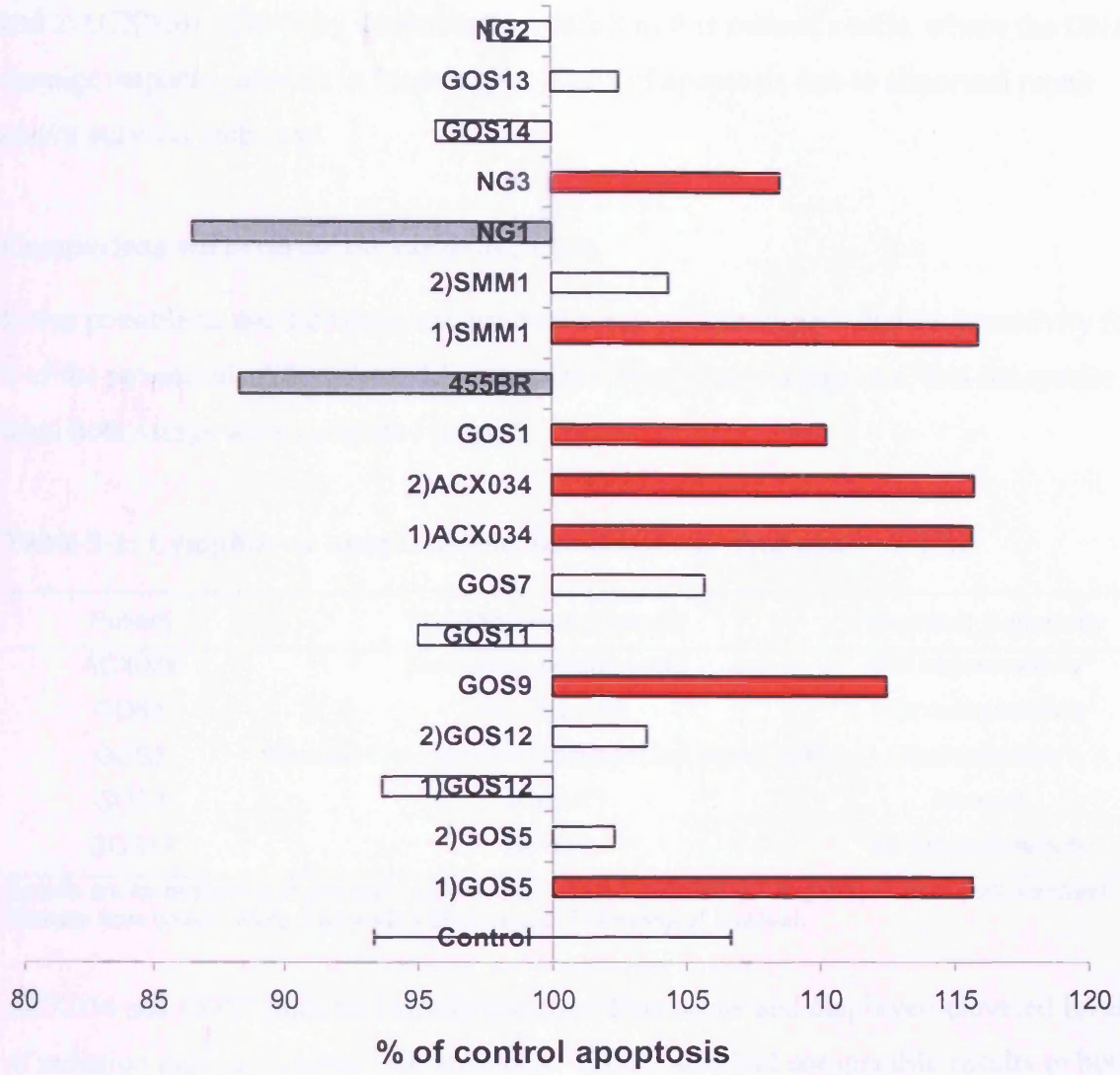

Figure 3-6: Bar chart of patient lymphocyte apoptosis 24 h after 3 Gy γ-radiation. Values are expressed as % of the mean of 14 control responses to 3 Gy γ-radiation. Error bars represent standard deviation. 9 responses fell within (clear bars), 2 below (grey bars) and 7 above (red bars) the normal range. 1) and 2) represent first and repeat experiments respectively.

This made it difficult to determine whether these patients were truly radiosensitive. There may be a factor (e.g. treatment, progression of disease) influencing the radiation response of lymphocytes from these patients that has changed between experiments, and due to the nature of studies using clinical samples we have been unable to control for this. GOS1, NG3 and GOS9 displayed elevated levels of apoptosis in response to radiation after one experiment. Further studies would be required to verify this result in light of the variability between experiments that has been observed. Patient GOS9 was being treated with dexamethasone at the time of this study, which may have affected the lymphocyte apoptotic response. Patient ACX034 is the only patient to show clearly

elevated apoptosis in response to radiation in two experiments (figure 3-6, 1)ACX034 and 2)ACX034). This may demonstrate a defect in this patient's cells, where the DNA damage response network induces higher levels of apoptosis due to abnormal repair and/or survival pathways.

Comparison with fibroblast survival assays

It was possible to use the fibroblast survival assay to determine radiation sensitivity for 5 of the patients also investigated for abnormal lymphocyte apoptosis, and the results from both assays were compared (table 3-1).

Table 3-1: Lymphocyte apoptosis and fibroblast survival assay results

Patient	Lymphocyte Apoptosis	Fibroblast Sensitivity
ACX034	Elevated (2 experiments))	Mild radiosensitivity*
GOS1	Mildly Elevated	Mild radiosensitivity
GOS5	Elevated (1st experiment) Normal (2nd experiment)	Radiosensitive
GOS7	Normal	Normal*
GOS14	Normal	Mild radiosensitivity

Results are for patients with a known result in both assays (Section 4.2 and results from collaborators).
**Results from collaborators (Laboratory of P. Jeggo, University of Sussex).*

ACX034 and GOS1 both had mildly sensitive fibroblasts and displayed elevated levels of radiation induced lymphocyte apoptosis. GOS7 also had comparable results in both assays, demonstrating normal fibroblast and lymphocyte sensitivities. Conversely, GOS14 displayed elevated fibroblast sensitivity to radiation, but normal levels of radiation-induced lymphocyte apoptosis. GOS5 exhibited radiosensitive fibroblasts but had variable lymphocyte apoptosis results, with elevated levels of radiation induced apoptosis in one experiment but normal levels in the repeat. These results demonstrate that a patient with radiosensitive fibroblasts can have a normal result in the lymphocyte apoptosis assay, and suggest that radiation induced lymphocyte apoptosis is not always a consistent measure of fibroblast sensitivity. Patients with radiosensitive fibroblasts generally displayed elevated levels of radiation induced lymphocyte apoptosis, but on two occasions this was not the case. Lymphocyte radiosensitivity therefore showed some correlation with fibroblast radiosensitivity, but does not appear reliable enough to use as a predictive assay.

3.3 Analysis of fibroblast radiosensitivity using CFSE

Colony forming assays have been widely used to identify patients with radiosensitive disorders and are the most reliable method of determining cellular radiosensitivity. These assays evaluate the relative survival of different fibroblast lines 2-3 weeks after irradiation, but give no insight into what happens to cells that survive the initial genotoxic insult but fail to proliferate and form colonies. We therefore developed a novel assay to look at what happens to fibroblasts during the course of a radiosensitivity survival assay, and what mechanisms may be influencing these cell fate decisions. Since there is increasing evidence that fibroblasts do not initiate apoptosis in response to radiation (Chung *et al*, 1998) (Dikomey *et al*, 1998) (Kawabe *et al*, 2001) (Zhang *et al*, 2001), we focused on cell division using the fluorescent dye CFSE.

CFSE is used for analysing cell division by monitoring serial dilution of the dye in labeled cells. CFSE consists of a fluorescein molecule containing two acetate moieties and a succinimidyl ester functional group. In this form, it is membrane permeate and non-fluorescent. After diffusion into the intracellular environment, endogenous esterases remove the acetate groups, rendering the molecule highly fluorescent and non-permeate to the cell. In addition, the succinimidyl ester reacts with free amine groups of intracellular proteins, forming covalent dye-protein adducts. Upon cell division CFSE is partitioned between daughter cells with remarkable fidelity.

3.3.1 Examination of fibroblast cell division using CFSE

There are no studies in the literature reporting the use of CFSE to monitor cell division in primary fibroblasts. Preliminary experiments therefore addressed whether this technique could be used for this purpose. Control cells harvested and fixed immediately after labeling with CFSE displayed a high level of fluorescence (figure 3-7, blue line). When the cells were incubated for 6 days this fluorescence decreased to a level that corresponded to 5-8 divisions in the majority of cells (figure 3-7, red line). The CFSE profile of dividing fibroblasts did not consist of well-defined peaks that represent each cell division as is the case with lymphocytes (Lyons, 2000). This may be explained by the greater heterogeneity in size between individual fibroblast cells compared to lymphocytes. Fibroblasts of a certain division number had a wider range of CFSE fluorescence, and therefore the corresponding peaks merged into a profile with poorer resolution compared to lymphocytes. In order to calculate the percentage of cells that

had achieved a certain number of divisions, the fluorescence level at the peak of the zero division control population was used as a baseline. This value was sequentially halved to calculate the fluorescence intensity that corresponded to cells of any subsequent division number.

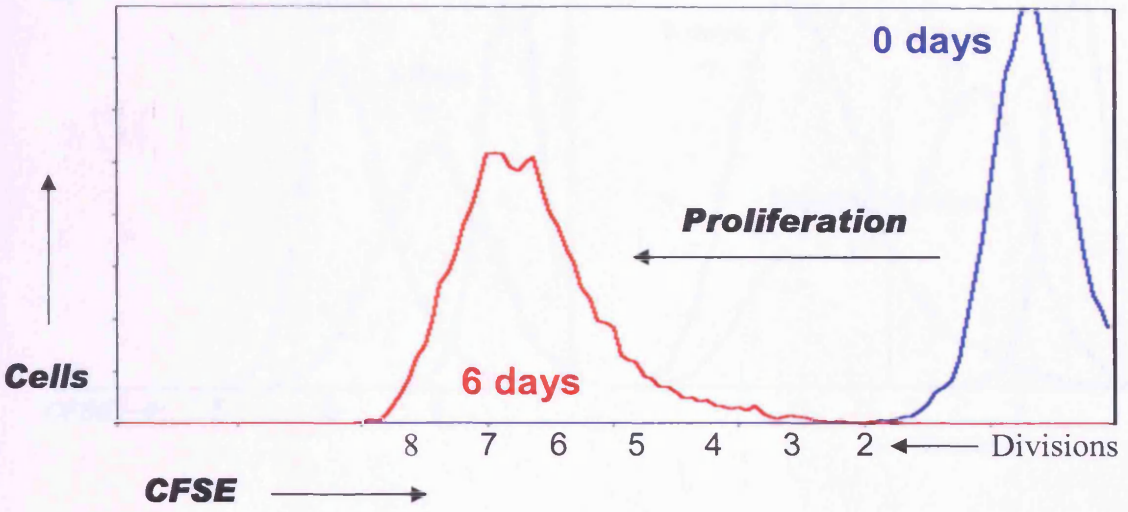

Figure 3-7. CFSE profile of control fibroblast division after 6 days. Cells were labelled with CFSE and fixed in Paraformaldehyde immediately (blue line) or incubated for 6 days (red line). Cells were then analysed by flow cytometry

3.3.2 Examination of control fibroblast division early after irradiation

After we demonstrated that CFSE could be used to monitor primary fibroblast division, we then investigated the effect of γ-radiation on the cell division profiles of control cells. Initial experiments involved labeling and irradiating cells on day 0, incubating the cultures for 3 and 6 days and then performing FACS analysis. Irradiated cells were compared to untreated cultures, and cells that were harvested and fixed immediately after labeling again served as 0 day controls. After a 3 day incubation the majority of cells in irradiated cultures had arrested after only 1 division whereas most of the unirradiated cells had completed 3 divisions (figure 3-8). This is consistent with the initiation of DNA damage checkpoints and the induction of cell cycle arrest. After a 6 day incubation, whereas the majority of unirradiated cells had completed 5 divisions, irradiation induced two distinct populations of cells. Whilst the majority of cells remained arrested after only 1-3 divisions, a minor population of cells had emerged to complete 5 divisions similar to the majority of unirradiated cells (figure 3-8). We hypothesised that these dividing cells may represent the surviving fraction of cells that

would proliferate to form colonies in clonogenic survival assays. We therefore went on to investigate whether this fraction of dividing cells could be used as a measure of radiosensitivity, and compare this endpoint between control cells and a line we knew to be radiosensitive, the Artemis deficient CJ179 line.

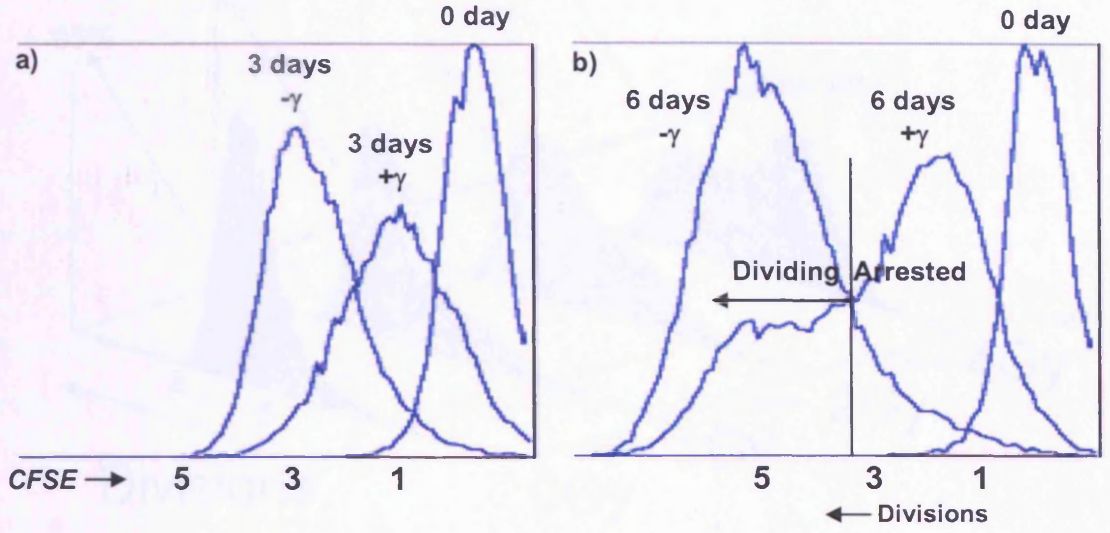

Figure 3-8: Effect of 4Gy γ-radiation on CFSE cell division profiles of control cells incubated for (a) 3 and (b) 6 days. Control 1BR cells were labeled with CFSE and then either mock irradiated (-γ) or exposed to 4Gy γ-radiation (+γ) on day 0. Cells were then incubated for (a) 3 or (b) 6 days after which FACS analysis was performed. (a) 3 days after irradiation the majority of cells had arrested after only 1 division (+γ), whereas mock irradiated cells had divided 3 times (-γ). (b) 6 days after irradiation although the majority of cells remained arrested after only 1-3 divisions, a minor population of cells had divided 5 times similar to mock irradiated cells.

3.3.3 Comparison of early post-irradiation division in control and radiosensitive cells

Control cells were labeled with CFSE and treated with increasing doses of γ-radiation up to 4Gy. Since preliminary experiments suggested that a 6 day incubation may be optimal to distinguish dividing from arrested cells (figure 3-8), this time point was used to asses the relative level of division after irradiation. This was taken as the percentage of cells that completed at least 5 divisions during the 6-day timeframe. In each experiment cells that were harvested and fixed immediately after labeling were used to set the 0 day level of CFSE fluorescence. This accounted for any variation in labeling between individual experiments and different cell lines.

As the dose of radiation increased the percentage of control (1BR) cells that completed 5 divisions decreased, from 85% in unirradiated cultures, to 33% in cells treated with 4Gy γ-radiation (figure 3-9a). This coincided with an equivalent increase in the amount

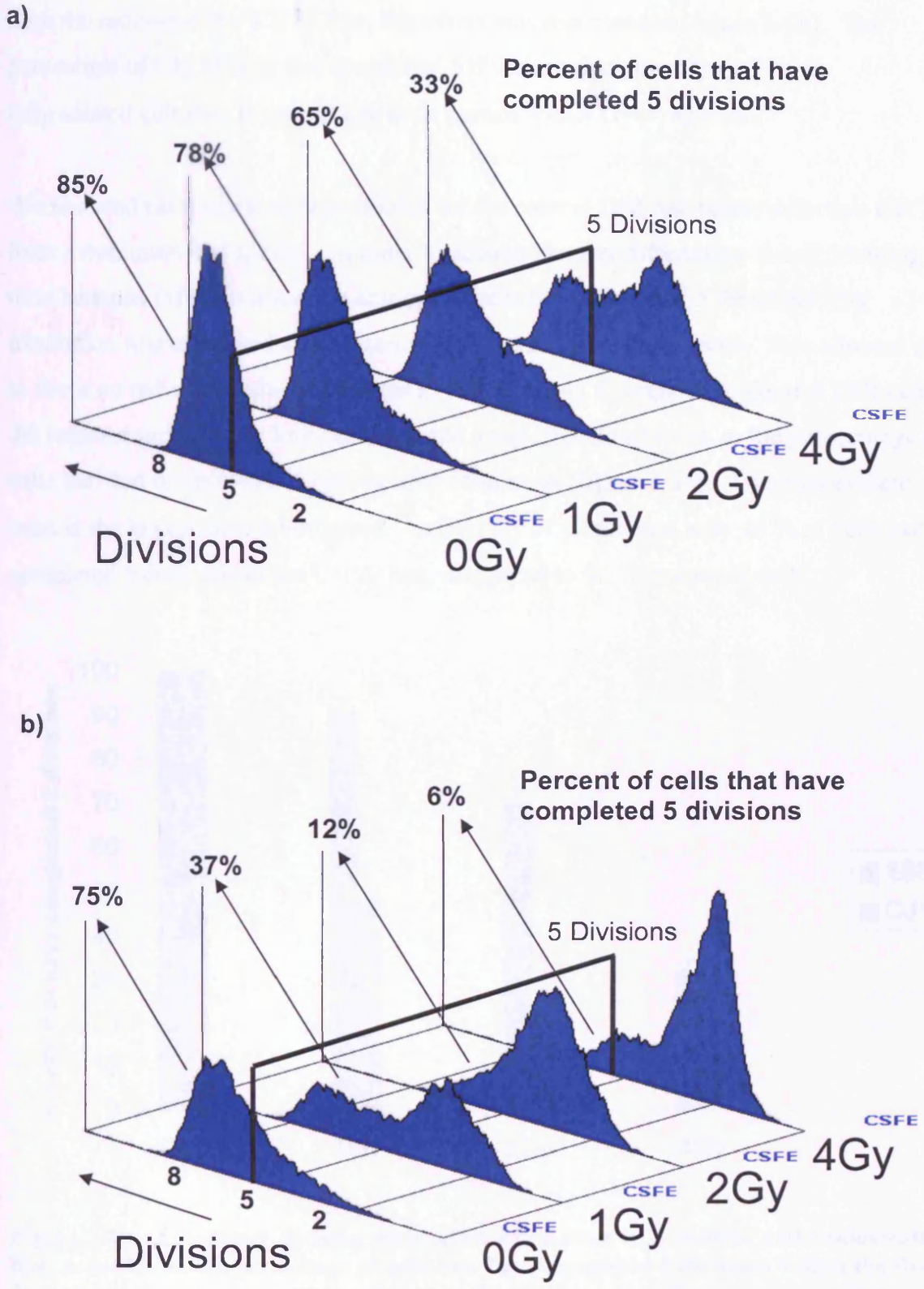

Figure 3-9: CFSE profiles of a) 1BR and b) CJ179 fibroblasts 6 days after irradiation. With increasing doses of radiation more cells arrested after only 1-3 divisions, and the percentage of cells that have completed 5 divisions decreased. This effect was more severe in the radiosensitive CJ179 line (b) than in control cells (a).

of cells arrested after only 1-3 cell divisions. When the same experiment was performed with the radiosensitive CJ179 line, this effect was more severe (figure 3-9b). The percentage of CJ179 cells that completed 5 divisions decreased from 75% in unirradiated cultures, to only 6% in cells treated with 4 Gy γ-radiation.

We repeated early division expermients for the control 1BR and repair defective CJ179 lines a minimum of 3 times. In order to account for any differences in cell doubling time between different lines, the amount of cells that completed 5 divisions after irradiation was expressed as a percentage of that in unirradiated cells. This allowed us to focus on radiation-induced changes in cell division. Compared to control 1BR cells, the radiosensitive CJ179 line demonstrated a significant reduction in the perecentage of cells that had completed 5 divisions after irradiation (figure 3-10). This was evident even at the lowest dose investigated. After 1Gy of γ-radiation only 48 % of cells had completed 5 divisions in the CJ179 line, compared to 91 % in control cells.

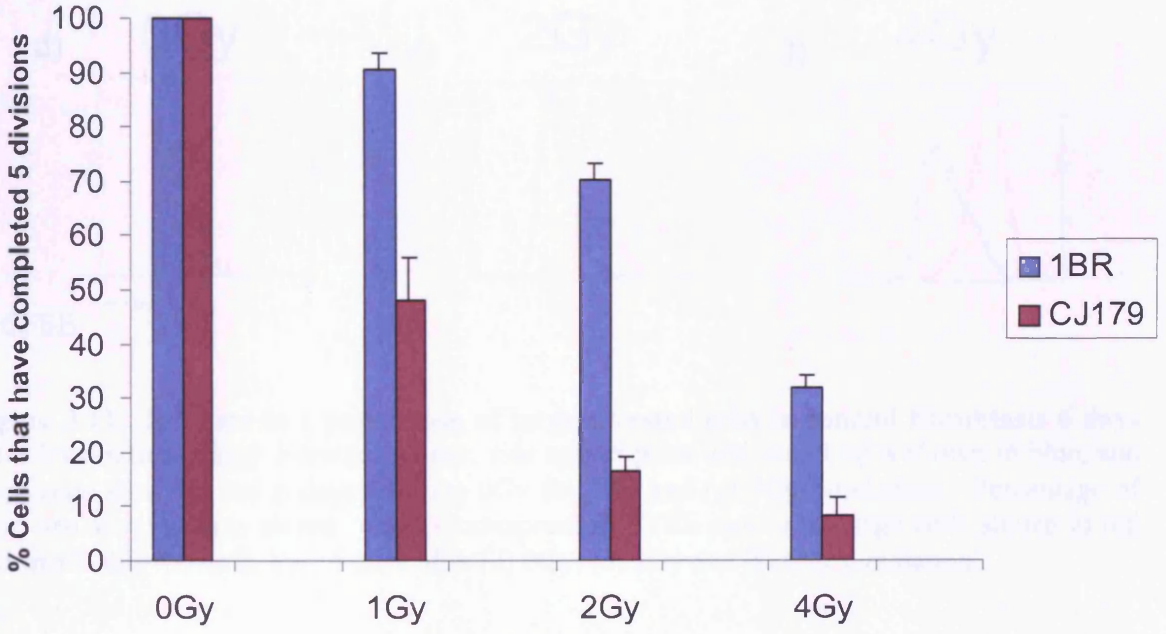

Figure 3-10: Fibroblast division early after irradiation in a control and radiosensitive line; reduction in the percentage of cells that have completed 5 divisions within the first 6 days of irradiation. Compared to control 1BR cells (blue bars) the radiosenstive line CJ179 (red bars) demonstrated a signgificant reduction in the percentage of cells that have completed 5 divisions. This was evident even at the lowest dose of 1 Gy. Error bars represent SEM (standard error of the mean).

During these early division experiments we noticed there was a consistent increase in the proportion of large cells within fibroblast cultures after irradiation, and this was evident in forward scatter (FS) side scatter (SS) plots (figure 3-11). This population of

large cells corresponded to those that had arrested after only 1-3 divisions. The remaining smaller cells within the culture corresponded to dividing cells that had completed at least 5 divisions (figure 3-11, blue cells). Since these cells were labeled with CFSE before irradiation, any increase in large cells with high CFSE fluorescence (i.e. arrested cells) after irradiation can be attributed to the genotoxic treatment, and not that larger cells simply incorporate more CFSE. This is consistent with the induction of a senescent like phenotype, which has been previously described to occur in primary fibroblasts after irradiation (Toussaint *et al*, 2000) and has been monitored using flow cytometry (Gorbunova *et al*, 2003).

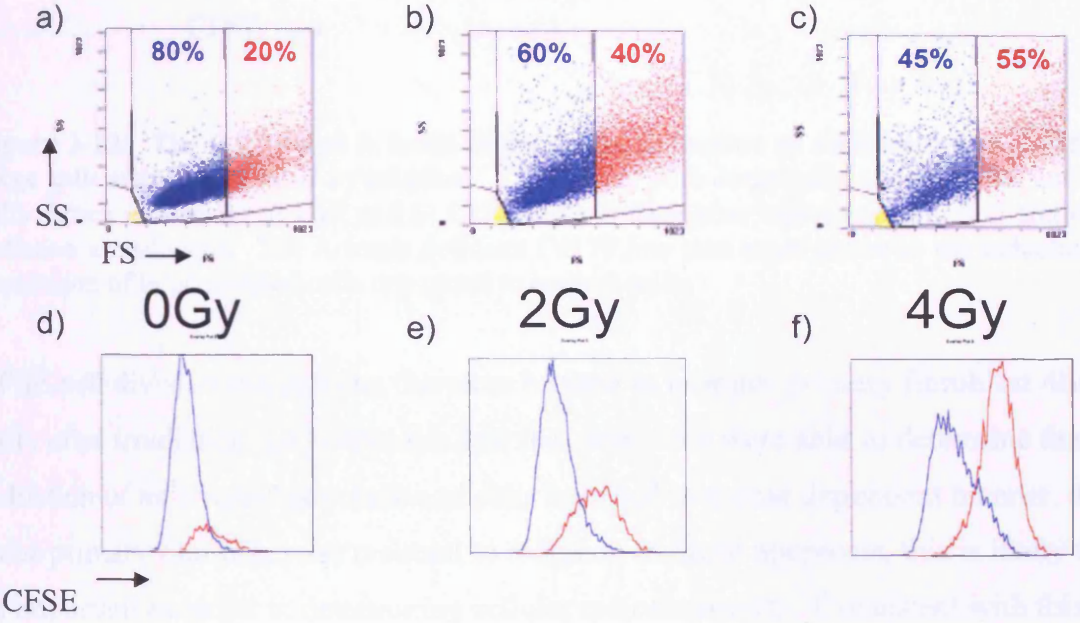

Figure 3-11: Increase in a population of large arrested cells in control fibroblasts 6 days after irradiation. (a-c) Forward scatter, side scatter plots with small cells shown in blue, and large cells shown in red 6 days after (a) 0Gy (b) 2Gy and (c) 4Gy γ-radiation. Percentage of large and small cells is shown. (d-e) Corresponding CFSE plots with large cells shown in red and small cells shown in blue 6 days after (d) 0Gy, (e) 2Gy and (f) 4Gy γ-radiation.

In early division experiments the Artemis deficient CJ179 line demonstrated a significant reduction in the percentage of cells that had completed 5 divisions after irradiation compared to control (figure 3-10). After further analysis we found that this line was much more prone to a radiation-induced population of large arrested cells, and this accounted for the significant reduction in cell division observed compared to the control line (figure 3-12).

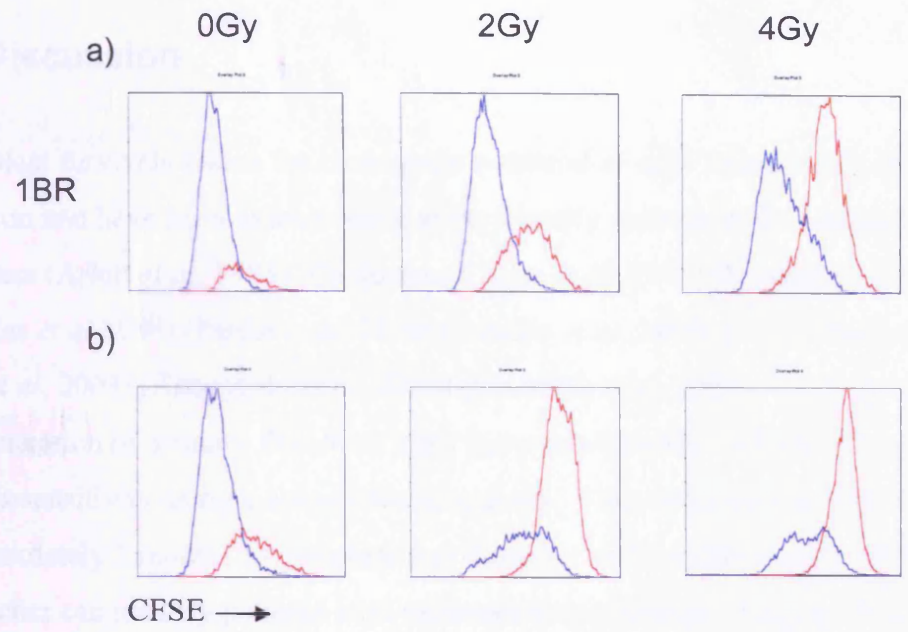

Figure 3-12: The CJ179 line is more prone to the induction of an arrested population of large cells within 6 days of irradiation. CFSE plots with large cells shown in red and small cells shown in blue for a) 1BR and b) CJ179 cells 6 days after treatment with 0, 2 and 4Gy γ-radiation as indicated. The Artemis deficient CJ179 line was more prone to the induction of a population of large arrested cells compared to control cells.

CFSE cell division analysis can therefore be used to monitor primary fibroblast division early after irradiation, i.e. within the first few days. We were able to determine that the induction of an arrested population of cells occurred in a dose dependent manner, and since primary fibroblasts are resistant to radiation-induced apoptosis, this is likely to be an important endpoint in determining cellular radiosensitivity. Consistent with this hypothesis, we were able to identify differences between control and radiosensitivie cells, and discover that the repair defective CJ179 line is more prone to the induction of an arrested population of cells. This resulted in a significant reduction in the proliferation of CJ179 cultures compared to controls after irradiation, and cell cycle arrest may therefore be a key mechanism by which the clonogenic potential of radiosensitive fibroblasts is affected. After irradiation we also observed an increase in the proportion of large cells within fibroblasts cultures, and these cells corresponded to those that had arrested after only 1-3 divisons. The CJ179 line was more prone to this large cell arrest phenotype than control cells, and this suggests that DNA repair defects have a substantial influence on cell survival outcome after irradiation. This assay should allow the further investigation of what happens to fibroblasts during the course of a clonogenic survival assay, and allow a better understanding of what factors may be influencing these cell fate decisions.

3.4 Discussion

Fibroblast survivals assess the clonogenic potential of cells treated with ionizing radiation and have been extensively used to identify patients with radiosensitive disorders (Arlett *et al*, 1988) (Cavazzana-Calvo *et al*, 1993) (Nicolas *et al* 1996) (Nicolas *et al* 1998) (Peake *et al*, 1999) (Riballo *et al*, 1999) (O'Driscoll *et al*, 2001) (Dai *et al*, 2003) (Kobayashi *et al*, 2003) (Noordzij *et al*, 2003). This process involves the generation of primary fibroblast lines from skin biopsies and the subsequent analysis of radiosensitivity using a colony-forming assay. This entire process takes approximately 2 months to complete and therefore restricts the speed with which the researcher can identify patients with radiosensitive disorders. The development of a more rapid screen for cellular radiosensitivity would therefore be beneficial to both the clinician and scientist in the investigation of patients with potential DNA damage response defects.

We investigated whether radiation-induced lymphocyte apoptosis could be used to identify radiosensitive patients more rapidly and less intrusively than the fibroblast survival assay. We found there was a high degree of inter-control variability in radiation induced lymphocyte apoptosis, and 2 patients displayed conflicting results between repeat experiments. This suggested there were external factors we could not control for, such as the subject's current state of health or treatment, which were influencing the apoptotic response of lymphocytes. Lymphocyte cell types have been shown to vary in their apoptotic response to DNA damage (Crompton *et al*, 2001) (Wilkins *et al*, 2002) (Schmitz *et al*, 2003), and differences in cell populations may have contributed the observed variability. Another problem encountered was that most of the patients described are children, and obtaining control samples from healthy children of a similar age is difficult. The lymphocyte apoptotic response has been shown to both decrease (6.5 % less apoptosis with each 10 years of life, Crompton *et al*, 2001) and increase (Schmitz *et al*, 2003) with age using two different experimental designs. Although we tried to obtain control blood from adults under 30, comparing samples from subjects of different ages is not ideal, and may have contributed to inter-control variability.

Patients with radiosensitive fibroblasts generally displayed elevated levels of radiation induced lymphocyte apoptosis, but on two occasions this was not the case. Previous

studies have failed to identify a robust correlation between fibroblast and lymphocyte radiosensitivity (Cole *et al*, 1988) (Geara *et al*, 1992), and it was suggested that tissue-specific characteristics, such as differentiation status, might variably modulate radiosensitivity. We investigated undefined immunodeficient patients that are likely to have abnormal blocks in lymphocyte development. The limited number of lymphocytes that remain in these patients were investigated for radiosensitivity, and may have given varied apoptotic responses depending on their differentiation status, and not just the intrinsic sensitivity of the patient. This may explain some of the observed discrepancies between radiation-induced lymphocyte apoptosis, and radiosensitivity in fibroblast lines; cells that should be of similar differentiation status between different patients.

Since radiation-induced lymphocyte apoptosis can be measured within 24 hours of irradiation, this was a good candidate system to use as a predictive assay for intrinsic cellular radiosensitivity. Despite showing some correlation with fibroblast survival assays, we found that radiation-induced lymphocyte apoptosis can be variable between repeat experiments, and certain control samples from apparently normal individuals may give an elevated response. Therefore, although this assay may have an application in the investigation of a predetermined radiosensitive phenotype, it does not appear reliable enough to use as a pre-screening assay for fibroblast radiosensitivity.

Whilst fibroblast survival assays take a relatively long time to perform, they also give no insight into the fate of cells that survive the initial genotoxic insult, but then fail to proliferate and form colonies. Many reports suggest that primary fibroblasts are not prone to the induction of apoptosis after irradiation (Chung *et al*, 1998) (Dikomey *et al*, 1998) (Kawabe *et al*, 2001) (Zhang *et al*, 2001a), but there is increasing evidence that a substantial fraction of primary fibroblasts are inactivated by a permanent growth arrest (Little *et al*, 1985) (Di Leonardo *et al*, 1994) (Yount *et al*, 1996) (Linke *et al*, 1997) (Williams *et al*, 1997) (Boyle *et al*, 1999) (Azzam *et al*, 2000). We therefore decided to examine the proliferation of primary fibroblasts after irradiation using CFSE cell division analysis. This allowed us to study the early effects of radiation on fibroblast growth, within the first few days of DNA damage.

Early division experiments demonstrated that 3 days after irradiation the majority of control cells had arrested after only 1 division, compared to unirradiated cultures where most cells had completed three cell divisions. This is consistent with the induction of

DNA damage checkpoints and the initiation of cell cycle arrest. 6 days after irradiation whilst the majority of cells remained arrested after only 1-3 divisions, a minor population of cells had emerged to complete 5 divisions similar to the majority of unirradiated cells. These dividing cells may represent the surviving fraction that proliferates to form colonies during clonogenic survival assays. A similar effect of radiation on cell division has been described in colon carcinoma cells, where although a strong damage-induced growth arrest occurred 3 days after treatment with chemotherapeutic agents, a substantial fraction of dividing cells emerged by day 6 after release from the drug (Chang *et al*, 1999b). The extent of this growth arrest was greatly diminished in the absence of p21, and partially reduced on a p53 null background (Chang *et al*, 1999a). A large proportion of the radiation induced growth arrest we have observed in primary fibroblasts is therefore likely to result form the induction of p21, via both p53 dependent and possibly p53 independent pathways.

We next demonstrated that the DSB repair defective CJ179 line is more prone to the induction of an arrested population of cells after irradiation compared to control cells, and this resulted in a reduced amount of cells that completed 5 divisions. An elevated level of radiation-induced chromosome damage has been previously observed in NHEJ defective cells (Badie *et al*, 1995a) (Badie *et al*, 1995b) (Evans *et al*, 1996) (Rooney *et al*, 2003). This could have led to an enhanced activation of the p53 pathway and a higher induction of growth arrested cells. A similar situation was previously described in NHEJ deficient cells undergoing V(D)J recombination, where the persistence of DSBs led to the enhanced activation of p53 and elevated levels of apoptosis (Guidos *et al*, 1996). The persistence of chromosomal damage after V(D)J recombination in lymphocytes or radiation exposure of fibroblasts may therefore lead to an enhanced activation of p53. Since fibroblasts are resistant to apoptosis, this manifests as elevated levels of growth arrest in this system.

Another possibility for enhanced growth arrest in the CJ179 line after DNA damage may be inactivation due to abnormal mitotic events. This involves the induction of chromosome aberrations that lead to the loss of DNA during mitosis in the form of micronuclei 2-3 divisions after irradiation (Joshi *et al*, 1982a) (Joshi *et al*, 1982b) (Joshi *et al*, 1982c) (Savage *et al*, 1989) (Cornforth and Goodwin, 1991). This mode of cell inactivation was shown to be associated with non- or slow- growing fibroblast colonies after irradiation, and would be expected to be more prevalent in Artemis deficient cells

due to the elevated levels of persistent radiation-induced chromosome damage frequently observed in radiosensitive lines (Badie *et al*, 1995a) (Badie *et al*, 1995b) (Evans *et al*, 1996) (Kawata *et al*, 2003) (Rooney *et al*, 2003).

We also observed an increase in the proportion of large cells within irradiated cultures, and these cells corresponded to those that had arrested after only 1-3 divisions. This is consistent with the induction of a senescent like phenotype that has been observed after exposure to radiation (Di Leonardo *et al*, 1994) (Oh *et al*, 2001), and previous reports have described a similar increase in forward scatter when analysing senescent fibroblasts by flow cytometry (Gorbunova *et al*, 2003). The repair defective CJ179 line was more prone to this endpoint than control cells, and due to the high level of residual chromosome damage described above may be more prone to the induction of a stress induced premature senescence (Toussaint *et al*, 2000). This is consistent with a model proposed by Naka *et al* (2004) in which DNA damage initially triggers the G1/S checkpoint by the activation of p53 by ATM. If DNA damage cannot be repaired within a few days of irradiation, then the cells undergo SIPS to prevent accumulation of genetic mutations. Since CJ179 cells are defective in DSB repair, this line is unable to deal with the same level of damage as controls and is therefore more prone to the induction of SIPS. This mechanism may be an important determinant of cellular radiosensitivity since a significant correlation has been observed between radiation-induced differentiation and fibroblast survival (Lara *et al*, 1996).

Since this analysis focused on the live cells that remained 6 days after irradiation, these experiments would not detect any differences in mitotic death associated with lethal chromosome damage that had occurred within the first few days of irradiation. This mode of cell inactivation was thought to be the most important process leading to a loss of proliferative capacity in irradiated cells (Cornforth and Bedford, 1987), but recent results have suggested that p53 dependent arrest accounts for at least half of the inactivation in irradiated primary fibroblasts (Borgmann *et al*, 2004). Analysis of cell division would be expected to identify arrested cells resulting from both p53 dependent processes and gross chromosomal damage, but may not account for any cells that were killed by mitotic death. Whilst this caveat may result in an underestimation of radiosensitivity, this assay was able to identify major differences in post radiation cell division between a wild type and NHEJ deficient line. This suggests that in primary fibroblasts growth arrest is one of the major cell fates after irradiation and is an

important determinant of cellular radiosensitivity. Further analysis of the distinct populations of dividing and growth arrested cells after irradiation may improve our understanding of the factors that influence cell fate decisions in response to DNA damage.

Chapter 4: Identification of radiosensitive patients and further investigation

4.1 Background

A main aim of this project was to identify undefined immunodeficient patients that demonstrated cellular radiosensitivity. Fibroblast survival assays have been widely used for this purpose (Arlett *et al*, 1988) (Cavazzana-Calvo *et al*, 1993) (Nicolas *et al* 1996) (Nicolas *et al* 1998) (Peake *et al*, 1999) (Riballo *et al*, 1999) (O'Driscoll *et al*, 2001) (Dai *et al*, 2003) (Kobayashi *et al*, 2003) (Noordzij *et al*, 2003) and involve the generation of primary fibroblast lines. We took skin biopsies from undefined patients with low T- and B- lymphocyte function and established primary fibroblast lines, which were then assessed for radiosensitivity using a colony-forming assay. Primary fibroblasts were treated with increasing doses of γ-radiation and incubated for 2-3 weeks until surviving colonies were visible to the naked eye. Colonies were then stained and counted which allowed the relative survival after irradiation to be calculated. Patient lines were compared to control cells and known radiosensitive mutants in order to classify radiosensitivity. This allowed the identification of a group of patients that demonstrated significant radiosensitivity compared to controls.

Section 3.2 described the development of a novel radiosensitivity assay that focused on cell division with the first few days of irradiation. Using CFSE we were able to monitor cell division early after irradiation and identified differences between control and radiosensitive cells in relation to survival outcome. This assay has the potential to investigate undefined radiosensitive lines and identify what happens to cells that survive the initial genotoxic insult but do not grow to form colonies in survival assays. Cell division analysis was therefore applied to the two undefined lines that demonstrated the most pronounced radiosensitivity in survival assays in order to gain some insight into the fate of these radiosensitive cells after irradiation.

4.2 Identification of radiosensitive patients

4.2.1 Generation of primary fibroblasts

Primary skin fibroblast lines were established from 19 undefined immunodeficient patients. All of these lines grew well with a similar doubling time to that of control cells except the GOS5 line. This line displayed poor growth and premature senescence at passage 9.

4.2.2 Fibroblast radiosensitivity survival assays

Primary fibroblast lines were investigated for radiosensitivity using the fibroblast survival assay described in section 2. This assay focuses on surviving colony formation after an incubation period of 2-3 weeks post irradiation. Two control lines (1BR and 48BR) demonstrated normal levels of survival after exposure to ionising radiation (figure 4-1). A typical AT cell line (A-T1BR) demonstrated severe radiosensitivity similar to that previously described (Taylor *et al*, 1975). CJ179 is a line derived from a patient with a large genomic deletion in the Artemis DSB repair gene that results in the absence of transcript and protein. These cells can therefore be considered as Artemis null (P. Jeggo, personal communication), and this line demonstrated an intermediate level of radiosensitivity (figure 4-1).

F96 cells are from an undefined immunodeficient patient and were previously shown to be radiosensitive (Peake *et al*, 1999). These cells demonstrated intermediate levels of radiosensitivity similar to the repair defective CJ179 cells. 2BN cells, from another undefined immunodeficient patient, are known to be extremely sensitive to ionising radiation and defective in DSB repair (Dai *et al*, 2003). This line demonstrated severe radiosensitivity that was more pronounced than AT cells (figure 4-1)

20 undefined immunodeficient patients were investigated for damage response defects using the fibroblast survival assay. As a population this group of 20 immunodeficient patients was not significantly more radiosensitive than the control population ($p=0.1$). This suggests that undefined immunodeficient patients do not represent a distinct population compared with normal individuals with respect to radiosensitivity. Moreover, patients demonstrated a variety of sensitivities ranging from normal to

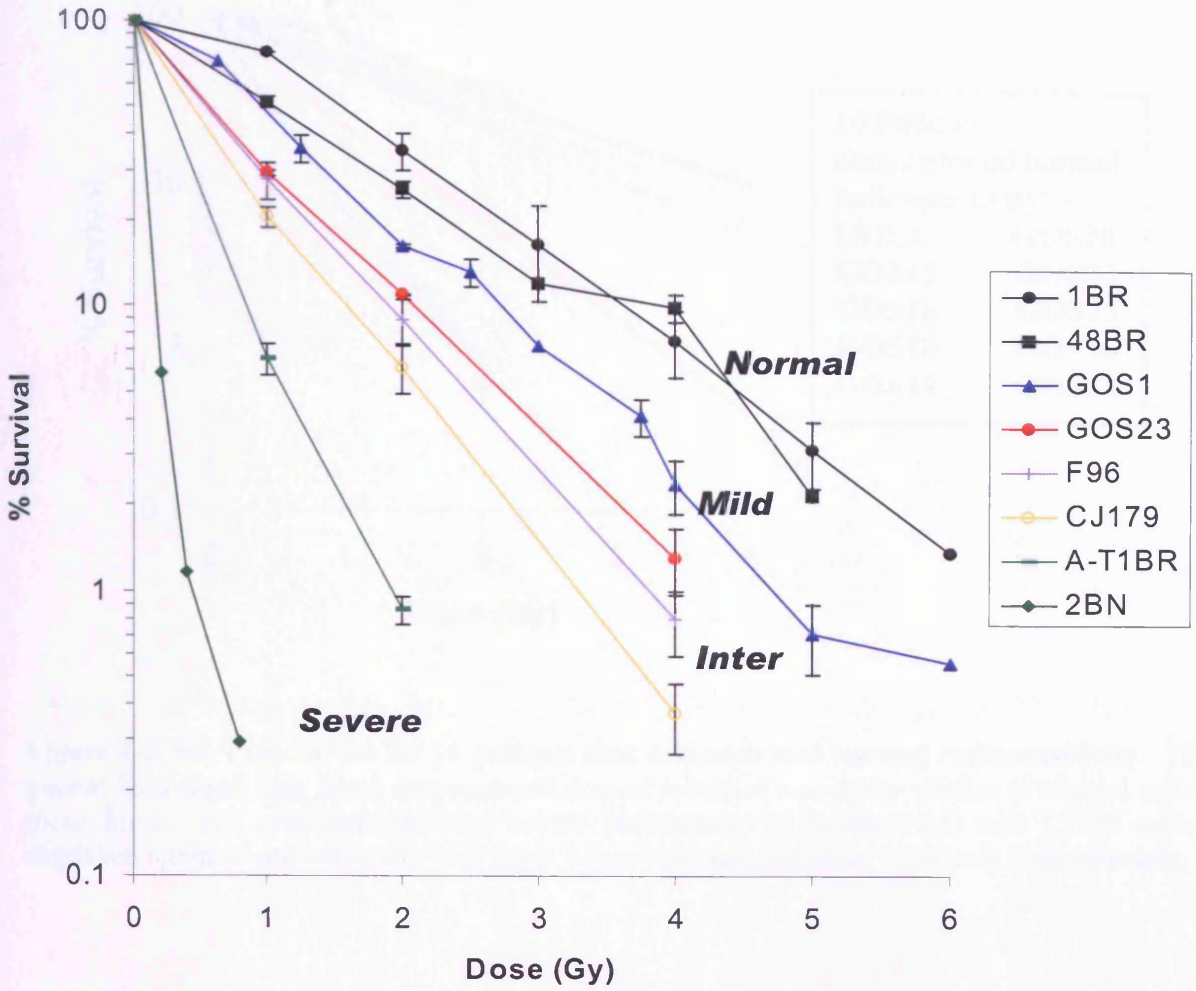

Figure 4-1 Sensitivity of control, mutant and patient fibroblasts to ionising radiation. Exponentially growing fibroblasts were treated with γ-radiation and plated immediately. Patient cells were compared to normal controls (1BR and 48BR), a typical AT cell line (A-T1BR), and a DSB repair deficient line (CJ179). Cells demonstrated normal, mild, intermediate or severe levels of radiosensitivity. Error bars represent SEM.

clearly radiosensitive. Subtle genetic differences and polymorphisms are likely to account for mild differences in radiosensitivity near to the control range, whilst more pronounced radiosensitivity is more likely to result from mutations that impair damage response protein function. On an individual level, we attempted to identify such patients by comparing the survival of each patient line to that of control cells after exposure to 4 Gy γ-radiation using a student t-test to see if the survival levels observed were statistically significant. Using this criterion, 10 patient lines demonstrated normal levels of sensitivity that were not significantly different from control cells after 4 Gy γ-radiation (figures 4-2 and 4-3).

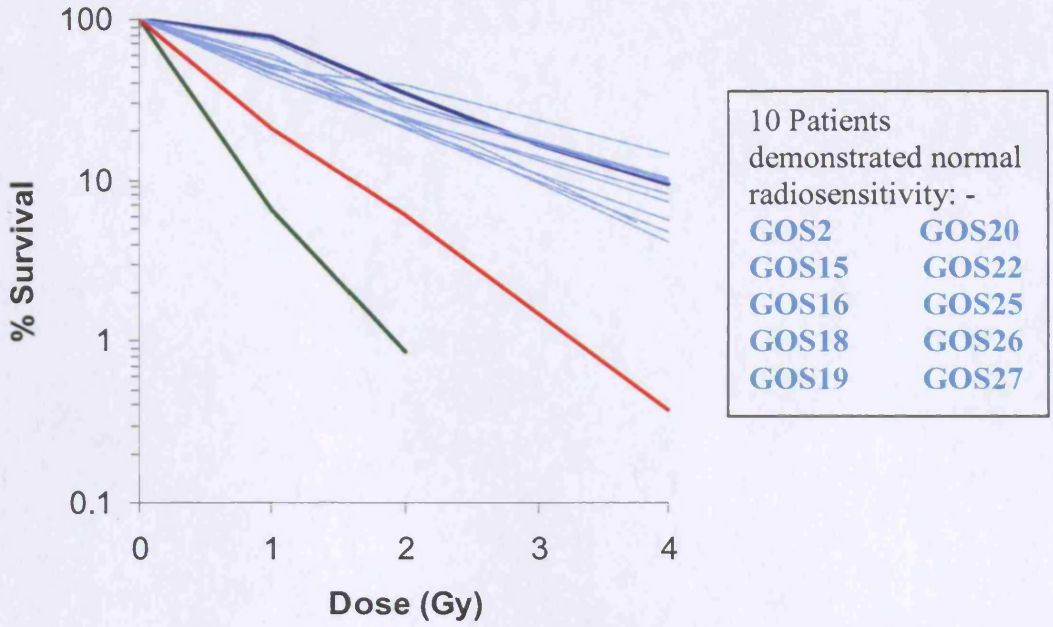

Figure 4-2: Survival curves for 10 patients that demonstrated normal radiosensitivity. 10 patient lines (light blue lines) demonstrated normal levels of sensitivity similar to control cells (blue line). AT cells demonstrated severe radiosensitivity (green line) and CJ179 cells displayed intermediate sensitivity (red line). Lines represent the mean of at least 2 experiments.

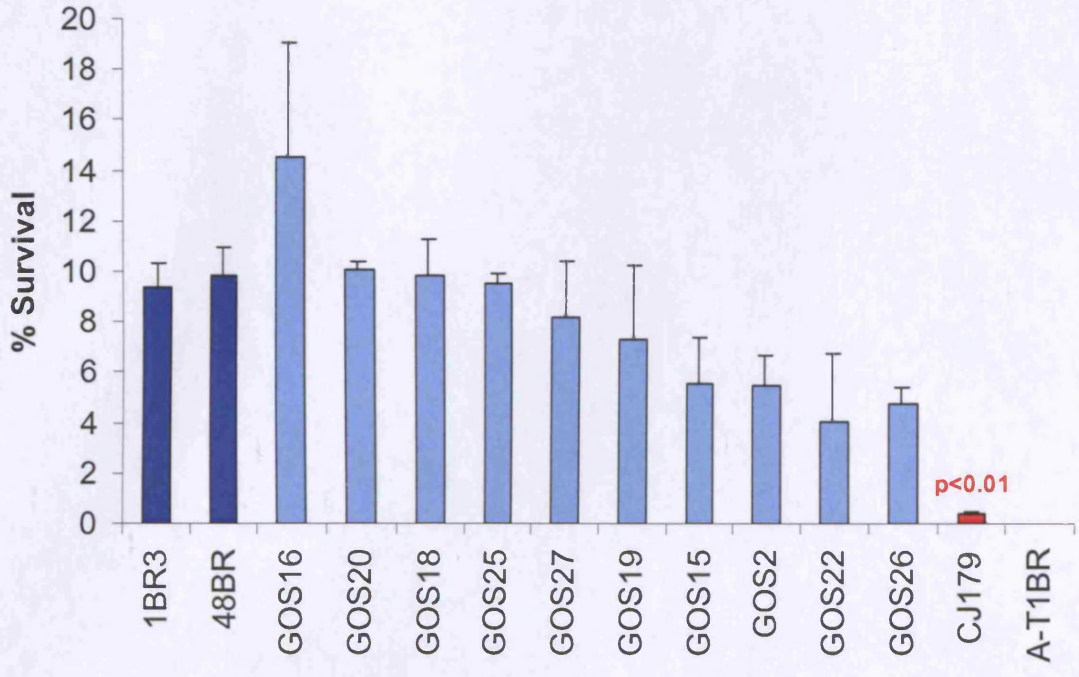

Figure 4-3: Bar chart of relative survival after 4 Gy γ-radiation for 10 patients that demonstrated normal radiosensitivity: 10 patients demonstrated normal sensitivity (light blue bars) that was not significantly different from controls (blue bars). CJ179 cells (red bar) displayed significantly less survival compared to the control lines. Error bars represent SEM.

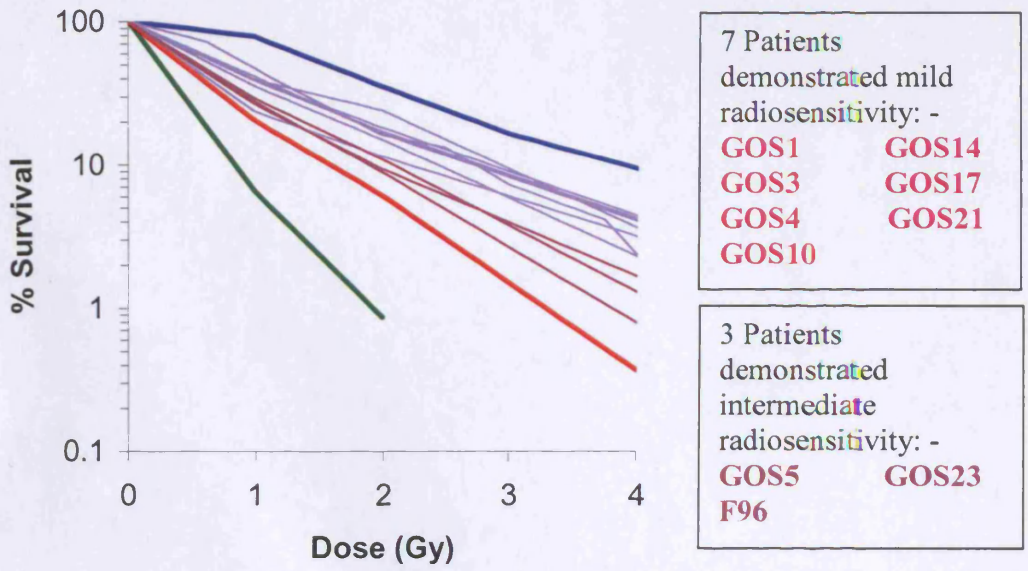

Figure 4-4: Survival curves for 10 patients that demonstrated significant radiosensitivity. 7 patient lines demonstrated mild radiosensitivity (light purple lines) and 3 patient lines displayed intermediate sensitivity (dark purple lines) compared to control cells (blue line). AT cells demonstrated severe radiosensitivity (green line) and CJ179 cells displayed intermediate sensitivity (red line). Lines represent the mean of at least 2 experiments.

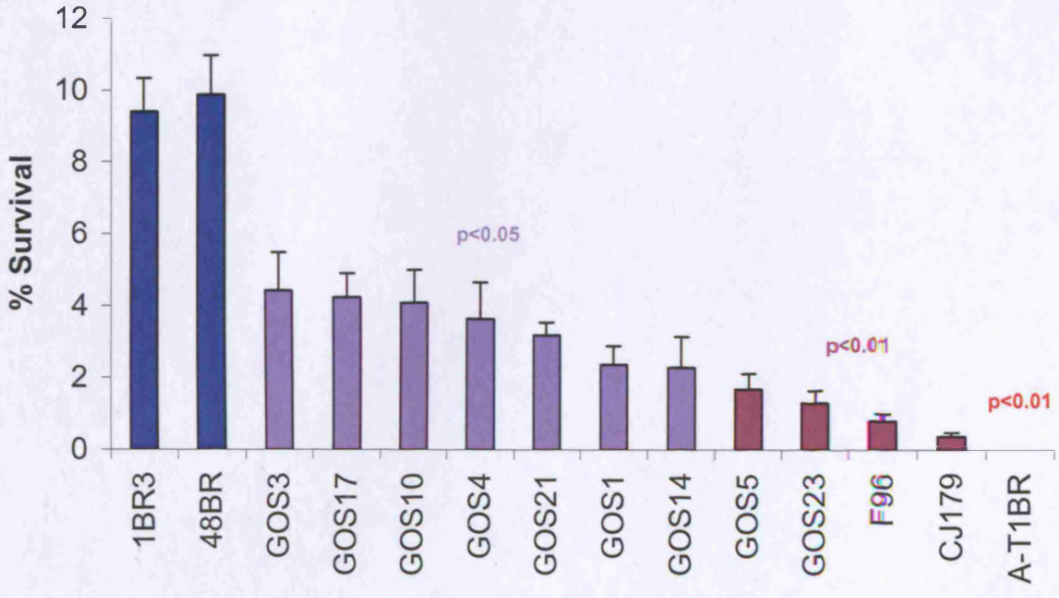

Figure 4-5: Bar chart of relative survival after 4 Gy γ-radiation for 10 patients that demonstrated significant radiosensitivity: 7 patients demonstrated mild radiosensitivity (light purple bars, $p<0.05$) and 3 patients displayed intermediate radiosensitivity (dark purple bars, $p<0.01$) compared to control cells (blue bars). CJ179 cells (red bar) displayed intermediate levels of radiosensitivity (red bar, $p<0.01$). No patients demonstrated severe radiosensitivity similar to that of the A-T1BR line. Error bars represent SEM.

10 patient lines demonstrated significant radiosensitivity compared to control cells (figures 4-4 and 4-5). This effect ranged from a mild sensitivity that was significantly different to control cells after 4Gy γ-radiation, to a more pronounced phenotype comparable to the Artemis defective CJ179 line. These radiosensitive patient lines were grouped into two categories of sensitivity according to the severity of this phenotype. 7 patients were defined as mildly radiosensitive compared to control cells (figures 4-4 and 4-5, light purple series, $p<0.05$) and 3 patients, with a more pronounced phenotype, were classified as displaying intermediate sensitivity (dark purple series, $p<0.01$) that was similar to that of the CJ179line. No patients demonstrated a severe radiosensitivity that was observed in the A-T1BR line.

Using the fibroblast survival assay we have identified a group of 10 undefined immunodeficient patients that demonstrated cellular radiosensitivity (table 4-1). These patients may therefore have defects in the response to DNA damage. The severity of radiosensitivity observed may reflect the extent to which the underlying mutation affects the repair and/or survival processes initiated by ionising radiation.

Table 4-1: Radiosensitivity of 20 undefined immunodeficient patients

Radiosensitivity	No. of patients	Comparable mutant	Cell line example
Normal	10	Controls	1BR, 48BR
Mild +	7	-	GOS1, GOS14
Intermediate ++	3	Artemis	GOS5, F96
Severe +++	0	ATM	-

4.3 Investigation of radiosensitive fibroblasts using CFSE cell division analysis

In chapter 3 we described the development of a novel assay for assessing the radiosensitivity of primary fibroblasts that focused on cell division within the first few days of irradiation. This technique allowed us to gain some insight into what may be happening to fibroblasts during the course of a clonogenic survival assay, and what happens to a large proportion of cells that do not survive to form colonies in radiosensitive lines. In order to further investigate the radiosensitive phenotype of the identified patient lines, we subjected these cells to CFSE cell division analysis after

irradiation. This was performed for the two undefined lines that demonstrated the most pronounced radiosensitivity, F96 and GOS5. Results for these patient lines were compared to the previously characterised CJ179 line, and the AT line A-T1BR.

4.3.1 Investigation of early cell division after irradiation

As described previously, cells were labelled with CFSE and irradiated on day 0, then analysed by FACS after a 6-day incubation. Compared to control 1BR cells, the radiosensitive CJ179 and A-T1BR lines demonstrated a significant reduction in the perecentage of cells that completed 5 divisions after irradiation (figure 4-6). The magnitude of this effect was similar between the two radiosensitive lines, which is in contrast to survial results where AT cells were considerbly more sensitive than the CJ179 line. The GOS5 line also demonstrated a reduced amount of cells that completed 5 divisions compared to controls. This effect was slightly less than that observed for the CJ179 line, and this is in agreement with survival results where the GOS5 line was slightly less radiosensitive than CJ179 cells (figure 4-5).

In fibroblast survival assays the F96 line demonstrated the most severe radiosensitivity compared to all other undefined patient lines (figure 4-5). Conversely, analysis of early cell division demonstrated only a modest reduction in the percentage of F96 cells that had completed 5 divisions after irradiation (figure 4-6). This mild reduction was significantly less than that observed for the CJ179 line at doses of 1 (CJ179 48%, F96 81% cells ≥5 divisions) and 2 Gy (CJ179 16%, F96 49% cells ≥5 divisions), and suggested that F96 cultures were initially able to recover from low doses of radiation relatively well.

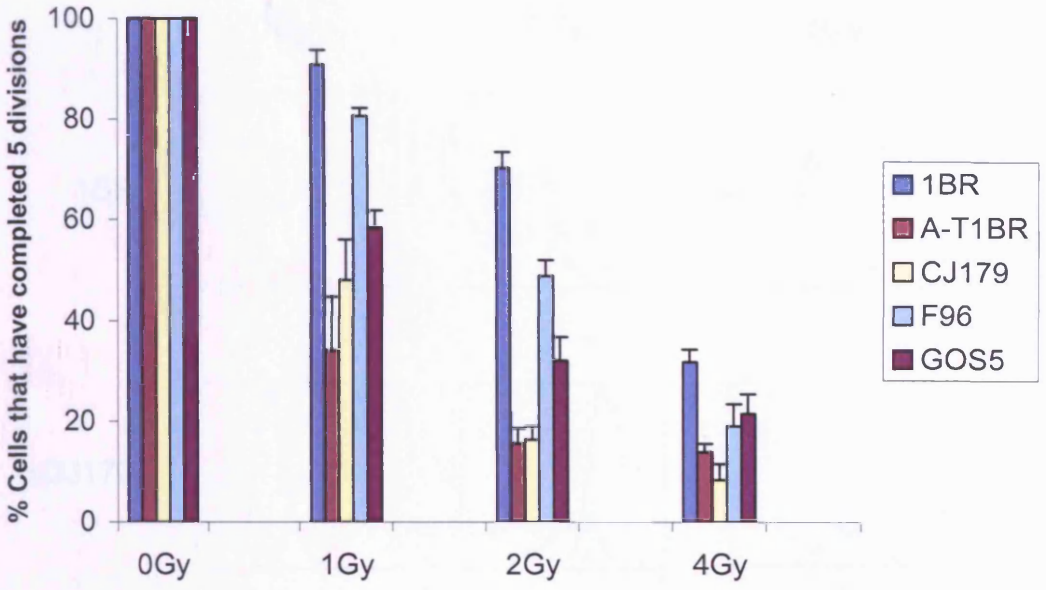

Figure 4-6: Early division experiments with radiosensitive fibroblasts; Reduction in the percentage of cells that have completed 5 divisions within the first 6 days of irradiation. CJ179 (cream bars) and A-T1BR (dark red bars) cells demonstrated an abnormal block on proliferation that was similar in magnitude between the two lines. GOS5 cells (purple) were also sensitive to this endpoint, although this effect was slightly less pronounced than that of the known mutant lines. F96 cells (pale green) demonstrated only a modest reduction in the percentage cells that have completed 5 divisions compared to controls. Error bars represent SEM.

In early division experiments with the CJ179 line, the significant reduction in the percentage of cells that had completed 5 divisions compared to controls was associated the induction of a population of large arrested cells (figure 3-12). This accounted for the significant reduction in cell division observed, and is consistent with the induction of a Stress Induced Premature Senescence (SIPS) that has been described in cells following irradiation (Toussaint *et al*, 2000) and has been monitored using FACS (Gorbunova *et al*, 2003). The GOS5 line was similar to the CJ179 line in this respect, and demonstrated a similar tendency for this radiation-induced population of large arrested cells (figure 4-7). In contrast, the F96 line displayed a more modest reduction in early cell division than the CJ179 (figure 4-6), and was not as prone to the induction of a population of large arrested cells (figure 4-7)

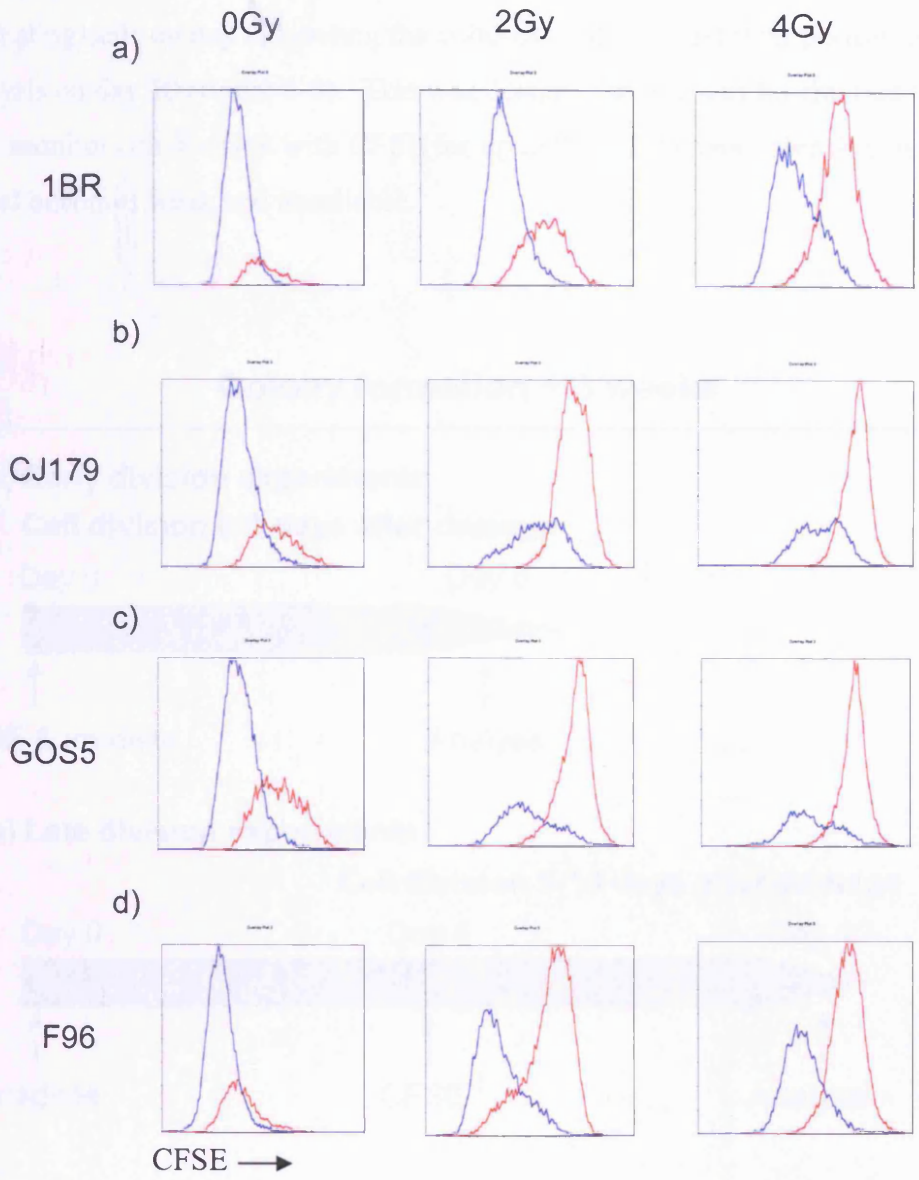

Figure 4-7: Radiosensitive lines are more prone to the induction of an arrested population of large cells within 6 days of irradiation. CFSE plots with large cells shown in red and small cells shown in blue for a) 1BR, b) CJ179, c) GOS5 and d) F96 cells 6 days after treatment with 0, 2 and 4 Gy γ-radiation as indicated. The Artemis deficient CJ179 line and undefined GOS5 line were more prone to the induction of a population of large arrested cells compared to control cells. The undefined F96 line was slightly more susceptible to this endpoint compared to controls, but not as sensitive as the CJ179 and GOS5 lines.

4.3.2 Investigation of late cell division after irradiation

Since we knew F96 cells were radiosensitive but observed only a modest reduction in early cell division compared to control, we went on to examine late cell division. This was intended to identify any abnormal blocks on cell division that occurred after the 0-6 day timeframe already examined. Late division experiments therefore focused on a

subsequent timeframe, between 5 and 10 days after irradiation. This involved irradiating cells on day 0, labeling the cultures on day 5, and then performing FACS analysis on day 10 (figure 4-8). This was designed to account for the fact that you can only monitor cell division with CFSE for up to 8-10 divisions, after this the fluorescent signal becomes weak and unreliable.

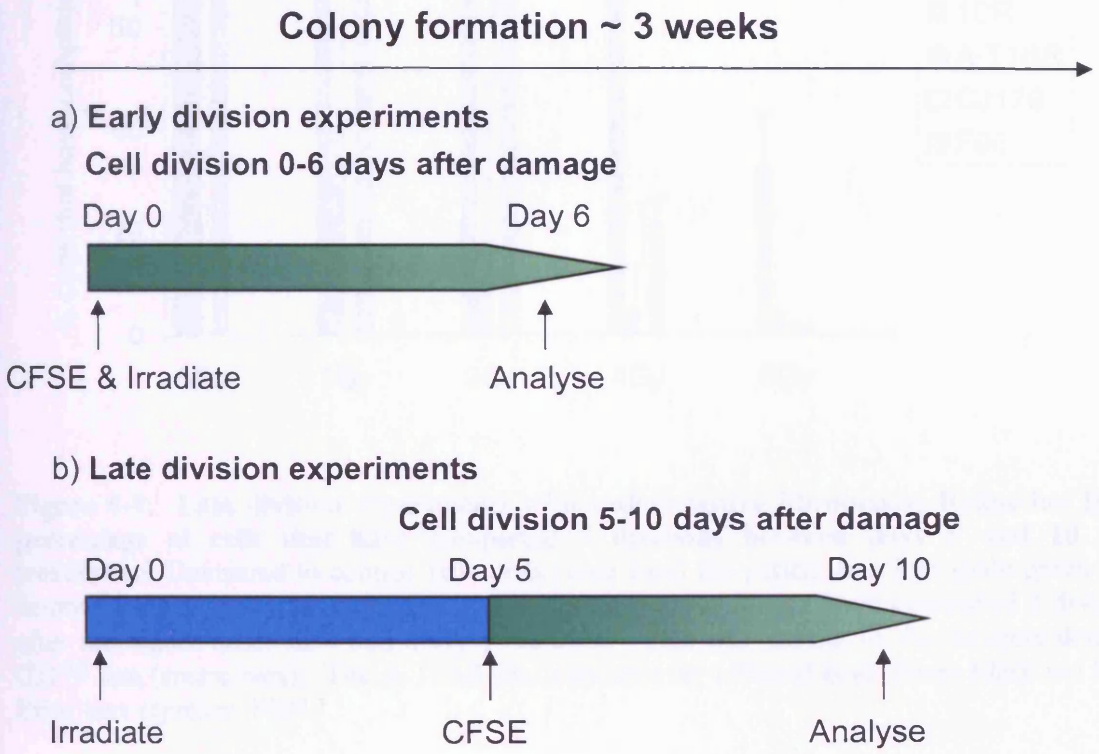

Figure 4-8: A combination of early and late CFSE division experiments examined cell division within the first 10 days of irradiation. a) Early division experiments focused on proliferation between 0 and 6 days after irradiation. b) Late division experiments focused on proliferation between 5 and 10 days after irradiation.

In late division expermients A-T1BR cells displayed a significant reduction in the percentage of cells that had completed 5 divisions at all doses compared to the control line 1BR (figure 4-9). At the lower doses of 1 and 2 Gy of γ-radiation CJ179 cells were able to recover from showing a significant reduction in proliferation in early division experiments (figure 4-6) to near control levels of division in this later timeframe. This demonstrates that unlike AT cells, CJ179 cultures are able to recover from low doses of radiation, and is compatible with survival assay results where they demonstrated a less severe phenotype than the A-T1BR line. At higher doses the CJ179 line was unable to

recover with only 2% of cells that had completed 5 divisions after 6 Gy γ-radiation compared to 33% in control cells.

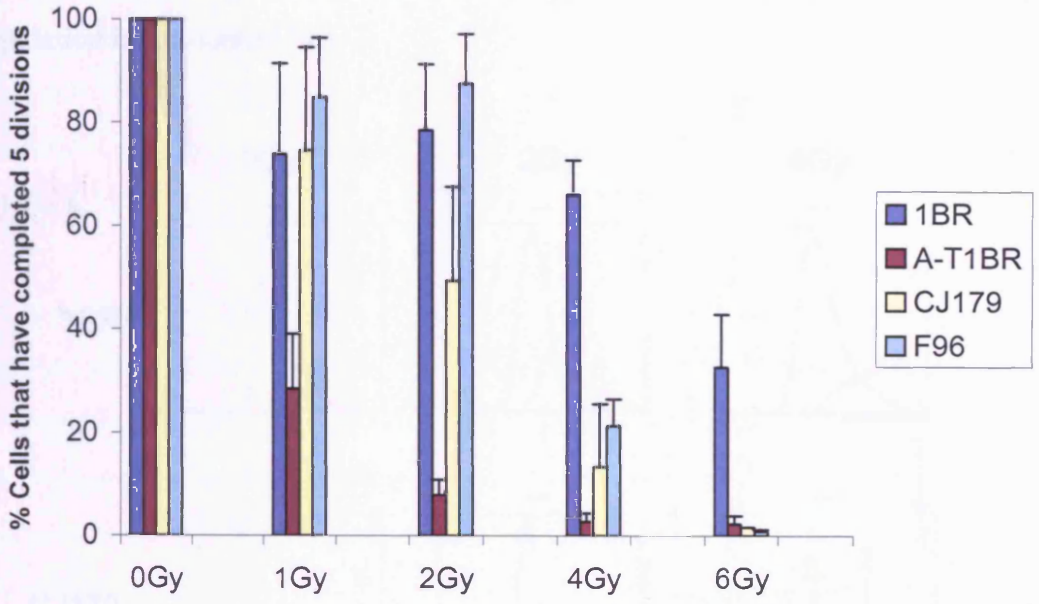

Figure 4-9: Late division experiments with radiosensitive fibroblasts; Reduction in the percentage of cells that have completed 5 divisions between days 5 and 10 after irradiation. Compared to control 1BR cells (blue bars) the patient line F96 (pale green bars) demonstrated a significant reduction in the percentage of cells that have completed 5 divisions after the higher doses of 4 and 6 Gy γ-radiation. This was similar to the Artemis deficient CJ179 line (cream bars). The A-T1BR line was severely affected at all doses (dark red bars). Error bars represent SEM.

Similar to CJ179 cells the F96 line was able to recover to control levels of proliferation after 1 and 2 Gy γ-radiation in this later timeframe (figure 4-9). At the higher doses of 4 and 6 Gy γ-radiation there was a significant reduction in the percentage of cells that had completed 5 divisions compared to controls (1BR 4 Gy; 66%, 6 Gy; 33%. F96 4 Gy; 21%, 6 Gy; 1% cells ≥5 divisions), and this was comparable to that for the CJ179 line (CJ179 4 Gy; 13%, 2 Gy; CJ179 2% cells ≥5 divisions). F96 cells were therefore similar to the CJ179 line in this late division timeframe, recovering well from low doses of γ-radiation but meeting with a significant block on proliferation at higher doses. These results suggested that although F96 cells can cope relatively well with the early effects of low doses of radiation, once a certain threshold is reached these cells are ultimately unable to recover. When we examined the morphological phenotype of cells in late division experiments we found that whereas at 4 Gy γ-radiation control cells recovered and produced a major population of small dividing cells, the CJ179 cultures

were still dominated at this point by large arrested cells (figure 4-10, population 1). We also noted a minor population of small cells that had ceased to divide after approximately one division (population 2), along with another minor population of small dividing cells (population 3) that corresponded to the dominant proliferating population in the control line.

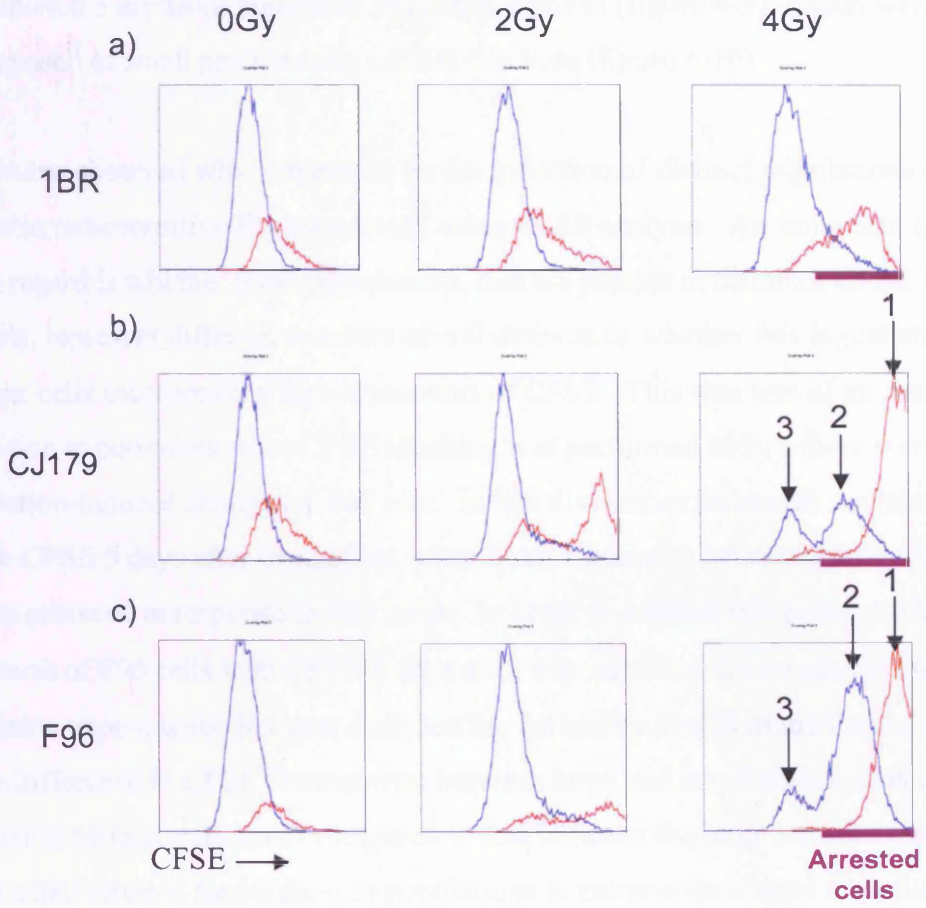

Figure 4-10: Radiation induces distinct populations of arrested cells in radiosensitive fibroblast lines 10 days after irradiation. CFSE plots with large cells shown in red and small cells shown in blue for a) 1BR, b) CJ179 and c) F96 cells 10 days after treatment with 0, 2 and 4Gy γ-radiation as indicated. Cells were labeled with CFSE 5 days after irradiation. After 2 Gy γ-radiation small dividing cells that have completed 5 divisions dominated 1BR, CJ179 and F96 cultures at this late time point. After 4 Gy γ-radiation the radiosensitive lines (CJ179 and F96) produced distinct populations of large (population 1) and small (population 2) arrested cells, along with a minor population of small dividing cells (population 3). CJ179 cells were more prone to a large cell arrest phenotype (population 1), compared to F96 cultures that contained a substantial proportion of small arrested cells (population 2).

Although the late division profile of the F96 line also contained 3 distinct populations of cells after 4 Gy γ-radiation (figure 4-10); large arrested (population 1), small arrested (population 2) and small dividing (population 3), there were reproducible differences in the proportion of these populations compared to CJ179 cells. The small arrested

population (population 2) was much more prominent in F96 cultures, and constituted a major proportion of the total arrested cells, whereas the majority of arrested CJ179 cells were of the large cell phenotype. Therefore, although the F96 line was not as sensitive as CJ179 to the earlier induction of a large arrested cell phenotype, at higher doses there was a subsequent arrest that occurred within the remaining population of small cells. This accounted for the significant reduction in the percentage of cells that had completed 5 divisions compared to control cultures (figure 4-9), which were mainly composed of small proliferating cells at this time (figure 4-10).

We have observed what appears to be the induction of distinct populations of arrested cells in radiosensitive fibroblast lines using CFSE analysis. An important question in this regard is whether these populations, that are present at different CFSE fluorescence levels, represent different numbers of cell division or whether this is just an artefact of larger cells incorporating higher amounts of CFSE. This was less of an issue with early division experiments since CFSE labelling was performed before there were any radiation-induced changes in cell size. In late division experiments we labelled cells with CFSE 5 days after irradiation, when there are sure to be changes in cell size that have occurred in response to this insult. In order to address this point, we labelled cultures of F96 cells with CFSE 5 days after exposure to 4 Gy γ-radiation just as in late division experiments, but then analysed the culture by FACS immediately afterwards. The difference in CFSE fluorescence between large and small cells in this culture was found to be relatively small compared to that between the large arrested (population 3) and small arrested (population 2) populations in cultures incubated for a further 5 days (figure 4-11). We therefore concluded that the difference between populations 2 and 3 in late division experiments was more than just an artefact of cell size, and represented at least one additional division which population 2 had completed before arresting in this time frame.

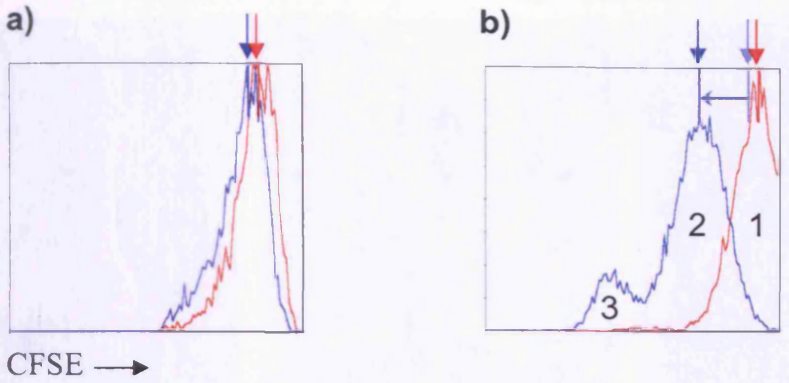

Figure 4-11: Affect of cell size on the incorporation of CFSE. CFSE plots with large cells shown in red and small cells shown in blue. F96 cultures were treated with 4Gy γ-radiation, incubated for 5 days and then labelled with CFSE. Cells were analysed by FACS either immediately (a) or after a further 5-day incubation (b). Larger cells incorporate slightly more CFSE than small cells (a), but this effect is substantially less than the difference between the arrested populations 1 and 2 after a further five-day incubation (b). Population 2 is therefore a distinct population, and represents at least one additional division during the labelled incubation period.

4.3.3 Investigation of the phenotype of arrested cells in radiosensitive lines

We were interested in identifying what mechanisms may be responsible for the induction of the different populations of arrested cells in the CJ179 and F96 lines 5-10 days after irradiation. Normal human fibroblasts have been reported to undergo SIPS in response to ionising radiation that involves the induction of a permanent G1 growth arrest, an increase in cell size and the expression of senescent markers. We investigated whether the different arrested populations observed in the F96 line after irradiation corresponded to the induction of SIPS. Late division experiments were repeated and cells were sorted into 3 populations according to their CFSE fluorescence. As described above, population 1 consisted of small dividing cells, population 2 of small arrested cells, and population 3 of large arrested cells. The 3 sorted populations were then seeded into tissue culture plates overnight, cell morphology was examined and cultures were stained for the senescence marker SA-βgal. This was performed for the control line 1BR and the undefined radiosensitive line F96.

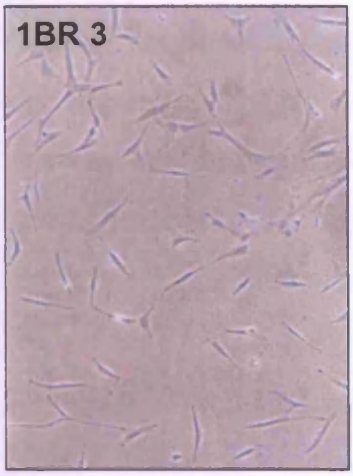
1BR 3

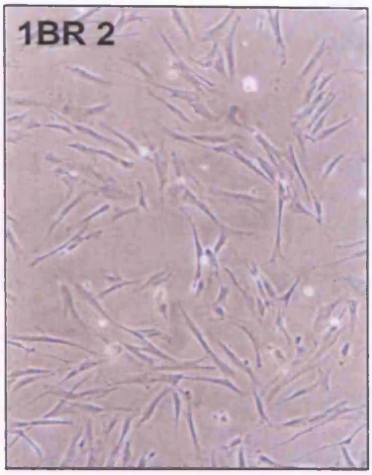
1BR 2

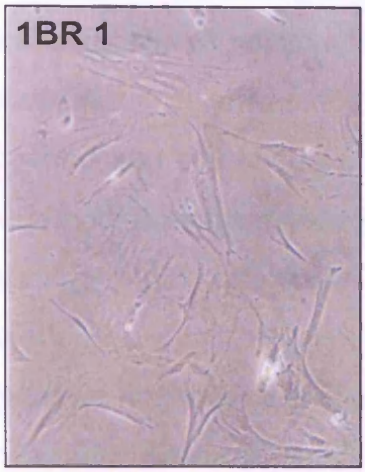
1BR 1

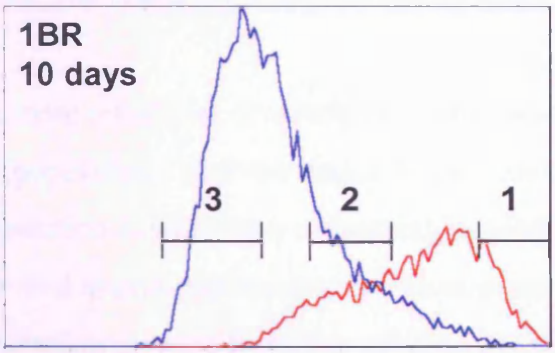
1BR
10 days
3
2
1


1BR 1
SA-βgal

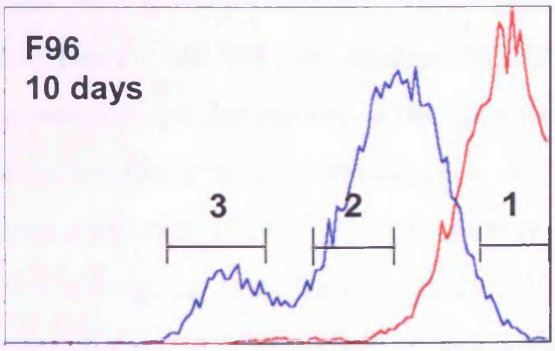
F96
10 days
3
2
1

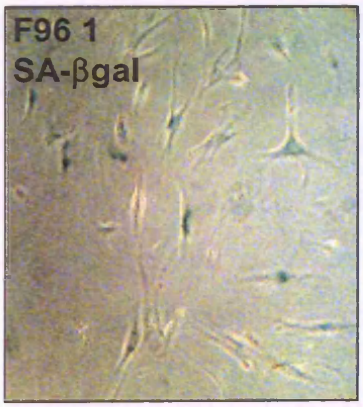
F96 1
SA-βgal

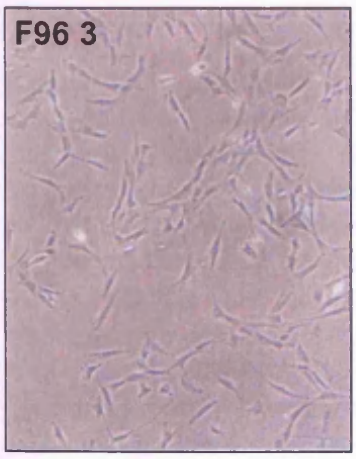
F96 3

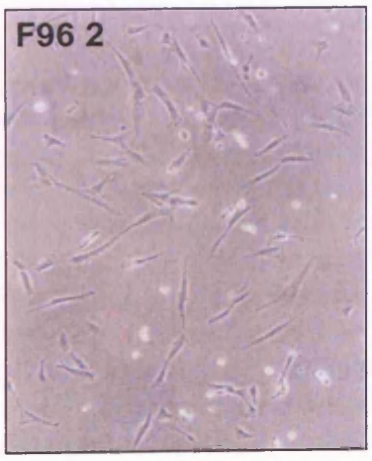
F96 2

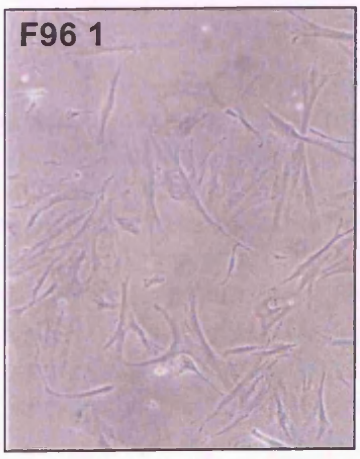
F96 1

For both the 1BR and F96 lines, population 1 consisted of cells that had a large, flattened, senescent like morphology, and 10-20% of these cells stained positive for SA-βgal (figure 4-12). This suggested that these large arrested cells resulted from the induction of a senescent like state. A longer incubation period after cell sorting may have increased the percentage of SA-βgal positive cells. In both lines the dividing population 3 consisted of small cells with a young morphology and no cells were positive for SA-βgal activity. The arrested cells in population 2 were also negative for SA-βgal, although 1BR cells at this level of CFSE fluorescence displayed a modest increase in size. There was also a relatively high level of cellular debris in population 2 cultures, and this was more pronounced in the F96 line.

From these results we concluded that the radiation-induced population of large arrested cells (population 1) corresponded to the induction of SIPS, and the small dividing cells in population 3, which were identical in morphology to cells that grow to form colonies in survival assays, represented the clonogenic surviving fraction. Indeed, when these two populations were further incubated, population 3 grew to confluence rapidly, whereas population 1 cells did not reach confluence after a two-week incubation. It was less clear what the small arrested cells in population 2, that were negative for SA-βgal and prominent in the F96 line, represented. Although these cells eventually reached confluence during a further two-week incubation, this growth was relatively slow and may have resulted from contamination with the dividing cells of population 3. The relatively high level of cellular debris in population 2 cultures suggested that these cells might be undergoing some form of death. We therefore investigated whether there were any detectable levels of apoptosis in this population.

Figure 4-12: Cellular morphology and SA-βgal staining of the distinct populations induced by γ-radiation in the control line 1BR and the radiosensitive line F96. Late division experiments were repeated for the control (1BR) and F96 lines, and cells were sorted according to their CFSE fluorescence level using the gates indicated, taking care to minimise any overlap between different populations. Sorted cells were incubated overnight in fibroblast growth medium, and cellular morphology was then examined (1BR top panel, F96 bottom panel). At this time SA-βgal staining was also performed, and only population 1 cultures contained any SA-βgal positive cells (shown in middle panel). In both lines the dividing population 3 consisted of small cells with a young morphology and no cells were positive for SA-βgal activity. The arrested cells in population 2 were also negative for SA-βgal, although 1BR cells in this population displayed a modest increase in size. There was a relatively high level of cellular debris in population 2 cultures, and this was more pronounced in the F96 line. For both lines the arrested population 1 consisted of large flattened cells with a senescent like morphology, and approximately 10-20 % of these stained positive for SA-βgal activity at this time.

Late division experiments with CFSE were repeated and cells were co-stained with Annexin V-PE and 7AAD. Annexin V binds to phosphatidylserine (PS) residues that translocate from the inner leaflet of the plasma membrane to the outer leaflet in the early stages of apoptosis. This exposes PS to the external environment and allows the percentage of cells undergoing apoptosis to be quantified. 7AAD is a DNA binding dye and identifies necrosis and the later stages of apoptosis, when the plasma membrane becomes highly permeable. These CFSE-Apoptosis experiments were performed for the control line 1BR, the Artemis deficient line CJ179 and the undefined radiosensitive line F96.

The total amount of Annexin V-PE positive cells for control (1BR) cells 10 days after 4Gy γ-radiation was 1.4 % compared to 1% for unirradiated cultures, which represented a 1.4 fold increase in apoptosis (figure 4-13). This is consistent with the low levels of radiation-induced apoptosis reported for primary fibroblast lines. We also noted that this small increase in apoptosis arose in cells with a medium level of CFSE fluorescence, corresponding to the population of small arrested cells identified in the radiosensitive CJ179 and F96 lines (figure 4-10), and gating on this population revealed that 3.7 % of these cells were apoptotic. This effect was more pronounced in the CJ179 line, which displayed a 3 fold increase in the total levels of apoptosis after irradiation. Similar to the 1BR line, the majority of the apoptotic CJ179 cells were in population 2, and when this population was gated 6.2 % of these cells had initiated apoptosis. This represents a relatively high proportion considering this analysis was performed 10 days after irradiation, and that primary fibroblasts are notoriously resistant to radiation-induced apoptosis. The F96 line demonstrated a 2.2 fold increase in apoptosis after irradiation, which comparable to the CJ179 line arose from cells within population 2. When this population was specifically gated, 3 % of these cells were positive for AnnexinV. Therefore, although primary fibroblasts do not display substantial levels of radiation-induced apoptosis 10 days after irradiation, the small increases that were observed were restricted to population 2. This may signify a delayed form of genomic instability that leads to the activation of p53 dependent pathways, resulting in growth arrest and a low level of apoptosis. The F96 line was exceptionally prone to this cell fate, which may reflect the nature of the underlying mutation.

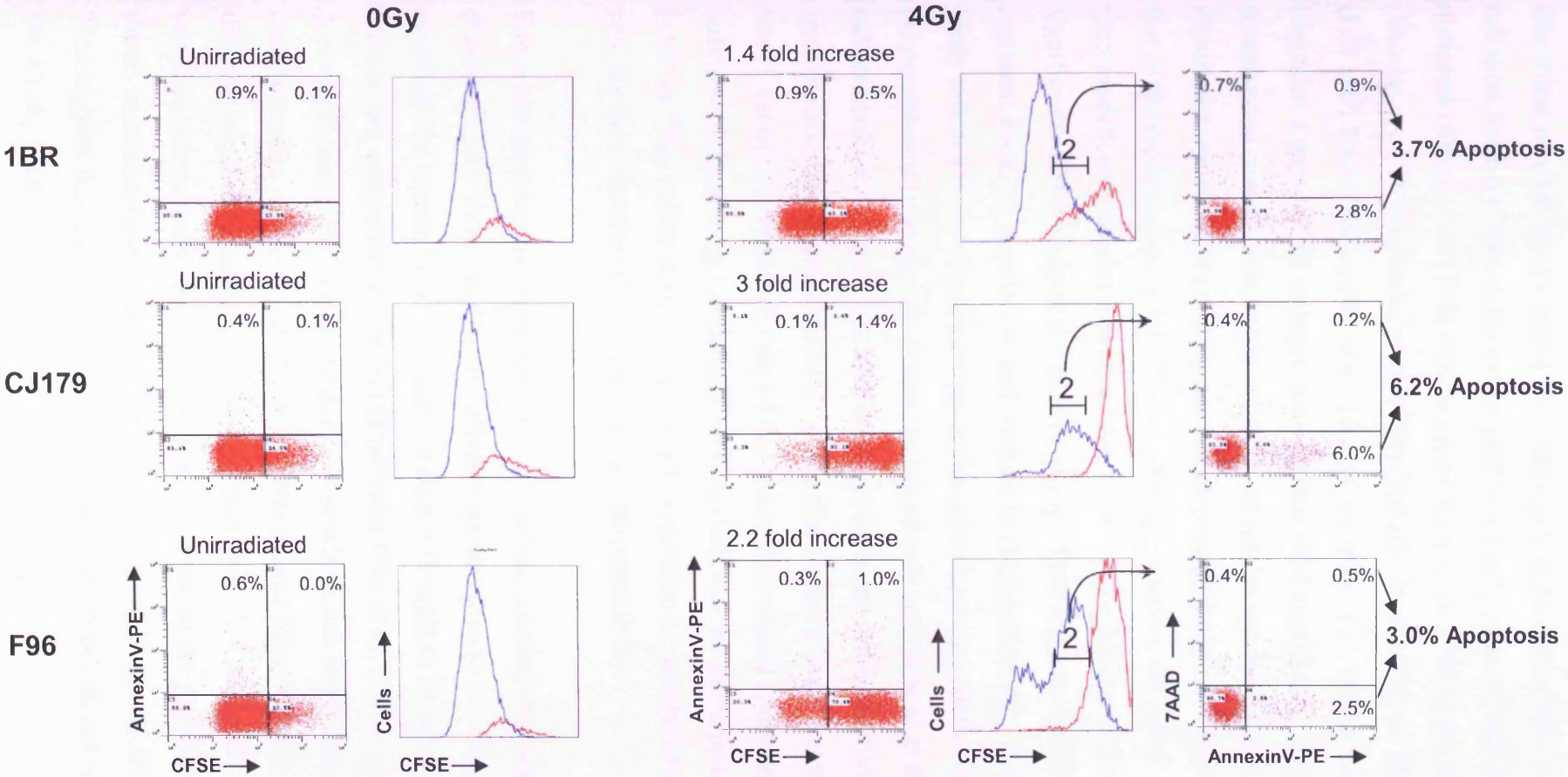

Figure 4-13: Levels of apoptosis in CFSE labelled cultures 10 days after exposure to 4Gy γ-radiation. Late division experiments were repeated for the control (1BR, top panel) and the radiosensitive CJ179 (middle panel) and F96 (bottom panel) lines. CFSE labelled cells were co-stained with Annexin V-PE and 7AAD to identify cells that had initiated apoptosis. Although the increase in Annexin V positive cells was low in 1BR, CJ179 and F96 cultures 10 days after irradiation (1.4, 3 and 2.2 fold respectively), the majority of apoptotic cells arose from the small arrested cells in population 2. When this population was specifically gated, 3.7, 6 and 3 % of these small arrested cells were positive for AnnexinV staining in the 1BR, CJ179 and F96 lines respectively. This suggests that a small percentage of cells in population 2 are in the early stages of apoptosis, and since fibroblasts are resistant to this endpoint, a more widespread instability may be present in these cells.

4.4 Discussion

Fibroblast survival assays assess the clonogenic potential of cells treated with ionizing radiation and have been extensively used to identify patients with radiosensitive disorders (Arlett *et al*, 1988) (Cavazzana-Calvo *et al*, 1993) (Nicolas *et al*, 1996) (Nicolas *et al*, 1998) (Peake *et al*, 1999) (Riballo *et al*, 1999) (O'Driscoll *et al*, 2001) (Dai *et al*, 2003) (Kobayashi *et al*, 2003) (Noordzij *et al*, 2003). Using this assay we identified a group of 10 patients that demonstrated significant cellular radiosensitivity compared to control cells. This ranged from a mild sensitivity that was marginally significant compared to controls, to a more pronounced phenotype that was similar to that of the repair defective CJ179 line. As a population, the group of undefined immunodeficient patients examined did not display a cellular radiosensitivity that was significantly different from the control group. This suggests that these patients do not represent a distinct population with respect to radiosensitivity. These results more likely reflect a range of sensitivities ensuing from subtle genetic differences and polymorphisms (that may be present in the normal population) at the more radioresistant end of the scale, to a more pronounced radiosensitivity that may result from mutations in damage response genes that impair protein function. Since only a few (3 out of 20) patients displayed this more pronounced phenotype, the incidence of radiosensitivity amongst undefined immunodeficient patients appears to be low (~10 %). This indicates that only a small proportion of undefined immunodeficient patients have disorders that affect cellular radiosensitivity.

Fibroblast lines derived from patients with distinct immunodeficient disorders have previously been shown to display different sensitivities to ionising radiation. The most sensitive line reported to date is 2BN, which is thought to have a defect in an unidentified component of the NHEJ pathway (Dai *et al*, 2003). Consistent with previous reports, 2BN cells were the most sensitive line examined in this study, and demonstrated a profound sensitivity that was greater than AT cells, which are among the most exquisitely radiosensitive lines described. A-T1BR cells demonstrated a severe radiosensitivity that was not observed in any of the undefined lines, and none of theses immunodeficient patients displayed any other symptoms common to AT patients. This suggests that the observed radiosensitive phenotypes do not result from defects in the ATM protein.

F96, GOS5 and GOS23 cells were among the most radiosensitive of all the undefined lines examined, and were classified as displaying an intermediate sensitivity that was slightly less pronounced than that of the Artemis deficient CJ179 line. These cells are therefore good candidate lines for defects in the NHEJ pathway, although the inherent mutations may not be as extreme as an Artemis null mutation, and may allow somewhat superior repair to marginally increase radioresistance. This would also be consistent with the limited number of T- and B- lymphocytes that were detected in these patients that could result from a partially functional V(D)J recombination pathway, compared to the more severe immunodeficient phenotype associated with inactivating mutations in Artemis (O'Driscoll *et al*, 2004).

Fibroblast lines derived from different normal individuals have previously been shown to display a broad variation in radiosensitivity, and this was attributed to genetic differences (Little *et al*, 1988) (Deschavanne and Fertil, 1996) (Dikomey *et al*, 2003). Although the two control lines used in this study demonstrated almost identical levels of survival after irradiation (1BR; 9.4% after 4 Gy, 48BR, 9.9% after 4 Gy), it was difficult to assess to what extent random genetic differences affected radiosensitivity with only 2 normal lines at our disposal. This issue became of particular relevance when examining lines that demonstrated a mild radiosensitivity that was on the borderline of significance.

We grouped 7 patient lines into a mild category of radiosensitivity based on their reduced survival after 4 Gy γ-radiation that was not as pronounced as that of the three intermediate radiosensitive lines (F96, GOS5, GOS23). Although this mild level of radiosensitivity was significantly different from 2 control lines, it was difficult to determine whether this represented a distinct pathological phenotype, or if this was the result of random genetic variation affecting sensitivity. Later in this study a patient that demonstrated borderline significance radiosensitivity (GOS10) was found to have a homozygous Y589X mutation in the RAG1 gene. Although this almost certainly accounts for the severe immunodeficiency observed in this patient, this protein is not thought to function in general DSB repair (Gellert *et al*, 2002) and RAG mutations have not been reported that affect radiosensitivity. This suggests that although patients that were borderline radiosensitive, such as GOS3, GOS17, GOS10 and GOS4, demonstrated a significant difference compared to controls, this mild phenotype may be the result of other genetic differences that do not directly affect DNA damage response

pathways. A similar borderline radiosensitivity has been reported in fibroblasts derived from a patient with Adenine Deaminase (ADA) deficiency after low dose rate irradiation (Sproston *et al*, 1997). ADA deficiency, the first known cause of a severe combined immunodeficient disorder (Giblett *et al*, 1972), is thought to result from abnormal purine metabolism during lymphocyte development (Aldrich *et al*, 2000) and is not implicated in the general response to DNA damage. This would further suggest that the marginal radiosensitivity observed in some SCID patients might be the result of global genetic variation and not mutations in specific damage response pathways. Further characterisation therefore concentrated on the lines that displayed intermediate radiosensitivity that may reflect pathological defects in the response to DNA damage.

In section 3.3 we described the development of a novel assay for cellular radiosensitivity using the fluorescent dye CFSE that focuses on cell division within the first week of irradiation. This system allowed us to identify differences in post-radiation division between control cells and a radiosensitive line (CJ179) with a null mutation in the Artemis DSB repair gene. We observed that a lower percentage of repair defective cells were able to complete five divisions after irradiation compared to controls, and this coincided with the induction of a population of large arrested cells, consistent with the initiation of Stress Induced Premature Senescence (SIPS). We next employed this test system to further characterise the GOS5 and F96 lines, which demonstrated intermediate radiosensitivity in clonogenic survival assays. The GOS5 line was more prone to the induction of a population of large arrested cells compared to controls, and hence significantly fewer cells completed 5 divisions. This suggests that similar to the CJ179 line, the radiosensitivity observed in GOS5 cells is conferred, at least in part, through the induction of abnormally high levels of radiation induced growth arrest within 6 days. This could result from a similar mechanism to that in CJ179 cells, involving deficient DSB repair, or a defect in the damage assessment process that leads to elevated levels of SIPS after irradiation. Since the GOS5 line also displayed premature senescence at passage 9 of normal tissue culture, deregulation of this tumour suppressor mechanism may be inherent to these cells. Further investigation was therefore required to determine whether a defect in DNA repair is associated with the GOS5 line (section 5).

Despite showing a similar radiosensitivity to that of the GOS5 and CJ179 lines in clonogenic survival assays, the F96 line displayed only a modest reduction in cell

division within the first 6 days of irradiation. This was especially evident after low doses of γ-radiation, which suggested that F96 cells are able to deal with the early effects of low doses relatively well. In order to further investigate this discrepancy between clonogenic survival and early cell division results, we decided to examine cell division at a later timeframe, between days 5 and 10 after irradiation. At the lower doses of 1 and 2 Gy the F96 line continued to divide well, and CJ179 cultures were also able to recover to produce a substantial proportion of dividing cells. This was in contrast to the A-T1BR line, which displayed low levels of division at all doses, consistent with the severe radiosensitivity of this line. After the higher doses of 4 and 6 Gy both the F96 and CJ179 lines met with a severe block on late cell division compared to controls. Whilst in the CJ179 line this was generally due to the continued presence of a population of large cells that had not divided in this timeframe, the F96 line displayed a high proportion of cells that had arrested after 1-2 additional divisions. These data suggest that unlike the CJ179 and AT-1BR lines, the F96 line is able to deal with low doses of γ-radiation relatively well, but once a certain threshold is reached these cells meet with a delayed block on proliferation.

There have been many reports on the delayed effects of ionising radiation on cultured cells. This has been documented as delayed chromosomal instability in surviving cells manifested as multiple rearrangements several generations after exposure to X rays (Marder and Morgan, 1993), and a high frequency of chromosome bridge formation and delayed reproductive death in the progeny of human embryonic cells surviving similar treatment (Suzuki *et al*, 1998). This delayed chromosomal instability was reduced by delayed plating, which allows more time for repair and suggests that the potentiality of genetic instability is determined by the repair process of the initial radiation damage (Roy *et al*, 1999). Therefore, the F96 line may harbour a subtle defect in the damage response that initially allows a normal rate of DNA repair and proliferation, but after a certain number of divisions high levels of delayed genetic instability and/or reactivation of growth arrest pathways impair clonogenic survival.

Delayed chromosomal instability has also been described as delayed induction of γ-H2AX foci, corresponding to a 0.5 – 1 Gy equivalent dose, which was observed in cells 30-50 population doublings post irradiation (Suzuki *et al*, 2003a). Since γ-H2AX foci are thought to represent sites of DNA DSBs (Rogakou *et al*, 1999) this may be expected to initiate a secondary p53 response. Consistent with this hypothesis, these studies

demonstrated the delayed activation of p53 in a significant number of colonies surviving the initial genotoxic insult (Suzuki *et al*, 2003b). Whilst these effects were seen in cells 30-50 population doublings after irradiation, a similar phenomenon has been described in human fibroblasts 5 days after irradiation, which is within the timeframe that the F96 line demonstrated a significant block on cell division. X-irradiation was shown to cause a primary transient induction of p53 followed by a reinduction of p53 5 days after irradiation (Rugo *et al*, 2002). This reinduction persisted for 2 days and coincided with the largest induction of apoptosis. The F96 line may therefore display high levels of delayed growth arrest due to the abnormal reinduction of p53, but this does not seem to be associated with high levels of apoptosis. Co-staining of CFSE labelled cells with Annexin V-PE revealed that although any limited increase in apoptosis was restricted to cells that had initiated a delayed growth arrest, less than 10 % of these cells were apoptotic. Levels of apoptosis in human fibroblasts have previously been reported to be maximal at about 5 days after irradiation, although this was evident in only a small proportion of cells (Belyakov *et al*, 1999). The same study observed that a larger proportion of cells were micronucleated, and this response peaked at around 5 days after irradiation. Micronuclei are formed in cells manifesting chromosome aberrations during cell division and result from nuclear membrane encapsulation of chromatin and chromosomal fragments that fail to properly segregate after mitosis (Muller *et al*, 1996). If the F96 line was prone to a form of delayed chromosome instability, which may involve the induction of secondary DSBs, micronuclei may be induced after several further divisions. Since p53 activation and cell cycle arrest have been shown to occur in response to micronuclei (Sablina *et al*, 1998), this may account for the delayed arrest observed in F96 cells.

Although the cells that demonstrated a delayed arrest in treated F96 cultures did not show signs of premature senescence, the radiation-induced populations of large arrested cells contained cells with a senescent-like, flattened morphology that were positive for the senescence marker SA-βgal. This is consistent with previous studies that separated dividing and growth retarded colon carcinoma cells after treatment with chemotherapeutic agents. The arrested population was shown to contain a high percentage of cells with increased granularity that stained positive for SA-βgal compared to the dividing population (Chang *et al*, 1999b). Of the few colonies that grew out of this growth retarded population, none stained positive for SA-βgal, suggesting that the senescent-like cells lost their long-term proliferative capacity. This

mechanism may therefore function as a means of inducing proliferative death in cells such as primary fibroblasts that are resistant to apoptosis but have persistent DSBs after irradiation, as suggested by Naka *et al*, 2004. In colon carcinoma cells this arrest was substantially dependent on p21, and partly dependent on p53 (Chang et al, 1999a) and was associated with inhibition of genes involved in cell proliferation and coinduction of multiple intracellular and secreted growth inhibitors (Chang *et al*, 2002). The induction of high levels of p21 has also been shown to be detrimental to growth-arrested cells that evade premature senescence and return to cycle. After release from growth arrest mediated by p21 over-expression from an inducible promoter, human fibrosarcoma cells failed to from colonies due to abnormal mitosis of the recovering cells (Chang *et al*, 2000). This was attributed to the p21-induced depletion of cellular pools of mitosis-control proteins, followed by the asynchronous resynthesis of such proteins after release from p21. Genetic destabilisation of cells recovering from p21-induced growth arrest may therefore contribute to the delayed effects of ionising radiation in the F96 line.

We have shown that a significant amount of primary fibroblasts initiate a senescent like growth retardation within the first 6 days of irradiation, and the repair defective line CJ179 is more prone to this endpoint than control cells. This suggests that unrepaired radiation-induced DSBs may promote growth retardation and the induction of premature senescence. Whilst GOS5 cells displayed a similar propensity for this endpoint, the F96 line was more disposed to a delayed arrest after higher doses of γ-radiation, which did not involve the induction of premature senescence at this time. Since there were also minimal levels of apoptosis in these cells, this may reflect a delayed instability that that promotes abnormal mitotic events and/or the reinduction of growth arrest pathways. These data suggest that the underlying mutation in this line allows for proliferation early after irradiation but promotes a delayed instability that is detrimental to long-term survival. In order to delineate the nature of the defects in these undefined radiosensitive lines, further characterisation was required in relation to p53 responses and DNA repair.

Chapter 5: Characterisation of radiosensitive fibroblast lines

5.1 Background

In the previous chapter we described a group of undefined immunodeficient patients that demonstrated cellular radiosensitivity in primary fibroblasts. These patients may have defects in the damage response network that impairs their ability to respond efficiently to radiation-induced DSBs. This could manifest as a failure to initiate appropriate cell cycle checkpoints through the activation of p53, and this phenotype has been described in AT cells that are defective in this process (Houldsworth and Lavin, 1980) (Kastan *et al*, 1992) (Lu and Lane, 1993) (Beamish and Lavin, 1994) (Khanna *et al*, 1995). Since these cells are unable to efficiently arrest the cell cycle after DNA damage, cells that have incurred high levels of damage are allowed to progress into S-phase. This is believed to exacerbate the damage sustained and induce a high level of genomic instability that ultimately impairs cell survival. The G1/S cell cycle checkpoint was therefore investigated in the most radiosensitive undefined line, F96, using BrdU cell cycle analysis. The efficient and sustained activation of the G1/S checkpoint depends on the induction of the Cdk inhibitor p21, a target gene of p53 (Waldman *et al*, 1995) (Brugarolas *et al*, 1999). We also examined whether p21 mRNA was induced normally in undefined radiosensitive lines using northern blot analysis. These responses were compared to those from control cells and the ATM deficient line A-T1BR.

Concurrent with the activation of cell cycle checkpoints, cells also initiate pathways that function to repair DNA damage and promote survival. This is an important aspect of the damage response, since the persistence of DNA DSBs after irradiation has been correlated with cellular radiosensitivity (Wurm *et al*, 1994) (Kiltie *et al*, 1997) (Dikomey *et al*, 1998) (Sarkaria *et al*, 1998) (Zhou *et al*, 1998) (Dikomey *et al*, 2000a) (Dikomey *et al*, 2000b). Radiosensitivity may therefore result from defects in DSB repair pathways, and this has been previously described in some patients with radiosensitive immunodeficiency (Moshous *et al*, 2001) (O'Driscoll *et al*, 2001) (Li *et al*, 2002a) (Kobayashi *et al*, 2003) (Noordzij *et al*, 2003). In order to investigate DSB repair in undefined radiosensitive lines we took two approaches. We first analysed

unrepaired chromosome breaks after irradiation by preparing metaphase spreads after a suitable incubation time for repair processes to function. This was complemented by work from our collaborators that examined the phosphorylated form of H2AX (γ-H2AX) after irradiation. Since this modification is believed to mark the site of DSBs, depreciation of γ-H2AX foci within cell nuclei can be used as a marker of DSB repair. These assays allowed us to gain an indication as to the presence of defective repair in undefined lines.

5.2 Initial checkpoint function in F96 cells

AT cells have defects in initial checkpoint function and this is likely to contribute to their poor survival after irradiation. To confirm that F96 cells are proficient in activating a G1/S checkpoint within hours of irradiation, we performed Bromodeoxyuridine (BrdU) cell cycle analysis before and after exposure to 4Gy γ-radiation. BrdU is a thymidine analogue and is specifically incorporated into DNA during DNA synthesis when incubated with cycling cells. Anti-bromodeoxyuridine monoclonal antibody can then be used to identify cells that have incorporated BrdU during S-phase. Co-staining with propidium iodide (PI) also allows the discrimination of G1 and G2 phases of the cell cycle.

In unirradiated control cultures 19 % of cells incorporated BrdU during a 30-minute incubation period and were considered to be in S-phase (Figure 5-1). When these cells were treated with 4 Gy of γ-radiation the amount of BrdU positive cells diminished to 2% 12 hrs after irradiation, which represented a 90 % reduction in the percentage of cells in S-phase and is consistent with the efficient activation of a G1/S DNA damage checkpoint. F96 cells demonstrated a similar reduction in DNA synthesis after irradiation, with 28 % of BrdU positive cells in unirradiated cultures diminishing to 2 % in cells 12hrs after exposure to 4Gy γ-radiation. This represented a 93 % reduction in the percentage of cells in S-phase and suggested that F96 cells are proficient in activation of an initial G1/S DNA damage checkpoint.

AT cells have defects in initial checkpoint function and consistent with this the A-T1BR line displayed only a 47 % reduction in the percentage of cells in S-phase 12 hrs after irradiation compared to 90 % in control cells. This is consistent with previous reports that document the failure of AT cells to efficiently activate a G1/S checkpoint after

radiation exposure (Beamish *et al*, 1994). Although some cells were able to initiate cell cycle arrest, many progressed into S-phase despite the genotoxic insult that was sustained.

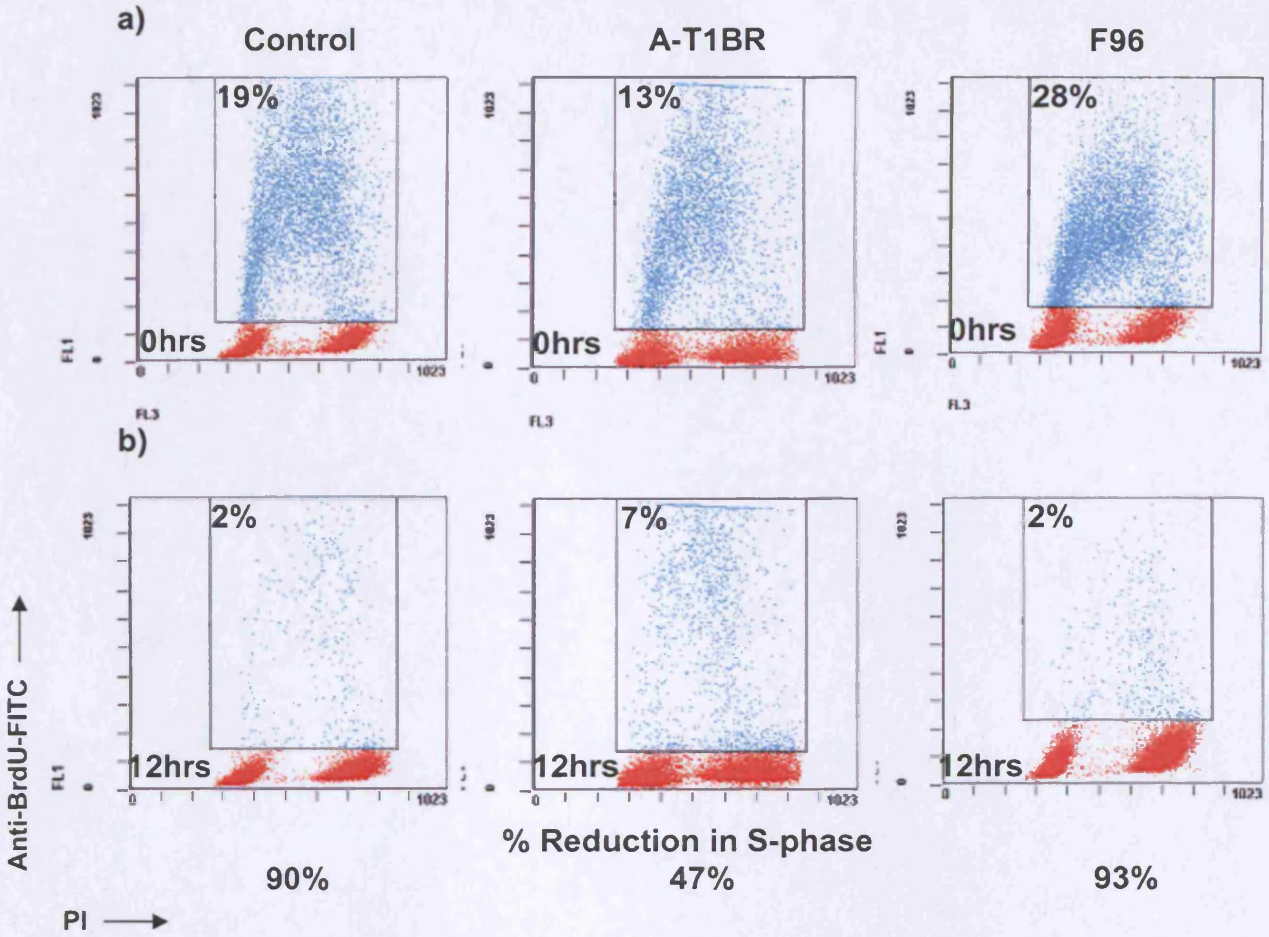

Figure 5-1: F96 cells demonstrate normal G1/S checkpoint function. Unirradiated cells (a) or cells incubated for 12 hrs (b) after exposure to 4Gy γ-radiation were labelled for 30 minutes with BrdU, fixed and analysed by FACS. Control and F96 cells demonstrated efficient activation of a G1/S checkpoint 12 hrs after irradiation with a ~90 % reduction of cells in S-phase. A-T1BR cells displayed abrogated activation of a G1/S checkpoint with only a 47 % reduction in the percentage of cells in S-phase 12 hrs after irradiation.

5.3 p53 dependent gene transcription in radiosensitive lines

In response to radiation induced DSBs, p53-dependent gene transcription is an important factor in the activation of DNA damage checkpoints and the induction of apoptosis (Vogelstein *et al*, 2000). p21 is a target gene of p53 and functions to arrest the cell cycle by inhibiting Cdks. This protein is crucial for the efficient and sustained

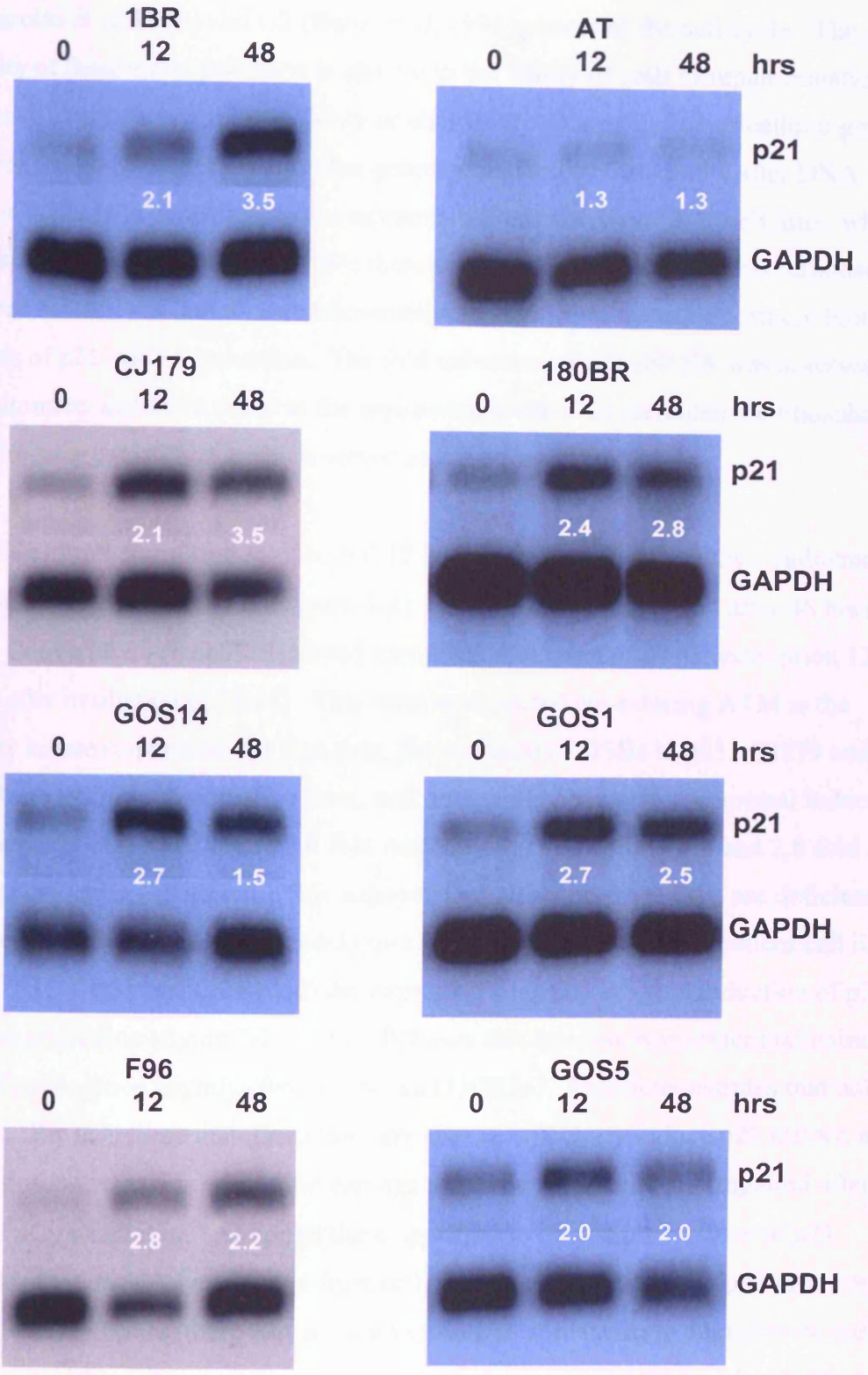

Figure 5-2. Northern blot of p21 mRNA induction in control, radiosensitive mutant and radiosensitive patient fibroblasts after exposure to 4Gy γ-radiation. The fold induction of p21 mRNA (white figures) was assessed using a densitometer and normalised to the expression level of Glyceraldehyde Phosphate Dehydrogenase (GAPDH). Control (1BR), repair defective (CJ179 and 180BR) and RS patient (F96, GOS1, GOS5 and GOS14) fibroblasts demonstrated efficient induction of p21 mRNA after irradiation. A-T cells displayed abrogated induction of p21 after irradiation.

activation of checkpoints that function at both the G1/S (Waldman *et al*, 1995) (Brugarolas *et al*, 1999) and G2 (Bunz *et al*, 1998) phases of the cell cycle. The integrity of these arrest pathways is critical to the ability of cells to repair mutations that otherwise might compromise viability or contribute to deregulation of cellular growth and proliferation. In this situation the genomic instability that results after DNA damage is likely to contribute to the extreme radiosensitivity of A-T cell lines, which are defective in signaling to p53. We therefore investigated whether this response occurred normally in undefined radiosensitive patient fibroblasts by northern blot analysis of p21 mRNA induction. The fold induction of p21 mRNA was assessed using a densitometer and normalised to the expression level of Glyceraldehyde Phosphate Dehydrogenase (GAPDH), which served as a loading control.

Induction of p21 transcription occurred 12 hours after exposure to 4Gy γ-radiation in the control cell line 1BR (2.1 fold, figure 5-2), and had further increased after 48 hrs (3.5 fold). Conversely, AT cells displayed abrogated induction of p21 transcription 12 and 48 hrs after irradiation (1.3fold). This may be expected considering ATM is the primary kinase responsible for signaling the presence of DSBs to p53. CJ179 and 180BR are DSB repair defective lines, and these cells demonstrated normal induction of p21 transcription 12 hrs (2 and 2.4 fold respectively) and 48 hrs (2.4 and 2.8 fold respectively) after irradiation. This suggests that although these cells are deficient in DSB repair, they retain normal checkpoint function. Radiosensitive patient cell lines F96, GOS1, GOS5 and GOS14 all demonstrated a normal 2-3 fold induction of p21 12 hrs after irradiation (figure 5-2). After 48 hours this increase was either maintained (GOS5) or declined slightly (F96, GOS1 and GOS14). This demonstrates that unlike the A-T1BR line, these undefined lines are able to efficiently induce p21 mRNA after irradiation, and that this arm of the damage response network is not impaired after a dose of 4Gy γ-radiation. Although there appeared to be distinct kinetics of p21 induction that could have resulted from different co-regulation of the p21 promoter in the different cell lines, there was not enough data to convincingly demonstrate these differences. The differences in p21 induction between 12 and 48 hrs after irradiation were small, and the number of replicates too low to know what variability is associated with these measurements, hence these differences may only reflect normal variation.

5.4 Analysis of double-strand break repair in radiosensitive lines

Primary immunodeficiency combined with cellular radiosensitivity has previously been described in patients with mutations in genes that function in DSB repair (Moshous *et al*, 2001) (O'Driscoll *et al*, 2001) (Li *et al*, 2002a) (Kobayashi *et al*, 2003) (Noordzij *et al*, 2003). These patients have defects in the NHEJ pathway of DSB repair, and are inefficient at performing V(D)J recombination during lymphocyte development and resolving DSBs induced by ionising radiation. Failure to efficiently repair DNA damage after irradiation is detrimental to cell survival and the number of residual DSBs have been found to be correlated with cellular radiosensitivity (Wurm *et al*, 1994) (Kiltie *et al*, 1997) (Dikomey *et al*, 1998) (Sarkaria *et al*, 1998) (Zhou *et al*, 1998) (Dikomey *et al*, 2000a) (Dikomey *et al*, 2000b). We therefore investigated whether a defect in repair could be observed in the identified radiosensitive patient lines. This was performed by examining unrepaired chromosome breaks after irradiation, and the disappearance of γ-H2AX foci in similarly treated cells. These assays may give an indication as to the presence of defective repair.

5.4.1 Analysis of chromosome breakage after irradiation

Radiation induced chromosome damage can be assessed by preparing metaphase spreads and examining individual cells for abnormal structures. This was performed with the identified radiosensitive lines, with particular reference to unrepaired chromosome and chromatid breaks after irradiation. Exponentially growing cells were treated with 3 Gy γ-radiation and given time to repair the damage (8 hours) after which the addition of colcemid arrested cells at metaphase. Metaphase spreads were then prepared and the number of unrepaired breaks was assessed for each cell line (figure 5-3a and b). Chromosome breaks were defined as acentric chromosome fragments that may have formed by irradiation in G1 or early S-phases of the cell cycle. Chromatid breaks were defined as chromatid gaps or fragments that may have arisen by irradiation during late S- or G2 phases of the cell cycle, or by other poorly defined mechanisms (Bryant *et al*, 2004)

Considering both chromosome and chromatid breaks together, the control line 1BR demonstrated the normal level of un-repaired breakage after irradiation (1.65 breaks per cell, figure 5-3a). CJ179 cells are defective in the Artemis DSB repair protein and

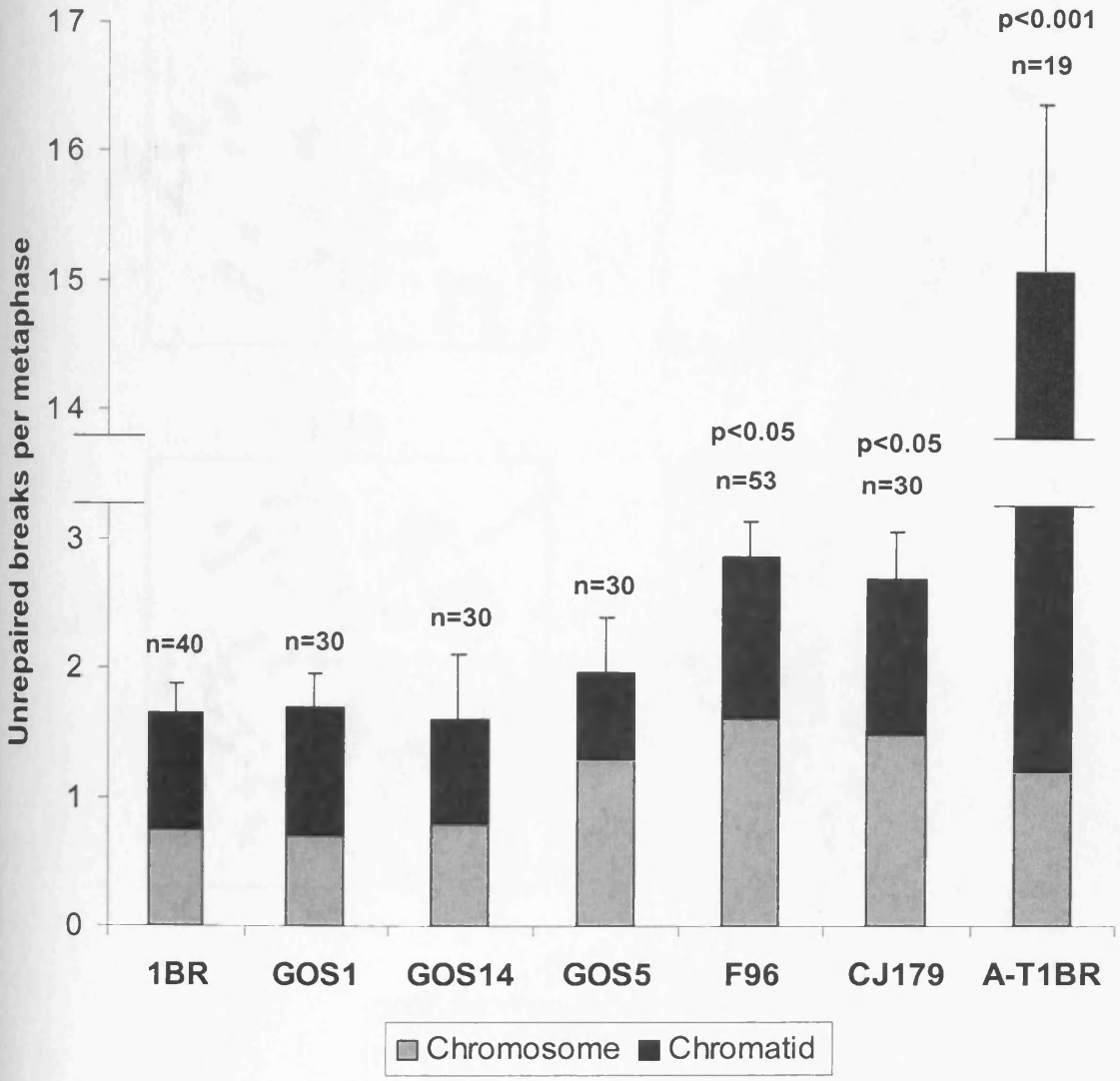

Figure 5-3a): Levels of unrepaired chromosome and chromatid breaks after irradiation of primary fibroblasts. The A-T1BR and CJ179 lines displayed significantly elevated levels of unrepaired breaks after irradiation compared to control (1BR) cells. For the A-T1BR line, this was mostly due to high levels of chromatid breaks. The GOS1, GOS14, and GOS5 patient lines demonstrated normal levels of unrepaired breaks similar to the control line 1BR. F96 cells exhibited significantly higher levels of unrepaired breaks after irradiation compared to controls, and this was similar in magnitude to that of CJ179 cells. This suggests that the F96 line may have a defect in DSB repair.

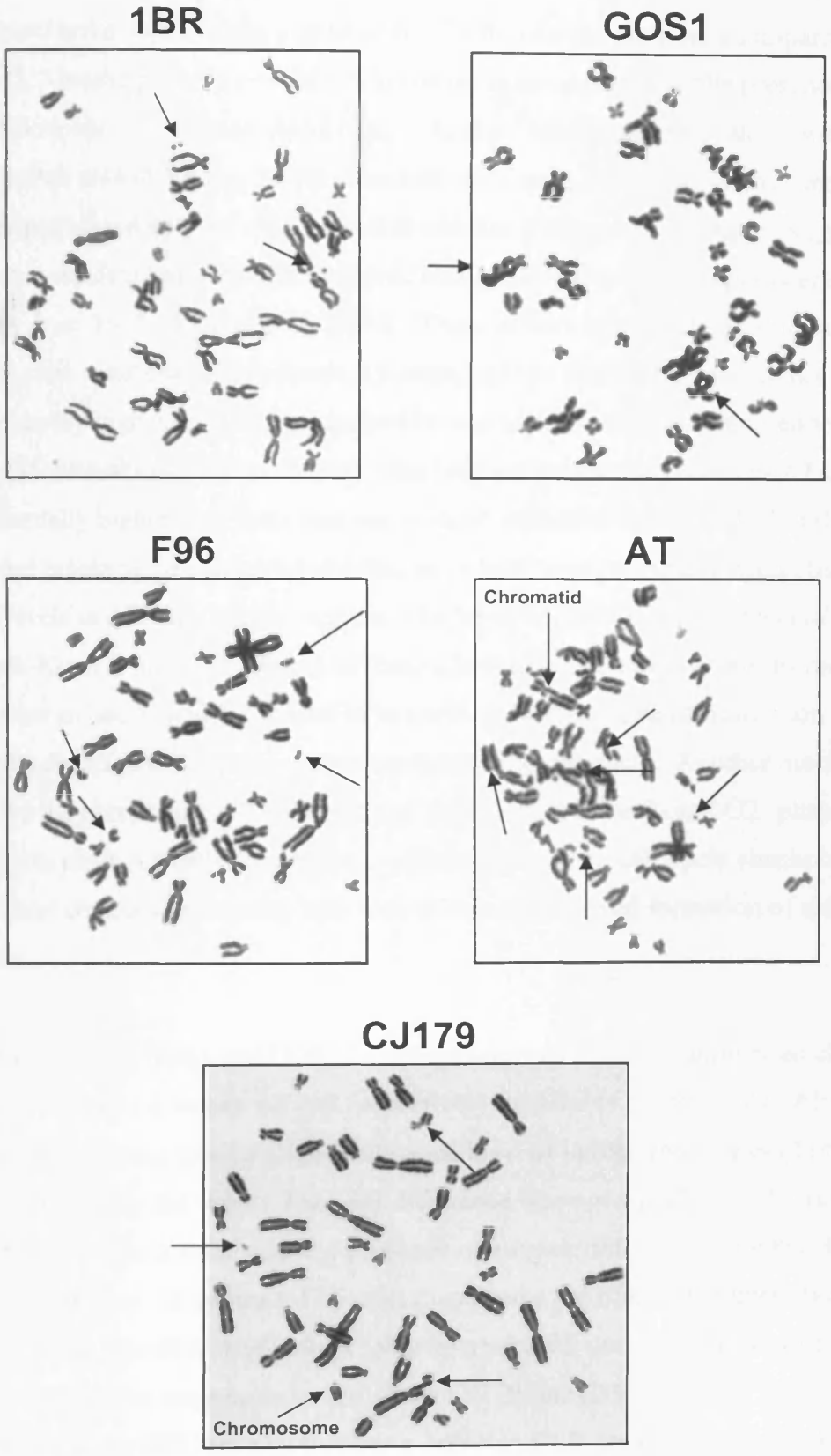

Figure 5-3b: Representative metaphase spreads of unrepaired chromosome and chromatid breaks for the control line 1BR, the known mutant lines A-T1BR (ATM) and CJ179 (Artemis), and the undefined radiosensitive lines F96 and GOS1. Examples of unrepaired damage are indicated by arrows.

demonstrated a significantly higher level of total unrepaired breaks compared to control cells (2.7 breaks per cell, $p<0.05$). This result is consistent with the presence of a defect in DSB repair. AT cells are defective in checkpoint activation (Houldsworth and Lavin, 1980) (Painter and Young, 1980) (Beamish and Lavin, 1994) (Jorgensen and Shiloh, 1996) and have displayed a high level of residual DSBs after irradiation suggesting a defect in repair (Cornforth and Bedford, 1985) (Sasai *et al*, 1994) (Foray *et al*, 1995), (Foray *et al*, 1997) (Khune *et al*, 2004). These effects combine to produce a high level of genomic instability in irradiated AT cells, and the A-T1BR line therefore exhibited significantly higher levels of unrepaired breaks after irradiation compared to control cells (15.1 breaks per cell, $p<0.001$). The level of unrepaired breaks in AT cells was substantially higher than that observed in repair defective CJ179 cells, but the majority of these breaks were chromatid aberrations, which have previously been observed at high levels in AT cells after irradiation (Taylor *et al*, 1976) (Nagasawa *et al*, 1985) (Virsik-Kopp *et al*, 2004). Some of these Chromatid breaks may have formed in cells that were in late S- and G2 phases of the cell cycle at the time of irradiation and reflect a specific defect in DNA repair at these points in the cell cycle. Another mechanism may involve the persistence of DSBs induced in G1 into the late S- and G2- phases of the cell cycle since AT cells are unable to efficiently activate cell cycle checkpoints. These persistent chromosome breaks may then initiate the delayed formation of chromatid breaks.

Patient cell lines GOS1 and GOS14 displayed normal levels of unrepaired chromosome breaks (1.7 and 1.6 breaks per cell respectively) similar to control cells. Although GOS5 cells demonstrated a slightly elevated level of unrepaired breaks (2 breaks per cell) compared to the control line, this difference was not significant. Therefore no evidence was found to suggest the presence of a repair defect in the GOS1, GOS5 or GOS14 cell lines. In contrast, F96 cells displayed a significantly higher level of unrepaired breaks after irradiation (2.9 breaks per cell) compared to control cells, and this was similar in magnitude to that of the CJ179 line (2.7 breaks per cell). This suggests that the F96 line may harbour a defect in DSB repair that has similar effects on the residual level of chromosome damage as that which occurs in the absence of the Artemis repair protein.

Dicentric chromosomes are reciprocal translocations between two different chromosomes that are believed to be formed by the aberrant repair of one or two DNA

DSBs (Pfeiffer *et al*, 2000). In order to investigate potential mis-rejoining of radiation-induced DSBs in radiosensitive lines, we counted the number of dicentric chromosomes present in each metaphase spread (table 5-1). Whilst the control line 1BR and the mildly radiosensitive line GOS1 displayed low levels of dicentric chromosomes (5 and 0 % of metaphases respectively contained at least one dicentric chromosome), the GOS14, CJ179 and A-T1BR lines demonstrated a slightly elevated level of this aberration (10, 10 and 11 % of metaphases respectively) that may suggest a subtle tendency for mis-rejoining. The radiosensitive lines F96 and GOS5 displayed relatively high levels of dicentric chromosomes (21 and 23 % of metaphases respectively), which may indicate that DSBs mis-rejoining is inherent to these lines.

Table 5-1: Frequency of dicentric chromosomes in primary fibroblast metaphase spreads

Primary cell line	Metaphases scored	Total dicentrics	Metaphases with a dicentric	% Metaphases with a dicentric
1BR	40	2	2	5 %
F96	53	12	11	21 %
GOS5	30	9	7	23 %
GOS1	30	0	0	0 %
GOS14	30	3	3	10 %
CJ179	30	4	3	10 %
A-T1BR	19	2	2	11 %

5.4.2 Results from our collaborators: γ-H2AX enumeration

Using a fluorescent antibody specific for the phosphorylated form of H2AX (γ-H2AX), discrete nuclear foci can be visualised at sites of DSBs induced by exogenous agents such as IR (Rogakou *et al*, 1999) (Burma *et al*, 2001), and the number of γ-H2AX foci were found to be closely correlated with the number of DSBs (Sedelnikova *et al*, 2002). Recent studies have demonstrated that enumerating γ-H2AX foci at various time points after irradiation can be used to measure the repair of DSBs in primary human fibroblasts (Rothkamm and Lobrich, 2003) (Khune *et al*, 2004) and Chinese hamster ovary cells (Rothkamm *et al*, 2003). This method is a more sensitive than Pulse Field Gel Electrophoresis (PFGE), which is limited to a dose of 10 Gy and has been widely used to measure DSB repair in the past. Using γ-H2AX foci analysis our collaborators (laboratory of P. Jeggo, University of Sussex) were able to assess DSB repair in response to more physiologically relevant doses of γ-radiation. Also, fewer cells are

required to perform this assay than PFGE and no radioactivity is involved apart from the dosing of cells. In order to analyse the rate of foci disappearance in undefined radiosensitive lines, fibroblasts were exposed to 2Gy γ-radiation, and incubated directly afterwards in fresh medium for 3 minutes, 15 minutes, 2 hrs, 6 hrs or 24 hrs repair time. After immunostaining with γ-H2AX antibodies, the number of initially induced foci, and residual foci, were counted.

About 30-40 foci/nucleus on average were present 3 minutes post irradiation and this number peaked at 40-60 after 15 minutes (not shown). Following this induction period foci levels continuously fell, until after 24 hours there was only 2.6 and 2.4 foci per cell present in the control lines 1BR and 48BR respectively (figure 5-4).

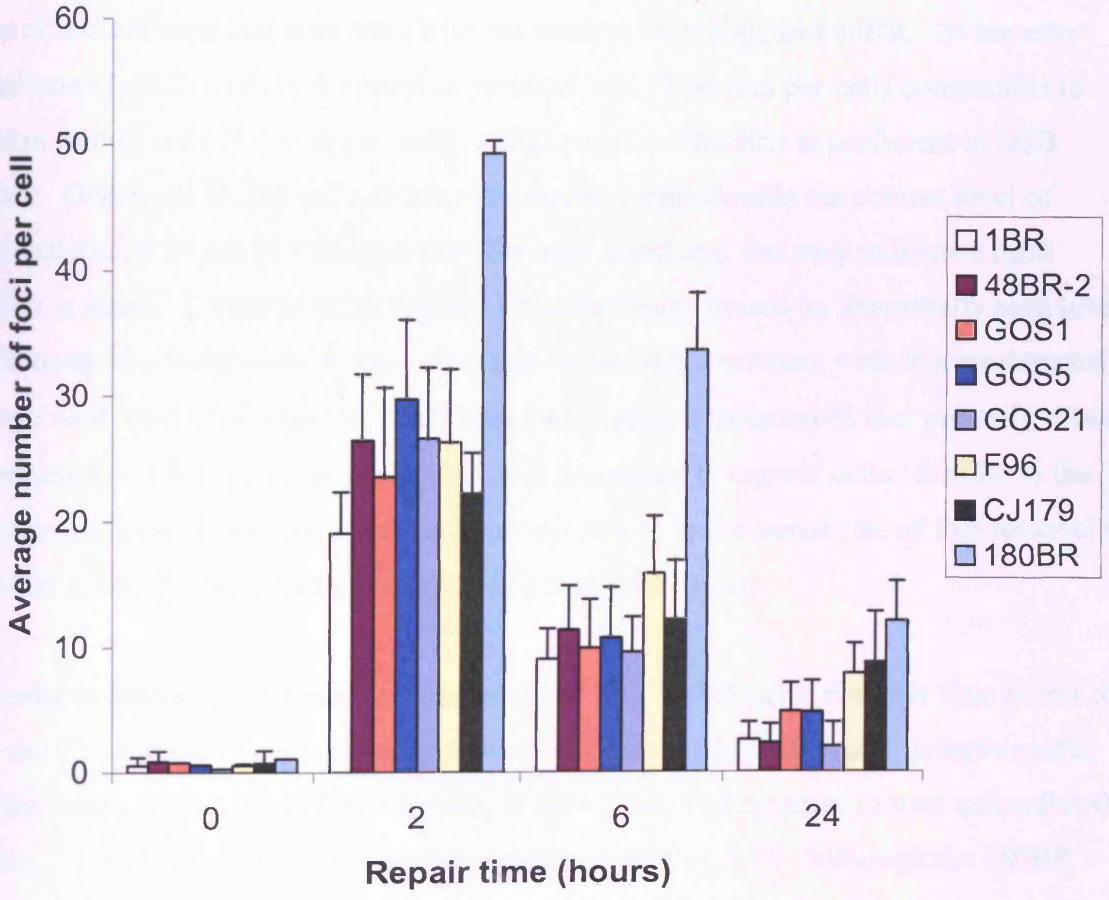

Figure 5-4: Average number of γ-H2AX foci counted in nuclei of control (1BR and 48BR), radiosensitive patient and radiosensitive mutant fibroblasts at indicated periods of repair time after irradiation with 2Gy. Whereas the ligase IV deficient 180BR line demonstrated a deficiency in the initial rate of foci removal, Artemis deficient cells (CJ179) demonstrated elevated levels of residual foci after 24 hours. Similar to this, the F96 line displayed higher levels of residual foci at 24 hours compared to control, and this may indicate comparable defect in DSB repair. GOS1 and GOS5 demonstrated a mild increase in residual foci, while the GOS21 line was similar to control cells. Error bars represent standard deviation (SD).

180BR is a primary line derived from a patient with mutations in the Ligase IV DSB repair gene (Riballo *et al*, 1999), and as expected these cells demonstrated a slower rate of foci removal compared to control cells, with 12 foci per cell remaining after 24 hrs. CJ179 is a primary fibroblast line with a null mutation in the Artemis DSB repair protein, and although these cells displayed a relatively normal rate of foci removal up to 6 hrs after irradiation, at 24 hrs they had an elevated level of residual foci (9 foci per cell) that was comparable to that of the 180BR line. This is consistent with the notion that Artemis is required for the resolution of a subset of DSBs. Although these cells can rapidly repair the majority of breaks, a percentage remains that is refractory to repair in the absence of Artemis.

The undefined radiosensitive lines GOS1, GOS5 and GOS21 all demonstrated an initial rate of foci removal that was similar to the control lines 1BR and 48BR. 24 hrs after irradiation GOS21 cells had a level of residual foci (2.08 foci per cell) comparable to that in control cells (2.4 foci per cell), which suggests this line is proficient in DSB repair. GOS1 and GOS5 cells displayed approximately double the control level of residual foci at 24 hrs (4.9 foci per cell for both lines) and this may indicate a mild defect in repair. Earlier in this chapter F96 cells demonstrated an abnormally high level of unrepaired chromosome breaks after irradiation and consistent with this we detected an elevated level of residual γ-H2AX foci 24 hrs after irradiation (8 foci per cell). This represented a 3 fold increase in residual foci compared to control cells. Similar to the Artemis deficient lines, there was no apparent deficit in the initial rate of foci removal in F96 cells, which may suggest a similar defect in DSB repair.

In order to further investigate residual levels of foci in F96 cells, the later time points of 48 and 72 hrs were examined and compared to control and DSB repair defective cells. In the control lines 1BR and 48BR the number of foci had returned to near unirradiated levels (~1 foci per cell) by 48 hrs after irradiation (figure 5-5). Although the 180BR line displayed a slower rate of foci removal, the number of foci eventually returned to baseline 72 hrs after irradiation, and this is consistent with the presence of a hypomorphic mutation in ligase IV that produces a partially functional protein (Riballo *et al*, 2001). CJ179 do not express Artemis and may be considered null for this DSB repair protein. These cells demonstrated an elevated level of residual foci 24 hrs after irradiation (10.6 foci per cell) similar to the 180BR line, but unlike 180BR cells the number of foci did not decrease substantially by 72 hrs and remained high (5 foci per

cell). This suggests that a certain number of breaks are not repaired in CJ179 cells and is consistent with the role of Artemis in repairing a subset of DSBs. Since these cells have no functional Artemis protein, these complex breaks persist for extended periods beyond 72 hrs (Riballo *et al*, 2004).

Similar to the CJ179 line, F96 cells demonstrated elevated levels of residual foci 24 hours after irradiation. Although still exceeding the control value at 48 hrs, foci levels continued to decrease until they were similar to control cells at 72 hours post irradiation. F96 cells were therefore characterised by a normal initial rate of foci removal (figure 5-4) until 24 hrs when there was an elevated level of residual breaks, but this had returned to normal after 72 hours (figure 5-5).

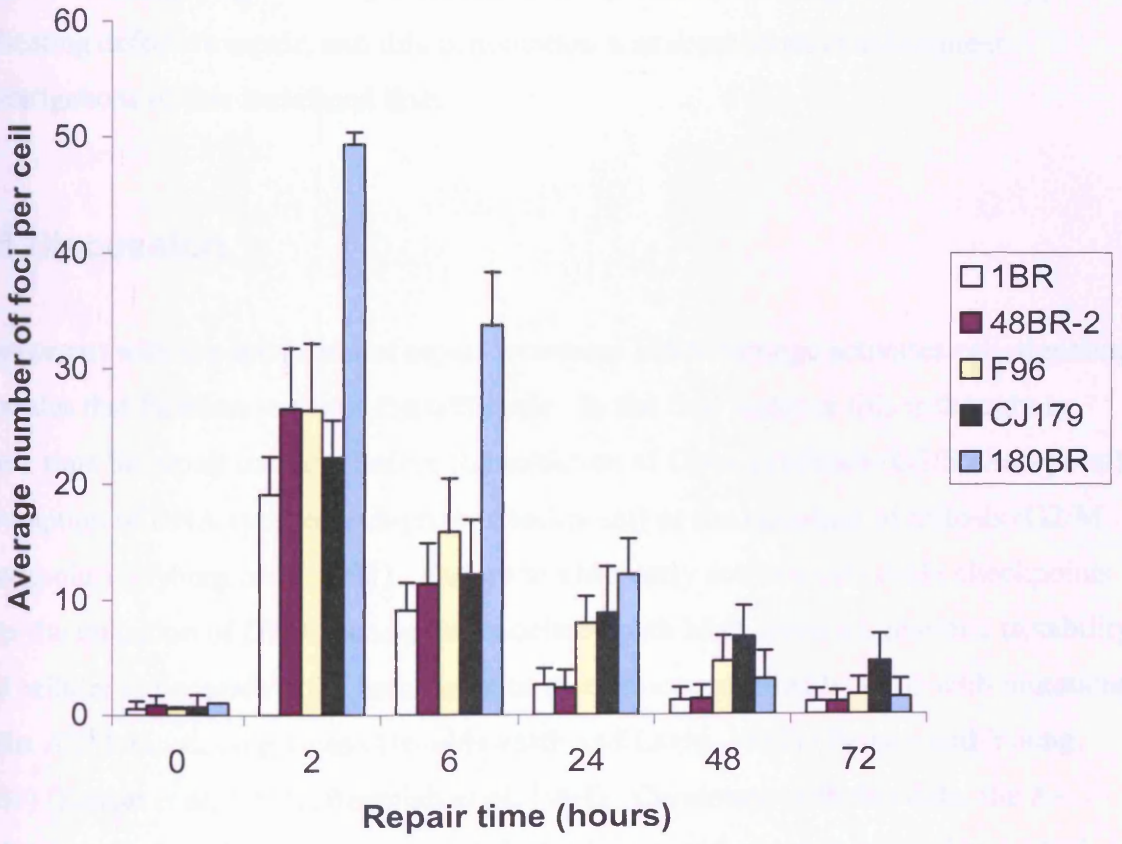

Figure 5-5: Average number of γ-H2AX foci counted in nuclei of control (48BR), repair defective (180BR and CJ179) and undefined F96 fibroblasts at late time points after irradiation with 2Gy. Foci levels in 180 BR cells that have a slow initial rate of removal eventually return to pre-irradiation values 72 hours after irradiation. The high level of residual breaks in CJ179 cells at 24 hrs remains elevated even after 72 hrs of repair time. F96 cells that have a normal initial rate of foci removal demonstrated elevated levels of foci 24 and 48 hours after irradiation compared to controls, but this decreased to control levels after 72 hours. Error bars represent SD.

These results indicate that although F96 cells may harbour a defect in the repair of a subset of DSBs, unlike CJ179 cells these are eventually resolved with delayed kinetics. The underlying mutation therefore does not affect the repair of all DSBs as proposed for Ligase IV deficiency, and is not as severe as an Artemis null mutation regarding the persistence of residual breaks.

Using a combination of chromosome break analysis and γ-H2AX foci enumeration we have been able to gain an indication of whether a defect in the repair of radiation-induced DSBs is present in undefined radiosensitive lines. Although GOS5 cells demonstrated slightly elevated levels of residual damage in both assays compared to controls, this was not significant enough to suggest any substantial defect in repair. F96 cells demonstrated significantly elevated levels of residual damage in both assays indicating defective repair, and this connotation was considered in subsequent investigations of this undefined line.

5.5 Discussion

Concurrent with the activation of repair processes DNA damage activates cell-signaling cascades that function to arrest the cell cycle. In the first instance this is thought to allow time for repair to occur before the initiation of DNA synthesis (G1/S checkpoint), resumption of DNA synthesis (S-phase checkpoint) or the initiation of mitosis (G2/M checkpoint) (Nyberg *et al*, 2002). Failure to efficiently activate cell cycle checkpoints after the induction of DNA damage is associated with high levels of genomic instability and cellular radiosensitivity, characteristics that are exemplified by cells with mutations in the ATM transducing kinase (Houldsworth and Lavin, 1980) (Painter and Young, 1980) (Kastan *et al*, 1992) (Beamish *et al*, 1994). Consistent with this data, the A-T1BR line displayed a deficiency in G1/S checkpoint activation compared to control cells as shown by BrdU cell cycle analysis. In contrast, the F96 line demonstrated efficient G1 arrest after irradiation and, apart from immunodeficiency, the F96 patient did not show any of the clinical characteristics of A-T. This suggests that the F96 line does not have defects in ATM that confer checkpoint deficiency. These results are consistent with previous investigations into the F96 line that described normal checkpoint function (Peake *et al*, 1999).

AT cells fail to efficiently stabilise p53 after exposure to ionising radiation (Lu and Lane, 1993) (Khanna *et al*, 1995) an event that is required for efficient G1/S arrest. In order to determine whether the undefined radiosensitive lines identified in section 4 are deficient in the activation of p53, we examined the induction of p21, a p53 target gene that is required for efficient G1/S arrest after exposure to γ-radiation. Consistent with BrdU cell cycle analysis results, the A-T1BR line demonstrated a deficiency in the induction of p21 mRNA after irradiation compared to control. The minimal increase (1.3 fold) in p21 mRNA levels that was observed may result from activation of ATR, which has been proposed as a compensatory mechanism for the delayed activation of p53 in the absence of ATM (Abraham, 2001). In contrast, the repair defective lines 180BR and CJ179, which have mutations in the Ligase IV and Artemis DSB repair genes respectively, displayed a normal induction of p21 mRNA after irradiation. This is consistent with previous reports that have described the efficient initiation of a G1/S checkpoint and induction of p21 after irradiation in NHEJ defective cells (Badie *et al*, 1997) (Jhappen *et al*, 2000). Therefore, although wild type Ligase IV and Artemis are required for normal levels of survival after irradiation, these defects are not associated with impaired checkpoint signaling regarding the induction of p21 after irradiation. Similar to the repair defective lines examined, the undefined radiosensitive lines GOS1, GOS5, GOS14 and F96 all demonstrated a robust induction of p21 mRNA after irradiation. This may be expected for the F96 line, considering the efficient activation of a G1/S checkpoint as shown by BrdU analysis, and since p21 protein induction after irradiation was previously found to be normal in F96 cells (Peake *et al*, 1999). Thus, in contrast to AT cells, these undefined radiosensitive lines do not show any evidence of an attenuated p53 response. Since none of these patients presented with the characteristic clinical symptoms of AT, it is unlikely that the observed radiosensitive phenotypes result from defects in the ATM protein associated with impaired p53 signaling.

Whilst the undefined radiosensitive lines have demonstrated robust activation of the p53 signaling pathway, this was also observed in DSB repair defective lines. In this situation, concurrent with the activation of DNA damage checkpoints, these mutant lines initiate repair pathways that are insufficient to effectively repair DNA damage. This can result in an increased number of residual DSBs after irradiation (Borgmann and Dikomey, 1997) (Dikomey *et al*, 1998) (Wachsberger *et al*, 1999), and since this endpoint has been associated with poor survival after irradiation (Wurm *et al*, 1994)

(Kiltie *et al*, 1997) (Dikomey *et al*, 1998) (Sarkaria *et al*, 1998) (Zhou *et al*, 1998) (Dikomey *et al*, 2000a) (Dikomey *et al*, 2000b), we investigated whether any of the undefined radiosensitive lines showed any evidence of defective repair. This was initially performed by examining levels of unrepaired chromosome and chromatid breaks after irradiation.

AT cells have previously demonstrated a high level of unrepaired chromatin breaks after irradiation (Taylor *et al*, 1976) (Sasai *et al*, 1994) or treatment with a radio-mimetic drug (Shaham *et al*, 1983), which may lead to increased levels of chromosomal deletions (Cornforth and Bedford, 1985) (Mozdarani and Bryant, 1989) (Martin *et al*, 2003). Consistent with these previous findings, the A-T1BR line demonstrated significantly higher levels of unrepaired breaks compared to control cells. Whilst the A-T1BR line displayed an elevated level of residual breaks that was approximately ten-fold higher than that that of control cells, the Artemis deficient CJ179 line demonstrated only a two-fold increase. This difference in chromosomal radiosensitivity is consistent with results obtained for cellular radiosensitivity using these lines, in which the A-T1BR line was found to be considerably more radiosensitive that the CJ179 line (section 4).

The majority of unrepaired breaks observed in the A-T1BR line after irradiation corresponded to chromatid breaks, in contrast to other lines that displayed approximately equal numbers of chromosome and chromatid breaks. AT cells have previously been shown to convert more DSBs into chromatid deletions than do normal cells (Mozdarani and Bryant, 1989). Whereas chromosome breaks are thought to arise from DSBs induced in G1, chromatid breaks are initiated by an undetermined mechanism involving DSBs induced in late S- or G2 phases of the cell cycle (Bryant, 2004). Since there appears to be no correlation between G1 chromosomal radiosensitivity and G2 chromatid radiosensitivity (Scott *et al*, 1999) different mechanisms are thought to convert DSBs into chromosomal aberrations at different stages of the cell cycle. The high levels of chromatid breaks observed in A-T cells may therefore result from a specific defect in DSB repair in G2. Since Homologous Recombination (HR) DSB repair is restricted to the late S- and G2 phases of the cell cycle (Takata *et al*, 1998) (Johnson and Jansin, 2000), and ATM has been implicated in this pathway (Chen *et al*, 1999b) (Morrison *et al*, 2000), the high levels of chromatid breaks observed in AT cells may reflect a specific defect in HR DSB repair. High

levels of chromatid breaks may also result from the lack of checkpoint function associated with AT cells (Houldsworth and Lavin, 1980) (Painter and Young, 1980) (Kastan *et al*, 1992) (Beamish *et al*, 1994) (section 5.3). Recent work has supported the notion that chromatid breaks result from a signaling pathway initiated by the presence of a DSB in a distinct loci, which involves either intra- or inter- chromatid recombination (Bryant *et al*, 2004). Since DSBs induced in G1 are expected to persist into the later stages of the cell cycle in A-T cells due checkpoint deficiency, this effect may promote chromatid break formation at this time.

The CJ179 line displayed significantly higher levels of unrepaired chromatin breaks compared to control cells. This is consistent with the complete lack of functional Artemis protein in this line (P. Jeggo, personal communication). Previous studies on murine cells have demonstrated increased levels of chromosomal instability in the absence of Artemis protein (Rooney *et al*, 2002), and this effect was enhanced in ES cells by treatment with ionising radiation (Rooney *et al*, 2003). Our results confirm that Artemis deficiency leads to increased chromosomal instability in human cells after irradiation, and may suggest a genome caretaker role for this protein in humans. The higher levels of chromatin breaks observed are likely to reflect the DSB repair defect associated with Artemis deficient cells as shown using the H2AX DSB repair assay (section 5.6.2) and pulse field gel electrophoresis to measure DSB rejoining (Riballo *et al*, 2004). The mildly radiosensitive lines GOS1 and GOS14 demonstrated a normal level of unrepaired chromatin breaks after irradiation, and although GOS5 cells had slightly elevated levels compared to control, this difference was not significant. This suggests that these cells are able to rejoin DNA DSBs efficiently and argues against the presence of a major defect in DSB repair. Conversely, the F96 line demonstrated significantly higher levels of unrepaired chromatin breaks compared to controls and this was to a similar extent as that observed in the Artemis deficient CJ179 line. These results indicated that the F96 line may harbour a similar defect in DSB repair, and we were able to further investigate this eventuality using the H2AX DSB repair assay.

Recent studies have demonstrated that enumerating γ-H2AX foci at various time points after irradiation can be used to measure the repair of DNA DSBs in primary human fibroblasts (Rothkamm and Lobrich, 2003) (Khune *et al*, 2004) and Chinese hamster ovary cells (Rothkamm *et al*, 2003). This method can also be employed at more physiologically relevant doses of ionising radiation compared to the more established

DSB repair assay involving PFGE (Badie *et al*, 1995a), which is restricted to doses of at least 10 Gy therefore limiting sensitivity. Compared to control cells, the radiosensitive 180BR line that harbours a hypomorphic mutation in the Ligase IV DSB repair gene (Riballo *et al*, 1999) (Riballo *et al*, 2001) displayed a slower initial rate of DSB repair. The number of foci returned to pre-treatment levels 48 hours after irradiation, while control cells achieved this within 24 hours. This is consistent with a hypomorphic mutation in Ligase IV that limits the initial rate of DSB rejoining but eventually, and with slower kinetics, is able to reduce the level of residual DSBs to pre-treatment levels. A slower initial rate of DSB repair has previously been reported in the 180BR line that was associated with reduced, but not abolished, double stranded DNA end ligation (Riballo *et al*, 2001). Since DNA end ligation is likely to be required for all NHEJ reactions, this should affect the repair of most, if not all, of the DSBs induced by ionising radiation.

In contrast the Artemis null CJ179 line displayed an initial rate of DSB rejoining that was similar to control cells until 24 hours after irradiation, when an elevated level of residual breaks remained. This elevated level of residual breaks did not dissipate significantly up to 72 hours after irradiation, suggesting a defect in DSB repair distinct from that observed in the Ligase IV defective 180BR line. This may indicate that while the Artemis protein is not required for the repair of the majority of radiation induced DSBs that occurs within the first 24 hours of radiation, a subset of breaks persist and are refractory to repair. This is consistent with the notion that Artemis is required for the repair of complex DSBs, i.e. those with base lesions and single strand breakage in the proximity of the DSB that require processing before ligation (Jeggo an O'Neil, 2002). From biophysical simulations, the proportion of IR induced DSBs that are complex is significant and may represent 30-40 % for sparsely ionising radiations such as γ-rays, rising to ~95 % for densely ionising α-radiation (Nikjoo *et al*, 2001). A consequence of the increased complexity of DSB is seen as a decrease in the proportion of DSB rejoined in mammalian cells on increasing ionisation density of the radiation (Jenner *et al*, 1993). Therefore, a fraction of complex breaks may require nucleolytic processing before ligation, and this does not occur in the absence of Artemis and leads to cell inactivation. Previous studies that report normal DSB repair in Artemis deficient cells utilising doses of 20-60 Gy followed by PFGE (Nicolas *et al*, 1996) (Zhang *et al*, 2004) may not be able to detect this residual fraction of unrepaired DSBs due to the poor sensitivity of this assay. In addition, the Zhang *et al*, 2004 study did not examine the

residual level of DSBs beyond 4 hours after irradiation, when the elevated level of residual DSBs is most apparent in the Artemis null CJ179 line. Indeed, recent work examining extended time points after irradiation confirmed that Artemis deficient cells are unable to repair a subset of DSBs, and this defect is enhanced by agents that induce relatively high levels of complex DSBs (Riballo *et al*, 2004).

Similar to the Artemis null CJ179 line, although the F96 line displayed a normal initial rate of DSB repair, an elevated level of residual H2AX foci remained 24 hours after irradiation. This is consistent with chromosome breakage results, which demonstrated an elevated level of chromatin breaks after irradiation in F96 cells. Whilst an elevated level of foci was still present at 48 hours, this had returned to control levels 72 hours after irradiation, in contrast to the Artemis null CJ179 line that retained elevated levels of foci at this late time point. These results indicate that whilst the F96 line may harbour a similar defect to that of CJ179 cells in the repair of a subset of DSBs, this deficiency may not be as severe since the level of foci eventually returned to normal. The underlying mutation may therefore confer enough residual function to repair complex breaks with reduced kinetics and/or fidelity, but the extended persistence and/or poor stability of such rejoined breaks may lead to cell inactivation. This would be consistent with the high level of dicentric chromosomes observed in the F96 that may result from mis-rejoining of radiation induced DSBs (Pfeiffer *et al*, 2000) and have been observed at high levels after irradiation in DNA-PK deficient cells (Evans *et al*, 1996). Indeed dicentric chromosomes have been proposed as a surrogate maker for the quality of DSB repair and were reduced by stimulation of DNA-PK activity (Dittmann *et al*, 2003). Our results suggest that a high level of misrepair occurs in the F96 line after irradiation.

A previous investigation into DSB repair in the F96 line described a fast rate of initial rejoining with normal levels of residual breaks 24 hours after exposure to γ-radiation (Peake *et al*, 1999). This was performed using the relatively insensitive PFGE technique after a dose of 30 Gy. Although these results disagree with our findings, the observed defect in DSB repair is subtle and only detectable within a restricted timeframe after irradiation. The poor sensitivity associated with PFGE and large doses of γ-radiation employed may have masked this subtle defect in DSB repair. Indeed, the fact that PFGE was unable to detect any defects in DSB repair in Artemis deficient cells similar to the CJ179 line (Nicolas *et al*, 1996) (Zhang *et al*, 2004) would suggest that

the less severe deficiency inherent to F96 cells would go undetected using this technique. The results from our chromosome breakage study further support the notion of defective repair in the F96 line.

The radiosensitive GOS1 and GOS5 lines demonstrated a normal rate of initial DSB repair as shown by γ-H2AX foci enumeration, and although there were slightly elevated levels of residual breaks 24 hours after irradiation, this effect was not significant compared to controls. The GOS5 line also demonstrated a slightly elevated level of unrepaired chromosome breaks compared to control that was not significant, and therefore displayed comparable results in both test systems. Although these results suggest no overt defect in repair is associated with the GOS1 and GOS5 lines, GOS5 cells did display a high level of dicentric chromosomes that could result from poor DSB repair fidelity. The radiosensitive GOS1 line was found to be comparable to control cells in both the chromosome breakage and γ-H2AX enumeration assays systems, therefore a defect in DSB repair is unlikely to be responsible for the observed radiosensitivity of this line.

These results indicate that unlike AT cells, the radiosensitive lines examined are able to efficiently activate p53 dependent gene transcription. The observed radiosensitivity of these lines is therefore not expected to be associated with defective G1/S checkpoint activation. Whilst all of the GOS lines have shown no convincing evidence of a defect in DSB repair, the F96 line is a good candidate to have a mild defect in this aspect of the damage response similar, but not as severe, to that observed in the Artemis null CJ179 line. The repair deficiency observed in F96 cells may also be associated with a high level of DSB misrejoining.

Chapter 6: Analysis of candidate genes associated with radiosensitive immunodeficiency

6.1 Background

We have identified a group of undefined immunodeficient patients that have demonstrated cellular radiosensitivity in fibroblast survival assays. After further investigation, one radiosensitive line (F96) displayed evidence of defective DNA repair. Defects in DNA repair have been previously described in radiosensitive immunodeficient patients with mutations in the Ligase IV (O'Driscoll *et al*, 2001) and Artemis (Moshous *et al*, 2001) (Li *et al*, 2002a) (Kobayashi *et al*, 2003) (Moshous *et al*, 2003) (Noordzij *et al*, 2003) DSB repair genes. Such deficiencies impair the ability to perform V(D)J recombination during lymphocyte development and result in poor cellular survival after radiation-induced DSBs.

To investigate the possibility that the radiosensitive patients identified in this project have similar mutations in DSB repair genes, we analysed the coding region of candidate genes obtained by RT-PCR of primary fibroblast cDNA. This was performed for the Artemis, Ligase IV and XRCC4 DSB repair genes. The Artemis protein is a nuclease that is thought to remove several end nucleotides prior to DSB rejoining, since pathological and physiological DSBs usually result in incompatible ends (Moshous *et al*, 2001) (Jeggo and O'Neill, 2002). The XRCC4/Ligase IV complex then functions in the final ligation stage of NHEJ, where the XRCC4 protein appears to stabilise and enhance the activity of Ligase IV in the rejoining of DSBs (Grawunder *et al*, 1997) (Grawunder *et al*, 1998). Although patients with mutations in XRCC4 have not been previously described, such defects would be expected to result in a similar human disorder to Ligase IV syndrome since the proteins function in the same step of NHEJ and their interaction is required for V(D)J recombination and DSB repair (Grawunder *et al*, 1998).

The sequencing of candidate genes can be a laborious process depending on the size of the coding region in question. We therefore restricted our efforts to 3 genes with a coding region of reasonable size (less than 3 kb) that was amenable to RT-PCR followed by DNA sequencing. We also focused on the F96, GOS5 and GOS23

undefined lines that displayed intermediate radiosensitivity in section 4.2.2., since it is more likely these patients have mutations in specific DNA repair genes compared to the patients that demonstrated a mild radiosensitivity, which could possibly result from random genetic variation. Consistently, no data was found for a defect in DNA repair in lines that demonstrated mild radiosensitivity (section 5.4), whereas one line with intermediate radiosensitivity (F96) displayed evidence of defective repair. Hence, this line in particular was a strong candidate to harbour a mutation in the repair genes under investigation.

6.2 Sequencing of candidate DNA repair genes

6.2.1 XRCC4 sequencing

A pair of PCR primers (UX and LX) was designed to amplify a 1283 bp fragment that spans the entire human XRCC4 coding sequence using cDNA as a template (figure 6-1). These primers target XRCC4 transcript variant 3 (GenBank identifier NM 022550), which includes the 3' portion of non-coding exon 1 that is missing in the other two known variants (1 and 2). The protein-coding region of transcript 3 is the same as that of variant 1, coding for full length XRCC4. Transcript 3 was sequenced here since the optimal design of PCR primers was easily achieved using this transcript as a template. PCR conditions were optimised to generate a clear 1283 bp band after gel electrophoresis on a 1 % agarose gel (figure 6-1), and the amplified product was then gel purified to be used as a template for DNA sequencing. The original PCR primers (UX and LX) were used in conjunction with sequencing primers located at approximately 500 bp intervals along the amplified product (U1 and U2; upper strand, L1 and L2; lower strand, figure 6-1) in order to sequence the coding region. This was performed in both directions for 3 templates generated in separate PCR reactions, after which the sequence data was pooled for analysis in each cell line. This process was completed for the control line 48BR and the radiosensitive patient lines F96, GOS5 and GOS23. All of these lines had wild type XRCC4 coding sequence identical to the published sequence.

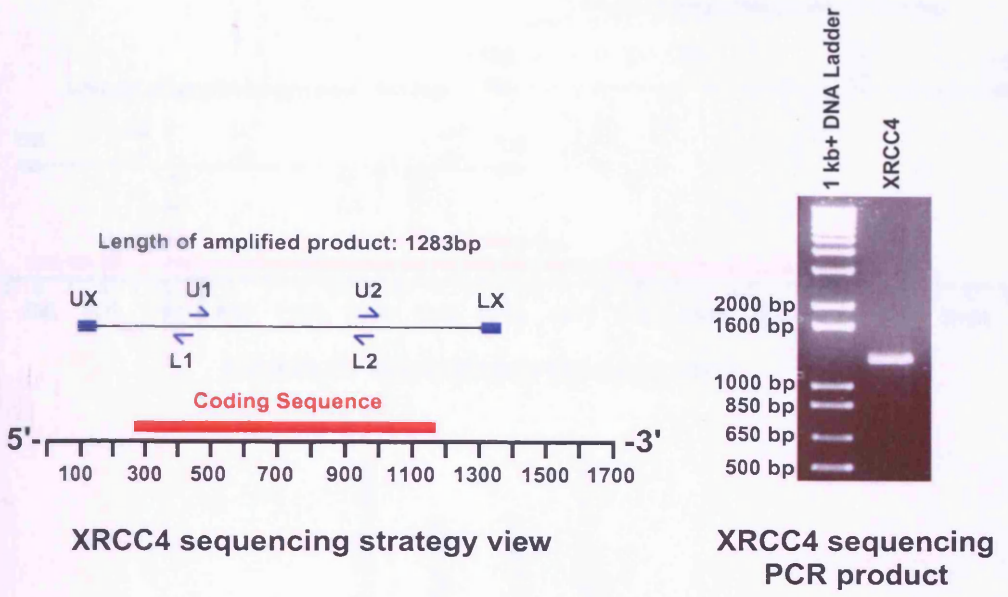

Figure 6-1: Strategy for sequencing human XRCC4. PCR primers UX and LX were designed to amplify the entire coding sequence of XRCC4. These were first used to amplify XRCC4 from cDNA, and then in conjunction with primers U1, U2, L1 and L2, were again used to sequence the gel purified PCR product.

6.2.2 Ligase IV sequencing

The Ligase IV coding region is 2734 bp long and was amplified in two overlapping sections. Primers UB and LB were designed to amplify a 1473 bp fragment that encompassed the 5' half of the coding region (figure 6-2). These PCR primers were then used in conjunction with primers U2, U3, U4 (upper strand), L1 and L2 (lower strand) in order to sequence the gel purified product in both directions. The 3' half of the coding region was amplified using primers UA and LA, which produce a 1496 bp PCR product (figure 6-2). These primers were then used in conjunction with primers U6, U7 (upper strand) L4 and L5 (lower strand) in order to sequence the gel purified PCR product in both directions. For both the 5' and 3' fragment, 3 templates produced in separate PCR reactions were sequenced in both directions, and the resulting sequence data pooled to construct the full coding sequence for each cell line. This process was completed for the control line 48BR and the radiosensitive patient lines GOS5 and GOS23. All of these lines had wild type Ligase IV coding sequence identical to the published sequence.

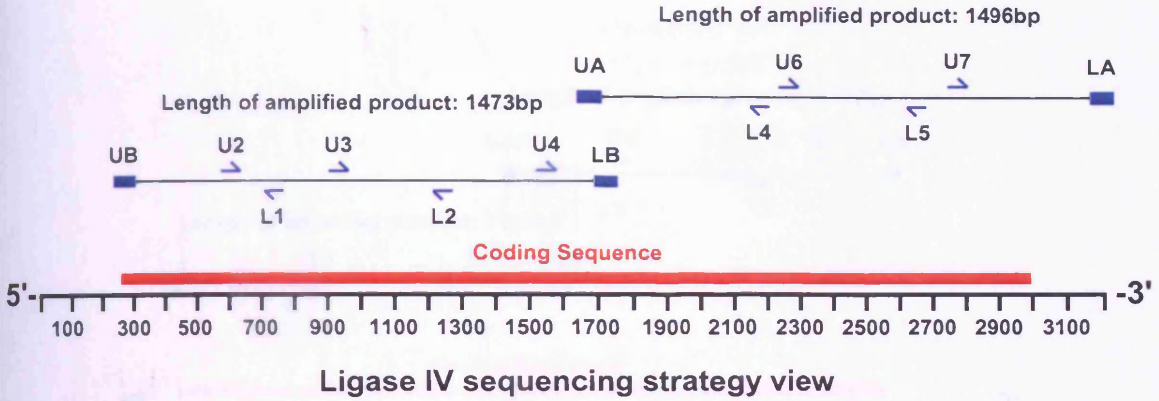

Ligase IV sequencing strategy view

Ligase IV sequencing PCR product

Figure 6-2: Strategy for sequencing human Ligase IV. PCR primers UB and LB were designed to amplify the 5' coding sequence of Ligase IV. These were first used to amplify the 5' region from cDNA, and then in conjunction with primers U2, U3, U4, L1 and L2, were again used to sequence the gel purified PCR product. PCR primers UA and LA were designed to amplify the 3' coding sequence of Ligase IV. These were first used to amplify the 3' region from cDNA, and then in conjunction with primers U6, U7, L4 and L5, were again used to sequence the gel purified PCR product. The resulting sequence data was then pooled in order to construct the full coding sequence of Ligase IV for each primary cell line.

6.2.3 Artemis sequencing

The Artemis coding region is over 2000 bp long, and similar to the strategy used to sequence Ligase IV, this gene was initially amplified to two sections. Primers UA and LA1 were designed to amplify a 1160 bp fragment that encompassed the 5' half of the coding region (figure 6-3). These PCR primers were then used in conjunction with primers U2, U3, (upper strand), L4 and L5 (lower strand) in order to sequence the gel purified product in both directions. The 3' half of the coding region was amplified using primers UA2 and LA, which produce a 1177 bp PCR product (figure 6-3).

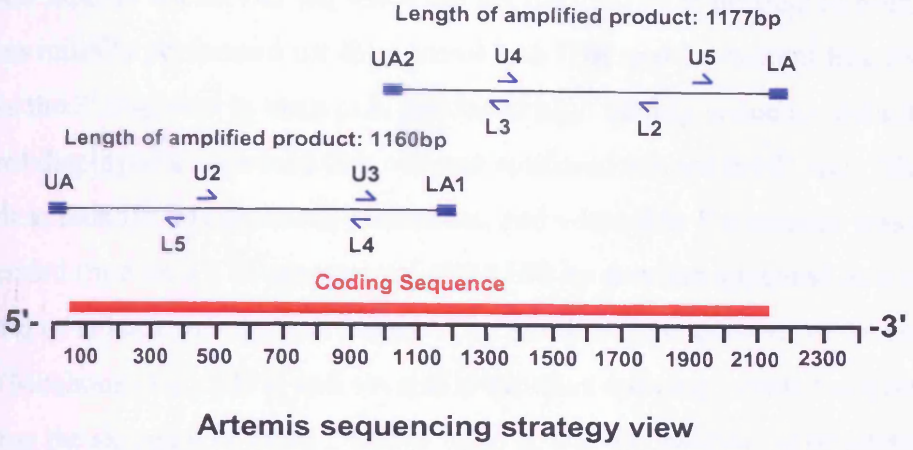

Artemis sequencing strategy view

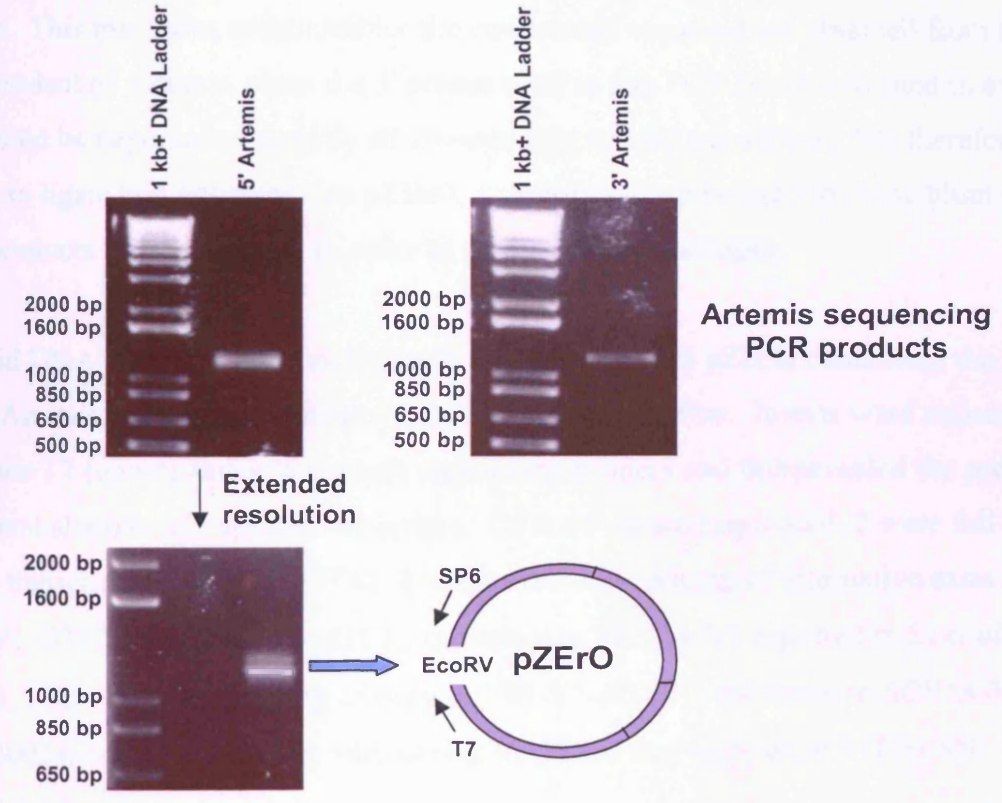

Figure 6-3: Strategy for sequencing human Artemis. PCR primers UA and LA1 were designed to amplify the 5' coding sequence of Artemis. These were first used to amplify the 5' region from cDNA, and then in conjunction with primers U2, U3, L4 and L5, were again used to sequence the gel purified PCR product. PCR primers UA2 and LA were designed to amplify the 3' coding sequence of Artemis. These were first used to amplify the 3' region from cDNA, and then in conjunction with primers U4, U5, L2 and L3, were again used to sequence the gel purified PCR product. Whereas the 3' fragment produced high quality sequence data, the 5' fragment generated sequence that became confused toward the 5' end, and appeared as a smear when resolved for an extended time on a 1% agarose gel (b). The gel purified 5' fragment was therefore blunt end ligated into pZErO and clones were sequenced using the T7 (forward) and SP6 (reverse) sequencing primers.

These primers were then used in conjunction with primers U4, U5 (upper strand) L2 and L3 (lower strand) in order to sequence the gel purified PCR product in both directions. This was initially performed for the control line 1BR and the patient line F96, but whereas the 3' fragment in each case produced high quality sequence data, the 5' fragment displayed a sequence that became confused toward the 5' end. This made it difficult to identify any potential mutations, and when this 5' fragment was resolved for an extended time on a 1 % agarose gel, the 1160 bp product appeared as a smear that consisted of at least two distinct bands. The Artemis gene consists of 14 constitutive exons (Moshous *et al*, 2001) and several alternative splicing events have been reported involving the skipping of exon 2 and/or exon 5, and the in-splicing of alternative exons 2b, 2c and 3b, all of which occur in the 5' region of the coding sequence (Li *et al*, 2002a). This may have accounted for the convoluted sequence we obtained from the 5' PCR product of Artemis, since the 5' primer used in this PCR (UA) is located in exon 1 and would be expected to amplify all alternatively spliced transcripts. We therefore decide to ligate this fragment into pZErO, a vector that can be used to clone blunt ended PCR products for sequencing, in order to further study this region.

Plasmid DNA was isolated from 6 clones transformed with pZErO containing the 5' half of the Artemis coding region from the radiosensitive F96 line. Inserts were sequenced using the T7 (upper) and SP6 (lower) sequencing primers and this revealed the presence of several alternatively spliced transcripts. Of the 6 clones sequenced, 2 were full-length transcripts (2 x F96-G377A), 2 involved the in-splicing of alternative exon 2b (F96-V1-G377A and F96-V1-ΔGTT, equivalent to SCIDA-V1 reported in Li *et al*, 2002a), 1 involved the skipping of exon 5 (F96-V3-ΔGTT, equivalent to SCIDA-V3, Li *et al*, 2002a) and 1 novel splice variant was identified that skips exon 9 (F96-V9-G377A) (table 6-1).

Table 6-1: Range of alternatively spliced transcripts and potential mutations in cloned F96 Artemis 5' fragment *(Numbered from translation initiation codon)*

Transcript	Exon deletion	Alternative exons	Frequency	Changes to published sequence
F96-G377A	-	-	2/6	G377A, A728G
F96-V1-G377A	-	2b	1/6	G377A, A728G
F96-V1-ΔGTT	-	2b	1/6	ΔGTT207-9, T643C
F96-V3-ΔGTT	5	-	1/6	ΔGTT207-9, T643C
F96-V9-G377A	9	-	1/6	G377A, A728G

In addition, there were 4 potential mutations present in the F96 Artemis gene that occurred in pairs that seemed to be mutually exclusive. This suggested that 2 Artemis alleles were represented in F96 cDNA, each of which contained two mutations. One allele contained G377A and A728G (numbered from the translation initiation codon) point mutations, whilst the other harboured a GTT207-209 codon deletion and a T681C point mutation (table 6-1).

6.2.4 Cloning of full length Artemis cDNA and confirmation of F96 Artemis mutations.

In order to confirm the potential Artemis mutations identified in the F96 line and fully characterise the range of transcripts expressed, we attempted to clone the entire Artemis coding region from control (1BR) and F96 cells. This was achieved using the gateway cloning system (Invitrogen). A pair of PCR primers (Art-F and Art-R) was designed to amplify the entire Artemis coding region and incorporate a CACC motif exactly 5′ to the ATG translation initiation codon. The sequence of the forward primer was therefore CACC ATG GTT CTT TCG AGG G. After a successful amplification reaction the CACC motif would allow the PCR product to be cloned directly into a Gateway TOPO directional cloning vector. The reverse primer was designed to anneal at the translation stop codon and modify this to code for tryptophan. This would allow the Artemis protein to be tagged at the C-terminus for later expression studies.

After optimisation of PCR conditions, primers Art-F and Art-R produced a band of the correct size (2083 bp) using both control (1BR) and F96 cDNA as a template (figure 6-4). The fragments produced using a PCR reaction containing 1mM $MgCl_2$ were cloned into pcDNA3.2/V5/GW/D-TOPO (Invitrogen) using the TOPO cloning system, whereby a GTGG overhang in the vector anneals to the CACC tagged PCR product, and *Vaccinia* virus topoisomerase I present at the cloning site recombines the two DNA molecules to clone the insert in the correct orientation. The T7 (forward) and TKR (reverse) primers where then used in combination with the Artemis sequencing primers described earlier (figure 6-3) to sequence the cloned inserts.

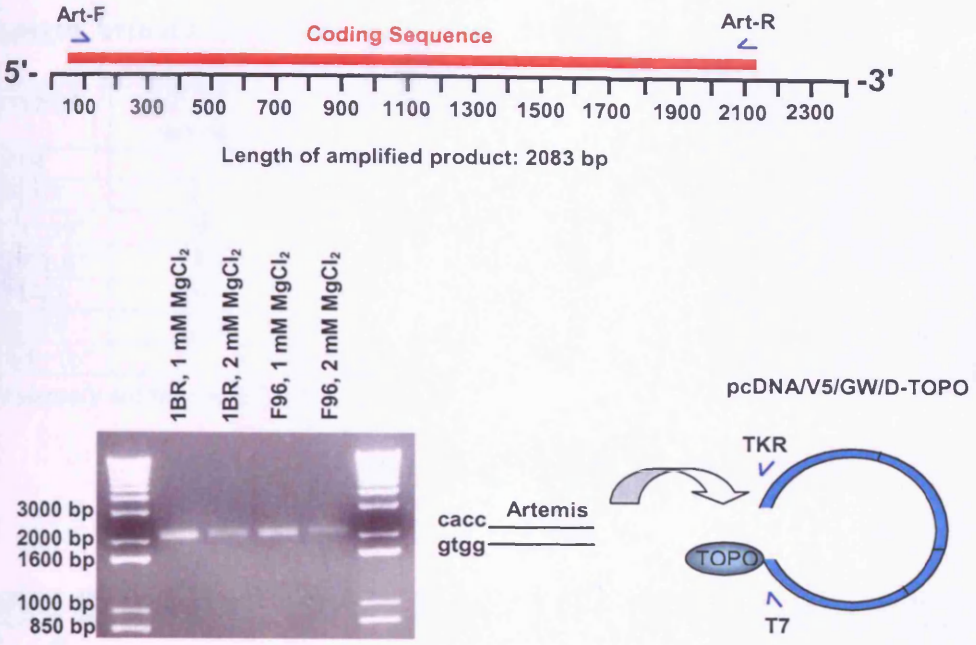

Figure 6-4: Strategy for cloning the full coding region of Artemis. The Art-F and Art-R PCR primers were designed to amplify the entire coding region of Artemis, and incorporate a CACC motif exactly 5′ to the ATG translation initiation codon. The gel purified PCR products could then be cloned directly into a gateway expression vector using the TOPO cloning system. Cloned inserts were sequence using a combination of the original PCR primers (Art-F and Art-R) and the sequencing primers described in figure 6-3.

In order to gain sufficient insight into the range of Artemis transcripts expressed in normal primary fibroblasts, 25 clones derived from 1BR cDNA and 22 clones derived from F96 cDNA were sequenced. Consistent with the preliminary results described above, along with the primary Artemis transcript there were many alternatively spliced products present in the F96 line, and this was also reflected in 1BR cells. Similar alternatively spliced transcripts have been described in SCID patients of Athabascan-speaking native Americans harbouring a common founder mutation (Y192X) (Li *et al*, 2002a), and since a single point mutation is unlikely to cause all splicing events, these alternative transcripts may also be expected in wild type cells. In addition to these previously characterised splice events, we also identified 3 novel variant transcripts in the 1BR line (table 6-2). These either involved the skipping of exon five, or the in-splicing of a previously uncharacterised 134 bp alternative exon that lies between exon 1 and 2, designated exon 1b (figure 6-5).

Table 6-2: Range of alternatively spliced transcripts and polymorphisms in cloned full length Artemis from 1BR cells *(Numbered from translation initiation codon)*

Transcript	Exon deletion	Alternative exons	Frequency	Differences to published sequence
1BR	-	-	7/25	T643C, G1678T, C1809T
1BR-V1	-	2b	7/25	T643C, G1678T, C1809T
1BR-V1Δ5*	5	2b	3/25	T643C, G1678T, C1809T
1BR-V2Δ5*	5	2c	2/25	T643C, G1678T, C1809T
1BR-V3	5	-	2/25	T643C, G1678T, C1809T
1BR-V4	2, 5	-	3/25	T643C, G1678T, C1809T
1BR-V1+1b*		1b, 2b	1/25	T643C, G1678T, C1809T

** Previously undescribed splice variants*

The organisation of the 1BR Artemis gene

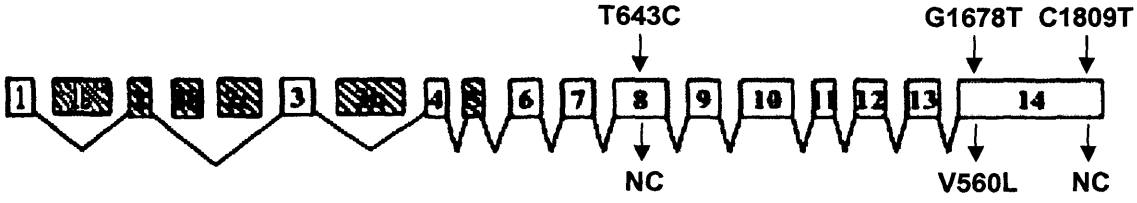

Sequence of exon 1b

5′ggagtcagccaccatgcctagctaatgtttgtatttttattattattttgag**GTGGAGTCTCCATCACCCTGG**
AGTGCAGTGGCGTGATCTCTGTTCACTGCAACCTCCGCCTCCTGGGTTCAAGCG
ATTCTCGTGCCTCAGCCTCCCAAGTAGCTGGAGTTACAGGCACGCACCACCACA
CCCAGgtaatttttgtgtttttagtagagatgatgtttcacc**3′**

Figure 6-5: The organisation of the 1BR Artemis gene and the sequence of exon 1b. The exon-intron organisation is depicted. The constitutive exons are shown as □ and the alternative exons are shown as ▩. In addition to the previously described variants (Li *et al*, 2001a), 1BR cells expressed V1 and V2 transcripts with deletion of exon 5 (1BR-V1Δ5 and 1BR-V2Δ5). One transcript (1BR-V1+1b) was also identified that utilised a novel 134 bp alternative exon that lies between exon 1 and 2, designated exon 1b. The sequence of exon 1b is displayed in bold upper case, and the intron sequence directly 5′ and 3′ is shown in lower case. No transcripts were found that involved alternative exons 2c, and 3b. 3 differences to the published sequence were also present. T643C and C1809T are silent polymorphisms that are not expected to change the primary sequence of the Artemis protein, whereas G1678T results in a Valine560Leucine amino acid change.

The 1BR Artemis gene also had 3 differences to the published wild type sequence. T643C and C1809T in exons 8 and 14 respectively were classed as silent polymorphisms since these changes do not affect the predicted amino acid sequence of the Artemis protein. Conversely, the G1678T difference identified in exon 14 results in a V560L amino acid change in the Artemis protein. Since this represents the exchange of one hydrophobic amino acid for another, and the 1BR line is derived from a normal

individual, this change in sequence was considered to be a polymorphism that is unlikely to have any significant affect on Artemis protein function.

Novel Artemis splice variants were also expressed in the F96 line (table 6-3), one resulting from the in-splicing of alternative exon 2b as well as 2c, and the other involving the use of an alternative splice site in the middle of exon 9 and deletion of exon 11 (figure 6-6). All of the F96 Artemis clones contained the C1678T and C1809T polymorphisms characterised previously in the control line 1BR.

Table 6-3: Range of alternatively spliced transcripts and mutations in cloned full length Artemis from F96 cells *(Numbered from translation initiation codon)*

Transcript	Exon deletion	Alternative exons	Frequency	Differences to published sequence
F96-ΔGTT	-	-	4/22	**ΔGTT207-209, T643C,** G1678T, C1809T
F96-V1-ΔGTT	-	2b	4/22	**ΔGTT207-209, T643C,** G1678T, C1809T
F96-V3-ΔGTT	5	-	1/22	**ΔGTT207-209, T643C,** G1678T, C1809T
F96-V2bc-ΔGTT*	5	2b, 2c	1/22	**ΔGTT207-209, T643C,** G1678T, C1809T
F96-G377A	-	-	8/22	**G377A, A728G,** G1678T, C1809T
F96-V1-G377A	-	2b	2/22	**G377A, A728G,** G1678T, C1809T
F96-V3-G377A	5	-	1/22	**G377A, A728G,** G1678T, C1809T
F96-V9/11-G377A*	9# 11	-	1/22	**G377A** G1678T, C1809T

** Previously undescribed splice variants, # Deletion of the 5′ half of exon 9*

Exon 9 alternative splice site

5′atttcacataatttgcatgtatgtattatttgccttag**GTTCATGTGAATAAGCTAGACATGTTTAGGA**
ACATGCCTGAGATCCTTCATCGTCTCACAACAGACCGCAACACTCAGATCCATG
CATGCCGGCATCCCAAGgtacgtgtgcaagtgattcctctcgtattgtttgtgtaa3′

Figure 6-6: The exon 9 alternative splice site involved in transcript F96-V9/11-G377A. Transcript F96-V9/11-G377A involved the splicing of exon 8 to an alternative splice site in the middle of exon 9. Exon 9 sequence is depicted in bold upper case, and intron sequence is shown in lower case. The 3′ exon 9 sequence that was present in transcript F96-V9/11-G377A is depicted in blue bold upper case. The A728G polymorphism present on the G377A F96 allele is shown in red and therefore did not occur in transcript F96-V9/11-G377A.

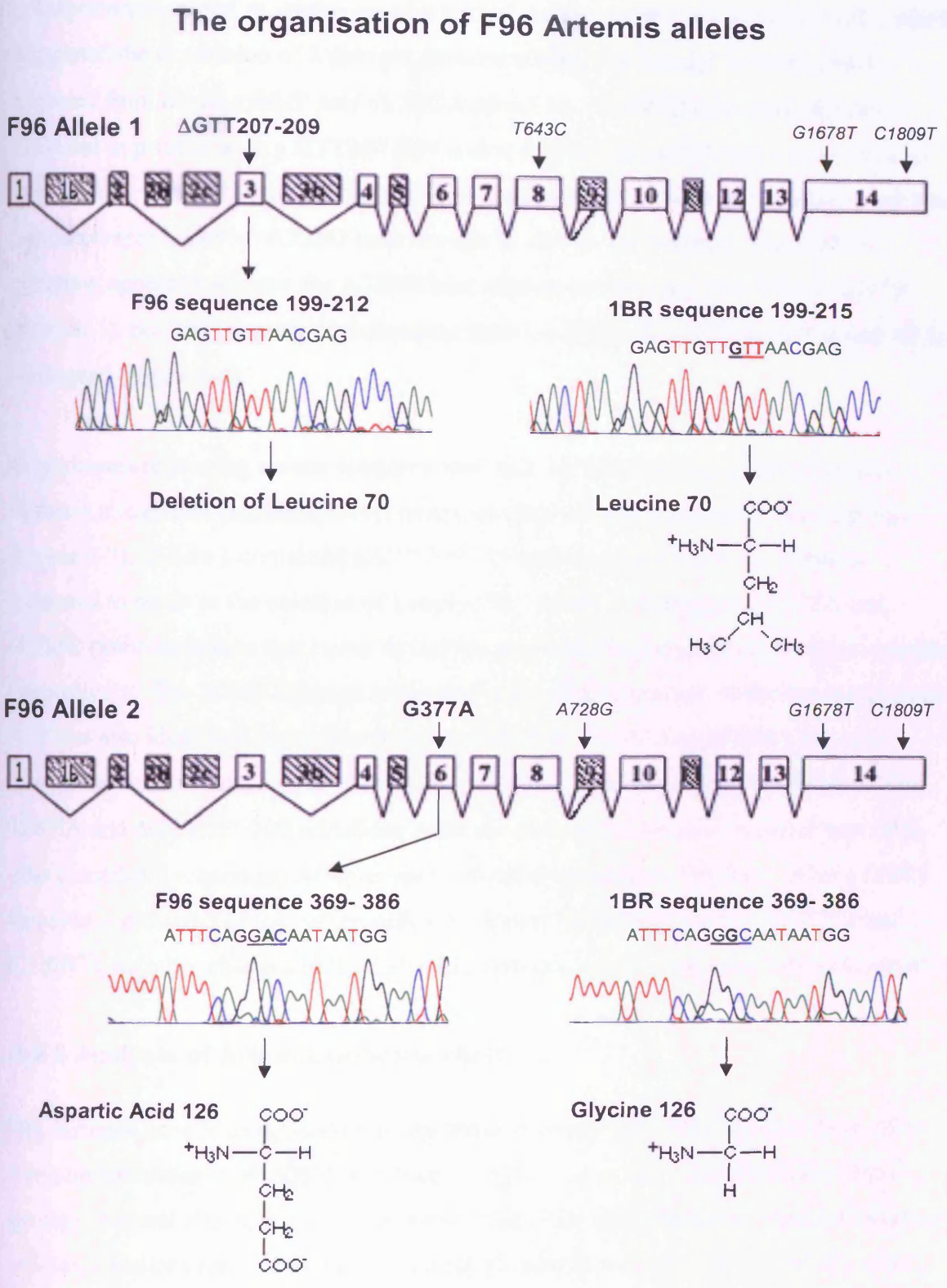

Figure 6-7: The F96 line is a compound heterozygote for mutations in the Artemis gene. F96 cells express 2 mutant Artemis alleles. Allele 1 harbors a GTT207-209 deletion in exon 3 that is predicted to result in the deletion of Leucine 70. Allele 2 contains a G377A point mutation in exon 6 that results a Glycine126Aspartic acid change in the Artemis protein. All the other differences compared to the published Artemis mRNA sequence are likely to be polymorphisms, since they were found in control cells and the draft sequence of the human genome (*italics*).

The T643C silent polymorphism identified in 1BR cells was also present in the F96 line but this only occurred in approximately half of the transcripts sequenced (10/22), which suggested the expression of 2 distinct Artemis alleles. Consistent with the results obtained from cloning the 5′ half of F96 Artemis, the T643C polymorphism only occurred in parallel with a GTT207-209 codon deletion in exon 3 that was specific to the F96 line. The remaining 13 transcripts contained a G377A point mutation, and this was accompanied by an A728G base change in all but one instance. The G377A mutation appeared without the A728G base change in transcript F96-V9/11-G377A (table 6-3), but this transcript involved the deletion of the 5′ half of exon 9 where A728 is situated (figure 6-6).

From these sequencing results we concluded that the F96 line expressed 2 distinct Artemis alleles that contained novel mutations that were not present in the 1BR line (figure 6-7). Allele 1 contained a GTT207-209 codon deletion in exon 3 that is expected to result in the deletion of Leucine 70. Allele 2 comprised G3777A and A728G point mutations that result in G126D and H243A changes in the Artemis protein respectively. The A728G change is present in the draft sequence of the human genome and was also identified in another primary fibroblast control line (48BR) that was sequenced for Artemis, and this is therefore likely to represent a polymorphism. The G377A and ΔGTT207-209 mutations were not present in this other control line. We also cloned and sequenced Artemis from the radiosensitive GOS5 line. Whilst GOS5 Artemis contained 3 of the polymorphisms already identified (T643C, G1678T and C1809T), no other changes to the published Artemis mRNA sequence were identified.

6.2.5 Analysis of Artemis splice variants

The Artemis gene is composed of 14 constitutive exons with sizes ranging from 52 to 1160 bp (Moshous *et al*, 2001), and exon 14 spans the entire C-terminal half of the protein. Several alternative splicing events have been reported involving the skipping of exon 2 and/or exon 5, and the in-splicing of alternative exons 2b, 2c and 3b, all of which occur in the 5' region of the coding sequence (Li *et al*, 2002). These alternative splicing events were reported in a group of Athabascan speaking Native Americans that harboured a common founder nonsense mutation (Y192X) that is unlikely to be responsible for all splicing events. Consistent with these previous findings, amongst the control (1BR) clones sequenced, we identified transcripts with deletions involving

exons 2 and 5, and inclusions of exon 2b or 2c (Table 6-4). These alternative transcripts code for severely truncated Artemis proteins, since the splicing-out of exons 2 or 5 as well as the addition of exons 2b or 2c, leads to a frameshift.

Table 6-4: Analysis of alternative Artemis transcripts identified in 1BR and F96 cells in sections 6.2.3 and 6.2.4

Transcript	Exon deletion	Alternative exons	Frequency (rel)	(%)	Frameshift after exon	Protein length (res)
1BR	-	-	7/25	28	-	692
1BR-V1	-	2b	7/25	28	2	54
1BR-V1Δ5*	5	2b	3/25	12	2	54
1BR-V2Δ5*	5	2c	2/25	8	2	56
1BR-V3	5	-	2/25	8	4	108
1BR-V4	2, 5	-	3/25	12	1	38
1BR-V1+1b*		1b, 2b	1/25	4	1b	82
F96 (G377A or ΔGTT)	-	-	14/28	50	-	692 or 691
F96-V1 (G377A or ΔGTT)	-	2b	8/28	29	2	54
F96-V2bc* (ΔGTT)	5	2b, 2c	1/28	3.3	2	54
F96-V3 (G377A or ΔGTT)	5	-	3/28	11	4	108 or 107
F96-V9* (G377A)	9	-	1/28	3.3	-	658
F96-V9/11* (G377A)	9# 11	-	1/28	3.3	-	625

** Previously undescribed splice variants, # Deletion of the 5' half of exon 9*

We also described the sequence of the novel alternative exon 1b, identified in a wild type variant that also incorporated exon 2b. Whilst the inclusion of exon 1b leads to the incorporation of 45 additional amino acids in the Artemis protein sequence, this leads to a frameshift when spliced to exon 2 and codes for a severely truncated protein of 82 amino acids (figure 6-8).

MSSFEGQMAEYPTISIDRFDRENLRARAYFLSHCHK**GGVSITLECSGVISVHCNLRLLGSSDSR**
ASASQVAGVTGTHHHTQIT. 82 Amino acids

Figure 6-8: The protein sequence coded for by Artemis variant transcript 1BR-V1+1b that involves inclusion of alternative exons 1b and 2b. The novel sequence encoded by exon 1b is shown in bold that when spliced to exon 2 results in a frameshift and a severely truncated protein of 82 amino acids.

Similar to the control line 1BR, F96 cells expressed alternatively spliced Artemis transcripts that involved deletions of exon 5, and additions of exons 2b and 2c. These variants contained either a G377A point mutation or a ΔGTT 207-9 codon deletion, and code for severely truncated proteins. There were also 2 transcripts expressed in the F96 line that contained the G377A point mutation and involved deletions of exon 9. F96-V9 involved deletion of exon 9 and codes for an Artemis protein with a 34 amino acid internal deletion in the metallo-ß-lactamase-associated CPSF Artemis SNM1/PSO2 (β-CASP) domain. F96-V9/11 involved the use of an alternative splice site within exon 9 and the deletion of exon 10. Whilst the use of this alternative splice site leads to a frameshift, the deletion of exon 10 brings the sequence back into frame and codes for an Artemis protein of 625 amino acids, which incorporates 13 amino acids of novel sequence within the β-CASP domain of Artemis (figure 6-9).

MSSFEGQMAEYPTISIDRFDRENLRARAYFLSHCHKDHMKGLRAPTLKRRLECSLKVYLYCSPV
TKELLLTSPKYRFWKKRIISIEIETPTQISLVDEASGEKEEIVVTLLPAGHCPGSVMFLFQGNN
GTVLYTGDFRLAQGEAARMELLHSGGRVKDIQSVYLDTTFCDPRFYQIPSREECLSGVLELVRS
WITRSPYHVVWLNCKAAYGYEYLFTNLSEELGVQ**TATLRSMHAGIPR**TGESSYRACFSFHSSYS
EIKDFLSYLCPVNAYPNVIPVGTTMDKVVEILKPLCRSSQSTEPKYKPLGKLKRARTVHRDSEE
EDDYLFDDPLPIPLRHKVPYPETFHPEVFSMTAVSEKQPEKLRQTPGCCRAECMQSSRFTNFVD
CEESNSESEEEVGIPASLQGDLGSVLHLQKADGDVPQWEVFFKRNDEITDESLENFPSSTVAGG
SQSPKLFSDSDGESTHISSQNSSQSTHITEQGSQGWDSQSDTVLVSSQERNSGDITSLDKADYR
PTIKENIPASLMEQNVICPKDTYSDLKSRDKDVTIVPSTGEPTTLSSETHIPEEKSLLNLSTNA
DSQSSSDFEVPSTPEAELPKREHLQYLYEKLATGESIAVKKRKCSLLDT. 625 Amino
acids

Figure 6-9: The protein sequence coded for by Artemis variant transcript F96-V9/11 that involves the use of an alternative splice site within exon 9 and deletion of exon 10. The novel 13 amino acid sequence introduced into the Artemis protein primary structure by use of the alternative splice site is shown in bold.

In control (1BR) and F96 cells the full length Artemis transcript was found in 28 % and 50 % of sequenced plasmids respectively. Although PCR can distort the proportions of particular transcripts in a mixed population, these results suggest that the full length transcript, possibly followed by variant 1 transcript, are the dominant species of Artemis mRNA expressed in these primary human fibroblasts. Most of the alternatively spliced transcripts, involving deletion of exons 2 and 5 or the addition of alternative exons 1b, 2b and 2c, result in a frameshift and code for severely truncated Artemis proteins. Only two alternative splicing modes identified amongst the F96 transcripts, F96-V9 and F96-V9/11, produce non-truncated proteins that may retain some residual function. These transcripts were found in only one of the sequenced plasmids in each case (3.3 %), and may therefore represent only a small fraction of the total complement of Artemis transcripts expressed by the F96 line.

6.2.6 Summary of candidate gene sequencing results

We have investigated 3 undefined radiosensitive lines for evidence of mutations in candidate genes associated with radiosensitive immunodeficiency. A summary of the results from these experiments is displayed in table 6-5.

Table 6-5: Summary of candidate gene sequencing results

Line	XRCC4	Artemis	Ligase IV
GOS5	WT	WT	WT
F96	WT	**ΔGTT207-209, G377A***	ND
GOS23	WT	ND	WT

*WT Wild type, ND Not done, * Compound heterozygote*

6.3 Expression of wild type and mutant Artemis proteins in human cells

We have identified two novel mutations in the Artemis gene of a radiosensitive line derived from an undefined immunodeficient patient. The Artemis protein can be divided into three regions. The first 155 amino acids of Artemis have marked homology to proteins of the metallo-β-lactamase family, which were first described in bacteria mediating the cleavage of β-lactam antibiotics (Aravind, 1999). This analogy was the first indication that Artemis probably has some kind of enzyme activity. The metallo-β-lactamase domain is followed by the β-CASP region (up to amino acid 385), which defines a family of metallo-β-lactamases that act on nucleic acids (Callebaut *et al*, 2002). Finally the last 307 amino acids of Artemis do not have any marked homology to other known proteins.

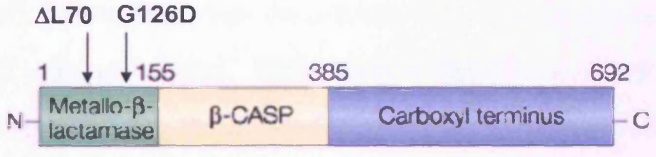

Figure 6-10: The Artemis protein can be divided into 3 regions. The metallo-β-lactamase homology domain, which contains four out of five conserved catalytic residues, spans the first 155 amino acids. This is followed by the β-CASP region that is common to metallo-β-lactamases that act in nucleic acids. The last 307 amino acids has no homology to any known proteins. The novel F96 mutations identified lie within the metallo-β-lactamase domain.

The ΔL70 and G126D mutations identified in F96 cells lie within the metallo-β-lactamase domain (figure 6-10), which contains four out of five of the conserved residues that define the catalytic site of these enzymes. Although the F96 mutations do not alter these residues directly, their presence may impair the catalytic activity and/or stability of this protein.

6.3.1 Expression of wild type Artemis in human cells

In order to assess the stability of the F96 mutant Artemis proteins in human cells, we first attempted to transfect cells with an expression vector containing the coding region of wild type Artemis isolated from 1BR cells. This was performed using 1BR Artemis that was cloned into the pcDNA/V5/GW/D-TOPO gateway vector for sequencing in section 6.2.4. A clone containing full length 1BR Artemis transcript was selected. The

TOPO system used to clone this fragment ensured that the insert was cloned in-frame with a C-terminal V5 tag, which can then be used to monitor expression with an anti-V5 antibody.

Initial attempts to transfect Artemis into primary human fibroblasts and human fibroblasts immortalised by stable expression of human telomerase (F96-hTERT) were unsuccessful using a transfection method involving Lipofectin/Integrin-targeting peptide 1/DNA complexes previously shown to efficiently transfect this cell type (Estruch *et al*, 2001). This was despite achieving a transfection efficiency of >50% with a GFP expression vector using the same transfection method and cells. We therefore attempted to express Artemis in cell lines. 293T cells are a human kidney tumour cell line and were initially used to confirm that we could express wild type Artemis by detection of a c-terminal V5 tag. 293T cells were either mock transfected or transfected with pEXP3.2-Artemis-V5 and after a 24 hr incubation period cell lysates were prepared. Cell lysates were run on a 10 % SDS-PAGE denaturing gel and an immunoblot for V5 was performed. Wild type Artemis is a 78 kD protein and the addition of a c-terminal V5 tag should result in a 5 kD increase in size. Consistent with this, 24 hrs after transfection with pEXP3.2-Artemis-V5 a band was observed corresponding to a protein of 83 kD, and this was absent in the mock transfected control (figure 6-11a). There were also secondary bands present in transfected cells at approximately 75 and 50 kD that are likely to represent degradation products of the transfected protein.

We next investigated whether transfected Artemis protein was expressed in the appropriate sub-cellular compartment to perform its role in DNA repair, i.e. the nucleus. Wild type Artemis coding region was transferred from pEXP-Artemis-V5 into the Gateway destination vector pDEST 47 in order to create an Artemis expression vector that produces a c-terminal GFP tagged Artemis protein (pEXP47-Artemis-GFP). pEXP47-Artemis-GFP was transiently transfected into 293T cells and the expression of GFP tagged Artemis was visualised by fluorescence microscopy 24 hrs after transfection. All positive cells (~20 %) showed the tagged protein essentially exclusively in the nucleus (excluding nucleoli) (figure 6-11b), which is consistent with its role in DNA repair. Cells transfected with pGFP and pEXP47-Artemis-GFP were

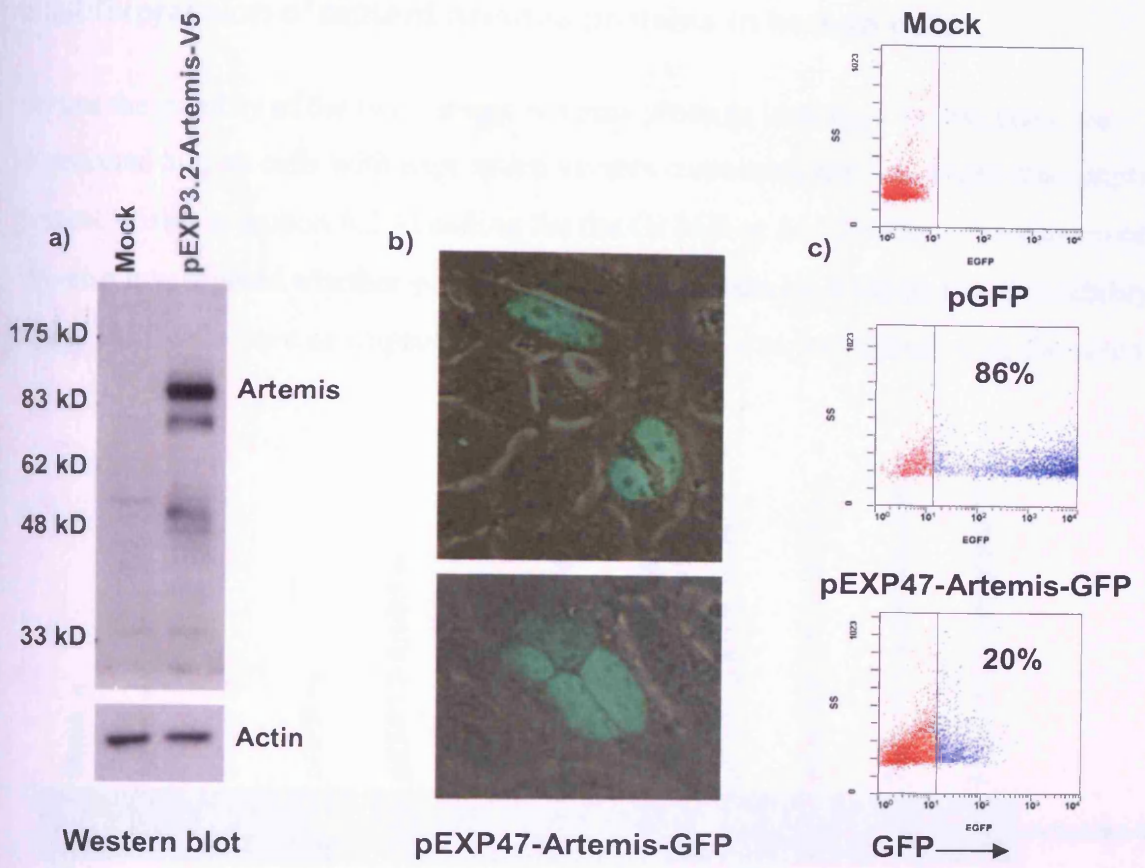

Figure 6-11: Expression of wild type Artemis protein in 293T cells shows a nuclear localisation. a) Western blot of Artemis expression. 293T cells were transiently transfected with pEXP3.2-Artemis-V5 and cell lysates prepared after a 24 hr incubation. Immunoblot analysis was performed using anti-V5 antibody, and a band of the correct size (83 kD) for V5-tagged Artemis was visualised. Actin expression levels were used as a loading control (bottom panel). b) 293 cells were transfected with pEXP47-Artemis-GFP and the sub-cellular localisation of GFP tagged Artemis was visualised by fluorescence microscopy 24 hrs after transfection. Artemis expression was confined to the nucleus (excluding nucleoli). c) Expression levels of transfected GFP tagged Artemis compared with GFP alone as measured by FACS analysis. Compared to transfection with GFP alone, there were less GFP-tagged Artemis positive cells, and those that were positive displayed a lower level of fluorescence.

also analysed by FACS to compare expression levels (figure 6-11c). Compared to transfection with GFP alone, the GFP tagged Artemis transfections resulted in a lower percentage of GFP positive cells, and those that were positive displayed considerably less fluorescence. This was despite using the same method of transfection for each plasmid, both of which utilised the Cytomegalovirus (CMV) promoter. The reason for the difficulties in expressing high levels of exogenous Artemis protein in human cells remains unclear. Similar problems using Artemis expression vectors were encountered by our collaborators (P. Jeggo, personal communication).

6.3.2 Expression of mutant Artemis proteins in human cells

To test the stability of the two mutant Artemis proteins identified in F96 cells, we transfected human cells with expression vectors containing the full length transcripts (characterised in section 6.2.4) coding for the G126D or ΔL70 mutant Artemis proteins. We also investigated whether γ-radiation had any effects on Artemis protein stability. Since 293T cells have an impaired p53 pathway, this was performed using the colon

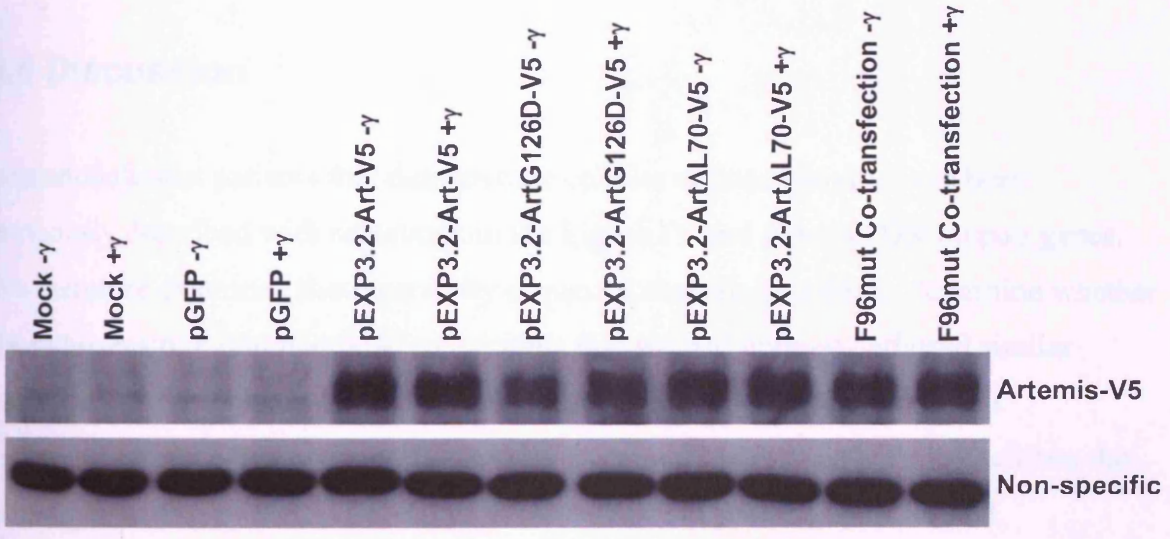

Figure 6-12: F96 mutant Artemis proteins are stable in the human carcinoma cell line HCT116. HCT116 cells were transfected with pEXP3.2-V5 expression vectors coding for V5 tagged wild type Artemis (pEXP3.2-Art-V5), G126D mutant Artemis (pEXP3.2-ArtG126D-V5) or ΔL70 mutant Artemis (pEXP3.2-ArtΔL70-V5). The two F96 mutants were also co-transfected (F96mut Co-transfection). Mock and GFP (pGFP) transfected cells were used as controls. 24 hrs after transfection the cells were either treated with 1 Gy γ-radiation (+γ) or mock irradiated (-γ), and cell lysates prepared after a further 4 hr incubation. The expression of the Artemis-V5 proteins, as detected by immunoblot analysis, is shown in the upper panel; non-specific binding is shown below.

carcinoma cell line HCT116, which retains p53 function and typical DNA damage response pathways. HCT116 cells were either mock transfected or transfected with GFP (pGFP), wild type Artemis (pEXP3.2-Art-V5), G126D Artemis (pEXP3.2-ArtG126D-V5) or ΔL70 Artemis (pEXP3.2-ArtΔL70-V5) expression vectors. We also co-transfected cells with both the G126D and ΔL70 Artemis mutants (F96mut Co-transfection). 24 hours after transfection cells were either treated with 1 Gy γ-radiation or mock irradiated, and cell lysates prepared after a further 4 hour incubation. Using an antibody directed against the c-terminal V-5 tag, an immunoblot of cell lysates was performed (figure 6-12). We found that the wild type and both mutant Artemis proteins were stable in eukaryotic cells with some differences in expression levels. Whilst the

wild type and ΔL70 Artemis proteins were expressed at a similar level, the G126D mutant appeared to be expressed at a lower level. This may indicate that G126D mutant Artemis is not as stable in human cells as the wild type protein, although differences in transfection efficiency may have contributed to this effect. After irradiation the expression level of G126D Artemis appeared to increase. γ-radiation did not have any substantial effect on the expression levels of wild type or ΔL70 mutant Artemis expression.

6.4 Discussion

Immunodeficient patients that demonstrate cellular radiosensitivity have been previously described with mutations in the Ligase IV and Artemis DSB repair genes. We therefore examined these genes by sequence analysis in order to determine whether the radiosensitive immunodeficient patients that we had defined harbored similar mutations in these repair genes. The XRCC4 gene was also included in this investigation since this protein functions in a complex with Ligase IV to facilitate the final ligation step of NHEJ DSB repair. Although not previously described, hypomorphic mutations in XRCC4 that impair this function may be expected to result in abrogated DSB repair and V(D)J recombination, resulting in radiosensitive immunodeficiency. These three genes were therefore good candidates for investigation by sequence analysis, and have sufficiently small coding regions to allow this method of investigation. The three patient lines that demonstrated the clearest radiosensitivity in fibroblast survival assays, GOS5, GOS23 and F96, were subjected to this candidate gene sequencing.

Patient GOS23 was an undefined immunodeficient patient that displayed developmental delay, which is also a characteristic observed in Ligase IV defective patients (O'Driscoll *et al*, 2001). Since this patient's fibroblasts were found to be radiosensitive (section 4-2), this line was a good candidate to have mutations in either Ligase IV, or its closely associated partner XRCC4. Despite these indications we were unable to find any mutations in either of these genes amplified from GOS23 cDNA, confirming that any potential defect in this patient must lie elsewhere in the DNA damage response. Since we received this biopsy in the closing stages of this project, time and resources did not permit a full characterisation of this line.

In the previous section we examined certain radiosensitive lines for evidence of defective DSB repair by the analysis of unrepaired radiation-induced chromosome breaks and the removal of γ-H2AX foci after irradiation. Despite being one of the most exquisitely radiosensitive of all undefined lines examined (section 4), the GOS5 line showed no evidence of a defect in DSB repair (section 5.4). Consistent with this finding, sequence analysis of the Ligase IV, XRCC4 and Artemis DSB repair genes confirmed there were no mutations in the coding region of these genes in GOS5 cells. These findings support the notion that the GOS5 line has a defect in another aspect of the damage response network that does not necessarily affect DSB repair, but is severe enough to confer a radiosensitive phenotype. This may involve the survival assessment process, whereby a certain cell fate (apoptosis or permanent arrest) is initiated once a specific threshold of DNA damage is achieved. A defect in this process may set this threshold at an abnormally low level of damage, and confer radiosensitivity without any observable effects on DSB repair. Indeed, the GOS5 line grew slowly and displayed premature senescence at passage 9 (section 4.2), which may indicate that DSB arising from endogenous sources during routine tissue culture may be enough to induce an abnormal permanent arrest. After irradiation this survival outcome may result after an unusually low level of exogenous DNA damage in GOS5 cells that would not be sufficient to impair survival in control cells. This is consistent with FACS data that demonstrated the GOS5 line is more prone to the induction of a population of senescent like growth arrested cells after irradiation (section 4.3).

Although the F96 line had previously been shown to have no observable defect in DSB repair (Peake *et al*, 1999), we observed an elevated level of unrepaired chromosome breaks after irradiation in these cells (section 5). Consistent with this finding, analysis of the removal of radiation-induced γ-H2AX foci demonstrated an elevated level of residual breaks in the F96 line that suggested a partial defect in DSB repair. This line was therefore a good candidate to harbor a mutation in a DSB repair gene, and we were able to identify two novel mutations in the Artemis DSB repair gene from F96 cells that was not present in two control lines (1BR and 48BR). We also found that the Artemis gene undergoes a complex series of alternative splicing events that required thorough investigation in order to determine exactly what transcripts were present in control and F96 cells.

Full length Artemis is a 78 kD protein encoded by 692 amino acids. Based on protein sequence analysis, Artemis can be divided into three distinct regions (figure 6-13a). The first 155 amino acids, encoded for by exons 1-6, corresponds to the metallo-β-lactamase domain. Metallo-β-lactamase fold proteins, also known as class B β-lactamases, are a large family of proteins that were first described in bacteria, where they are responsible for the hydrolysis of the β-lactam ring of certain antibiotics (Wang *et al*, 1999). A variety of proteins widely expressed in all living organisms have subsequently been shown to possess a metallo-β-lactamase fold (Aravind *et al*, 1999). These enzymes have a broad range of substrates, most of which present an ester bond and a negative charge. Artemis was first identified through its loose sequence homology with the yeast and murine DNA repair factors PSO2 and SNM1 that represent a group of metallo-β-lactamase enzymes involved in the metabolism of nucleic acids, which also includes the cleavage and polyadenylation-specific factor (CPSF) (Moshous *et al*, 2001). Further analysis revealed that residues 156-385, encoded by exons 7-13, displayed significant homology with both SNM1 and PSO2 but also with a whole range of other proteins present in a wide range of organisms, including CPSF (Callebaut *et al*, 2002). This domain was therefore termed the β-CASP domain (**β**-Lactamase-**C**PSF, **A**rtemis, **S**NM1 and **P**SO2 domain), and is not an independent domain but is always found linked to a metallo-β-lactamase domain in proteins involved in nucleic acid metabolism. Finally, residues 386-692, encoded by exon 14, is designated the C-terminal domain and shows no homology with any known proteins.

The structure of metallo-β-lactamase enzymes consists of a four-layered β-sandwich with two mixed β-sheets flanked by α-helices, with a catalytic site composed of two metal-binding sites located at one edge of the β-sandwich (Wang *et al*, 1999). The binuclear Zn(II) centre (thought to utilise Mg in the case of Artemis), used to perform the cleavage reaction, is located at the bottom of a wide shallow grove. The catalytic site of metallo-β-lactamases is constituted by five highly conserved sequence motifs consisting mostly of histidine and aspartic acid residues, which participate in metal coordination and hydrolysis reaction. The first four motifs of Artemis were easily recognised (Moshous *et al*, 2001), and motif I corresponds to a conserved aspartic acid residue at position 17 (figure 6-13a). The highly conserved HxHxDH signature that begins at residue 33 of human Artemis typifies the second motif, which is representative

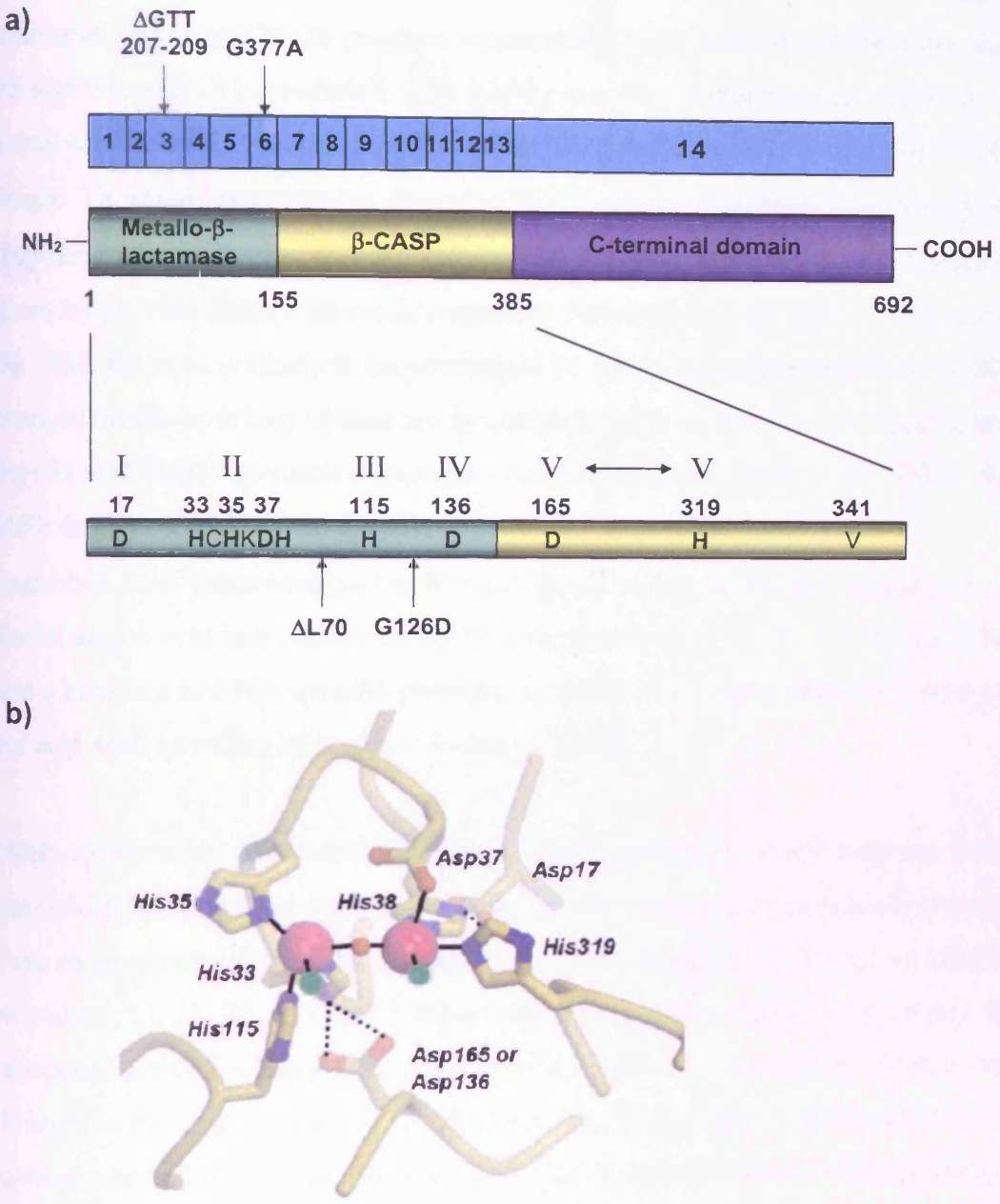

Figure 6-13: Analysis of Artemis protein sequence and the proposed active site. a) Artemis is composed of three identifiable regions, the metallo-β-lactamase homology domain (amino acids 1-155) coded by exons 1-6, the associated β-CASP domain (amino acids 156-385) coded by exons 7-13, and the COOH-terminal region (amino acids 386-692) coded by exon 14. Five motifs (I-V) that compose the catalytic site of bacterial β-lactamases are conserved in Artemis. Two residues may constitute the fifth domain, since both residues are required for nuclease activity. A hydrophobic amino acid, such as valine, at position 341 is typical of metallo-β-lactamases that act on DNA rather than RNA. The mutations identified in the F96 line resulting in ΔL70 and G126D changes to the Artemis protein are indicated. b) The catalytic site of Artemis proposed by Pannicke *et al*, 2004, involves the coordination of two metal ions by the conserved residues that constitute the metallo-β-lactamase/β-CASP active site. Residues thought to function in metal binding are shown in ball-and-stick representation (with yellow carbons, blue nitrogen, and red oxygen atoms). Two metal ions (magenta spheres) are bound by Asp37 and histidines 33, 35, 38, 115 and 319 and Asp 17, 136 and/or 165 may orient histidines 38 and 33 for efficient metal coordination (dashed lines). A putative water molecule might complete the coordination pocket (red sphere) and two coordination sites on the active site metals (green spheres) may bind the DNA substrate. (adapted from Pannicke *et al*, 2004)

of the entire family of metallo-β-lactamases. The third and fourth motifs correspond to the conserved H115 and D136 residues respectively. Since the length between the fourth and fifth motifs is predicted to be highly variable in this class of enzymes (Aravind *et al*, 1999) (Wang *et al*, 1999), the fifth motif of Artemis was more difficult to assign. Thorough examination of the β-CASP domain suggested that this region participates in the formation of the metallo-β-lactamase enzymatic pocket within these enzymes by providing the fifth motif necessary for metal coordination (Callebaut *et al*, 2002). This function is likely to be performed by either the conserved D165 or H319 residues, although both hypotheses are in fact supported by the loss of Artemis activity in Asp165 and His319 mutants (Pannicke *et al*, 2004) (Poinsignon *et al*, 2004). Finally, β-CASP family members that specifically interact with DNA targets can be distinguished from those involved in RNA metabolism regarding the nature of a particular amino acid in a conserved motif corresponding to V341 in Artemis, which is always a histidine in RNA specific proteins, whereas it is substituted by a hydrophobic amino acid such as valine in proteins acting on DNA.

The high conservation of the active site histidines and aspartic acids between Artemis and metallo-β-lactamases suggests that Artemis binds two metal cofactors, consistent with the requirement of Artemis nuclease activity for magnesium (Ma *et al*, 2002). D37 and histidines 33, 35, 38, 115 and 319 have been proposed to directly coordinate the two proposed active site metals, whereas aspartic acids 17, 136 and/or 165 may form salt bridges to the HxHxDH motif backbone and the side chain of H38 and H33, respectively, to optimally stabilise this active site structure (figure 6-13b) (Pannicke *et al*, 2004). Mutation of any one of the residues proposed to function in metal coordination results in abrogation of endonuclease (but not exonuclease) activity, although this effect was less severe with mutation of H38, since this change may only affect the binding of one metal (Pannicke *et al*, 2004). The severe effect of mutation of either D136 or D165 on endonuclease activity (Pannicke *et al*, 2004) suggests that both of these residues are located in the in the active site of Artemis and participate in metal binding. Although the metallo-β-lactamase/βCASP domain of Artemis has been shown to be sufficient for V(D)J recombination on chromosomal substrates, this region did not complement the radiosensitivity of Artemis deficient cells (Poinsignon *et al*, 2004). This suggests that while the C-terminal region of Artemis is dispensable for the repair of DSBs during V(D)J recombination, it is required for the efficient repair of radiation damage.

Artemis transcripts can be spliced in multiple combinations, and we detected several alternative transcripts in both control and F96 cells. The majority of alternative transcripts involved a frameshift that incorporates a premature stop codon within the metallo-β-lactamase domain, and results in severe truncation of the Artemis protein at a range of locations between residues 38 (variant 4) and 108 (variant 3). Since these proteins retain only two of the five conserved metal binding motifs proposed to form the catalytic site of Artemis (figure 6-13), it is highly unlikely that these putative proteins would have any residual catalytic activity. Furthermore, transcripts with premature stop codons are subject to nonsense-mediated decay (Hilleren and Parker, 1999), and thus their proportion does not necessarily have to represent later protein levels.

2 variants expressed in the F96 line involved either deletion of exon 9 (F96-V9) or deletion of the 5′ portion of exon 9 and deletion of exon 10 (F96-V9/11). Both of these splicing modes retain the original reading frame, and result in a small internal deletion within the β-CASP domain of Artemis. In the case of F96-V9/11, 13 extra amino acids are incorporated at the site of this deletion due to a frameshift at the exon 9 alternative splice site, which is restored back to the original reading frame when spliced to exon 11. These changes to Artemis protein structure occur between the two residues proposed to function as the fifth catalytic domain of Artemis (figure 6-13), and do not directly affect either of these motifs. Although this may allow some residual catalytic activity, F96-V9 and F96-V9/11 result in an internal deletion of 34 and 67 amino acids respectively, and such large deletions within the β-CASP domain are likely to have a significant impact on the function of the catalytic site, albeit indirectly. Further work is required in order to investigate the physiological significance of the many Artemis splice variants observed in this project.

Half (14/28) of the Artemis transcripts cloned from F96 cells were full length transcripts, which suggests this may be the dominant species of Artemis mRNA in these cells. Using these sequences, we identified two novel mutations in the F96 Artemis gene that were mutually exclusive and therefore expressed from separate alleles. These mutations, deletion of codon 70 and a G377A missense mutation, are predicted to result in the production of two distinct Artemis proteins, one harboring a deletion of leucine 70, and the other with a substitution of glycine 126 for aspartic acid. Both leucine 70 and glycine 126 are conserved in mouse and chicken Artemis homologues (figure 6-14)

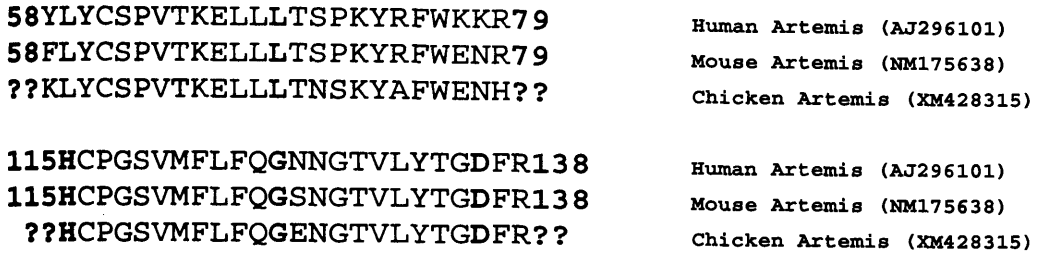

Figure 6-14: Conservation of leucine 70 and glycine 126 in human, mouse and chicken Artemis proteins. Homologous sequence is shown in blue, with residues proposed to function in metal binding shown in bold. Residues corresponding to leucine 70 and glycine 126 of human Artemis are shown in red, and differences to the human sequence are shown in green. The chicken Artemis protein sequence was predicted from partial mRNA sequence by automated computational analysis, and is therefore incomplete. Numbers in parenthesis are GenBank identifiers.

As predicted, the mutations observed in the F96 line allow expression of viable Artemis proteins, shown by the transfection of HCT116 cells with expression vectors coding for each mutant. Although both mutations are within the metallo-β-lactamase domain, neither of the changes involves residues that are proposed to function in metal coordination within the active site (figure 6-13). Despite this, these changes may still have a deleterious influence on the catalytic site of Artemis, since their close proximity to essential residues may indirectly affect active site structure. This may not be to the same extent which mutations in metal binding residues abolish nuclease activity (Pannicke *et al*, 2004), but could result in a partially functional protein. This would be consistent with the modest post-radiation cell division phenotype displayed by the F96 line compared to Artemis null cells (section 4.3), and the progressive lymphopaenia associated with apparently normal V(D)J recombination observed in patient F96 (Peake *et al*, 1999). In order to finally confirm the pathogenicity of the F96 Artemis mutations, each of the mutant proteins could be stably expressed in Artemis deficient cells of the same genetic background, for example in CJ179 cells. Once achieved, DNA hairpin opening activity of these proteins could be compared to that with expression of the wild type protein. Similar expression experiments could be performed to determine whether each mutant Artemis protein was able to fully rescue the poor division observed in CJ179 cells during experiments with CFSE.

Most of the Artemis mutations identified in RS-SCID patients seem to represent null alleles, which result from genomic deletions covering several of the 5′ exons or involve the production of severely truncated proteins (Moshous *et al*, 2001). This is likely to

result in the complete inactivation of the metallo-β-lactamase/βCASP domain, reflected by the severe T-B-SCID phenotype of these patients. In addition, a patient homozygous for a D165N mutation, a residue proposed to function in metal binding within the active site (figure 6-13), was reported as being clinically indistinguishable from patients with null mutations in Artemis (Ma *et al*, 2002). This emphasises the importance of the proposed metal binding residues within the active site of Artemis, but other patients have been described with mutations in surrounding residues similar to those observed in the F96 line. RS-SCID patients have been described with S32C (Le Deist *et al*, 2004), G118V and G135E (Noordzij *et al*, 2003) missense mutations, which lie within the metallo-β-lactamase/βCASP domain of Artemis but do not involve the residues proposed to function in metal binding. Compared to a patient with a truncation at codon 269 of the β-CASP domain, the patient harboring a G118V mutation demonstrated relatively high frequencies of precursor B cells which suggested a partially functional V(D)J recombination pathway (Noordzij *et al*, 2003). Since patient F96 initially displayed relatively normal numbers of lymphocytes, but subsequently developed lymphopaenia that was progressive with age, the Artemis mutations identified here are likely to be hypomorphic (Peake *et al*, 1999). This may allow a relatively normal level of V(D)J recombination to occur, but the coding joins formed may be abnormal or unstable, a situation that could trigger the elevated levels of spontaneous apoptosis observed in this patient. At this point other genetic factors, which may have an effect on lymphocyte survival, could contribute to this immunodeficient phenotype.

Chapter 7: Analysis of p53 function and radiation induced gene expression in F96 cells

7.1 Background

Radiation induced DSBs activate the ATM kinase that phosphorylates transducer proteins that can signal the presence of DNA damage to the cell cycle and apoptotic machinery. The p53 tumour suppressor protein plays a key role in this part of the DNA damage response, and acts as a node or hub for the incoming stress signals it receives. ATM can directly and indirectly facilitate an accumulation and activation of the p53 tumour suppressor, the function of which largely depends on its transcriptional activator properties. ATM directly phosphorylates p53 on serine 15 (Banin *et al*, 1998) (Canman *et al*, 1998) (Khanna *et al*, 1998) (Nakagawa *et al*, 1999), which seems to enhance its transcriptional activator function (Lambert *et al*, 1998) (Dumaz and Meek, 1999). Serine 15 phosphorylation is then thought to nucleate a series of subsequent post-translational modifications on p53 that contribute to both its stabilisation and biochemical activation (as many as 17 sites in p53 undergo phosphorylation or acetylation) (Appella and Anderson, 2001). Phosphorylation of serine-15, threonine 18 and serine-20 stimulates the recruitment of transcription factors including p300, CBP (both transcriptional co-activators and histone acetyl-transferases [HATs]) and P/CAF that stimulate p53 sequence specific DNA binding (Sakaguchi *et al*, 1998) (Liu *et al*, 1999). Once activated, p53 is able to induce expression of target genes involved in growth arrest and apoptosis.

Whilst investigating the cause of radiosensitivity in the F96 line, and concurrent with our characterisation of the associated defect in repair, we obtained results that hinted at an enhanced p53 response in these cells. Furthermore, the F96 patient displayed a cellular radiosensitivity that was associated with increased spontaneous apoptosis of lymphocytes (Peake *et al*, 1999), a characteristic that may be associated with augmented p53 activity. Whilst this could result from unrepaired endogenous DSBs that promote p53 signaling and apoptosis, other genetic factors may also contribute to such a phenotype. We were therefore interested in determining the status of the p53 signaling pathway in this line. In order to differentiate between these effects in control and F96 cells, we employed low doses of γ-radiation that should be more physiologically

relevant. This allowed us to identify important differences between control and F96 cells with regard to p53 activation after irradiation. This differential response was then analysed on a genomic scale using oligonucleotide microarrays.

7.2 Characterisation of the p53 response in F96 cells

7.2.1 Analysis of p53 status in control and F96 cells

The radiosensitive line F96 is defective in DNA repair and we have identified two novel mutations in the Artemis DSB repair gene. This is likely to contribute to the poor survival of F96 cells after irradiation, although the exact mechanism of cell inactivation is unknown. ATM signals the presence of DNA DSBs to the p53 tumour suppressor by direct and indirect mechanisms involving phosphorylation of p53 on serine-15. This is believed to stabilise p53 levels within the nucleus and may also contribute to the activation of p53 dependent gene transcription that promotes cell cycle arrest and apoptosis. In order to detect any abnormalities in this process in the F96 line, we investigated p53 levels and serine-15 phosphorylation status in control and F96 cells. This was performed before and after exposure to γ-radiation.

Control (1BR) cells exposed to 1Gy γ-radiation demonstrated a marked increase in p53 serine-15 phosphorylation 2 hours after treatment. There was also an increase in total p53 levels, although this was not as striking because unirradiated cells contained a significant amount of non-phosphorylated p53. By 8 hours the amount of serine-15 phosphorylation and total p53 had decreased to near baseline levels (Figure 7-1). Compared to control cells, the induction of serine-15 phosphorylation was more prominent in the F96 line 2 hours after irradiation, and this was sustained to a greater degree in these cells, with relatively high levels remaining after 8 hours compared with the near baseline level in controls.

We also noted that p53 isolated from F96 cells appeared to migrate at a slightly larger size both before and after irradiation. We hypothesised that this slight increase in size could result from certain post-translational modifications that were not present in control cells. We therefore investigated whether this shift was due to post-translational modifications such as phosphorylation or acetylation.

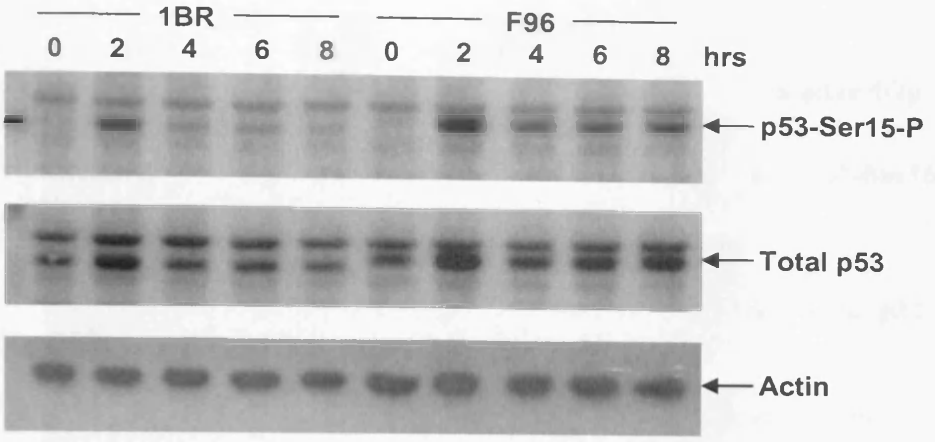

Figure 7-1: p53 isolated from F96 cells displays retarded migration and elevated levels of radiation-induced serine-15 phosphorylation compared to control. In control cells there was a marked increase in the level of p53 serine-15 phosphorylation 2 hours after irradiation, but this had decreased to near baseline levels after 8 hours. The F96 line demonstrated more pronounced phosphorylation of p53 serine-15 2 hours after irradiation, and compared to control cells this was maintained at a relatively high level up to 8 hours post-irradiation. The amount of total p53 demonstrated a modest increase 2 hours after irradiation in both lines, with a substantial amount of non-phosphorylated p53 being present before irradiation. F96 p53 migrated more slowly than p53 from the control cells, which may suggest the presence of additional post-translational modifications, or that p53 may not be wild type in the F96 line

In order to investigate whether additional phosphorylations were responsible for the shift in F96 p53, protein lysate isolated from control (1BR) or F96 cells before and after irradiation was subjected to phosphatase treatment using Calf Intestinal Alkaline Phosphatase (CIAP). This should remove any phosphate groups that are present on p53, and comparing the migration of total p53 from treated extracts to mock treated lysate can confirm whether the slight shift in size observed was due to phosphorylation. The p53 serine-15 phosphorylation specific antibody used previously was employed to confirm that phosphatase treatment was successful, and as expected incubation with CIAP removed all detectable p53 serine-15 phosphorylation in both cell lines, before and after irradiation (figure 7-2a). When total p53 levels were examined these had not changed as a result of the phosphatase treatment, and the slower migration of F96 p53 was still observed. These results confirmed that the slow migration of F96 p53 compared to control p53 was not due to additional phosphorylations.

We next investigated whether the slow migration of F96 p53 was due to the presence of additional acetylations using Anacardic Acid (AA), a potent non-competitive inhibitor

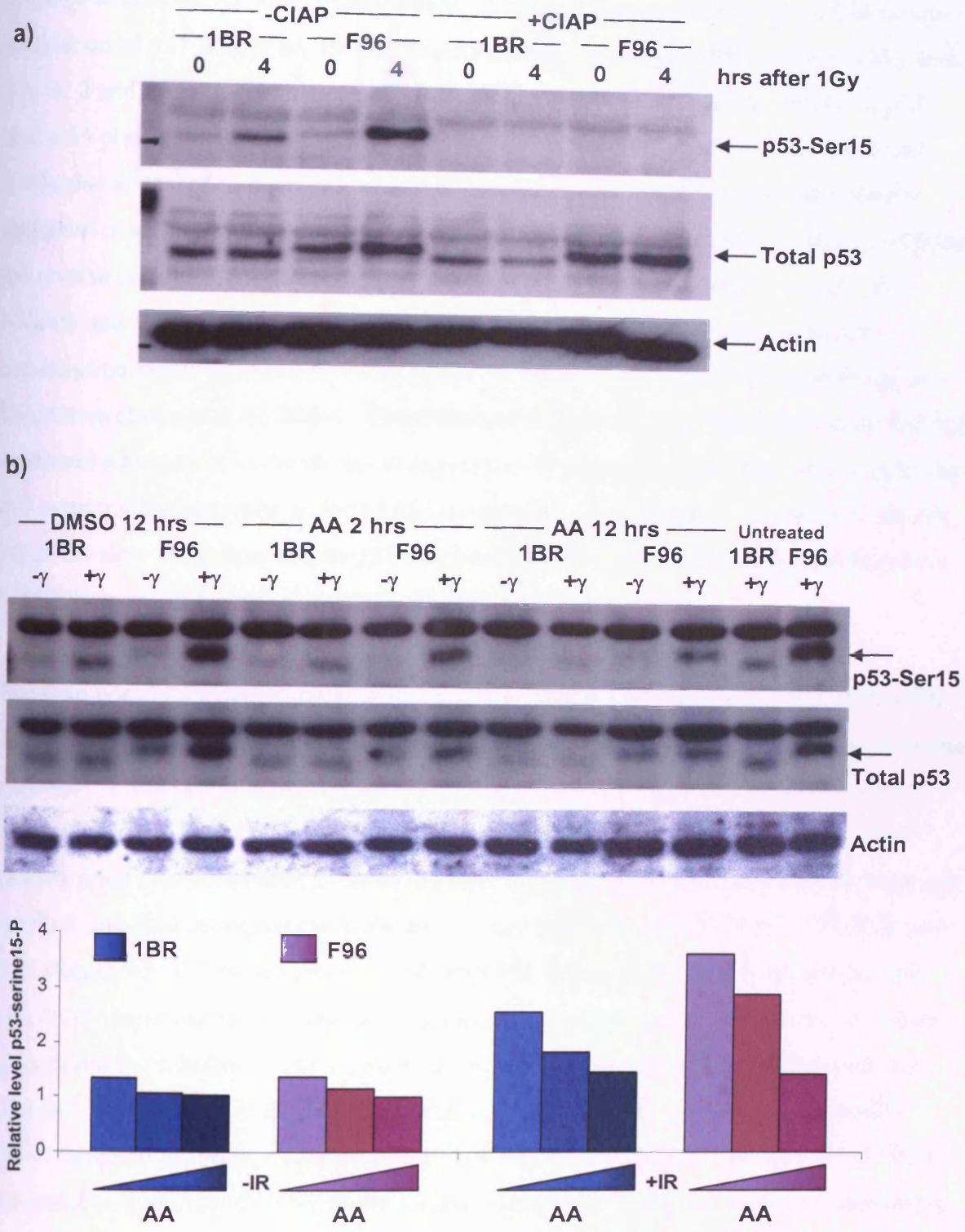

Figure 7-2: Phosphorylation and acetylation are not responsible for the slow migration of F96 p53, but acetylation may facilitate p53 stabilisation and phosphorylation. a) Phosphatase treatment successfully removed p53 serine-15 phosphorylation in both the control and F96 lines, but did not affect the slow migration of total p53 from F96 cells. b) Control (1BR) and F96 cells were pre-treated with the acetylation inhibitor Anacardic Acid (AA) for 2 or 12 hrs, before irradiation with 1 Gy and a further 4 hr incubation. DMSO only controls were treated for 12 hours prior to irradiation and a further 4 hr incubation. Cell lysates were then prepared and western blotted. AA did not affect the slow migration of F96 p53, although levels of total p53 and serine 15 phosphorylation were reduced for both the control and F96 lines in a dose dependent manner. This western blot was analysed by densitometry and the relative levels of p53 serine-15 phosphorylation are shown.

of the p300 and P/CAF acetyltransferases, which are thought to be responsible for the acetylation of p53 (Liu *et al*, 1999). Pre-treatment of control (1BR) and F96 cells with AA for 2 and 12 hours prior to irradiation substantially decreased the induction p53 serine-15 phosphorylation after a further 4 hour incubation (figure 7-2b). Total p53 levels also appeared to decrease with AA treatment, but it is impossible to state if a reduction in serine-15 phosphorylation caused a decrease in total p53 levels, or whether the reverse is true. Acetylation of p53 has previously been shown to promote p53 stability and activity (Sakaguchi *et al*, 1998) (Ito *et al*, 2001), and an oncogenic transcription factor has recently been shown to impair p53 function by promoting de-acetylation (Insinga *et al*, 2004). Consistent with these studies our results show that AA conferred a reduction in the ability to signal to p53 after DNA damage, and suggest that this compound effectively inhibited p53 acetylation. Since treatment with AA did not affect the slow migration of F96 p53 compared to that from controls, this difference is not likely to result from the presence of additional acetylations.

The final possibility investigated to explain the apparently larger size of p53 from F96 cells was to examine the coding sequence of this gene and compare this to the published sequence. Primers P5F and P7R were designed to amplify a 1426 bp fragment that encompassed the entire coding region of p53 using F96 cDNA as a template. This amplification was performed in three separate reactions and the PCR products were gel purified, and then sequenced in both directions using primers P5F, P6F, P7F, P7R and P5R (figure 7-3a). The sequence of F96 p53 was found to be normal except for one previously described polymorphism in codon 72, which involves a CGC to CCC base change and the substitution of arginine for proline in the translated protein sequence (figure 7-3b). Although single amino acid substitutions are not usually expected to affect the electrophoretic mobility of proteins, this polymorphism has previously been described to significantly alter the biochemical properties of p53. p53 with arginine at position 72 ($p53_{Arg}$) has been shown to migrate more rapidly on denaturing gels than the proline72 form ($p53_{Pro}$), and a mixture of both forms results in a doublet (Matlashewski *et al*, 1987). The single, slow migrating band of p53 isolated from the F96 line is consistent with a homozygous $p53_{Pro}$ genotype, compared to the fast migrating p53 from control (1BR) cells that indicated $p53_{Arg}$.homozygosity. In order to confirm that 1BR cells were homozygous for $p53_{Arg}$ we amplified p53 from 1BR cDNA as described for the F96 line, and sequenced the 5′ section of the coding region that contained codon 72 using primers P5F and P5R.

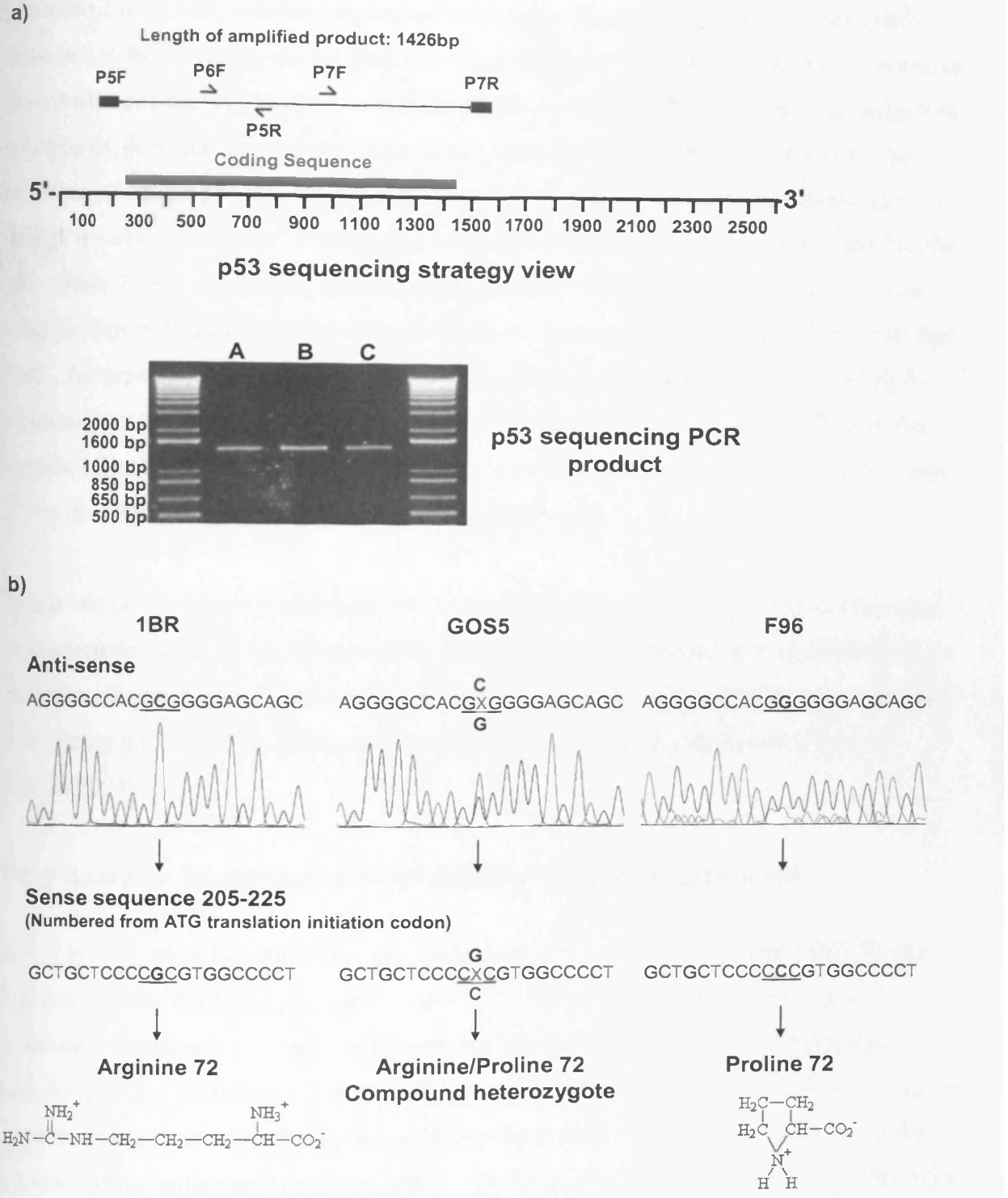

Figure 7-3: Strategy for sequencing human p53 and the identification of codon 72 polymorphisms in different fibroblast lines. a) PCR primers P5F and P7R were designed to amplify the entire coding sequence of p53. These were first used to amplify p53 from cDNA, and then in conjunction with primers P6F, P7F and P5R, were again used to sequence the gel purified PCR products. b) Chromatogram of anti-sense sequencing results for the region 205-225 bp from the ATG translation initiation codon that contains codon 72. 1BR cells appeared to be homozygous for C**G**C codon 72 sequence, which codes for arginine in the p53 protein, whereas F96 cells were homozygous for C**C**C in this position, which codes for proline. GOS5 cells seem to be heterozygous for this polymorphism, illustrated by the double **G/C** peak for the middle base of codon 72 on the GOS5 sequence chromatogram.

Consistent with 1BR cells displaying only the fast-migrating form of p53, these cells appeared to be homozygous for the CGC form of codon 72, which codes for Arginine in this position of the p53 protein. Analysis of p53 status in GOS5 cells demonstrated that this line expressed both the slow- and fast- migrating forms of p53, indicated by the presence of a tight p53 doublet after gel electrophoresis for extended periods (figure 7-4a and results not shown). This suggested that GOS5 cells may be heterozygous for the p53 codon 72 polymorphism, and this was confirmed by sequence analysis. p53 was amplified from GOS5 cDNA as described above, and sequenced using primers P5F and P5R. As expected, a mixture of PCR products harbouring either the CGC (coding for arginine) or CCC (coding for proline) codon 72 polymorphism were amplified in this reaction, illustrated by the presence of a G/C double peak for the middle base of codon 72 on the GOS5 sequence chromatogram (figure 7-3b).

These two polymorphic variants of p53 have been reported to have different biological characteristics, with $p53_{Pro}$ being a more functional transcriptional activator (Thomas *et al*, 1999). Further investigation revealed that whilst $p53_{Pro}$ appears to be more efficient at inducing growth arrest, $p53_{Arg}$ is more effective at initiating apoptosis (Pim and Banks, 2004).

7.2.2 Analysis of p53 status in control and radiosensitive lines

Initial investigation into the status and activation of p53 in the radiosensitive F96 line has shown these cells display high levels of p53 serine-15 phosphorylation after irradiation compared to control cells, and that this line is homozygous for the slow migrating $p53_{Pro}$ polymorph, whereas the control line 1BR is homozygous for $p53_{Arg}$. In order to evaluate whether the enhanced phosphorylation of p53 observed in F96 cells occurs in other radiosensitive lines, and to determine if any other radiosensitive lines are homozygous for $p53_{Pro}$, we performed a western blot of p53 phosphorylation for a range of different lines. This should indicate whether elevated levels of DNA damage contribute to the enhanced p53 signalling observed, or if this is more likely to result from the specific p53 isoform expressed in F96 cells. This analysis involved the additional control line 48BR, the undefined radiosensitive line GOS5, the Artemis deficient line CJ179, the Ligase IV deficient line 180BR and the AT line A-T1BR, along with the previously characterised 1BR and F96 lines (figure 7-4)

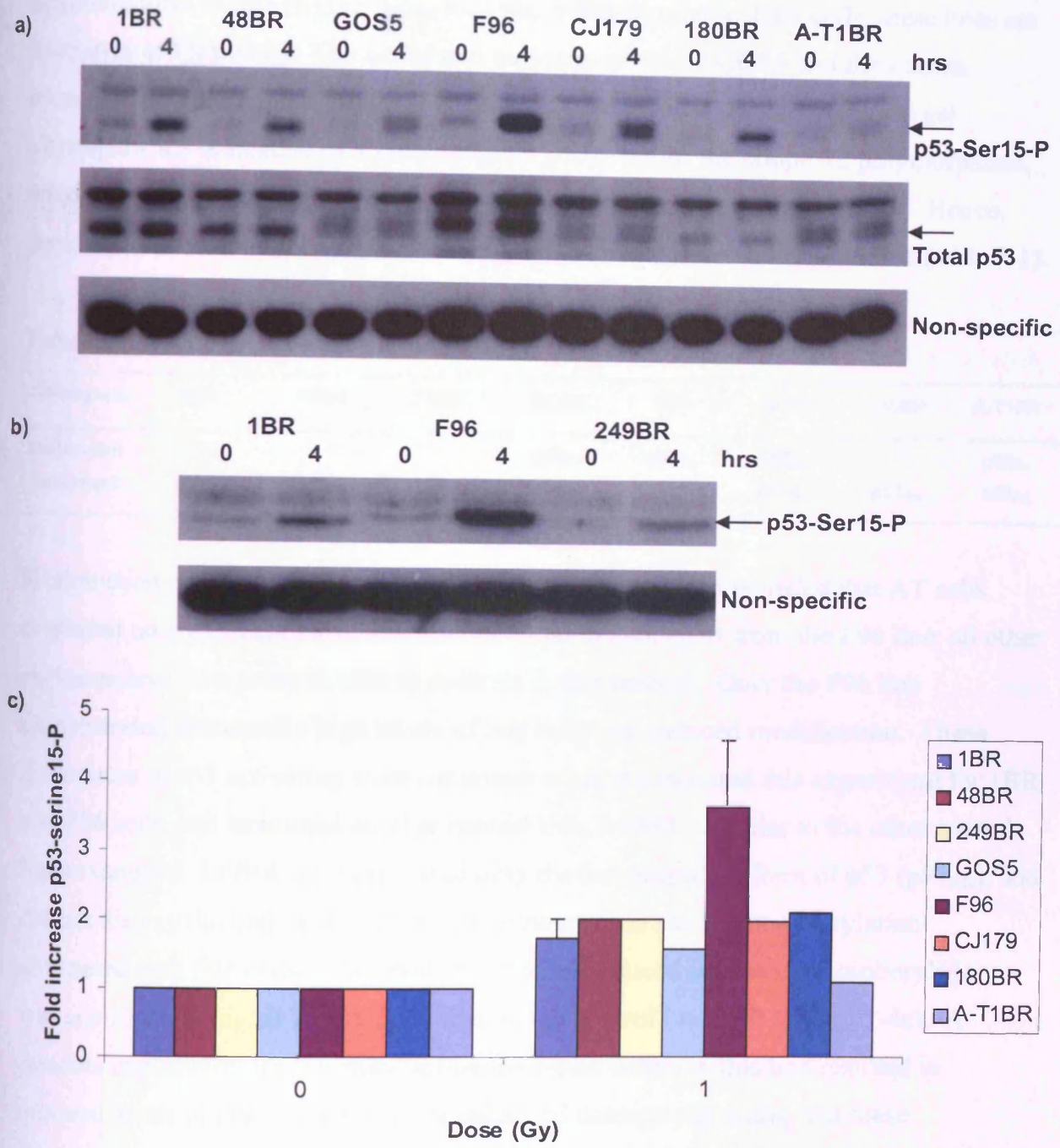

Figure 7-4: p53 status and radiation induced serine-15 phosphorylation in control and radiosensitive lines. a-b) Western blots of total p53 and serine-15 phosphorylation 4 hours after exposure to 1Gy γ-radiation. The control lines 1BR, 48BR and 249BR all displayed only the fast migrating form of p53 indicative of $p53_{Arg}$. The Ligase IV defective line 180BR also contained only this form of p53, but the other radiosensitive lines GOS5 (undefined), CJ179 (Artemis deficient), and A-T1BR (ATM deficient) all displayed a p53 doublet indicative of heterozygosity for the codon 72 polymorphism. Only the radiosensitive line F96 was associated with a single, slow migrating p53 band consistent with the homozygous $p53_{Pro}$ genotype of this line. These blots were analysed by densitometry and the normalised fold induction of p53 serine-15 phosphorylation is presented in graph form (c). This experiment was repeated at least 3 times for control and F96 cells; error bars represent 1 SD of the mean. All lines examined demonstrated radiation-induced p53 serine-15 phosphorylation except the A-T1BR line. Whilst F96 cells displayed significantly higher levels of radiation-induced serine-15 phosphorylation than the control line 1BR, all the remaining lines demonstrated normal induction of serine-15 phosphorylation.

The control line 48BR and the Ligase IV deficient line 180BR expressed only the fast migrating form of p53 (figure 7-4a) indicating that, similar to 1BR cells, these lines are homozygous for $p53_{Arg}$. The undefined radiosensitive line GOS5 and the known mutants CJ179 (Artemis) and A-T1BR (ATM) displayed a p53 doublet after gel electrophoresis indicative of a heterozygous genotype for the codon 72 polymorphism, which was confirmed in GOS5 cells by p53 sequence analysis (figure 7-3b). Hence, none of the lines examined expressed only $p53_{Pro}$ comparable to the F96 line (table 7-1).

Table 7-1: F96 was the sole line to express only the $p53_{Pro}$ isoform

Primary line	1BR	48BR	249BR	GOS5	F96	CJ179	180BR	A-T1BR
Polymorph expressed	$p53_{Arg}$	$p53_{Arg}$	$p53_{Arg}$	$p53_{Pro}$ $p53_{Arg}$	$p53_{Pro}$	$p53_{Pro}$ $p53_{Arg}$	$p53_{Arg}$	$p53_{Pro}$ $p53_{Arg}$

Examination of radiation-induced serine-15 phosphorylation revealed that AT cells displayed no significant induction after irradiation and, apart from the F96 line, all other radiosensitive lines were similar to controls in this respect. Only the F96 line demonstrated abnormally high levels of this radiation-induced modification. These differences in p53 activation were consistent when we repeated this experiment for 1BR and F96 cells, and examined another control line, 249BR. Similar to the other control lines examined, 249BR cells expressed only the fast migrating form of p53 ($p53_{Ala}$), and did not display the high levels of radiation-induced serine-15 phosphorylation associated with F96 cells. The level of radiation-induced serine-15 phosphorylation was significantly higher in F96 cells than in the control line 1BR (figure 7-4c). A possible explanation for this may be that the repair defect in this line resulted in elevated levels of DSBs and therefore enhanced damage signalling, but these experiments were performed 4 hours after irradiation, when the levels of unrepaired DSBs were comparable between F96 and control cells (section 5.4.2). Furthermore, compared to controls the Ligase IV defective line 180BR displayed substantially higher levels of DSBs 4 hours after irradiation, but did not demonstrate the enhanced damage signalling associated with the F96 line. Together, these results suggest that the elevated levels of radiation-induced p53 signalling observed in F96 cells is not due to high levels of unrepaired DSBs, and is more likely to result from other factors present in this line. Since the heterozygous $p53_{Pro}$ isoform expressed in CJ179 cells did not specifically display enhanced radiation-induced phosphorylation, it is unlikely this form of p53 is more susceptible to this modification, unless the presence of $p53_{Arg}$ interferes with this

effect in some way. Therefore, other factors present in F96 cells may have contributed to the enhanced levels of radiation-induced serine-15 phosphorylation. This enhanced damage signalling may be further amplified during the induction of p53 target genes, since $p53_{Pro}$ has been shown to be a more potent transcriptional activator than $p53_{Arg}$ (Thomas *et al*, 1999).

During this experiment it became apparent that whilst γ-irradiation of primary fibroblasts induced the rapid phosphorylation of p53 serine-15, the total levels of p53 did not increase substantially after treatment. In most primary lines this was associated with a significant amount of unphosphorylated p53 that was present in unirradiated samples. Although it is not clear why basal levels of total p53 were relatively high in this experiment, the lack of active p53 as suggested by differences in serine-15 phosphorylation indicates that the p53 at time 0 is unlikely to be active and is probably located in the cytoplasm.

7.2.3 Examination of p21 induction after irradiation in control and F96 cells

The F96 line had demonstrated abnormally high levels of signalling to p53 after irradiation in the form of serine-15 phosphorylation, which is thought to be involved in the stabilisation and activation of p53. We therefore investigated whether a target gene of p53, the Cdk inhibitor p21, was also induced at an abnormally high level in the F96 line. Examination of p21 mRNA levels by northern blot revealed that this gene was induced at significantly higher levels in F96 cells compared to the control line 1BR (figure 7-5a). Consistent with this result, radiation-induced p21 protein levels were also significantly higher in the F96 line compared to control (figure 7-5b). The AT line A-T1BR displayed no significant induction of p21 mRNA or protein, which demonstrates the downstream effects of defective signalling to p53. These results are coherent with the abnormally high levels of p53 serine-15-phosporylation observed after irradiation in F96 cells, and suggest that an unusually elevated p53 response is initiated in this line. This then manifests with the strong induction of at least one p53 target gene.

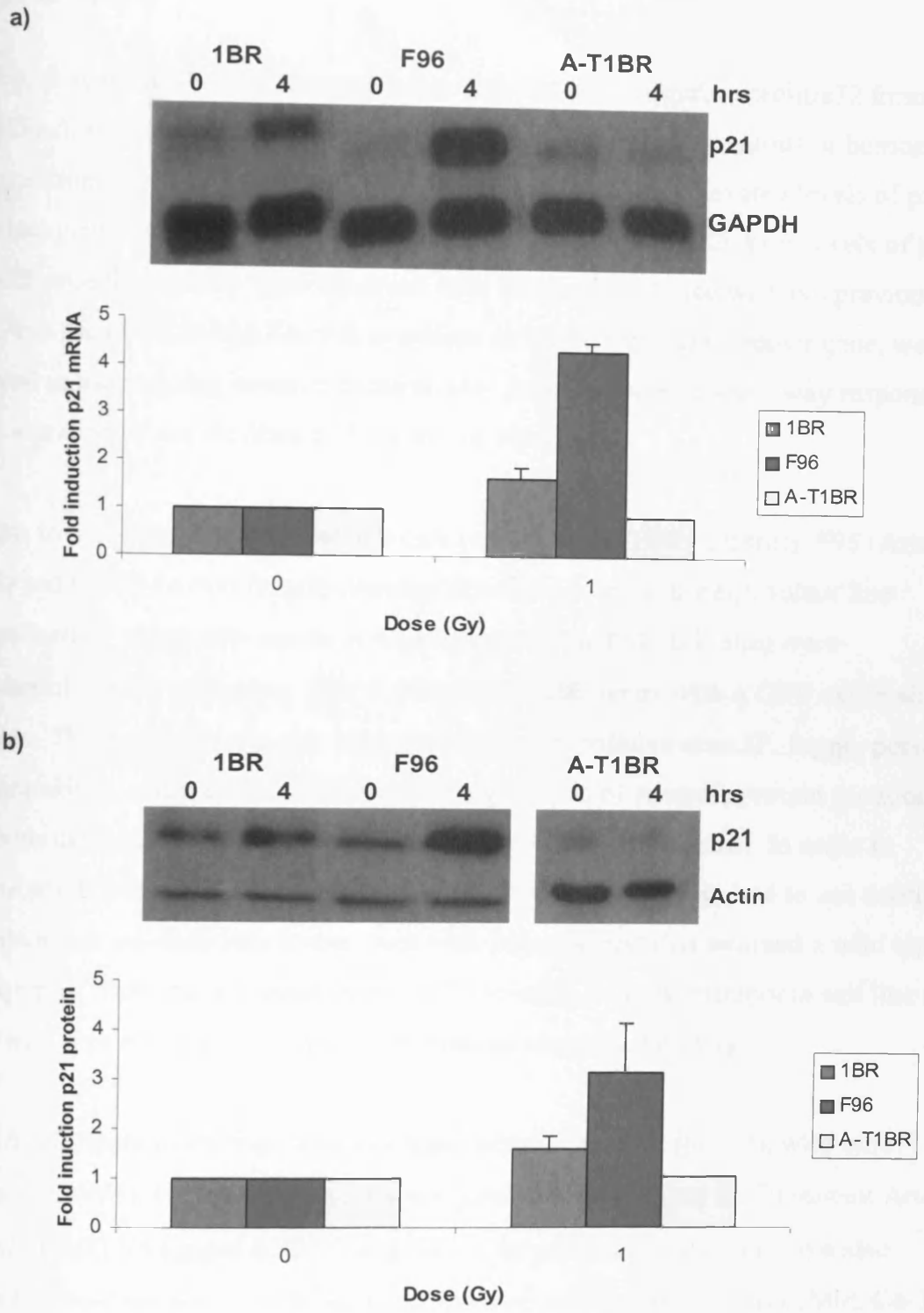

Figure 7-5: F96 cells display elevated levels of p21 induction after irradiation. a) Northern blot of p21 mRNA levels 4 hours after exposure to 1Gy γ-radiation. b) Western blot of p21 protein levels 4 hours after exposure to 1Gy γ-radiation. For control and F96 cells these experiments were repeated at least twice and the normalised fold induction of p21 calculated to give an average value, displayed in bar chart form underneath each representative blot. Error bars represent 1 SD of the mean. The F96 line displayed higher levels of p21 mRNA and protein induction after irradiation compared to control. The AT line A-T1BR demonstrated no significant induction of p21.

7.2.4 Effect of F96 Artemis mutations on radiation-induced p53 serine-15 phosphorylation

We have shown that the F96 line expresses only the fast migrating proline72 form of p53 ($p53_{Pro}$), whereas all other lines examined were either heterozygous or homozygous for expression of $p53_{Ala}$. F96 cells were also found to display elevated levels of p53-dependent gene transcription compared to control, and abnormally high levels of p53 serine-15 phosphorylation were observed after irradiation. Since we have previously shown that the F96 line has 2 novel mutations in the Artemis DSB repair gene, we were interested in ascertaining whether these mutant proteins were in some way responsible for the initiation of the elevated p53 responses observed.

Attempts to transiently express the Artemis protein in the 1BR (control), F96 (Artemis mutant) and CJ179 (Artemis null) primary fibroblast lines or the equivalent line immortalised by stable expression of human telomerase (hTERT line) were unsuccessful despite achieving ~50 % transfection efficiency with a GFP expression construct. This problem was also experienced by our collaborators (P. Jeggo, personal communication), and we concluded that the high levels of Artemis protein produced by exogenous expression constructs were toxic to these fibroblast lines. In order to examine any effects of these Artemis mutants on p53 we therefore had to use another cell system that we were able to transfect with Artemis, and that retained a wild type p53 response. This was achieved using HCT116 cells, a colon carcinoma cell line that retains wild type p53 and a normal DNA damage response pathway.

HCT116 cells were mock transfected or transfected with GFP (pGFP), wild type Artemis (pArt-V5), G126D mutant Artemis (pArt-G126D-V5) or ΔL70 mutant Artemis (pArt-ΔL70-V5) V5 tagged EXP3.2 expression constructs in duplicate. We also performed a co-transfection with equal amounts of each Artemis mutant (Mut. Co-T) in an attempt to recreate the situation within F96 cells. After a 24-hour incubation to allow expression of Artemis protein, one of each transfected plate was exposed to 1 Gy γ-radiation, and the other was mock irradiated. The cells were then incubated for a further 4 hours, before the isolation of total cellular protein. The western blot of Artemis expression displayed in section 6.3.2, figure 6-12, was generated using lysate from this experiment. This western blot was re-probed for p53 serine-15 phosphorylation (figure 7-6a). Protein isolated from 1BR and F96 primary fibroblasts

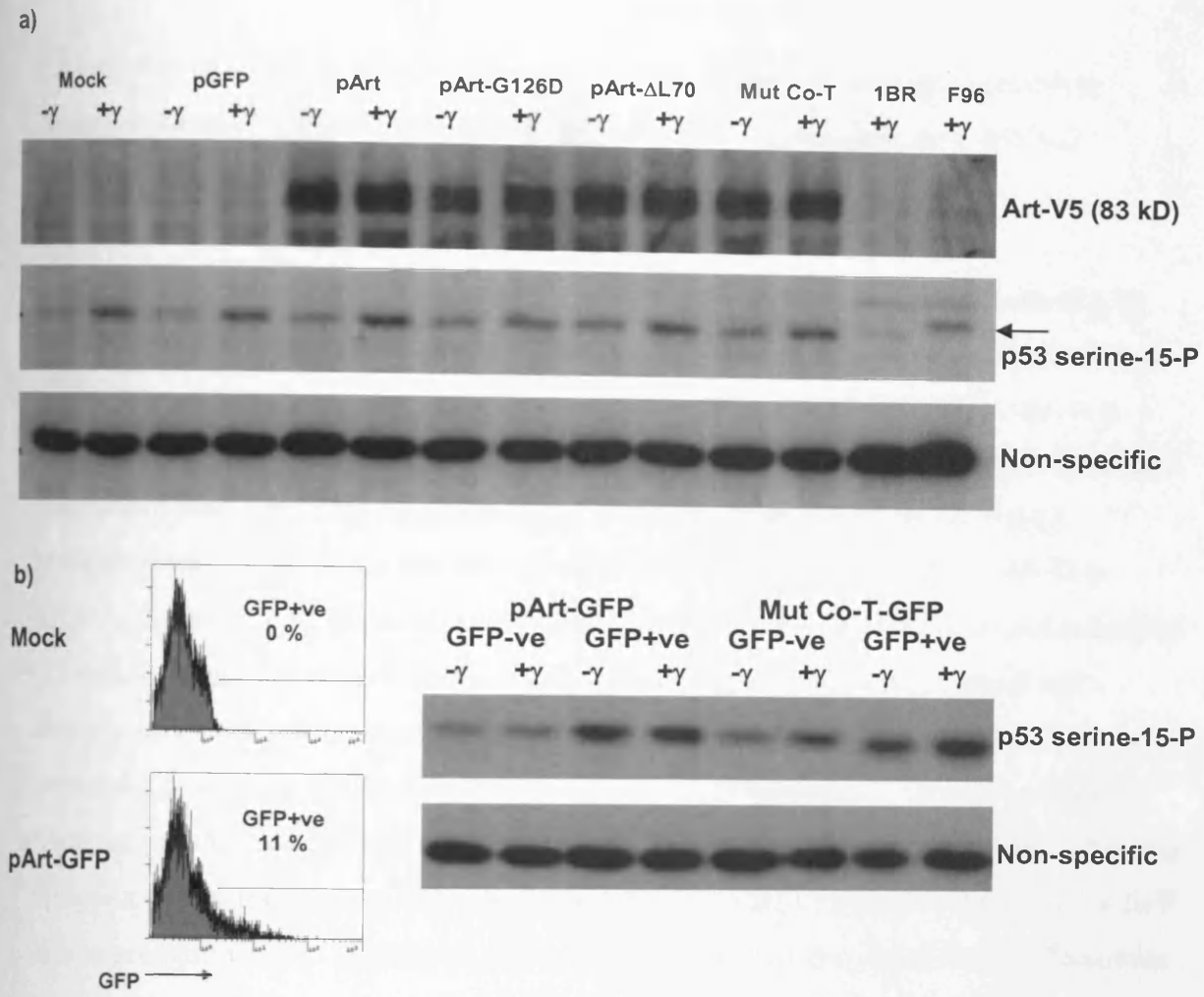

Figure 7-6: The presence of the F96 mutant Artemis proteins does not enhance radiation-induced p53 serine-15 phosphorylation in HCT116 cells. a) Western blot of HCT116 cells either mock transfected or transfected with V5-tagged EXP3.2 expression vectors coding for wild type Artemis (pArt), G126D Artemis (pArt-G126D), or ΔL70 Artemis (pArt-ΔL70). A co-transfection with equal amounts of each Artemis mutant (Mut. Co-T) is also included, as well as transfection with GFP alone (pGFP). 24 hours after transfection cells were either mock irradiated (-γ) or exposed to 1Gy γ-radiation (+γ) and total cellular protein isolated after a further 4-hour incubation. The final 2 lanes represent protein isolated from the 1BR and F96 primary fibroblast lines 4 hours after 1Gy irradiation. Similar to the 1BR line, HCT116 cells express only the fast migrating form of p53 ($p53_{Ala}$). The G126D Artemis mutant was expressed at a lower level compared to the other Artemis transfections, which produced comparable amounts of 83 kD V5 tagged protein. The presence of the F96 Artemis mutants did not significantly affect radiation induced serine-15 phosphorylation. b) HCT116 cells were transfected with either a GFP-tagged wild type Artemis EXP47 expression vector (pArt-GFP) or co-transfected with equal amounts of each GFP-tagged F96 mutant (G126D and ΔL70) EXP47 expression vector (Mut Co-T-GFP). 24 hours after transfection, half of each sample was either mock irradiated (-γ) or exposed to 1 Gy γ-radiation (+γ), and after a further 4-hour incubation cells were sorted into GFP negative (GFP-ve) and GFP positive (GFP+ve) populations. Total cellular protein was then isolated and a western blot of p53 serine-15 phosphorylation performed. Transfection with either wild type Artemis or the F96 mutants resulted in a significant increase in p53 serine-15 phosphorylation in untreated cells, and irradiation only marginally increased this modification. The expression of the F96 mutant Artemis proteins did not result in the specific amplification of radiation-induced p53 serine-15 phosphorylation compared to that with wild type Artemis.

4 hours after exposure to 1Gy γ-radiation was also run on the same gel in order to determine whether the HCT116 cells expressed the fast ($p53_{Ala}$) or slow ($p53_{Pro}$) migrating polymorphic forms of p53.

Similar to 1BR cells, the HCT116 line expressed only the fast migrating form of p53, suggesting this line is homozygous for $p53_{Ala}$. A V5-tagged protein was detected in all of the Artemis transfections at the expected size of 83 kD. The G126D mutant was expressed at a lower level compared to the other Artemis transfections, which produced comparable amounts of V5 tagged protein. Irradiation increased p53 serine-15 phosphorylation in all of the transfected cells, and the presence of either G126D or ΔL70 Artemis mutants, either alone or after co-transfection, did not increase the level of this radiation-induced modification. Although we were able to detect significant amounts of V5 tagged Artemis protein after these transfections, there was likely to be a substantial proportion of untransfected cells in these populations. This was reflected when we transfected HCT116 cells with a GFP tagged Artemis construct and could only achieve a ~10 % transfection efficiency, despite achieving ~80 % efficiency with a GFP only expression vector. In order to address the problem of low transfection efficiencies using Artemis constructs we performed an experiment that involved sorting the populations of transfected and untransfected cells within a sample. HCT116 cells were transfected with a GFP-tagged wild type Artemis EXP47 expression vector (pArt-GFP) or co-transfected with equal amounts of each GFP-tagged F96 mutant (G126D and ΔL70) EXP47 expression vector. After a 24 hour incubation, half of the transfected cells were exposed to 1 Gy γ-radiation, while the remainder were mock irradiated. 4 hours later these samples were sorted into GFP positive (therefore Artemis positive) and GFP negative (Artemis negative) populations. Total cellular protein was then isolated and a western blot of p53 serine-15 phosphorylation was performed (figure 7-6b). Successful transfection of cells with either wild type Artemis or the F96 mutants resulted in a significant increase in p53 serine-15 phosphorylation in untreated cells, and irradiation only marginally increased this modification. This suggests that either the transfection process or the exogenous expression of any form of Artemis protein may initiate a damage response pathway that results in activation of p53.

The expression of the F96 mutant Artemis proteins did not result in the specific amplification of radiation-induced p53 serine-15 phosphorylation, even after sorting specifically for transfected cells. The presence of the F96 Artemis mutants was

therefore not sufficient to induce abnormally high levels of p53 activation and confer an F96 phenotype on another cell line. Since no evidence was obtained to suggest the F96 mutant Artemis proteins are directly responsible for the enhanced p53 signalling observed, this phenotype is most likely to result from the homozygous expression of the $p53_{Pro}$ isoforms, the presence of a subset of DSBs particularly potent in triggering p53, or other genetic factors specific to the F96 line, such as a reduced level of p53 negative regulation. The separate expression of each of the polymorphic forms of p53 ($p53_{Arg}$ and $p53_{Pro}$) in p53 mutant cells of the same genetic background would finally confirm whether radiation induced serine-15 phosphorylation is differentially regulated in an isoform specific manner.

7.3 Microarray analysis of the Artemis mutant F96 in response to ionising radiation

Because we had observed that the p53 response was elevated in the F96 line with respect to p53 serine-15 phosphorylation and the induction of p21, we investigated this phenotype on a genomic scale by microarray analysis of radiation-induced gene expression. F96 cells were compared to the control line 1BR, both before and after exposure to 1 Gy γ-radiation.

12 Affymetrix U133A microarrays (3 x 1BR 0 Gy, 3 x 1BR 1Gy, 3 x F96 0Gy and 3 x F96 1Gy) were hybridised with cRNA prepared from the corresponding total RNA sample. Each replicate sample represented a separate RNA isolation experiment and quality control was performed using an Agilent Bioanalyser 2100 (section 2.15.1). Data was collected on an Affymetrix Scanner 3000, and primary expression data was summarised using the MAS5.0 algorithm. The data generated was then transferred to Genespring 6 for further analysis.

7.3.1 GeneChip Quality Control

Table 7-2: GeneChip Quality Control

Chip name	Q	Scale Factor	Background	% Call	Av Signal	GAPDH	B-actin
1BR 0Gy A	2.46	0.456	53.13	52.50%	266.6	1.17	1.96
1BR 0Gy B	2.54	0.458	56.41	51.60%	273.2	1.11	1.81
1BR 0Gy C	2.24	0.376	48.21	54.90%	248	1.2	2.02
1BR 1Gy A	2.47	0.32	55.49	54.50%	243.4	1.06	1.59
1BR 1Gy B	2.87	1.124	58.51	36.00%	372.1	1.06	2.38
1BR 1Gy C	2.76	0.684	59.12	47.50%	281.4	1.26	1.53
F96 0Gy A	2.64	0.471	60.11	53.40%	251.1	1	1.27
F96 0Gy B	5.27	0.439	141.58	47.20%	273.2	0.99	1.75
F96 0Gy C	2.39	0.584	53.41	50.20%	265.3	1.15	1.31
F96 1Gy A	2.32	0.535	52.19	51.80%	265.5	1.05	1.25
F96 1Gy B	2.26	0.577	50.01	51.80%	269	1.14	1.32
F96 1Gy C	2.16	0.39	47.48	55.40%	247	1.32	2.51
Limits	5.0	3.5 fold	150	25 %	200-400	3	3

BioB spike-in control was detected in all arrays (sensitivity > 3 copies per cell).

1BR 1Gy B has a lower % call and a higher scale factor (table 7-2), indicating low yield from the IVT, therefore the chip may have been slightly under-loaded. 1BR 1Gy B and F96 1Gy C have slightly higher B-actin ratios, indicating slightly lower RNA quality. F96 0Gy B has a slightly higher background. Overall, no arrays were outside the limits of acceptability (as defined by experience), and therefore all are included in the analysis.

7.3.2 Distributions

1BR 1Gy B and F96 1Gy C had a slightly flattened distribution, but were within acceptable limits (figure 7-7). Ideally the 1BR 1Gy B experiment would have been repeated but the resources available did not allow for this. Subsequent examination of differentially expressed genes did not reveal any major bias conferred by this array.

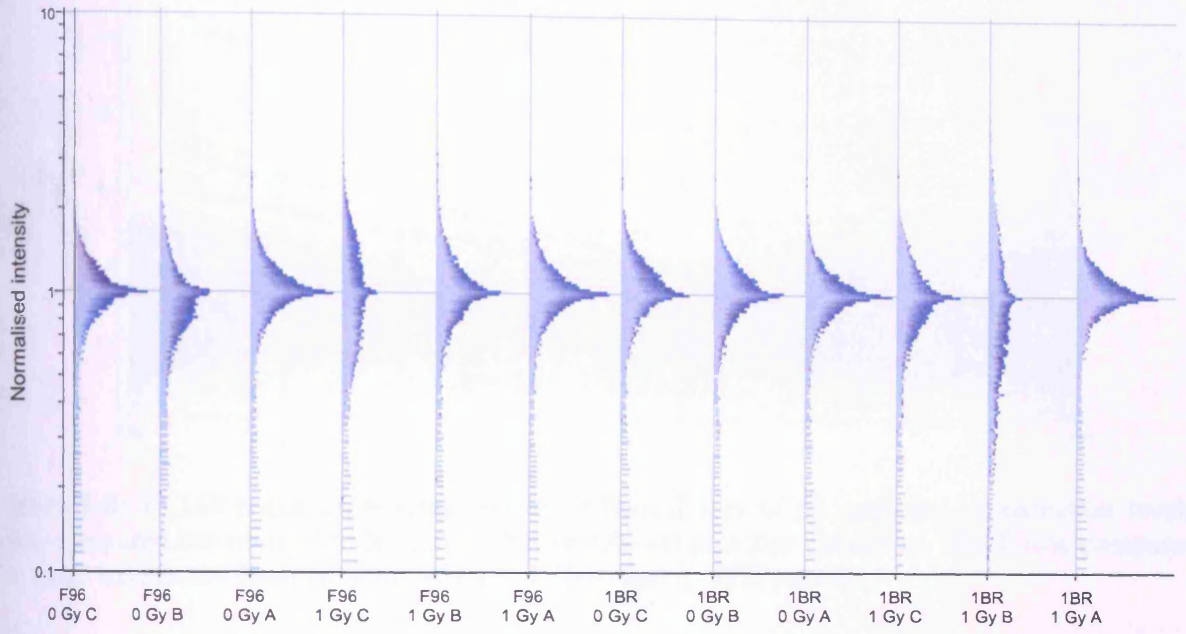

Figure 7-7: Distribution of normalised intensity for each of the 12 U133A microarrays used for analysis of radiation-induced gene expression

Initially we normalised the data within arrays to the median of all genes (i.e. genes at the median level on each array had a value of 1). Genes were then normalised across arrays to the median value of that gene across all 12 arrays, to give a relative expression value per gene, per array.

7.3.3 Detection

Detection was based on the Affymetrix MAS5.0 algorithm, which gives a p value for the call of each probeset. We relaxed this to <0.1 (from <0.06) as we find from experience the Affymetrix detection limit to be over rigorous. On this basis 13,168 transcripts, out of a total of 22283 total transcripts and controls, were detected in at least 2 (out of 12) samples on the Affymetrix U133A array (figure 7-8).

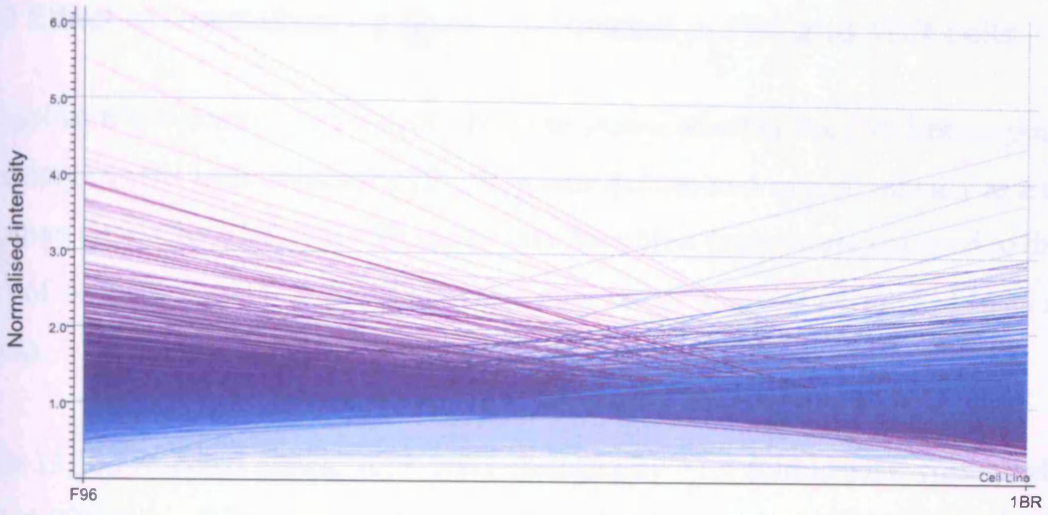

Figure 7-8: 13,168 transcripts detected in at least 2 out of 12 samples. Expression levels were compared between F96 (left) and 1BR (right) cells in any condition. Each line compares the mean expression level of a transcript in F96 to that in 1BR (n=6).

7.3.4 Cell specific variation

The majority of genes were expressed in both populations but 650 genes show a 2 fold or greater difference between 1BR and F96 samples irrespective of radiation treatment. 273 of these show statistical significance (t test n = 6 $p<0.05$), and 51 survive Benjamini Hochberg false discovery correction. These represent the most robust differences between cell lines independent of irradiation (figure 7-9), and are included in Appendix 1 (7.3 Gene lists CD). Among groups of related genes in this set are a large group of Hox and Sox genes (HoxA11, B2, B7, C6; Sox9 and 13), all but one (Sox 13) of which are high in F96 and low in 1BR samples. The significance of this is not apparent, but the variation that exists between different fibroblast cell lines emphasises the possibility that additional "background" factors may affect p53 signalling.

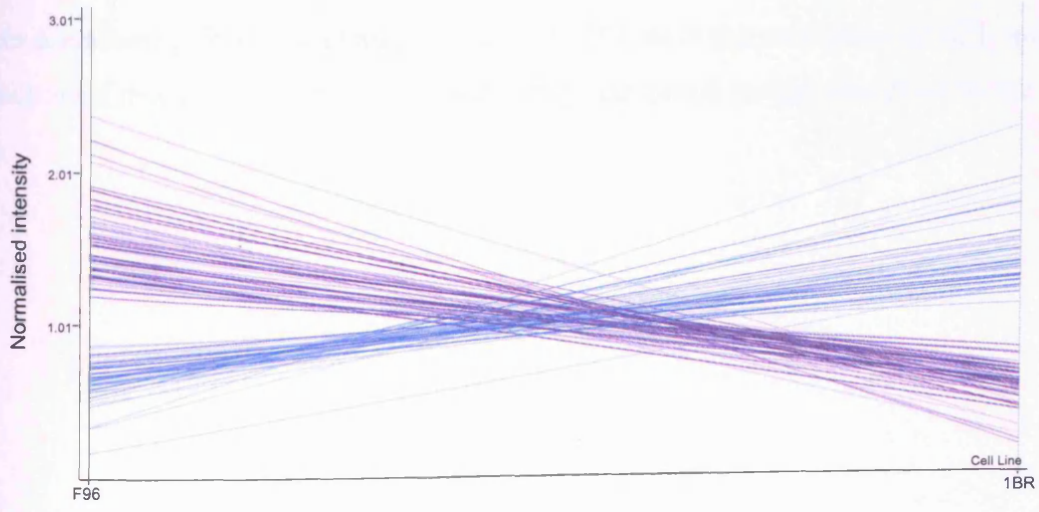

Figure 7-9: 51 genes differentially expressed in F96 (left) and 1BR (right) cells irrespective of irradiation.

7.3.5 Effect of irradiation on gene expression in F96 and 1BR cells

We applied a low dose of γ-radiation (1Gy) to assess whether the F96 line responded differently to 1BR cells following IR. 1Gy was determined experimentally as a non-saturating dose after 1BR and F96 (and other fibroblast lines) were exposed to different doses of γ-radiation (0, 1, 3, and 6 Gy) and microarray analysis performed (data not shown).

Of the 13,168 detected genes, 2650 were changed by >1.4 fold in 1BR compared to 2054 in F96 cells. Of these, 74 were significantly changed in 1BR (t test $p < 0.05$) and 144 in F96 cells. Lists of significantly changed genes are included in Appendix 1 (7.3 Gene lists CD). From these 74 (1BR) and 144 (F96) genes changed by irradiation, 40 were up regulated in 1BR and 80 in F96 cells. However, there was very little overlap between these groups. Only 2 genes, p21cip1 and 217542_at, appear in both categories, although several others classify together if the stringency of the t-test is relaxed. This is in contrast to comparable groups derived from higher doses of irradiation (3 and 6 Gy), where many more genes classify together.

Many of the differentially induced genes do not elevate above the pre-irradiation levels observed in the opposite cell line (shown for the F96 line, genes highlighted in black, figure 7-10), which suggests these changes may not be functionally important in the response to DNA damage. A small group of genes were activated above 1BR irradiated levels in the F96 line, and this list contained at least 8 genes known to be targets of p53 (Velasco-Miguel *et al*, 1999) (Takimoto and El-Deiry, 2000) (Hellborg *et al*, 2001) (Tan and Chu, 2002) (Vousden and Lu, 2002) (Burns *et al*, 2003) (figure 7-11). These genes are missing from the changes found in 1BR with the exception of p21, and the induction of this gene is reduced considerably compared to that observed in the F96 line.

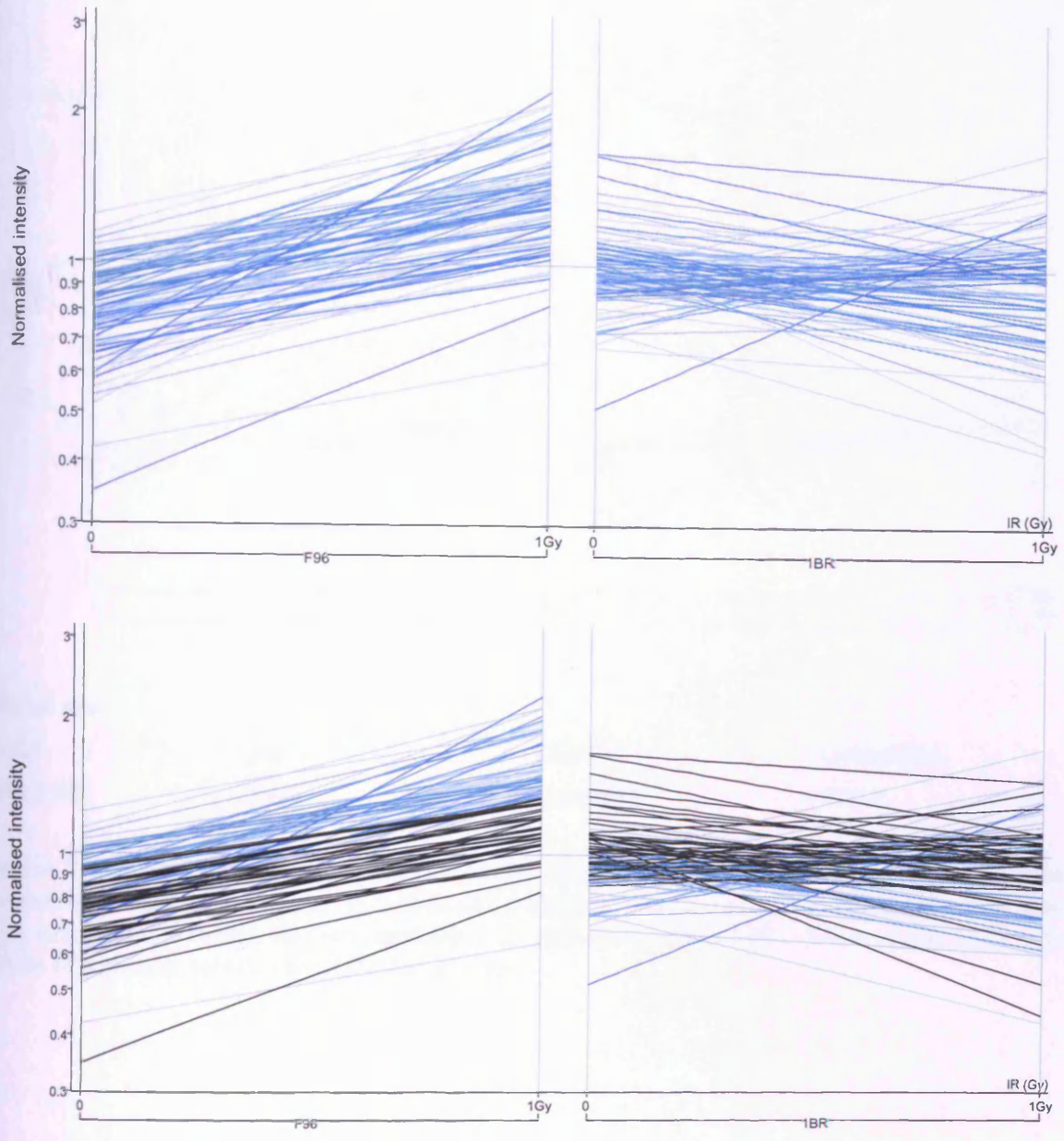

Figure 7-10: 80 genes were upregulated in the F96 line. Whilst many of the genes upregulated by IR in the F96 line did not show a similar pattern of expression in 1BR cells (top panel), many of the F96 upregulated genes increased only to a level similar to that in 1BR cells before irradiation (highlighted in black, bottom panel). A small group of genes were elevated after IR in F96 cells above that of 1BR irradiated levels (blue genes, bottom panel).

In order to confirm whether such p53 target genes are induced by higher doses of IR in the 1BR line, we analysed a preliminary experiment performed with Affymetrix U95A microarrays that involved doses of 6 Gy γ-radiation. After this higher dose of γ-radiation, many more p53 target genes were induced in the 1BR line similar to that observed in F96 cells (figure 7-12), and some of these genes corresponded to those that were selectively induced in the F96 line after 1Gy γ-radiation. This indicates that 1BR cells are capable of inducing this wider p53 response, but only after higher levels of DNA damage.

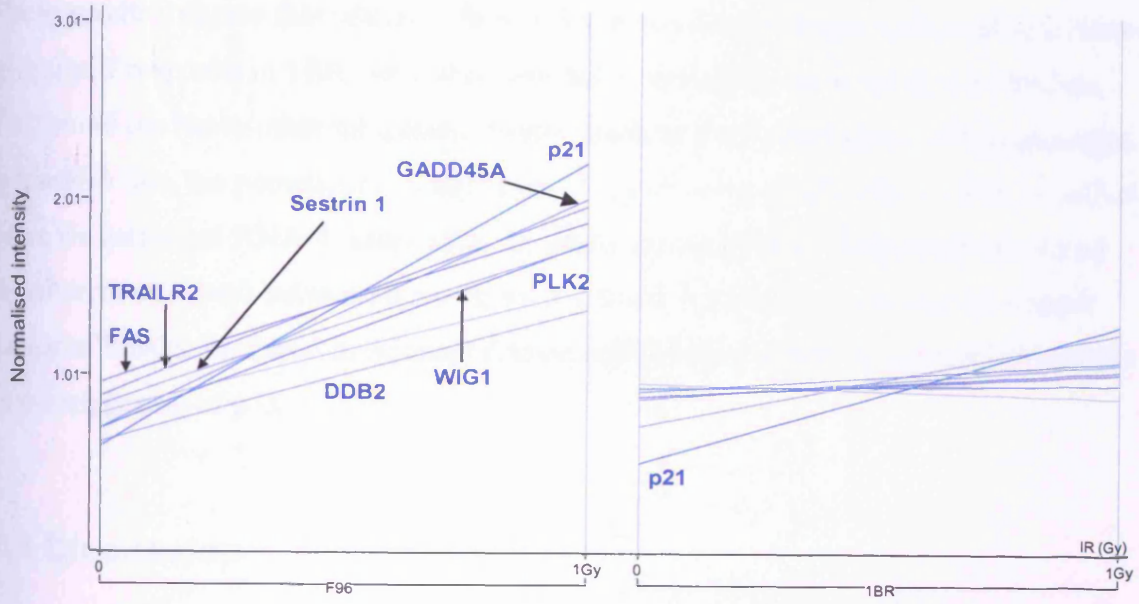

Genes are:

PLK2	p21	DDB2	GADD45A
TRAILR2	FAS	Sestrin1	WIG1

Figure 7-11: 7 p53 target genes elevated by IR in F96 cells but not in 1BR cells after exposure to 1Gy γ-radiation. p21 was the only p53 target gene to be induced in both lines after irradiation, although this was considerably reduced in 1BR cells. Lines connect the mean values of triplicate measurements at the 2 doses.

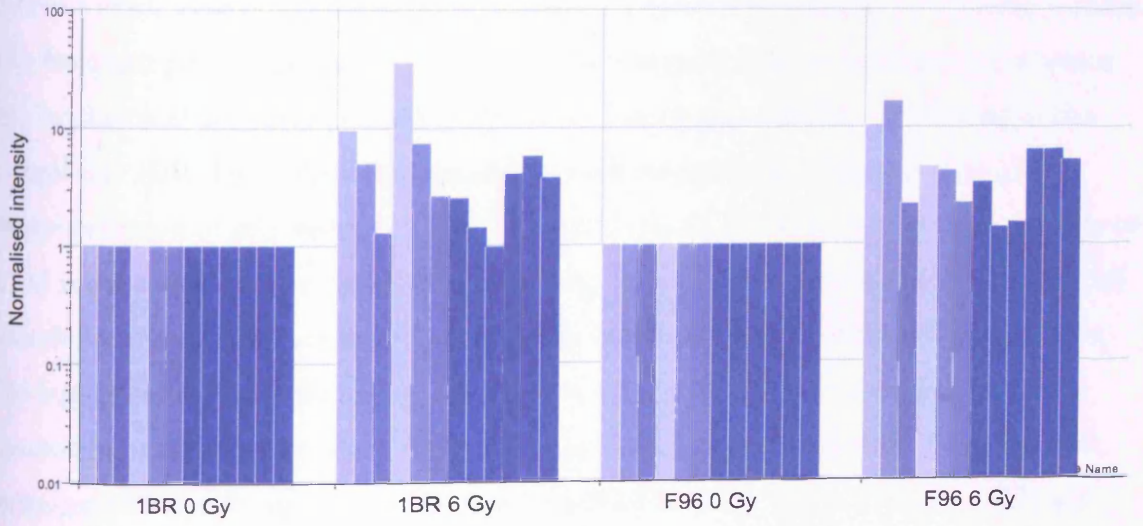

Figure 7-12: Selection of p53 target genes induced in 1BR and F96 cells after exposure to 6 Gy γ-radiation measured using Affymetrix U95A microarrays. Gene order is Cyclin G, Bax, Fas, PCNA, Fas (alt splice), Bax, DDB2, Bax (alt splice), PLK, GADD45, p21, IGFBP4, IGFBP3

These results indicate that whilst a dose of 1 Gy γ-radiation was insufficient to initiate a global p53 response in 1BR cells, this network was clearly activated in the F96 line. This could be due to inherent genetic factors such as the homozygous $p53_{Pro}$ genotype of the F96 line, the persistence of elevated levels of unrepaired DSBs (which is unlikely since we measured RNA 4 hours after IR where no significant differences in overall repair were observed between these lines, section 5.4.2.) or the existence of a small subset of breaks, enriched in Artemis deficient F96 cells, which are particularly potent in the triggering of p53.

7.4 Discussion

We have identified a mild defect in DSB repair in the radiosensitive line F96 and confirmed the presence of 2 novel mutations on separate alleles of the Artemis gene. Although this repair defect is likely to contribute to the poor survival of F96 cells after irradiation due to a fraction of persistent, slowly repaired breaks, we also investigated p53 signalling in this line in order to identify any anomalies in the wider response to DNA damage.

ATM directly phosphorylates p53 on serine-15 (Banin *et al*, 1998) (Canman *et al*, 1998) (Khanna *et al*, 1998) (Nakagawa *et al*, 1999), which is then thought to nucleate a series of subsequent post-translational modifications that contribute to both the stabilisation and biochemical activation of p53 (Appella and Anderson, 2001). Compared to the control line 1BR, F96 cells demonstrated a more pronounced radiation-induced phosphorylation of p53 serine-15. Previous work has indicated that the total activity of ATM is dependent on the yield of DNA lesion, and this was associated with enhanced phosphorylation of p53 serine-15 after higher levels of damage (Buscemi *et al*, 2004). The higher induction of this modification observed in F96 cells may therefore have resulted from elevated levels of DNA damage 4 hours after irradiation that triggered enhanced p53 signalling, but results from the H2AX repair assay (section 5.4.2) are inconsistent with this hypothesis. H2AX analysis demonstrated that the repair defect in F96 cells does not become apparent until 24 hours after irradiation, and at 2 and 6 hours of repair time the F96 line has comparable levels of unrepaired DSBs to that of control cells. Furthermore, although the 180BR line (which is deficient in Ligase IV) displayed

elevated levels of H2AX foci 2-6 hours after irradiation, abnormally high levels of radiation induced p53 phosphorylation were not observed. Together, these results suggest that high levels of unrepaired DSBs are not responsible for the enhanced p53 signalling observed in the F96 line.

Whilst elevated levels of total DNA DSBs do not appear to be responsible for the enhanced p53 signalling associated with F96 cells, another possibility may be a difference in the species of DNA lesion that predominates after 4 hours. Artemis has been implicated in the repair of a subset of DNA DSBs, possibly complex lesions that require nucleolytic processing (Jeggo and O'Neill, 2002) (Riballo *et al*, 2004) and the accumulation of p53 has been shown, within limits, to be enhanced after high LET irradiation that produces more complex DSBs (Fournier *et al*, 2004). The persistence of complex breaks in the F96 line, although masked by the total level of breaks, may therefore have promoted p53 signalling. If this were due to the absent repair of complex DSBs then the Artemis null CJ179 line may also be expected to display enhanced p53 signalling, but this was not observed. Therefore, if the initiating signal, i.e. the damage lesion itself, was responsible for the p53 effects observed in F96 cells, then the mutant Artemis proteins present must have modified the lesion in such a way to promote DSB signalling, an effect associated with hypomorphic mutations and not the total absence of Artemis protein. Whilst there is no precedence for this situation in the literature, the possibility cannot be dismissed.

In order to investigate whether the presence of mutant Artemis proteins in the F96 line were responsible for the enhanced p53 signalling observed, we transfected colon carcinoma cells, which retain a non mutated p53 pathway, with F96 mutant Artemis constructs. Previous experiments with expression vectors that incorporate a C-terminal GFP tag demonstrated relatively poor transfection efficiencies using Artemis constructs (~10 %), but we were able to sort cells into non-transfected (GFP -) and transfected (GFP +) populations by FACS. Cells transfected with either wild type or mutant Artemis constructs displayed increased p53 serine-15 phosphorylation, which may be attributed to the transfection procedure introducing DNA DSBs in a non-specific manner. Since there was no specific increase in radiation-induced p53 serine-15 phosphorylation in cells expressing the F96 mutant Artemis proteins, this would suggest that these mutants are not responsible for the p53 effects observed. Certain limitations should be appreciated when interpreting results from these experiments. Despite

achieving favourable transfection efficiencies with other expression vectors, we were unable to express Artemis proteins in either primary fibroblasts or fibroblasts immortalised by stable expression of human telomerase catalytic subunit (hTERT). More appropriate experiments would have involved the transfection of Artemis null CJ179 cells with mutant Artemis proteins, but since this was not possible we were restricted to the use of cell lines. HCT116 cells are expected to express endogenous Artemis and this is not an ideal system to look for the effects of exogenous mutant counterparts, since the endogenous protein may interfere with any mutant effects. In addition, the Cycle 3 GFP tag incorporated at the Artemis C-terminal in these experiments is predicted to add 27 kD to expressed proteins. Such a large modification may have impaired any function of the mutant Artemis proteins that promotes p53 signalling. Whilst acknowledging these caveats, no evidence was obtained to suggest the F96 mutant Artemis proteins were responsible for the enhanced p53 signalling phenotype observed in this line.

To further investigate the enhanced damage signalling associated with F96 cells, we began to examine the p53 protein itself. After extended resolution on a denaturing gel, p53 from F96 cells displayed retarded electrophoretic mobility compared to that from control cells, indicative of a small increase in size. Although this could have resulted from additional post-translational modifications, we demonstrated this shift did not involve phosphorylation, and was also unlikely to result from additional acetylations, shown by treatment of cells with anacardic acid, a potent non-competitive inhibitor of the p300 and PCAF acetyltransferases. p300 and PCAF are thought to be responsible for the acetylation of p53 (Liu *et al*, 1999), which enhances its stabilisation and activity (Sakaguchi *et al*, 1998) (Ito *et al*, 2001). Consistent with this, the apparent inhibition of these enzymes induced a dose dependent decrease in the stability of p53, and this was associated with reduced levels of serine-15 phosphorylation in control and F96 cells. Despite these changes, the electrophoretic mobility of F96 p53 was still retarded. We therefore began to examine the coding sequence of p53 in F96 cells for any differences that may account for this apparent discrepancy in size compared to p53 from control cells.

Analysis of the p53 coding region from F96 cells revealed expression of a transcript that was wild type, but which contained a polymorphism in codon 72 that has been previously reported (Harris *et al*, 1986) (Matlashewski *et al*, 1987). The amino acid

change that results from this polymorphism was shown to affect the electrophoretic mobility of p53, with $p53_{Pro}$ (Proline in position 72) demonstrating reduced electrophoretic mobility compared to the $p53_{Arg}$ (Arginine in position 72) (Harris *et al*, 1986) (Matlashewski *et al*, 1987). Since the p53 gene expressed in F96 cells coded for $p53_{Pro}$, this may have explained the differences in migration compared to p53 from the control line 1BR, and sequence analysis confirmed this hypothesis, revealing that 1BR cells expressed transcript coding for $p53_{Arg}$. Furthermore, GOS5 cells that displayed a p53 doublet after gel electrophoresis, expressed transcripts coding for both the $p53_{Pro}$ and $p53_{Arg}$ forms, indicating this line was heterozygous for this polymorphism.

Out of the 8 primary lines examined, the F96 line was the only one to express just the fast migrating form of p53 indicating a homozygous $p53_{Pro}$ genotype. A highly significant association between the p53 codon 72 polymorphism and ethnicity has been reported, with the frequency of the $p53_{Pro}$ allele showing a north-south cline from 17 % in Swedish Saamis to 63 % in African Blacks (Nigerians) (Beckman *et al*, 1994). In White non-Hispanic Americans a homozygous $p53_{Pro}$ genotype was shown to account for only 9 % of the population (Inserra *et al*, 2003) and a similar low frequency was reflected in the UK for two different White control populations (Rosenthal *et al*, 1998). Whilst the ethnicity of most patients in this project was unknown, the low frequency (0.12) of homozygous $p53_{Pro}$ expression observed is consistent with a North European population, and since patient F96 was of White UK ethnicity, the homozygous $p53_{Pro}$ genotype observed is likely to represent a relatively rare occurrence.

F96 was also the only line to display enhanced p53 activation compared to controls. It is therefore tempting to speculate that the presence of only the $p53_{Pro}$ variant in the F96 line contributed to the elevated levels of p53 signalling. Whilst there have been no reports of either polymorphic form of p53 being more prone to serine 15 phosphorylation, their transcriptional activities have been examined in detail. Compared to the $p53_{Arg}$ form, the $p53_{Pro}$ variant has previously been shown to be a more potent transcriptional activator by a magnitude of approximately 2-fold (Thomas *et al*, 1999). This effect was observed using a reporter plasmid for the p21 promoter-enhancer, and consistent with this the $p53_{Pro}$ variant was later found to induce a higher level of G1 arrest than the $p53_{Arg}$ form (Pim and Banks, 2004). Our results compare well with these findings, since the homozygous $p53_{Pro}$ F96 line was found to induce p21 mRNA and protein to a level approximately double that of the homozygous $p53_{Arg}$ 1BR

line. It is therefore likely that the $p53_{Pro}$ genotype of the F96 line contributed to the elevated levels of p53-dependent gene transcription observed. Our results also suggest that the $p53_{Pro}$ variant, when present in a homozygous setting, may be more prone to radiation-induced serine-15 phosphorylation than $p53_{Arg}$, although other genetic effects such as Artemis mutations may contribute to this phenotype. The net result manifests as enhanced DNA damage signalling in the F96 line.

Another difference between the codon 72 variants of p53 has been reported in their ability to induce apoptosis. In human tumour cells the $p53_{Arg}$ form was shown to be more efficient at inducing apoptosis than $p53_{Pro}$ (Thomas *et al*, 1999) (Pim and Banks, 2004). This difference was related to the ability of $p53_{Arg}$ to more efficiently translocate to the mitochondria (Dumont *et al*, 2003) where p53 may promote apoptosis independent of its transcriptional activator properties (Mihara *et al*, 2003) (Leu *et al*, 2004), but this translocation seems to occur only in tumour cells (Marchenko *et al*, 2000). Consistent with this, no evidence was found for the localisation of p53 to the mitochondria in non-transformed human fibroblasts, and no correlation was observed between the p53 codon 72 polymorphism and apoptosis in normal human fibroblast lines homozygous for either allele after DNA damage (Dumont *et al*, 2003). This suggests that unlike in tumour cells, the enhanced ability of $p53_{Arg}$ to induce apoptosis directly at the mitochondria may not be relevant in primary cells. Conversely, in primary cells the differential transcriptional activator properties of the p53 variants may be more important. In this respect the expression of $p53_{Pro}$ may lead to enhanced p53 dependent gene transcription, and we therefore investigated this on a genomic scale in the F96 line using Affymetrix microarray analysis.

Consistent with the enhanced p53 signalling observed in the F96 line, microarray analysis revealed an elevated p53 transcriptional response after irradiation in F96 cells compared to the control line 1BR. The induction of p21 was elevated compared to control, and at least 7 other p53 target genes that did not change in controls were selectively induced in F96 cells. These results suggested that whilst a dose of 1 Gy γ-radiation was insufficient to initiate a global p53 response in 1BR cells, this network was clearly activated in the F96 line. This could be due to the persistence of elevated levels of unrepaired DSBs, but this is unlikely since we measured RNA 4 hours after irradiation where no significant differences in overall repair were observed between these lines (section 5.4.2.).

The relatively high level of p21 induction observed in F96 cells may promote a more stringent growth arrest in this line after non-saturating doses of γ-radiation. Whilst this would allow time for repair mechanisms to function, such high levels of p21 may not be desirable. Cells released from p21 mediated overexpression have previously displayed growth retardation, cell death and decreased clonogenicity that was associated with abnormal mitotic events in subsequent divisions (Chang *et al*, 2000). These effects were correlated with the induction level of p21, which at high levels resulted in the depletion of proteins involved in the control and execution of mitosis. This study was performed in fibrosarcoma cells, and if similar mechanisms exist in primary fibroblasts they may contribute to the delayed growth retardation observed in the F96 line after irradiation (section 4.3.2). Thus, the enhanced p53 signalling observed early after irradiation may have deleterious effects on survival during subsequent divisions in cells that would otherwise recover from the initial genotoxic insult.

The elevated level of p21 induction and selective induction of certain p53-target genes in the F96 line is likely to result, at least in part, from the elevated levels of p53 serine-15 phosphorylation observed in these cells after irradiation. Previous results have indicated that the role of p53 serine-18 phosphorylation, the murine counterpart of serine 15, in regulating the transcription of p53 target genes is promoter specific (Chao *et al*, 2003). In addition to abrogated p21 induction, thymocytes homozygous for a p53 mutant refractory to serine-18 phosphorylation ($p53^{S18A}$) displayed impaired induction of certain p53 target genes after irradiation, whilst others were unaffected. Amongst the transcriptional changes severely impaired in $p53^{S18A}$ homozygous cells was the induction of the p53 target PLK2/SNK, which was also selectively induced in the F96 line after irradiation. The high levels of radiation-induced serine-15 phosphorylation in F96 cells may therefore contribute not only to elevated p21 induction, but also to the induction of certain p53 target genes in a promoter specific manner.

Of the group of p53 target genes selectively induced in F96 fibroblasts it is noteworthy that Fas and TRAILR2, both apoptosis inducing death receptors (Walczak and Krammer, 2000), were included. Primary fibroblasts are notoriously resistant to apoptosis (Chung *et al*, 1998) (Dikomey *et al*, 1998) (Kawabe *et al*, 2001) (Zhang *et al*, 2001a) and the p53-dependent induction of TRAILR2 has been shown to be restricted to cell types undergoing apoptosis and not cells undergoing exclusively p53 dependent G1

arrest such as normal lung fibroblasts (Wu *et al*, 1999). Since F96 fibroblasts have demonstrated insignificant levels apoptosis at both early (Peake *et al*, 1999) and delayed (section 4.3.3.) time points after irradiation, it is intriguing that the expression of these death receptor genes should be induced. Whilst the induction of death receptors may not lead to the initiation of fibroblast apoptosis *in vitro*, it is tempting to speculate this may not be the case *in vivo*, where the ligands for such receptors (Fas-L and TRAIL) may be more readily available. The induction of death receptors may represent a mechanism whereby highly damaged fibroblasts are targeted for apoptosis by the Fas-L and/or TRAIL expressed on infiltrating lymphocytes in order to facilitate tissue repair. Indeed, primary human fibroblasts modified to express relatively high levels of Fas receptor displayed widespread apoptosis after incubation with the Fas cross-linking antibody CH-11 (Freiberg *et al*, 1997). Similarly, in murine fibroblasts UVB irradiation was shown to increase death receptor expression and subsequent levels of apoptosis after incubation with the respective ligand (Kimura *et al*, 2001). F96 fibroblasts may therefore be particularly sensitive to death receptor activation when presented with the cognate ligand after irradiation, a characteristic that could be investigated by incubating control and F96 fibroblasts with either TRAIL or Fas-L after irradiation and comparing levels of apoptosis.

The selective radiation-induced expression of Fas and TRAILR2 observed in F96 fibroblasts may also have important implications for other cell types in the F96 patient. As well as demonstrating cellular radiosensitivity, this patient displayed a progressive immunodeficiency that was associated with increased levels of lymphocyte apoptosis (Peake *et al*, 1999). Although this increased apoptosis did not seem to be associated with deregulated Fas signalling, sensitivity to TRAIL-induced apoptosis was not examined. Human lymphoid cell lines differ in their sensitivity to TRAIL-induced apoptosis and whilst peripheral T cells appear resistant (Jeremias *et al*, 1998), activated thymocytes are sensitive to TRAIL mediated apoptosis (Simon *et al*, 2001). Since V(D)J recombination is monitored by the p53 pathway to limit aberrant recombination events (Guidos *et al*, 1996) (Perkins *et al*, 2002), the repair defect present in F96 cells may combine with the enhanced DNA damage signalling observed to promote TRAIL mediated thymocyte apoptosis and confer clinical immunodeficiency. Indeed, common variable immunodeficiency has previously been associated with high expression levels of other receptors of the TNF receptor family (TNF-R1 and TNF-R2) (Di Renzo *et al*, 2001).

We have described enhanced DNA damage signalling in the Artemis mutant line F96 after irradiation. This manifested as elevated levels of radiation-induced p53 serine-15 phosphorylation, p21 induction, and the specific induction of certain p53 target genes that was not observed in control cells after un-saturating doses of γ-radiation. There was no evidence to suggest these effects resulted from the direct activity of the F96 mutant Artemis proteins or elevated levels of total unrepaired DSBs, although a subset of DSBs particularly potent in triggering the p53 response and enriched in F96 cells may have been involved. In contrast to all other primary lines examined, the F96 line was found to be homozygous for the $p53_{Pro}$ polymorphic form of p53, and this genetic variation may contribute to the elevated p53 responses described. F96 cells may therefore be hard-wired to induce p53 dependent endpoints such as growth arrest and apoptosis more readily. This enhanced damage signalling may combine with the deficiency in DNA repair observed, and possibly other factors intrinsic to the patient, to impair the survival of fibroblasts irradiated *in vitro*, and hinder the development of functional lymphocytes *in vivo*.

Chapter 8: Conclusions

Double strand breaks (DSBs) in genomic DNA are induced by exogenous sources such as ionising radiation, but also arise during normal physiological processes such as V(D)J recombination during lymphocyte development. The induction of DSBs leads to the activation of proteins involved in DNA repair, and may initiate p53 dependent pathways that result in cell cycle arrest and/or apoptosis. Defects in this damage response network that impair the ability of cells to repair DSBs, both during V(D)J recombination and after irradiation, may therefore result in radiosensitive immunodeficiency. Radiosensitive immunodeficiency has been previously described in patients with mutations in DSB repair genes, whilst others have been described with no apparent deficiency in DNA repair. These patients may have defects in the damage assessment process that commits highly damaged cells to either permanent growth arrest or apoptosis. This project aimed to investigate undefined immunodeficient patients for evidence of DNA damage response defects using established and novel techniques in order to gain insight into the processes involved in cellular radiosensitivity. Further investigation allowed us to delineate how incongruities in certain pathways may contribute to radiosensitive immunodeficiency.

As a population, the group of 20 undefined immunodeficient patients examined were not significantly more radiosensitive than controls, suggesting these patients do not represent a distinct population with respect to cellular radiosensitivity. The range of sensitivities observed more likely reflects subtle genetic differences and polymorphisms that promote minor variations in radiosensitivity near to the control range. A more pronounced radiosensitivity similar to repair defective cells may be more indicative of a mutation in a damage response protein that impairs protein function. Only a small proportion (~10 %) of the undefined immunodeficient patients examined displayed this more pronounced phenotype. This indicates that the majority of undefined immunodeficient cases are not associated with radiosensitivity. Only those patients displaying a pronounced cellular radiosensitivity, similar to previously defined damage response mutants, should be classed as radiosensitive and further investigated along those lines.

Fibroblast survival assays were used to identify radiosensitive patient lines that were classified into mild and intermediate groups of radiosensitivity. This is the established method of assessing cellular radiosensitivity, but such clonogenic assays are very time consuming. We therefore investigated radiation-induced lymphocyte apoptosis as a measure of cellular radiosensitivity, since this endpoint can be measured as early as 24 hours after treatment. Despite some correlation with fibroblast survivals, radiation-induced lymphocyte apoptosis was found to be highly variable between different controls, and there were some discrepancies between repeat experiments with some patient samples. We therefore concluded that this endpoint was not reliable enough to use as a measure for cellular radiosensitivity.

Another limitation of fibroblast survival assays is they give no insight into the fate of cells that survive the initial genotoxic insult, but then fail to proliferate and form colonies. Primary fibroblasts are not prone to the induction of apoptosis after irradiation (Chung *et al*, 1998) (Dikomey *et al*, 1998) (Kawabe *et al*, 2001) (Zhang *et al*, 2001a), but a substantial fraction of primary fibroblasts seem to be inactivated by a permanent growth arrest (Little *et al*, 1985) (Di Leonardo *et al*, 1994) (Yount *et al*, 1996) (Linke *et al*, 1997) (Williams *et al*, 1997) (Boyle *et al*, 1999) (Azzam *et al*, 2000). We therefore developed a novel assay for cellular radiosensitivity that focused on fibroblast division early after irradiation, and this was able to identify important differences between a control and repair defective line. The Artemis deficient CJ179 line was more prone to the induction of a senescent like growth arrest than control cells, which is likely to result from the persistence of unrepaired breaks for at least 3 days after irradiation as shown by γ-H2AX foci enumeration. Consistently, the persistence of breaks too severe for repair for several days after irradiation has previously been proposed as an initiation signal for stress-induced premature senescence (Naka *et al*, 2004).

Despite showing impaired radiosensitivity survival similar to that of the Artemis null CJ179 line, the F96 line was only slightly more sensitive than control cells to the induction of an early, senescent-like growth arrest. Instead, after higher doses of radiation the dividing F96 cells that emerged underwent a delayed growth arrest that was not associated with senescent like characteristics or substantial levels of apoptosis. The specific causes of this delayed arrest are unknown. Previous studies have described reactivation of p53 numerous divisions after irradiation (Rugo *et al*, 2002) (Suzuki *et al*,

2003b) and the induction of delayed chromosomal damage (Marder and Morgan, 1993) that is associated with delayed reproductive death (Chang and Little, 1991) (Suzuki *et al*, 1998). The observation that delayed chromosomal instability can be reduced by delayed plating, which allows more time for repair, suggests that these effects may be determined by the repair process of the initial radiation damage (Roy *et al*, 1999).

Chromosome break analysis and H2AX enumeration demonstrated an elevated level of unrepaired DNA damage in F96 cells 24 hours after irradiation suggesting defective repair, and sequence analysis confirmed this line was compound heterozygote for G126D and ΔL70 mutations in Artemis. Since these mutations do not directly modify any residues proposed to function in metal binding within the metallo-β-lactamase catalytic site (Pannicke *et al*, 2004) (Poinsignon *et al*, 2004), these mutant proteins are likely to retain partial function. This would be consistent with extended γ-H2AX enumeration studies. In contrast to the Artemis null CJ179 line where γ-H2AX foci persisted, in F96 cells these foci had returned to control levels by 72 hours. This slow repair is likely to represent the rejoining of complex breaks that require nucleolytic processing before rejoining, a function previously proposed for Artemis (Jeggo and O'Neill, 2002). In addition, the high incidence of dicentrics observed in F96 cells after irradiation may also indicate a high level of DSB misrejoining. The mutant Artemis proteins in the F96 line may therefore eventually allow the repair of complex breaks, albeit with slower kinetics and reduced fidelity. This could permit cells to divide a limited number of times before the induction of a delayed growth arrest or cell death, possibly resulting from a delayed instability similar to that described above. Indeed, higher levels of delayed reproductive death are observed in cells that retain a functional NHEJ pathway compared to those deficient in this process (Chang and Little, 1992). In Artemis null cells, the persistent level of unrepaired breaks may simply induce premature senescence within the first 6 days of irradiation. The arrested populations observed in these cell division experiments could be further investigated for γ-H2AX foci, p53 signalling and chromosomal damage after cell sorting in order to better understand why these different cell fates are initiated.

The activity of the F96 mutant Artemis proteins is currently being examined by our collaborators using an *in vitro* functional assay. The results presented here suggest these mutations are hypomorphic, which is consistent with the phenotype of the F96 patient. Although this patient displayed lymphopaenia that was progressive with age,

this was relatively mild compared to that observed in Artemis null patients. There was also no appreciable alteration in the distribution of lymphocyte subsets and T cells did not consist of single or multiple abnormal clones (Peake *et al*, 1999). A partially functional V(D)J recombination pathway where RAG induced breaks are eventually rejoined, possibly with reduced fidelity, may be expected to confer such a phenotype. This would result in a significant amount of mature lymphocytes, but these cells may be unstable. Just as F96 fibroblasts treated with γ-radiation are destined to arrest after a certain amount of divisions, F96 lymphocytes *in vivo* may be prone to apoptosis. Indeed, elevated spontaneous apoptosis was observed in this patient's lymphocytes *in vitro* (Peake *et al*, 1999). Since the ATM-p53 pathway is reported to monitor V(D)J recombination and remove abnormal cells (Guidos *et al*, 1996) (Perkins *et al*, 2002), we investigated this side of the damage response network to determine if any other factors may contribute to this radiosensitive immunodeficiency.

The F96 line demonstrated enhanced levels of radiation-induced serine-15 phosphorylation compared to controls that did not coincide with the elevated level of unrepaired DSBs observed at later time points. This suggested other factors intrinsic to F96 cells may promote p53 signalling, but no evidence was found to suggest the mutant Artemis proteins were responsible for this effect. Further investigation revealed that out of 8 primary lines examined, the F96 line was the only one to be homozygous for proline at position 72 of p53 ($p53_{Pro}$), a previously described polymorphism (Harris *et al*, 1986) (Matlashewski *et al*, 1987). Compared to the $p53_{Arg}$ form, the $p53_{Pro}$ variant was shown to be a more potent transcriptional activator by a magnitude of approximately 2-fold (Thomas *et al*, 1999). This effect was observed using a reporter plasmid for the p21 promoter-enhancer, and consistent with these results the F96 line was found to induce p21 to a level approximately double that of control cells. This may not be desirable since cells released from p21 mediated overexpression have displayed growth retardation, cell death and decreased clonogenicity that was associated with abnormal mitotic events in subsequent divisions (Chang *et al*, 2000). Such an effect may therefore contribute to the delayed arrest observed in F96 cells using cell division analysis. Microarray analysis of gene expression revealed a group of p53 target genes were specifically induced in F96 fibroblasts after a non-saturating dose of irradiation, and this included certain pro-apoptotic death receptors. Although this response may not have significant effects on fibroblast survival *in vitro*, this may not be the situation in vivo where death receptor ligands are available to induce apoptosis. Indeed, the

initiation of such a response in lymphocytes may be expected to enhance death signalling, which may contribute to the elevated levels of spontaneous apoptosis observed in lymphocytes from this patient.

Whilst we cannot be certain that the $p53_{Pro}$ genotype of F96 cells is solely responsible for this enhanced damage signalling, it is likely to contribute to this phenotype. The F96 patient died before this study began, therefore it was not possible to investigate other cell types such as lymphocytes for the enhanced damage signalling observed in fibroblasts. Although transient transfection of primary fibroblasts was not successful, it may be possible to generate stable cell lines from Artemis deficient cells that express each of the F96 mutant Artemis proteins. If this line was not homozygous for $p53_{Pro}$, then any contribution of the Artemis mutants to enhanced damage signalling could be examined more thoroughly than was possible here. These lines could also be used to determine if the expression of these mutants promotes the delayed arrest observed after irradiation, and what role the p53 codon 72 polymorphism may have in such delayed effects.

This thesis describes the discovery of 2 novel Artemis mutations in a patient with progressive immunodeficiency associated with increased apoptosis of lymphocytes and radiosensitivity of fibroblasts. Comparing fibroblasts from this patient to those from an Artemis null line allowed us to investigate what mechanisms may promote such phenotypes (figure 8-1). In Artemis null patients, the absent repair of complex DSBs in fibroblasts after irradiation leads to the early induction of premature senescence, whereas lymphocytes *in vivo* are not able to repair coding ends during V(D)J recombination and are removed by apoptosis. This leads to severe immunodeficiency and radiosensitivity of fibroblasts. In the F96 patient, partially functional Artemis proteins may allow the slow repair of complex breaks, possibly with reduced fidelity. Whilst this is sufficient to escape early premature senescence, this aberrant repair may promote instability in subsequent divisions and lead to delayed cell inactivation. Similarly in lymphocytes, coding ends induced during V(D)J recombination may be rejoined in an unstable manner that after subsequent division and development triggers apoptosis. At this point, other genetic factors that enhance damage signalling may contribute to the induction of apoptosis in lymphocytes and the delayed growth arrest of fibroblasts.

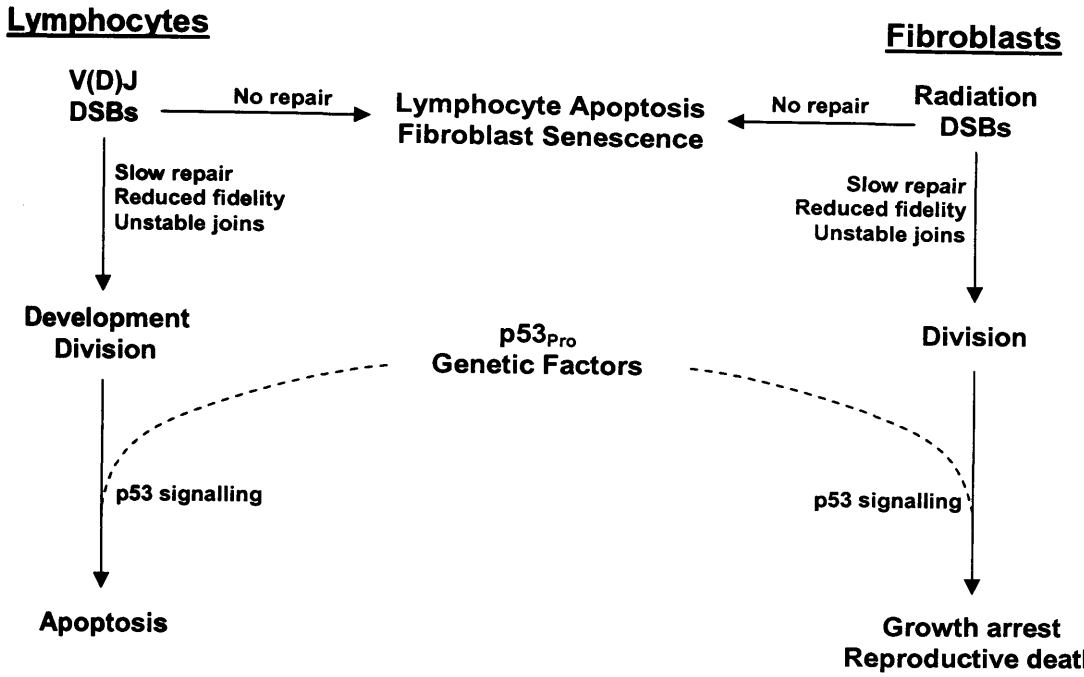

Figure 8-1: Mechanisms that may lead to distinct cell fates of lymphocytes *in vivo* and fibroblasts *in vitro* after DSB induction in Artemis deficient cells.

Further work is underway to evaluate the biochemical phenotype of the F96 mutant Artemis proteins described in this thesis using functional assays for nuclease activity. Each mutant protein will be expressed in Artemis null cells and the relative efficiency of DNA hairpin and overhang cutting will be compared to that in the same cells expressing wild type protein. This should determine to what extent these changes in Artemis primary structure affect nuclease function, and confirm if these changes do indeed represent the hypomorphic ("leaky") mutations suggested by the results presented here. Once confirmed, these mutant Artemis proteins will be a useful resource for exploring the link between ATM, the repair of DSB subsets and, given the enhanced p53 signalling observed in F96 cells, the possible effect of the repair complex on ATM mediated p53 activity, cell cycle arrest and apoptosis.

Appendix 1

7.3 Gene Lists CD

This CD contains 5 Gene lists identified in the microarray analysis section 7.3 and is attached to the inside of the back cover.

Lists are: -

51 Genes differently expressed between 1BR and F96 lines irrespective of irradiation (51F96v1BRnoIR)

74 Genes changed with irradiation in 1BR cells (74changed1BR1Gy)

144 Genes changed with irradiation in F96 cells (144changedF961Gy)

40 Genes upregulated with irradiation in 1BR cells (40up1BR1Gy)

80 Genes upregulated with irradiation in F96 cells (80upF961Gy)

Appendix 2

Summary table of results obtained for each cell line

Cell line	Lymphocyte apoptosis	Fibroblast survival	Early division	Late division	G1 Arrest	Chromo break	γ-H2AX	Sequencing	P53/p21
1BR		n	n	n	n	n	n	n	n
48BR		n					n	n	
GOS1	+	+				n	n		n
GOS2		n							
GOS3		+							
GOS4		+							
GOS5	+/n	++	++			n	n	n	n
GOS10		+							
GOS14	n	+				n			n
GOS15		n							
GOS16		n							
GOS17		+							
GOS18		n							
GOS19		n							
GOS20		n							
GOS21		+					n		
GOS22		n							
GOS23		++						n	
GOS25		n							
GOS26		n							
GOS27		n							
F96	*Spontaneous*	++	+	++	n	+	+	*Artemis*	*Elevated*
CJ179		++	++	+		+	++		n
AT1BR		+++	++	++	*Impaired*	++			*Impaired*

n = normal response, + = mild positive result, ++ = positive result, +++ strong positive result.

References

1. Abraham,R.T. (2001). Cell cycle checkpoint signaling through the ATM and ATR kinases. Genes Dev. *15*, 2177-2196.
2. Adachi,K., Toyota,M., Sasaki,Y., Yamashita,T., Ishida,S., Ohe-Toyota,M., Maruyama,R., Hinoda,Y., Saito,T., Imai,K., Kudo,R., and Tokino,T. (2004). Identification of SCN3B as a novel p53-inducible proapoptotic gene. Oncogene *23*, 7791-7798.
3. Adachi,N., Ishino,T., Ishii,Y., Takeda,S., and Koyama,H. (2001). DNA ligase IV-deficient cells are more resistant to ionizing radiation in the absence of Ku70: Implications for DNA double-strand break repair. Proc. Natl. Acad. Sci. U. S. A *98*, 12109-12113.
4. Aldrich,M.B., Blackburn,M.R., and Kellems,R.E. (2000). The importance of adenosine deaminase for lymphocyte development and function. Biochem. Biophys. Res. Commun. *272*, 311-315.
5. Andegeko,Y., Moyal,L., Mittelman,L., Tsarfaty,I., Shiloh,Y., and Rotman,G. (2001). Nuclear retention of ATM at sites of DNA double strand breaks. J. Biol. Chem. *276*, 38224-38230.
6. Anderson,L., Henderson,C., and Adachi,Y. (2001). Phosphorylation and rapid relocalization of 53BP1 to nuclear foci upon DNA damage. Mol. Cell Biol. *21*, 1719-1729.
7. Appella,E. and Anderson,C.W. (2001). Post-translational modifications and activation of p53 by genotoxic stresses. Eur. J. Biochem. *268*, 2764-2772.
8. Aravind,L. (1999). An evolutionary classification of the metallo-beta-lactamase fold proteins. In Silico. Biol. *1*, 69-91.
9. Arlett,C.F. and Priestley,A. (1983). Defective recovery from potentially lethal damage in some human fibroblast cell strains. Int. J. Radiat. Biol. Relat Stud. Phys. Chem. Med. *43*, 157-167.
10. Arlett,C.F., Green,M.H., Priestley,A., Harcourt,S.A., and Mayne,L.V. (1988). Comparative human cellular radiosensitivity: I. The effect of SV40 transformation and immortalisation on the gamma-irradiation survival of skin derived fibroblasts from normal individuals and from ataxia-telangiectasia patients and heterozygotes. Int. J. Radiat. Biol. *54*, 911-928.
11. Azzam,E.I., de Toledo,S.M., Waker,A.J., and Little,J.B. (2000). High and low fluences of alpha-particles induce a G1 checkpoint in human diploid fibroblasts. Cancer Res. *60*, 2623-2631.
12. Badie,C., Iliakis,G., Foray,N., Alsbeih,G., Cedervall,B., Chavaudra,N., Pantelias,G., Arlett,C., and Malaise,E.P. (1995a). Induction and rejoining of DNA double-strand breaks and interphase chromosome breaks after exposure to X rays in one normal and two hypersensitive human fibroblast cell lines. Radiat. Res. *144*, 26-35.
13. Badie,C., Iliakis,G., Foray,N., Alsbeih,G., Pantellias,G.E., Okayasu,R., Cheong,N., Russell,N.S., Begg,A.C., Arlett,C.F., and . (1995b). Defective repair of DNA double-strand breaks and chromosome damage in fibroblasts from a radiosensitive leukemia patient. Cancer Res. *55*, 1232-1234.
14. Badie,C., Goodhardt,M., Waugh,A., Doyen,N., Foray,N., Calsou,P., Singleton,B., Gell,D., Salles,B., Jeggo,P., Arlett,C.F., and Malaise,E.P. (1997). A DNA double-strand break defective fibroblast cell line (180BR) derived from a radiosensitive patient represents a new mutant phenotype. Cancer Res. *57*, 4600-4607.
15. Bakkenist,C.J. and Kastan,M.B. (2003). DNA damage activates ATM through intermolecular autophosphorylation and dimer dissociation. Nature *421*, 499-506.
16. Banin,S., Moyal,L., Shieh,S., Taya,Y., Anderson,C.W., Chessa,L., Smorodinsky,N.I., Prives,C., Reiss,Y., Shiloh,Y., and Ziv,Y. (1998). Enhanced phosphorylation of p53 by ATM in response to DNA damage. Science *281*, 1674-1677.
17. Barnes,D.E., Tomkinson,A.E., Lehmann,A.R., Webster,A.D., and Lindahl,T. (1992). Mutations in the DNA ligase I gene of an individual with immunodeficiencies and cellular hypersensitivity to DNA-damaging agents. Cell *69*, 495-503.
18. Barnes,D.E., Stamp,G., Rosewell,I., Denzel,A., and Lindahl,T. (1998). Targeted disruption of the gene encoding DNA ligase IV leads to lethality in embryonic mice. Curr. Biol. *8*, 1395-1398.
19. Bartek,J. and Lukas,J. (2001). Pathways governing G1/S transition and their response to DNA damage. FEBS Lett. *490*, 117-122.
20. Baskaran,R., Wood,L.D., Whitaker,L.L., Canman,C.E., Morgan,S.E., Xu,Y., Barlow,C., Baltimore,D., Wynshaw-Boris,A., Kastan,M.B., and Wang,J.Y. (1997). Ataxia telangiectasia mutant protein activates c-Abl tyrosine kinase in response to ionizing radiation. Nature *387*, 516-519.
21. Bassing,C.H., Swat,W., and Alt,F.W. (2002a). The mechanism and regulation of chromosomal V(D)J recombination. Cell *109 Suppl*, S45-S55.

22. Bassing,C.H., Chua,K.F., Sekiguchi,J., Suh,H., Whitlow,S.R., Fleming,J.C., Monroe,B.C., Ciccone,D.N., Yan,C., Vlasakova,K., Livingston,D.M., Ferguson,D.O., Scully,R., and Alt,F.W. (2002b). Increased ionizing radiation sensitivity and genomic instability in the absence of histone H2AX. Proc. Natl. Acad. Sci. U. S. A *99*, 8173-8178.
23. Bassing,C.H. and Alt,F.W. (2004). The cellular response to general and programmed DNA double strand breaks. DNA Repair (Amst) *3*, 781-796.
24. Baumann,P. and West,S.C. (1997). The human Rad51 protein: polarity of strand transfer and stimulation by hRP-A. EMBO J. *16*, 5198-5206.
25. Beamish,H. and Lavin,M.F. (1994). Radiosensitivity in ataxia-telangiectasia: anomalies in radiation-induced cell cycle delay. Int. J. Radiat. Biol. *65*, 175-184.
26. Beckman,G., Birgander,R., Sjalander,A., Saha,N., Holmberg,P.A., Kivela,A., and Beckman,L. (1994). Is p53 polymorphism maintained by natural selection? Hum. Hered. *44*, 266-270.
27. Belyakov,O.V., Prise,K.M., Trott,K.R., and Michael,B.D. (1999). Delayed lethality, apoptosis and micronucleus formation in human fibroblasts irradiated with X-rays or alpha-particles. Int. J. Radiat. Biol. *75*, 985-993.
28. Bennett,M., Macdonald,K., Chan,S.W., Luzio,J.P., Simari,R., and Weissberg,P. (1998). Cell surface trafficking of Fas: a rapid mechanism of p53-mediated apoptosis. Science *282*, 290-293.
29. Benson,F.E., Baumann,P., and West,S.C. (1998). Synergistic actions of Rad51 and Rad52 in recombination and DNA repair. Nature *391*, 401-404.
30. Bergamaschi,D., Samuels,Y., O'Neil,N.J., Trigiante,G., Crook,T., Hsieh,J.K., O'Connor,D.J., Zhong,S., Campargue,I., Tomlinson,M.L., Kuwabara,P.E., and Lu,X. (2003). iASPP oncoprotein is a key inhibitor of p53 conserved from worm to human. Nat. Genet. *33*, 162-167.
31. Bertocci,B., De Smet,A., Flatter,E., Dahan,A., Bories,J.C., Landreau,C., Weill,J.C., and Reynaud,C.A. (2002). Cutting edge: DNA polymerases mu and lambda are dispensable for Ig gene hypermutation. J. Immunol. *168*, 3702-3706.
32. Bertocci,B., De Smet,A., Berek,C., Weill,J.C., and Reynaud,C.A. (2003). Immunoglobulin kappa light chain gene rearrangement is impaired in mice deficient for DNA polymerase mu. Immunity. *19*, 203-211.
33. Block,W.D., Yu,Y., Merkle,D., Gifford,J.L., Ding,Q., Meek,K., and Lees-Miller,S.P. (2004). Autophosphorylation-dependent remodeling of the DNA-dependent protein kinase catalytic subunit regulates ligation of DNA ends. Nucleic Acids Res. *32*, 4351-4357.
34. Bochar,D.A., Wang,L., Beniya,H., Kinev,A., Xue,Y., Lane,W.S., Wang,W., Kashanchi,F., and Shiekhattar,R. (2000). BRCA1 is associated with a human SWI/SNF-related complex: linking chromatin remodeling to breast cancer. Cell *102*, 257-265.
35. Bogue,M.A., Jhappan,C., and Roth,D.B. (1998). Analysis of variable (diversity) joining recombination in DNAdependent protein kinase (DNA-PK)-deficient mice reveals DNA-PK-independent pathways for both signal and coding joint formation. Proc. Natl. Acad. Sci. U. S. A *95*, 15559-15564.
36. Borgmann,K. and Dikomey,E. (1997). Relationship between PCC fragments and cell killing studied in X-irradiated CHO, CHO-K1 cells and two radiosensitive mutants xrs1 and xrs5. Int. J. Radiat. Biol. *72*, 667-674.
37. Borgmann,K., Dede,M., Wrona,A., Brammer,I., Overgaard,J., and Dikomey,E. (2004). For X-irradiated normal human fibroblasts, only half of cell inactivation results from chromosomal damage. Int. J. Radiat. Oncol. Biol. Phys. *58*, 445-452.
38. Bosma,G.C., Kim,J., Urich,T., Fath,D.M., Cotticelli,M.G., Ruetsch,N.R., Radic,M.Z., and Bosma,M.J. (2002). DNA-dependent protein kinase activity is not required for immunoglobulin class switching. J. Exp. Med. *196*, 1483-1495.
39. Bourdon,J.C., Renzing,J., Robertson,P.L., Fernandes,K.N., and Lane,D.P. (2002). Scotin, a novel p53-inducible proapoptotic protein located in the ER and the nuclear membrane. J. Cell Biol. *158*, 235-246.
40. Boyle,J.M., Greaves,M.J., Camplejohn,R.S., Birch,J.M., Roberts,S.A., and Varley,J.M. (1999). Radiation-induced G1 arrest is not defective in fibroblasts from Li-Fraumeni families without TP53 mutations. Br. J. Cancer *79*, 1657-1664.
41. Brugarolas,J., Moberg,K., Boyd,S.D., Taya,Y., Jacks,T., and Lees,J.A. (1999). Inhibition of cyclin-dependent kinase 2 by p21 is necessary for retinoblastoma protein-mediated G1 arrest after gamma-irradiation. Proc. Natl. Acad. Sci. U. S. A *96*, 1002-1007.
42. Bryant,P.E., Gray,L.J., and Peresse,N. (2004). Progress towards understanding the nature of chromatid breakage. Cytogenet. Genome Res. *104*, 65-71.
43. Bryant,P.E. (2004). Repair and chromosomal damage. Radiother. Oncol. *72*, 251-256.
44. Buckbinder,L., Talbott,R., Velasco-Miguel,S., Takenaka,I., Faha,B., Seizinger,B.R., and Kley,N. (1995). Induction of the growth inhibitor IGF-binding protein 3 by p53. Nature *377*, 646-649.

45. Bulavin,D.V., Saito,S., Hollander,M.C., Sakaguchi,K., Anderson,C.W., Appella,E., and Fornace,A.J., Jr. (1999). Phosphorylation of human p53 by p38 kinase coordinates N-terminal phosphorylation and apoptosis in response to UV radiation. EMBO J. *18*, 6845-6854.
46. Bunz,F., Dutriaux,A., Lengauer,C., Waldman,T., Zhou,S., Brown,J.P., Sedivy,J.M., Kinzler,K.W., and Vogelstein,B. (1998). Requirement for p53 and p21 to sustain G2 arrest after DNA damage. Science *282*, 1497-1501.
47. Burma,S., Chen,B.P., Murphy,M., Kurimasa,A., and Chen,D.J. (2001). ATM phosphorylates histone H2AX in response to DNA double-strand breaks. J. Biol. Chem. *276*, 42462-42467.
48. Burns,T.F., Fei,P., Scata,K.A., Dicker,D.T., and El Deiry,W.S. (2003). Silencing of the novel p53 target gene Snk/Plk2 leads to mitotic catastrophe in paclitaxel (taxol)-exposed cells. Mol. Cell Biol. *23*, 5556-5571.
49. Buscemi,G., Perego,P., Carenini,N., Nakanishi,M., Chessa,L., Chen,J., Khanna,K., and Delia,D. (2004). Activation of ATM and Chk2 kinases in relation to the amount of DNA strand breaks. Oncogene *23*, 7691-7700.
50. Caelles,C., Helmberg,A., and Karin,M. (1994). p53-dependent apoptosis in the absence of transcriptional activation of p53-target genes. Nature *370*, 220-223.
51. Callebaut,I., Moshous,D., Mornon,J.P., and De Villartay,J.P. (2002). Metallo-beta-lactamase fold within nucleic acids processing enzymes: the beta-CASP family. Nucleic Acids Res. *30*, 3592-3601.
52. Camplejohn,R.S., Perry,P., Hodgson,S.V., Turner,G., Williams,A., Upton,C., MacGeoch,C., Mohammed,S., and Barnes,D.M. (1995). A possible screening test for inherited p53-related defects based on the apoptotic response of peripheral blood lymphocytes to DNA damage. Br. J. Cancer *72*, 654-662.
53. Canman,C.E., Lim,D.S., Cimprich,K.A., Taya,Y., Tamai,K., Sakaguchi,K., Appella,E., Kastan,M.B., and Siliciano,J.D. (1998). Activation of the ATM kinase by ionizing radiation and phosphorylation of p53. Science *281*, 1677-1679.
54. Cary,R.B., Peterson,S.R., Wang,J., Bear,D.G., Bradbury,E.M., and Chen,D.J. (1997). DNA looping by Ku and the DNA-dependent protein kinase. Proc. Natl. Acad. Sci. U. S. A *94*, 4267-4272.
55. Cavazzana-Calvo,M., Le Deist,F., De Saint,B.G., Papadopoulo,D., De Villartay,J.P., and Fischer,A. (1993). Increased radiosensitivity of granulocyte macrophage colony-forming units and skin fibroblasts in human autosomal recessive severe combined immunodeficiency. J. Clin. Invest *91*, 1214-1218.
56. Celeste,A., Petersen,S., Romanienko,P.J., Fernandez-Capetillo,O., Chen,H.T., Sedelnikova,O.A., Reina-San-Martin,B., Coppola,V., Meffre,E., Difilippantonio,M.J., Redon,C., Pilch,D.R., Olaru,A., Eckhaus,M., Camerini-Otero,R.D., Tessarollo,L., Livak,F., Manova,K., Bonner,W.M., Nussenzweig,M.C., and Nussenzweig,A. (2002). Genomic instability in mice lacking histone H2AX. Science *296*, 922-927.
57. Celeste,A., Fernandez-Capetillo,O., Kruhlak,M.J., Pilch,D.R., Staudt,D.W., Lee,A., Bonner,R.F., Bonner,W.M., and Nussenzweig,A. (2003). Histone H2AX phosphorylation is dispensable for the initial recognition of DNA breaks. Nat. Cell Biol. *5*, 675-679.
58. Cerosaletti,K. and Concannon,P. (2004). Independent roles for nibrin and Mre11/Rad50 in the activation and function of Atm. J. Biol. Chem. *279*, 38813-38819.
59. Chan,D.W. and Lees-Miller,S.P. (1996). The DNA-dependent protein kinase is inactivated by autophosphorylation of the catalytic subunit. J. Biol. Chem. *271*, 8936-8941.
60. Chan,T.A., Hermeking,H., Lengauer,C., Kinzler,K.W., and Vogelstein,B. (1999). 14-3-3Sigma is required to prevent mitotic catastrophe after DNA damage. Nature *401*, 616-620.
61. Chang,B.D., Xuan,Y., Broude,E.V., Zhu,H., Schott,B., Fang,J., and Roninson,I.B. (1999a). Role of p53 and p21waf1/cip1 in senescence-like terminal proliferation arrest induced in human tumor cells by chemotherapeutic drugs. Oncogene *18*, 4808-4818.
62. Chang,B.D., Broude,E.V., Dokmanovic,M., Zhu,H., Ruth,A., Xuan,Y., Kandel,E.S., Lausch,E., Christov,K., and Roninson,I.B. (1999b). A senescence-like phenotype distinguishes tumor cells that undergo terminal proliferation arrest after exposure to anticancer agents. Cancer Res. *59*, 3761-3767.
63. Chang,B.D., Broude,E.V., Fang,J., Kalinichenko,T.V., Abdryashitov,R., Poole,J.C., and Roninson,I.B. (2000). p21Waf1/Cip1/Sdi1-induced growth arrest is associated with depletion of mitosis-control proteins and leads to abnormal mitosis and endoreduplication in recovering cells. Oncogene *19*, 2165-2170.
64. Chang,B.D., Swift,M.E., Shen,M., Fang,J., Broude,E.V., and Roninson,I.B. (2002). Molecular determinants of terminal growth arrest induced in tumor cells by a chemotherapeutic agent. Proc. Natl. Acad. Sci. U. S. A *99*, 389-394.
65. Chang,W.P. and Little,J.B. (1991). Delayed reproductive death in X-irradiated Chinese hamster ovary cells. Int. J. Radiat. Biol. *60*, 483-496.

66. Chang,W.P. and Little,J.B. (1992). Evidence that DNA double-strand breaks initiate the phenotype of delayed reproductive death in Chinese hamster ovary cells. Radiat. Res. *131*, 53-59.
67. Chao,C., Hergenhahn,M., Kaeser,M.D., Wu,Z., Saito,S., Iggo,R., Hollstein,M., Appella,E., and Xu,Y. (2003). Cell type- and promoter-specific roles of Ser18 phosphorylation in regulating p53 responses. J. Biol. Chem. *278*, 41028-41033.
68. Chehab,N.H., Malikzay,A., Stavridi,E.S., and Halazonetis,T.D. (1999). Phosphorylation of Ser-20 mediates stabilization of human p53 in response to DNA damage. Proc. Natl. Acad. Sci. U. S. A *96*, 13777-13782.
69. Chehab,N.H., Malikzay,A., Appel,M., and Halazonetis,T.D. (2000). Chk2/hCds1 functions as a DNA damage checkpoint in G(1) by stabilizing p53. Genes Dev. *14*, 278-288.
70. Chen,C.F., Chen,P.L., Zhong,Q., Sharp,Z.D., and Lee,W.H. (1999a). Expression of BRC repeats in breast cancer cells disrupts the BRCA2-Rad51 complex and leads to radiation hypersensitivity and loss of G(2)/M checkpoint control. J. Biol. Chem. *274*, 32931-32935.
71. Chen,G., Yuan,S.S., Liu,W., Xu,Y., Trujillo,K., Song,B., Cong,F., Goff,S.P., Wu,Y., Arlinghaus,R., Baltimore,D., Gasser,P.J., Park,M.S., Sung,P., and Lee,E.Y. (1999b). Radiation-induced assembly of Rad51 and Rad52 recombination complex requires ATM and c-Abl. J. Biol. Chem. *274*, 12748-12752.
72. Chen,J., Silver,D.P., Walpita,D., Cantor,S.B., Gazdar,A.F., Tomlinson,G., Couch,F.J., Weber,B.L., Ashley,T., Livingston,D.M., and Scully,R. (1998). Stable interaction between the products of the BRCA1 and BRCA2 tumor suppressor genes in mitotic and meiotic cells. Mol. Cell *2*, 317-328.
73. Chen,L., Trujillo,K., Sung,P., and Tomkinson,A.E. (2000). Interactions of the DNA ligase IV-XRCC4 complex with DNA ends and the DNA-dependent protein kinase. J. Biol. Chem. *275*, 26196-26205.
74. Chen,M.S., Hurov,J., White,L.S., Woodford-Thomas,T., and Piwnica-Worms,H. (2001). Absence of apparent phenotype in mice lacking Cdc25C protein phosphatase. Mol. Cell Biol. *21*, 3853-3861.
75. Chen,X., Ko,L.J., Jayaraman,L., and Prives,C. (1996). p53 levels, functional domains, and DNA damage determine the extent of the apoptotic response of tumor cells. Genes Dev. *10*, 2438-2451.
76. Chung,D.H., Zhang,F., Chen,F., McLaughlin,W.P., and Ljungman,M. (1998). Butyrate attenuates BCLX(L) expression in human fibroblasts and acts in synergy with ionizing radiation to induce apoptosis. Radiat. Res. *149*, 187-194.
77. Cole,J., Arlett,C.F., Green,M.H., Harcourt,S.A., Priestley,A., Henderson,L., Cole,H., James,S.E., and Richmond,F. (1988). Comparative human cellular radiosensitivity: II. The survival following gamma-irradiation of unstimulated (G0) T-lymphocytes, T-lymphocyte lines, lymphoblastoid cell lines and fibroblasts from normal donors, from ataxia-telangiectasia patients and from ataxia-telangiectasia heterozygotes. Int. J. Radiat. Biol. *54*, 929-943.
78. Constantinou,A., Davies,A.A., and West,S.C. (2001). Branch migration and Holliday junction resolution catalyzed by activities from mammalian cells. Cell *104*, 259-268.
79. Cooke,M.S., Evans,M.D., Dizdaroglu,M., and Lunec,J. (2003). Oxidative DNA damage: mechanisms, mutation, and disease. FASEB J. *17*, 1195-1214.
80. Cornforth,M.N. and Bedford,J.S. (1985). On the nature of a defect in cells from individuals with ataxia-telangiectasia. Science *227*, 1589-1591.
81. Cornforth,M.N. and Bedford,J.S. (1987). A quantitative comparison of potentially lethal damage repair and the rejoining of interphase chromosome breaks in low passage normal human fibroblasts. Radiat. Res. *111*, 385-405.
82. Cornforth,M.N. and Goodwin,E.H. (1991). Transmission of radiation-induced acentric chromosomal fragments to micronuclei in normal human fibroblasts. Radiat. Res. *126*, 210-217.
83. Cortez,D., Wang,Y., Qin,J., and Elledge,S.J. (1999). Requirement of ATM-dependent phosphorylation of brca1 in the DNA damage response to double-strand breaks. Science *286*, 1162-1166.
84. Cox,M.M. (2002). The nonmutagenic repair of broken replication forks via recombination. Mutat. Res. *510*, 107-120.
85. Cox,R., Debenham,P.G., Masson,W.K., and Webb,M.B. (1986). Ataxia-telangiectasia: a human mutation giving high-frequency misrepair of DNA double-stranded scissions. Mol. Biol. Med. *3*, 229-244.
86. Critchlow,S.E., Bowater,R.P., and Jackson,S.P. (1997). Mammalian DNA double-strand break repair protein XRCC4 interacts with DNA ligase IV. Curr. Biol. *7*, 588-598.
87. Critchlow,S.E. and Jackson,S.P. (1998). DNA end-joining: from yeast to man. Trends Biochem. Sci. *23*, 394-398.
88. Crompton,N.E., Shi,Y.Q., Emery,G.C., Wisser,L., Blattmann,H., Maier,A., Li,L., Schindler,D., Ozsahin,H., and Ozsahin,M. (2001). Sources of variation in patient response to radiation treatment. Int. J. Radiat. Oncol. Biol. Phys. *49*, 547-554.

89. Dai,Y., Kysela,B., Hanakahi,L.A., Manolis,K., Riballo,E., Stumm,M., Harville,T.O., West,S.C., Oettinger,M.A., and Jeggo,P.A. (2003). Nonhomologous end joining and V(D)J recombination require an additional factor. Proc. Natl. Acad. Sci. U. S. A *100*, 2462-2467.
90. Davies,A.A., Masson,J.Y., McIlwraith,M.J., Stasiak,A.Z., Stasiak,A., Venkitaraman,A.R., and West,S.C. (2001). Role of BRCA2 in control of the RAD51 recombination and DNA repair protein. Mol. Cell *7*, 273-282.
91. de Stanchina,E., McCurrach,M.E., Zindy,F., Shieh,S.Y., Ferbeyre,G., Samuelson,A.V., Prives,C., Roussel,M.F., Sherr,C.J., and Lowe,S.W. (1998). E1A signaling to p53 involves the p19(ARF) tumor suppressor. Genes Dev. *12*, 2434-2442.
92. de Toledo,S.M., Azzam,E.I., Dahlberg,W.K., Gooding,T.B., and Little,J.B. (2000). ATM complexes with HDM2 and promotes its rapid phosphorylation in a p53-independent manner in normal and tumor human cells exposed to ionizing radiation. Oncogene *19*, 6185-6193.
93. de Vries,E., van Driel,W., Bergsma,W.G., Arnberg,A.C., and van der Vliet,P.C. (1989). HeLa nuclear protein recognizing DNA termini and translocating on DNA forming a regular DNA-multimeric protein complex. J. Mol. Biol. *208*, 65-78.
94. DeFazio,L.G., Stansel,R.M., Griffith,J.D., and Chu,G. (2002). Synapsis of DNA ends by DNA-dependent protein kinase. EMBO J. *21*, 3192-3200.
95. Delacote,F., Han,M., Stamato,T.D., Jasin,M., and Lopez,B.S. (2002). An xrcc4 defect or Wortmannin stimulates homologous recombination specifically induced by double-strand breaks in mammalian cells. Nucleic Acids Res. *30*, 3454-3463.
96. Delia,D., Piane,M., Buscemi,G., Savio,C., Palmeri,S., Lulli,P., Carlessi,L., Fontanella,E., and Chessa,L. (2004). MRE11 mutations and impaired ATM-dependent responses in an Italian family with ataxia-telangiectasia-like disorder. Hum. Mol. Genet. *13*, 2155-2163.
97. Deschavanne,P.J. and Fertil,B. (1996). A review of human cell radiosensitivity in vitro. Int. J. Radiat. Oncol. Biol. Phys. *34*, 251-266.
98. Di Leonardo,A., Linke,S.P., Clarkin,K., and Wahl,G.M. (1994). DNA damage triggers a prolonged p53-dependent G1 arrest and long-term induction of Cip1 in normal human fibroblasts. Genes Dev. *8*, 2540-2551.
99. Di Renzo,M., Serrano,D., Zhou,Z., George,I., Becker,K., and Cunningham-Rundles,C. (2001). Enhanced T cell apoptosis in common variable immunodeficiency: negative role of the fas/fasligand system and of the Bcl-2 family proteins and possible role of TNF-RS. Clin. Exp. Immunol. *125*, 117-122.
100. Difilippantonio,M.J., Zhu,J., Chen,H.T., Meffre,E., Nussenzweig,M.C., Max,E.E., Ried,T., and Nussenzweig,A. (2000). DNA repair protein Ku80 suppresses chromosomal aberrations and malignant transformation. Nature *404*, 510-514.
101. Dikomey,E., Dahm-Daphi,J., Brammer,I., Martensen,R., and Kaina,B. (1998). Correlation between cellular radiosensitivity and non-repaired double-strand breaks studied in nine mammalian cell lines. Int. J. Radiat. Biol. *73*, 269-278.
102. Dikomey,E. and Brammer,I. (2000a). Relationship between cellular radiosensitivity and non-repaired double-strand breaks studied for different growth states, dose rates and plating conditions in a normal human fibroblast line. Int. J. Radiat. Biol. *76*, 773-781.
103. Dikomey,E., Brammer,I., Johansen,J., Bentzen,S.M., and Overgaard,J. (2000b). Relationship between DNA double-strand breaks, cell killing, and fibrosis studied in confluent skin fibroblasts derived from breast cancer patients. Int. J. Radiat. Oncol. Biol. Phys. *46*, 481-490.
104. Dikomey,E., Borgmann,K., Brammer,I., and Kasten-Pisula,U. (2003). Molecular mechanisms of individual radiosensitivity studied in normal diploid human fibroblasts. Toxicology *193*, 125-135.
105. Ding,H.F., McGill,G., Rowan,S., Schmaltz,C., Shimamura,A., and Fisher,D.E. (1998). Oncogene-dependent regulation of caspase activation by p53 protein in a cell-free system. J. Biol. Chem. *273*, 28378-28383.
106. Ding,Q., Reddy,Y.V., Wang,W., Woods,T., Douglas,P., Ramsden,D.A., Lees-Miller,S.P., and Meek,K. (2003). Autophosphorylation of the catalytic subunit of the DNA-dependent protein kinase is required for efficient end processing during DNA double-strand break repair. Mol. Cell Biol. *23*, 5836-5848.
107. Dittmann,K., Virsik-Kopp,P., Mayer,C., Rave-Frank,M., and Rodemann,H.P. (2003). Bowman-Birk protease inhibitor activates DNA-dependent protein kinase and reduces formation of radiation-induced dicentric chromosomes. Int. J. Radiat. Biol. *79*, 801-808.
108. Donehower,L.A. and Bradley,A. (1993). The tumor suppressor p53. Biochim. Biophys. Acta *1155*, 181-205.
109. Dumaz,N. and Meek,D.W. (1999). Serine15 phosphorylation stimulates p53 transactivation but does not directly influence interaction with HDM2. EMBO J. *18*, 7002-7010.
110. Dumont,P., Leu,J.I., Della,P.A., III, George,D.L., and Murphy,M. (2003). The codon 72 polymorphic variants of p53 have markedly different apoptotic potential. Nat. Genet. *33*, 357-365.

111. Dynan,W.S. and Yoo,S. (1998). Interaction of Ku protein and DNA-dependent protein kinase catalytic subunit with nucleic acids. Nucleic Acids Res. *26*, 1551-1559.
112. Eggleston,A.K., Mitchell,A.H., and West,S.C. (1997). In vitro reconstitution of the late steps of genetic recombination in E. coli. Cell *89*, 607-617.
113. El Deiry,W.S., Tokino,T., Velculescu,V.E., Levy,D.B., Parsons,R., Trent,J.M., Lin,D., Mercer,W.E., Kinzler,K.W., and Vogelstein,B. (1993). WAF1, a potential mediator of p53 tumor suppression. Cell *75*, 817-825.
114. Elledge,S.J. (1996). Cell cycle checkpoints: preventing an identity crisis. Science *274*, 1664-1672.
115. Espinosa,J.M., Verdun,R.E., and Emerson,B.M. (2003). p53 functions through stress- and promoter-specific recruitment of transcription initiation components before and after DNA damage. Mol. Cell *12*, 1015-1027.
116. Estruch,E.J., Hart,S.L., Kinnon,C., and Winchester,B.G. (2001). Non-viral, integrin-mediated gene transfer into fibroblasts from patients with lysosomal storage diseases. J. Gene Med. *3*, 488-497.
117. Evans,J.W., Liu,X.F., Kirchgessner,C.U., and Brown,J.M. (1996). Induction and repair of chromosome aberrations in scid cells measured by premature chromosome condensation. Radiat. Res. *145*, 39-46.
118. Fabbro,M., Savage,K., Hobson,K., Deans,A.J., Powell,S.N., McArthur,G.A., and Khanna,K.K. (2004). BRCA1-BARD1 complexes are required for p53Ser-15 phosphorylation and a G1/S arrest following ionizing radiation-induced DNA damage. J. Biol. Chem. *279*, 31251-31258.
119. Falck,J., Petrini,J.H., Williams,B.R., Lukas,J., and Bartek,J. (2002). The DNA damage-dependent intra-S phase checkpoint is regulated by parallel pathways. Nat. Genet. *30*, 290-294.
120. Falzon,M., Fewell,J.W., and Kuff,E.L. (1993). EBP-80, a transcription factor closely resembling the human autoantigen Ku, recognizes single- to double-strand transitions in DNA. J. Biol. Chem. *268*, 10546-10552.
121. Fang,L., Li,G., Liu,G., Lee,S.W., and Aaronson,S.A. (2001). p53 induction of heparin-binding EGF-like growth factor counteracts p53 growth suppression through activation of MAPK and PI3K/Akt signaling cascades. EMBO J. *20*, 1931-1939.
122. Ferguson,D.O., Sekiguchi,J.M., Chang,S., Frank,K.M., Gao,Y., DePinho,R.A., and Alt,F.W. (2000). The nonhomologous end-joining pathway of DNA repair is required for genomic stability and the suppression of translocations. Proc. Natl. Acad. Sci. U. S. A *97*, 6630-6633.
123. Ferguson,D.O. and Alt,F.W. (2001). DNA double strand break repair and chromosomal translocation: lessons from animal models. Oncogene *20*, 5572-5579.
124. Fernandez-Capetillo,O., Chen,H.T., Celeste,A., Ward,I., Romanienko,P.J., Morales,J.C., Naka,K., Xia,Z., Camerini-Otero,R.D., Motoyama,N., Carpenter,P.B., Bonner,W.M., Chen,J., and Nussenzweig,A. (2002). DNA damage-induced G2-M checkpoint activation by histone H2AX and 53BP1. Nat. Cell Biol. *4*, 993-997.
125. Flores,E.R., Tsai,K.Y., Crowley,D., Sengupta,S., Yang,A., McKeon,F., and Jacks,T. (2002). p63 and p73 are required for p53-dependent apoptosis in response to DNA damage. Nature *416*, 560-564.
126. Foray,N., Arlett,C.F., and Malaise,E.P. (1995). Dose-rate effect on induction and repair rate of radiation-induced DNA double-strand breaks in a normal and an ataxia telangiectasia human fibroblast cell line. Biochimie *77*, 900-905.
127. Foray,N., Priestley,A., Alsbeih,G., Badie,C., Capulas,E.P., Arlett,C.F., and Malaise,E.P. (1997). Hypersensitivity of ataxia telangiectasia fibroblasts to ionizing radiation is associated with a repair deficiency of DNA double-strand breaks. Int. J. Radiat. Biol. *72*, 271-283.
128. Foray,N., Marot,D., Gabriel,A., Randrianarison,V., Carr,A.M., Perricaudet,M., Ashworth,A., and Jeggo,P. (2003). A subset of ATM- and ATR-dependent phosphorylation events requires the BRCA1 protein. EMBO J. *22*, 2860-2871.
129. Fournier,C., Wiese,C., and Taucher-Scholz,G. (2004). Accumulation of the cell cycle regulators TP53 and CDKN1A (p21) in human fibroblasts after exposure to low- and high-LET radiation. Radiat. Res. *161*, 675-684.
130. Frank,K.M., Sharpless,N.E., Gao,Y., Sekiguchi,J.M., Ferguson,D.O., Zhu,C., Manis,J.P., Horner,J., DePinho,R.A., and Alt,F.W. (2000). DNA ligase IV deficiency in mice leads to defective neurogenesis and embryonic lethality via the p53 pathway. Mol. Cell *5*, 993-1002.
131. Freiberg,R.A., Spencer,D.M., Choate,K.A., Duh,H.J., Schreiber,S.L., Crabtree,G.R., and Khavari,P.A. (1997). Fas signal transduction triggers either proliferation or apoptosis in human fibroblasts. J. Invest Dermatol. *108*, 215-219.
132. Fugmann,S.D., Lee,A.I., Shockett,P.E., Villey,I.J., and Schatz,D.G. (2000). The RAG proteins and V(D)J recombination: complexes, ends, and transposition. Annu. Rev. Immunol. *18*, 495-527.
133. Fukumura,R., Araki,R., Fujimori,A., Tsutsumi,Y., Kurimasa,A., Li,G.C., Chen,D.J., Tatsumi,K., and Abe,M. (2000). Signal joint formation is also impaired in DNA-dependent protein kinase catalytic subunit knockout cells. J. Immunol. *165*, 3883-3889.

134. Fukushima,T., Takata,M., Morrison,C., Araki,R., Fujimori,A., Abe,M., Tatsumi,K., Jasin,M., Dhar,P.K., Sonoda,E., Chiba,T., and Takeda,S. (2001). Genetic analysis of the DNA-dependent protein kinase reveals an inhibitory role of Ku in late S-G2 phase DNA double-strand break repair. J. Biol. Chem. *276*, 44413-44418.
135. Gao,Y., Chaudhuri,J., Zhu,C., Davidson,L., Weaver,D.T., and Alt,F.W. (1998). A targeted DNA-PKcs-null mutation reveals DNA-PK-independent functions for KU in V(D)J recombination. Immunity. *9*, 367-376.
136. Gatei,M., Scott,S.P., Filippovitch,I., Soronika,N., Lavin,M.F., Weber,B., and Khanna,K.K. (2000). Role for ATM in DNA damage-induced phosphorylation of BRCA1. Cancer Res. *60*, 3299-3304.
137. Gatei,M., Sloper,K., Sorensen,C., Syljuasen,R., Falck,J., Hobson,K., Savage,K., Lukas,J., Zhou,B.B., Bartek,J., and Khanna,K.K. (2003). Ataxia-telangiectasia-mutated (ATM) and NBS1-dependent phosphorylation of Chk1 on Ser-317 in response to ionizing radiation. J. Biol. Chem. *278*, 14806-14811.
138. Geara,F.B., Peters,L.J., Ang,K.K., Wike,J.L., Sivon,S.S., Guttenberger,R., Callender,D.L., Malaise,E.P., and Brock,W.A. (1992). Intrinsic radiosensitivity of normal human fibroblasts and lymphocytes after high- and low-dose-rate irradiation. Cancer Res. *52*, 6348-6352.
139. Gellert,M. (2002). V(D)J recombination: RAG proteins, repair factors, and regulation. Annu. Rev. Biochem. *71*, 101-132.
140. Giblett,E.R., Anderson,J.E., Cohen,F., Pollara,B., and Meuwissen,H.J. (1972). Adenosine-deaminase deficiency in two patients with severely impaired cellular immunity. Lancet *2*, 1067-1069.
141. Girard,P.M., Foray,N., Stumm,M., Waugh,A., Riballo,E., Maser,R.S., Phillips,W.P., Petrini,J., Arlett,C.F., and Jeggo,P.A. (2000). Radiosensitivity in Nijmegen Breakage Syndrome cells is attributable to a repair defect and not cell cycle checkpoint defects. Cancer Res. *60*, 4881-4888.
142. Girard,P.M., Riballo,E., Begg,A.C., Waugh,A., and Jeggo,P.A. (2002). Nbs1 promotes ATM dependent phosphorylation events including those required for G1/S arrest. Oncogene *21*, 4191-4199.
143. Girard,P.M., Kysela,B., Harer,C.J., Doherty,A.J., and Jeggo,P.A. (2004). Analysis of DNA ligase IV mutations found in LIG4 syndrome patients: the impact of two linked polymorphisms. Hum. Mol. Genet. *13*, 2369-2376.
144. Goldberg,M., Stucki,M., Falck,J., D'Amours,D., Rahman,D., Pappin,D., Bartek,J., and Jackson,S.P. (2003). MDC1 is required for the intra-S-phase DNA damage checkpoint. Nature *421*, 952-956.
145. Golding,S.E., Rosenberg,E., Khalil,A., McEwen,A., Holmes,M., Neill,S., Povirk,L.F., and Valerie,K. (2004). Double strand break repair by homologous recombination is regulated by cell cycle-independent signaling via ATM in human glioma cells. J. Biol. Chem. *279*, 15402-15410.
146. Gorbunova,V., Seluanov,A., and Pereira-Smith,O.M. (2003). Evidence that high telomerase activity may induce a senescent-like growth arrest in human fibroblasts. J. Biol. Chem. *278*, 7692-7698.
147. Gottlieb,T.M. and Oren,M. (1996). p53 in growth control and neoplasia. Biochim. Biophys. Acta *1287*, 77-102.
148. Gottlieb,T.M., Leal,J.F., Seger,R., Taya,Y., and Oren,M. (2002). Cross-talk between Akt, p53 and Mdm2: possible implications for the regulation of apoptosis. Oncogene *21*, 1299-1303.
149. Grawunder,U., Wilm,M., Wu,X., Kulesza,P., Wilson,T.E., Mann,M., and Lieber,M.R. (1997). Activity of DNA ligase IV stimulated by complex formation with XRCC4 protein in mammalian cells. Nature *388*, 492-495.
150. Grawunder,U., Zimmer,D., Kulesza,P., and Lieber,M.R. (1998). Requirement for an interaction of XRCC4 with DNA ligase IV for wild-type V(D)J recombination and DNA double-strand break repair in vivo. J. Biol. Chem. *273*, 24708-24714.
151. Gudkov,A.V. and Komarova,E.A. (2003). The role of p53 in determining sensitivity to radiotherapy. Nat. Rev. Cancer *3*, 117-129.
152. Guidos,C.J., Williams,C.J., Grandal,I., Knowles,G., Huang,M.T., and Danska,J.S. (1996). V(D)J recombination activates a p53-dependent DNA damage checkpoint in scid lymphocyte precursors. Genes Dev. *10*, 2038-2054.
153. Guo,Z., Kumagai,A., Wang,S.X., and Dunphy,W.G. (2000). Requirement for Atr in phosphorylation of Chk1 and cell cycle regulation in response to DNA replication blocks and UV-damaged DNA in Xenopus egg extracts. Genes Dev. *14*, 2745-2756.
154. Ha,L., Ceryak,S., and Patierno,S.R. (2003). Chromium (VI) activates ataxia telangiectasia mutated (ATM) protein. Requirement of ATM for both apoptosis and recovery from terminal growth arrest. J. Biol. Chem. *278*, 17885-17894.
155. Haber,J.E. (1999). DNA recombination: the replication connection. Trends Biochem. Sci. *24*, 271-275.

156. Hammarsten,O., DeFazio,L.G., and Chu,G. (2000). Activation of DNA-dependent protein kinase by single-stranded DNA ends. J. Biol. Chem. *275*, 1541-1550.
157. Han,J.A., Kim,J.I., Ongusaha,P.P., Hwang,D.H., Ballou,L.R., Mahale,A., Aaronson,S.A., and Lee,S.W. (2002). P53-mediated induction of Cox-2 counteracts p53- or genotoxic stress-induced apoptosis. EMBO J. *21*, 5635-5644.
158. Harper,J.W., Adami,G.R., Wei,N., Keyomarsi,K., and Elledge,S.J. (1993). The p21 Cdk-interacting protein Cip1 is a potent inhibitor of G1 cyclin-dependent kinases. Cell *75*, 805-816.
159. Harris,N., Brill,E., Shohat,O., Prokocimer,M., Wolf,D., Arai,N., and Rotter,V. (1986). Molecular basis for heterogeneity of the human p53 protein. Mol. Cell Biol. *6*, 4650-4656.
160. Hartley,K.O., Gell,D., Smith,G.C., Zhang,H., Divecha,N., Connelly,M.A., Admon,A., Lees-Miller,S.P., Anderson,C.W., and Jackson,S.P. (1995). DNA-dependent protein kinase catalytic subunit: a relative of phosphatidylinositol 3-kinase and the ataxia telangiectasia gene product. Cell *82*, 849-856.
161. Hekmat-Nejad,M., You,Z., Yee,M.C., Newport,J.W., and Cimprich,K.A. (2000). Xenopus ATR is a replication-dependent chromatin-binding protein required for the DNA replication checkpoint. Curr. Biol. *10*, 1565-1573.
162. Hellborg,F., Qian,W., Mendez-Vidal,C., Asker,C., Kost-Alimova,M., Wilhelm,M., Imreh,S., and Wiman,K.G. (2001). Human wig-1, a p53 target gene that encodes a growth inhibitory zinc finger protein. Oncogene *20*, 5466-5474.
163. Hertveldt,K., Philippe,J., Thierens,H., Cornelissen,M., Vral,A., and De Ridder,L. (1997). Flow cytometry as a quantitative and sensitive method to evaluate low dose radiation induced apoptosis in vitro in human peripheral blood lymphocytes. Int. J. Radiat. Biol. *71*, 429-433.
164. Hilleren,P. and Parker,R. (1999). Mechanisms of mRNA surveillance in eukaryotes. Annu. Rev. Genet. *33*, 229-260.
165. Hofseth,L.J., Hussain,S.P., and Harris,C.C. (2004). p53: 25 years after its discovery. Trends Pharmacol. Sci. *25*, 177-181.
166. Horejsi,Z., Falck,J., Bakkenist,C.J., Kastan,M.B., Lukas,J., and Bartek,J. (2004). Distinct functional domains of Nbs1 modulate the timing and magnitude of ATM activation after low doses of ionizing radiation. Oncogene *23*, 3122-3127.
167. Houldsworth,J. and Lavin,M.F. (1980). Effect of ionizing radiation on DNA synthesis in ataxia telangiectasia cells. Nucleic Acids Res. *8*, 3709-3720.
168. Hsieh,C.L., Arlett,C.F., and Lieber,M.R. (1993). V(D)J recombination in ataxia telangiectasia, Bloom's syndrome, and a DNA ligase I-associated immunodeficiency disorder. J. Biol. Chem. *268*, 20105-20109.
169. Inserra,P., Abrahamsen,M., Papenfuss,M., and Giuliano,A.R. (2003). Ethnic variation of the P53 codon 72 polymorphism, HPV persistence, and cervical cancer risk. Int. J. STD AIDS *14*, 800-804.
170. Insinga,A., Monestiroli,S., Ronzoni,S., Carbone,R., Pearson,M., Pruneri,G., Viale,G., Appella,E., Pelicci,P., and Minucci,S. (2004). Impairment of p53 acetylation, stability and function by an oncogenic transcription factor. EMBO J. *23*, 1144-1154.
171. Ito,A., Lai,C.H., Zhao,X., Saito,S., Hamilton,M.H., Appella,E., and Yao,T.P. (2001). p300/CBP-mediated p53 acetylation is commonly induced by p53-activating agents and inhibited by MDM2. EMBO J. *20*, 1331-1340.
172. Jackson,S.P. (2001). Detecting, signalling and repairing DNA double-strand breaks. Biochem. Soc. Trans. *29*, 655-661.
173. Jeggo,P. and O'Neill,P. (2002). The Greek Goddess, Artemis, reveals the secrets of her cleavage. DNA Repair (Amst) *1*, 771-777.
174. Jeggo,P.A. and Concannon,P. (2001). Immune diversity and genomic stability: opposite goals but similar paths. J. Photochem. Photobiol. B *65*, 88-96.
175. Jenner,T.J., deLara,C.M., O'Neill,P., and Stevens,D.L. (1993). Induction and rejoining of DNA double-strand breaks in V79-4 mammalian cells following gamma- and alpha-irradiation. Int. J. Radiat. Biol. *64*, 265-273.
176. Jeremias,I., Herr,I., Boehler,T., and Debatin,K.M. (1998). TRAIL/Apo-2-ligand-induced apoptosis in human T cells. Eur. J. Immunol. *28*, 143-152.
177. Jhappan,C., Yusufzai,T.M., Anderson,S., Anver,M.R., and Merlino,G. (2000). The p53 response to DNA damage in vivo is independent of DNA-dependent protein kinase. Mol. Cell Biol. *20*, 4075-4083.
178. Jin,S., Tong,T., Fan,W., Fan,F., Antinore,M.J., Zhu,X., Mazzacurati,L., Li,X., Petrik,K.L., Rajasekaran,B., Wu,M., and Zhan,Q. (2002). GADD45-induced cell cycle G2-M arrest associates with altered subcellular distribution of cyclin B1 and is independent of p38 kinase activity. Oncogene *21*, 8696-8704.
179. Jin,S., Kalkum,M., Overholtzer,M., Stoffel,A., Chait,B.T., and Levine,A.J. (2003). CIAP1 and the serine protease HTRA2 are involved in a novel p53-dependent apoptosis pathway in mammals. Genes Dev. *17*, 359-367.

180. Johnson,R.D. and Jasin,M. (2000). Sister chromatid gene conversion is a prominent double-strand break repair pathway in mammalian cells. EMBO J. *19*, 3398-3407.
181. Jones,J.M. and Gellert,M. (2001). Intermediates in V(D)J recombination: a stable RAG1/2 complex sequesters cleaved RSS ends. Proc. Natl. Acad. Sci. U. S. A *98*, 12926-12931.
182. Jongmans,W., Vuillaume,M., Chrzanowska,K., Smeets,D., Sperling,K., and Hall,J. (1997). Nijmegen breakage syndrome cells fail to induce the p53-mediated DNA damage response following exposure to ionizing radiation. Mol. Cell Biol. *17*, 5016-5022.
183. Jorgensen,T.J. and Shiloh,Y. (1996). The ATM gene and the radiobiology of ataxia-telangiectasia. Int. J. Radiat. Biol. *69*, 527-537.
184. Joshi,G.P., Nelson,W.J., Revell,S.H., and Shaw,C.A. (1982a). Discrimination of slow growth from non-survival among small colonies of diploid Syrian hamster cells after chromosome damage induced by a range of x-ray doses. Int. J. Radiat. Biol. Relat Stud. Phys. Chem. Med. *42*, 283-296.
185. Joshi,G.P., Nelson,W.J., Revell,S.H., and Shaw,C.A. (1982b). Division probability and division delay in diploid Syrian hamster cells following a range of x-ray doses. Int. J. Radiat. Biol. Relat Stud. Phys. Chem. Med. *41*, 443-448.
186. Joshi,G.P., Nelson,W.J., Revell,S.H., and Shaw,C.A. (1982c). X-ray-induced chromosome damage in live mammalian cells, and improved measurements of its effects on their colony-forming ability. Int. J. Radiat. Biol. Relat Stud. Phys. Chem. Med. *41*, 161-181.
187. Kaeser,M.D. and Iggo,R.D. (2002). Chromatin immunoprecipitation analysis fails to support the latency model for regulation of p53 DNA binding activity in vivo. Proc. Natl. Acad. Sci. U. S. A *99*, 95-100.
188. Kastan,M.B., Onyekwere,O., Sidransky,D., Vogelstein,B., and Craig,R.W. (1991). Participation of p53 protein in the cellular response to DNA damage. Cancer Res. *51*, 6304-6311.
189. Kastan,M.B., Zhan,Q., El Deiry,W.S., Carrier,F., Jacks,T., Walsh,W.V., Plunkett,B.S., Vogelstein,B., and Fornace,A.J., Jr. (1992). A mammalian cell cycle checkpoint pathway utilizing p53 and GADD45 is defective in ataxia-telangiectasia. Cell *71*, 587-597.
190. Kawabe,S., Munshi,A., Zumstein,L.A., Wilson,D.R., Roth,J.A., and Meyn,R.E. (2001). Adenovirus-mediated wild-type p53 gene expression radiosensitizes non-small cell lung cancer cells but not normal lung fibroblasts. Int. J. Radiat. Biol. *77*, 185-194.
191. Kawata,T., Ito,H., George,K., Wu,H., Uno,T., Isobe,K., and Cucinotta,F.A. (2003). Radiation-induced chromosome aberrations in ataxia telangiectasia cells: high frequency of deletions and misrejoining detected by fluorescence in situ hybridization. Radiat. Res. *159*, 597-603.
192. Keeney,S. (2001). Mechanism and control of meiotic recombination initiation. Curr. Top. Dev. Biol. *52*, 1-53.
193. Khan,S., Guevara,C., Fujii,G., and Parry,D. (2004). p14ARF is a component of the p53 response following ionizing irradiation of normal human fibroblasts. Oncogene.
194. Khan,S.H., Moritsugu,J., and Wahl,G.M. (2000). Differential requirement for p19ARF in the p53-dependent arrest induced by DNA damage, microtubule disruption, and ribonucleotide depletion. Proc. Natl. Acad. Sci. U. S. A *97*, 3266-3271.
195. Khanna,K.K., Beamish,H., Yan,J., Hobson,K., Williams,R., Dunn,I., and Lavin,M.F. (1995). Nature of G1/S cell cycle checkpoint defect in ataxia-telangiectasia. Oncogene *11*, 609-618.
196. Khanna,K.K., Keating,K.E., Kozlov,S., Scott,S., Gatei,M., Hobson,K., Taya,Y., Gabrielli,B., Chan,D., Lees-Miller,S.P., and Lavin,M.F. (1998). ATM associates with and phosphorylates p53: mapping the region of interaction. Nat. Genet. *20*, 398-400.
197. Khanna,K.K. and Jackson,S.P. (2001). DNA double-strand breaks: signaling, repair and the cancer connection. Nat. Genet. *27*, 247-254.
198. Khosravi,R., Maya,R., Gottlieb,T., Oren,M., Shiloh,Y., and Shkedy,D. (1999). Rapid ATM-dependent phosphorylation of MDM2 precedes p53 accumulation in response to DNA damage. Proc. Natl. Acad. Sci. U. S. A *96*, 14973-14977.
199. Kiltie,A.E., Orton,C.J., Ryan,A.J., Roberts,S.A., Marples,B., Davidson,S.E., Hunter,R.D., Margison,G.P., West,C.M., and Hendry,J.H. (1997). A correlation between residual DNA double-strand breaks and clonogenic measurements of radiosensitivity in fibroblasts from preradiotherapy cervix cancer patients. Int. J. Radiat. Oncol. Biol. Phys. *39*, 1137-1144.
200. Kimura,H., Minakami,H., and Shoji,A. (2001). Ultraviolet B irradiation modulates susceptibility to tumour necrosis factor-alpha-induced apoptosis via induction of death receptors in murine fibroblasts. Cell Biol. Int. *25*, 1221-1228.
201. Ko,L.J. and Prives,C. (1996). p53: puzzle and paradigm. Genes Dev. *10*, 1054-1072.
202. Kobayashi,J., Tauchi,H., Sakamoto,S., Nakamura,A., Morishima,K., Matsuura,S., Kobayashi,T., Tamai,K., Tanimoto,K., and Komatsu,K. (2002). NBS1 localizes to gamma-H2AX foci through interaction with the FHA/BRCT domain. Curr. Biol. *12*, 1846-1851.

203. Kobayashi,N., Agematsu,K., Sugita,K., Sako,M., Nonoyama,S., Yachie,A., Kumaki,S., Tsuchiya,S., Ochs,H.D., Sugita,K., Fukushima,Y., and Komiyama,A. (2003). Novel Artemis gene mutations of radiosensitive severe combined immunodeficiency in Japanese families. Hum. Genet. *112*, 348-352.
204. Kraakman-van der Zwet,M., Overkamp,W.J., Friedl,A.A., Klein,B., Verhaegh,G.W., Jaspers,N.G., Midro,A.T., Eckardt-Schupp,F., Lohman,P.H., and Zdzienicka,M.Z. (1999). Immortalization and characterization of Nijmegen Breakage syndrome fibroblasts. Mutat. Res. *434*, 17-27.
205. Krejci,L., Chen,L., Van Komen,S., Sung,P., and Tomkinson,A. (2003). Mending the break: two DNA double-strand break repair machines in eukaryotes. Prog. Nucleic Acid Res. Mol. Biol. *74*, 159-201.
206. Kuerbitz,S.J., Plunkett,B.S., Walsh,W.V., and Kastan,M.B. (1992). Wild-type p53 is a cell cycle checkpoint determinant following irradiation. Proc. Natl. Acad. Sci. U. S. A *89*, 7491-7495.
207. Kuhne,M., Riballo,E., Rief,N., Rothkamm,K., Jeggo,P.A., and Lobrich,M. (2004). A double-strand break repair defect in ATM-deficient cells contributes to radiosensitivity. Cancer Res. *64*, 500-508.
208. Kysela,B., Doherty,A.J., Chovanec,M., Stiff,T., Ameer-Beg,S.M., Vojnovic,B., Girard,P.M., and Jeggo,P.A. (2003). Ku stimulation of DNA ligase IV-dependent ligation requires inward movement along the DNA molecule. J. Biol. Chem. *278*, 22466-22474.
209. Lahdesmaki,A., Taylor,A.M., Chrzanowska,K.H., and Pan-Hammarstrom,Q. (2004). Delineation of the role of the Mre11 complex in class switch recombination. J. Biol. Chem. *279*, 16479-16487.
210. Lambert,P.F., Kashanchi,F., Radonovich,M.F., Shiekhattar,R., and Brady,J.N. (1998). Phosphorylation of p53 serine 15 increases interaction with CBP. J. Biol. Chem. *273*, 33048-33053.
211. Lara,P.C., Russell,N.S., Smolders,I.J., Bartelink,H., Begg,A.C., and Coco-Martin,J.M. (1996). Radiation-induced differentiation of human skin fibroblasts: relationship with cell survival and collagen production. Int. J. Radiat. Biol. *70*, 683-692.
212. Le Deist,F., Poinsignon,C., Moshous,D., Fischer,A., and De Villartay,J.P. (2004). Artemis sheds new light on V(D)J recombination. Immunol. Rev. *200*, 142-155.
213. Leber,R., Wise,T.W., Mizuta,R., and Meek,K. (1998). The XRCC4 gene product is a target for and interacts with the DNA-dependent protein kinase. J. Biol. Chem. *273*, 1794-1801.
214. Lee,J. and Desiderio,S. (1999). Cyclin A/CDK2 regulates V(D)J recombination by coordinating RAG-2 accumulation and DNA repair. Immunity. *11*, 771-781.
215. Lee,J.H. and Paull,T.T. (2004a). Direct activation of the ATM protein kinase by the Mre11/Rad50/Nbs1 complex. Science *304*, 93-96.
216. Lee,J.W., Blanco,L., Zhou,T., Garcia-Diaz,M., Bebenek,K., Kunkel,T.A., Wang,Z., and Povirk,L.F. (2004b). Implication of DNA polymerase lambda in alignment-based gap filling for nonhomologous DNA end joining in human nuclear extracts. J. Biol. Chem. *279*, 805-811.
217. Lee,S.E., Moore,J.K., Holmes,A., Umezu,K., Kolodner,R.D., and Haber,J.E. (1998a). Saccharomyces Ku70, mre11/rad50 and RPA proteins regulate adaptation to G2/M arrest after DNA damage. Cell *94*, 399-409.
218. Lee,S.J., Dimtchev,A., Lavin,M.F., Dritschilo,A., and Jung,M. (1998b). A novel ionizing radiation-induced signaling pathway that activates the transcription factor NF-kappaB. Oncogene *17*, 1821-1826.
219. Leu,J.I., Dumont,P., Hafey,M., Murphy,M.E., and George,D.L. (2004). Mitochondrial p53 activates Bak and causes disruption of a Bak-Mcl1 complex. Nat. Cell Biol. *6*, 443-450.
220. Li,L., Drayna,D., Hu,D., Hayward,A., Gahagan,S., Pabst,H., and Cowan,M.J. (1998). The gene for severe combined immunodeficiency disease in Athabascan-speaking Native Americans is located on chromosome 10p. Am. J. Hum. Genet. *62*, 136-144.
221. Li,L., Moshous,D., Zhou,Y., Wang,J., Xie,G., Salido,E., Hu,D., De Villartay,J.P., and Cowan,M.J. (2002a). A founder mutation in Artemis, an SNM1-like protein, causes SCID in Athabascan-speaking Native Americans. J. Immunol. *168*, 6323-6329.
222. Li,M., Luo,J., Brooks,C.L., and Gu,W. (2002b). Acetylation of p53 inhibits its ubiquitination by Mdm2. J. Biol. Chem. *277*, 50607-50611.
223. Li,Z., Otevrel,T., Gao,Y., Cheng,H.L., Seed,B., Stamato,T.D., Taccioli,G.E., and Alt,F.W. (1995). The XRCC4 gene encodes a novel protein involved in DNA double-strand break repair and V(D)J recombination. Cell *83*, 1079-1089.
224. Lieber,M.R. (1999). The biochemistry and biological significance of nonhomologous DNA end joining: an essential repair process in multicellular eukaryotes. Genes Cells *4*, 77-85.
225. Lieber,M.R., Ma,Y., Pannicke,U., and Schwarz,K. (2003). Mechanism and regulation of human non-homologous DNA end-joining. Nat. Rev. Mol. Cell Biol. *4*, 712-720.
226. Lieber,M.R., Ma,Y., Pannicke,U., and Schwarz,K. (2004). The mechanism of vertebrate nonhomologous DNA end joining and its role in V(D)J recombination. DNA Repair (Amst) *3*, 817-826.

227. Lim,D.S., Kim,S.T., Xu,B., Maser,R.S., Lin,J., Petrini,J.H., and Kastan,M.B. (2000). ATM phosphorylates p95/nbs1 in an S-phase checkpoint pathway. Nature *404*, 613-617.
228. Lin,W.C., Lin,F.T., and Nevins,J.R. (2001). Selective induction of E2F1 in response to DNA damage, mediated by ATM-dependent phosphorylation. Genes Dev. *15*, 1833-1844.
229. Lin,Y., Ma,W., and Benchimol,S. (2000). Pidd, a new death-domain-containing protein, is induced by p53 and promotes apoptosis. Nat. Genet. *26*, 122-127.
230. Linke,S.P., Clarkin,K.C., and Wahl,G.M. (1997). p53 mediates permanent arrest over multiple cell cycles in response to gamma-irradiation. Cancer Res. *57*, 1171-1179.
231. Little,J.B. and Nagasawa,H. (1985). Effect of confluent holding on potentially lethal damage repair, cell cycle progression, and chromosomal aberrations in human normal and ataxia-telangiectasia fibroblasts. Radiat. Res. *101*, 81-93.
232. Little,J.B., Nove,J., Strong,L.C., and Nichols,W.W. (1988). Survival of human diploid skin fibroblasts from normal individuals after X-irradiation. Int. J. Radiat. Biol. *54*, 899-910.
233. Liu,L., Scolnick,D.M., Trievel,R.C., Zhang,H.B., Marmorstein,R., Halazonetis,T.D., and Berger,S.L. (1999). p53 sites acetylated in vitro by PCAF and p300 are acetylated in vivo in response to DNA damage. Mol. Cell Biol. *19*, 1202-1209.
234. Lou,Z., Minter-Dykhouse,K., Wu,X., and Chen,J. (2003a). MDC1 is coupled to activated CHK2 in mammalian DNA damage response pathways. Nature *421*, 957-961.
235. Lou,Z., Chini,C.C., Minter-Dykhouse,K., and Chen,J. (2003b). Mediator of DNA damage checkpoint protein 1 regulates BRCA1 localization and phosphorylation in DNA damage checkpoint control. J. Biol. Chem. *278*, 13599-13602.
236. Lou,Z., Chen,B.P., Asaithamby,A., Minter-Dykhouse,K., Chen,D.J., and Chen,J. (2004). MDC1 regulates DNA-PK autophosphorylation in response to DNA damage. J. Biol. Chem. *279*, 46359-46362.
237. Lu,X. and Lane,D.P. (1993). Differential induction of transcriptionally active p53 following UV or ionizing radiation: defects in chromosome instability syndromes? Cell *75*, 765-778.
238. Lukas,C., Melander,F., Stucki,M., Falck,J., Bekker-Jensen,S., Goldberg,M., Lerenthal,Y., Jackson,S.P., Bartek,J., and Lukas,J. (2004). Mdc1 couples DNA double-strand break recognition by Nbs1 with its H2AX-dependent chromatin retention. EMBO J. *23*, 2674-2683.
239. Lyons,A.B. (2000). Analysing cell division in vivo and in vitro using flow cytometric measurement of CFSE dye dilution. J. Immunol. Methods *243*, 147-154.
240. Ma,Y., Pannicke,U., Schwarz,K., and Lieber,M.R. (2002). Hairpin opening and overhang processing by an Artemis/DNA-dependent protein kinase complex in nonhomologous end joining and V(D)J recombination. Cell *108*, 781-794.
241. Ma,Y., Lu,H., Tippin,B., Goodman,M.F., Shimazaki,N., Koiwai,O., Hsieh,C.L., Schwarz,K., and Lieber,M.R. (2004). A Biochemically Defined System for Mammalian Nonhomologous DNA End Joining. Mol. Cell *16*, 701-713.
242. Mahajan,K.N., Nick McElhinny,S.A., Mitchell,B.S., and Ramsden,D.A. (2002). Association of DNA polymerase mu (pol mu) with Ku and ligase IV: role for pol mu in end-joining double-strand break repair. Mol. Cell Biol. *22*, 5194-5202.
243. Manis,J.P., Gu,Y., Lansford,R., Sonoda,E., Ferrini,R., Davidson,L., Rajewsky,K., and Alt,F.W. (1998). Ku70 is required for late B cell development and immunoglobulin heavy chain class switching. J. Exp. Med. *187*, 2081-2089.
244. Manke,I.A., Lowery,D.M., Nguyen,A., and Yaffe,M.B. (2003). BRCT repeats as phosphopeptide-binding modules involved in protein targeting. Science *302*, 636-639.
245. Marchenko,N.D., Zaika,A., and Moll,U.M. (2000). Death signal-induced localization of p53 protein to mitochondria. A potential role in apoptotic signaling. J. Biol. Chem. *275*, 16202-16212.
246. Marder,B.A. and Morgan,W.F. (1993). Delayed chromosomal instability induced by DNA damage. Mol. Cell Biol. *13* , 6667-6677.
247. Martensson,S. and Hammarsten,O. (2002). DNA-dependent protein kinase catalytic subunit. Structural requirements for kinase activation by DNA ends. J. Biol. Chem. *277*, 3020-3029.
248. Martin,M., Genesca,A., Latre,L., Ribas,M., Miro,R., Egozcue,J., and Tusell,L. (2003). Radiation-induced chromosome breaks in ataxia-telangiectasia cells remain open. Int. J. Radiat. Biol. *79*, 203-210.
249. Matlashewski,G.J., Tuck,S., Pim,D., Lamb,P., Schneider,J., and Crawford,L.V. (1987). Primary structure polymorphism at amino acid residue 72 of human p53. Mol. Cell Biol. *7*, 961-963.
250. Matsuda,K., Yoshida,K., Taya,Y., Nakamura,K., Nakamura,Y., and Arakawa,H. (2002). p53AIP1 regulates the mitochondrial apoptotic pathway. Cancer Res. *62*, 2883-2889.
251. Matsumoto,Y., Suzuki,N., Namba,N., Umeda,N., Ma,X.J., Morita,A., Tomita,M., Enomoto,A., Serizawa,S., Hirano,K., Sakaia,K., Yasuda,H., and Hosoi,Y. (2000). Cleavage and phosphorylation of XRCC4 protein induced by X-irradiation. FEBS Lett. *478*, 67-71.

252. Maya,R., Balass,M., Kim,S.T., Shkedy,D., Leal,J.F., Shifman,O., Moas,M., Buschmann,T., Ronai,Z., Shiloh,Y., Kastan,M.B., Katzir,E., and Oren,M. (2001). ATM-dependent phosphorylation of Mdm2 on serine 395: role in p53 activation by DNA damage. Genes Dev. *15*, 1067-1077.
253. Mayo,L.D. and Donner,D.B. (2001). A phosphatidylinositol 3-kinase/Akt pathway promotes translocation of Mdm2 from the cytoplasm to the nucleus. Proc. Natl. Acad. Sci. U. S. A *98*, 11598-11603.
254. Mayo,L.D., Dixon,J.E., Durden,D.L., Tonks,N.K., and Donner,D.B. (2002). PTEN protects p53 from Mdm2 and sensitizes cancer cells to chemotherapy. J. Biol. Chem. *277*, 5484-5489.
255. McBlane,J.F., van Gent,D.C., Ramsden,D.A., Romeo,C., Cuomo,C.A., Gellert,M., and Oettinger,M.A. (1995). Cleavage at a V(D)J recombination signal requires only RAG1 and RAG2 proteins and occurs in two steps. Cell *83*, 387-395.
256. Meek,D.W. (2004). The p53 response to DNA damage. DNA Repair (Amst) *3*, 1049-1056.
257. Merkle,D., Douglas,P., Moorhead,G.B., Leonenko,Z., Yu,Y., Cramb,D., Bazett-Jones,D.P., and Lees-Miller,S.P. (2002). The DNA-dependent protein kinase interacts with DNA to form a protein-DNA complex that is disrupted by phosphorylation. Biochemistry *41*, 12706-12714.
258. Michael,D. and Oren,M. (2003). The p53-Mdm2 module and the ubiquitin system. Semin. Cancer Biol. *13*, 49-58.
259. Mihara,M., Erster,S., Zaika,A., Petrenko,O., Chittenden,T., Pancoska,P., and Moll,U.M. (2003). p53 has a direct apoptogenic role at the mitochondria. Mol. Cell *11*, 577-590.
260. Mirzoeva,O.K. and Petrini,J.H. (2001). DNA damage-dependent nuclear dynamics of the Mre11 complex. Mol. Cell Biol. *21*, 281-288.
261. Mirzoeva,O.K. and Petrini,J.H. (2003). DNA replication-dependent nuclear dynamics of the Mre11 complex. Mol. Cancer Res. *1*, 207-218.
262. Mizuta,R., Cheng,H.L., Gao,Y., and Alt,F.W. (1997). Molecular genetic characterization of XRCC4 function. Int. Immunol. *9*, 1607-1613.
263. Mochan,T.A., Venere,M., DiTullio,R.A., Jr., and Halazonetis,T.D. (2003). 53BP1 and NFBD1/MDC1-Nbs1 function in parallel interacting pathways activating ataxia-telangiectasia mutated (ATM) in response to DNA damage. Cancer Res. *63*, 8586-8591.
264. Mochan,T.A., Venere,M., DiTullio,R.A., Jr., and Halazonetis,T.D. (2004). 53BP1, an activator of ATM in response to DNA damage. DNA Repair (Amst) *3*, 945-952.
265. Morrison,C., Sonoda,E., Takao,N., Shinohara,A., Yamamoto,K., and Takeda,S. (2000). The controlling role of ATM in homologous recombinational repair of DNA damage. EMBO J. *19*, 463-471.
266. Moshous,D., Li,L., Chasseval,R., Philippe,N., Jabado,N., Cowan,M.J., Fischer,A., and De Villartay,J.P. (2000). A new gene involved in DNA double-strand break repair and V(D)J recombination is located on human chromosome 10p. Hum. Mol. Genet. *9*, 583-588.
267. Moshous,D., Callebaut,I., de Chasseval,R., Corneo,B., Cavazzana-Calvo,M., Le Deist,F., Tezcan,I., Sanal,O., Bertrand,Y., Philippe,N., Fischer,A., and De Villartay,J.P. (2001). Artemis, a novel DNA double-strand break repair/V(D)J recombination protein, is mutated in human severe combined immune deficiency. Cell *105*, 177-186.
268. Moshous,D., Pannetier,C., Chasseval,R.R., Deist,F.F., Cavazzana-Calvo,M., Romana,S., Macintyre,E., Canioni,D., Brousse,N., Fischer,A., Casanova,J.L., and Villartay,J.P. (2003). Partial T and B lymphocyte immunodeficiency and predisposition to lymphoma in patients with hypomorphic mutations in Artemis. J. Clin. Invest *111*, 381-387.
269. Moynahan,M.E., Chiu,J.W., Koller,B.H., and Jasin,M. (1999). Brca1 controls homology-directed DNA repair. Mol. Cell *4*, 511-518.
270. Moynahan,M.E., Pierce,A.J., and Jasin,M. (2001). BRCA2 is required for homology-directed repair of chromosomal breaks. Mol. Cell *7*, 263-272.
271. Mozdarani,H. and Bryant,P.E. (1989). Cytogenetic response of normal human and ataxia telangiectasia G2 cells exposed to X-rays and ara C. Mutat. Res. *226*, 223-228.
272. Muller,W.U., Nusse,M., Miller,B.M., Slavotinek,A., Viaggi,S., and Streffer,C. (1996). Micronuclei: a biological indicator of radiation damage. Mutat. Res. *366*, 163-169.
273. Murphy,M., Hinman,A., and Levine,A.J. (1996). Wild-type p53 negatively regulates the expression of a microtubule-associated protein. Genes Dev. *10*, 2971-2980.
274. Nagasawa,H., Latt,S.A., Lalande,M.E., and Little,J.B. (1985). Effects of X-irradiation on cell-cycle progression, induction of chromosomal aberrations and cell killing in ataxia telangiectasia (AT) fibroblasts. Mutat. Res. *148*, 71-82.
275. Naka,K., Tachibana,A., Ikeda,K., and Motoyama,N. (2004). Stress-induced premature senescence in hTERT-expressing ataxia telangiectasia fibroblasts. J. Biol. Chem. *279*, 2030-2037.
276. Nakagawa,K., Taya,Y., Tamai,K., and Yamaizumi,M. (1999). Requirement of ATM in phosphorylation of the human p53 protein at serine 15 following DNA double-strand breaks. Mol. Cell Biol. *19*, 2828-2834.

277. Nakano,K. and Vousden,K.H. (2001). PUMA, a novel proapoptotic gene, is induced by p53. Mol. Cell *7*, 683-694.
278. New,J.H., Sugiyama,T., Zaitseva,E., and Kowalczykowski,S.C. (1998). Rad52 protein stimulates DNA strand exchange by Rad51 and replication protein A. Nature *391*, 407-410.
279. Nick McElhinny,S.A., Snowden,C.M., McCarville,J., and Ramsden,D.A. (2000). Ku recruits the XRCC4-ligase IV complex to DNA ends. Mol. Cell Biol. *20*, 2996-3003.
280. Nicolas,N., Finnie,N.J., Cavazzana-Calvo,M., Papadopoulo,D., Le Deist,F., Fischer,A., Jackson,S.P., and De Villartay,J.P. (1996). Lack of detectable defect in DNA double-strand break repair and DNA-dependent protein kinase activity in radiosensitive human severe combined immunodeficiency fibroblasts. Eur. J. Immunol. *26*, 1118-1122.
281. Nicolas,N., Moshous,D., Cavazzana-Calvo,M., Papadopoulo,D., de Chasseval,R., Le Deist,F., Fischer,A., and De Villartay,J.P. (1998). A human severe combined immunodeficiency (SCID) condition with increased sensitivity to ionizing radiations and impaired V(D)J rearrangements defines a new DNA recombination/repair deficiency. J. Exp. Med. *188*, 627-634.
282. Nikjoo,H., O'Neill,P., Wilson,W.E., and Goodhead,D.T. (2001). Computational approach for determining the spectrum of DNA damage induced by ionizing radiation. Radiat. Res. *156*, 577-583.
283. Noordzij,J.G., Verkaik,N.S., van der,B.M., van Veelen,L.R., Bruin-Versteeg,S., Wiegant,W., Vossen,J.M., Weemaes,C.M., de Groot,R., Zdzienicka,M.Z., van Gent,D.C., and van Dongen,J.J. (2003). Radiosensitive SCID patients with Artemis gene mutations show a complete B-cell differentiation arrest at the pre-B-cell receptor checkpoint in bone marrow. Blood *101*, 1446-1452.
284. North,P., Ganesh,A., and Thacker,J. (1990). The rejoining of double-strand breaks in DNA by human cell extracts. Nucleic Acids Res. *18*, 6205-6210.
285. Nyberg,K.A., Michelson,R.J., Putnam,C.W., and Weinert,T.A. (2002). Toward maintaining the genome: DNA damage and replication checkpoints. Annu. Rev. Genet. *36*, 617-656.
286. O'Driscoll,M., Cerosaletti,K.M., Girard,P.M., Dai,Y., Stumm,M., Kysela,B., Hirsch,B., Gennery,A., Palmer,S.E., Seidel,J., Gatti,R.A., Varon,R., Oettinger,M.A., Neitzel,H., Jeggo,P.A., and Concannon,P. (2001). DNA ligase IV mutations identified in patients exhibiting developmental delay and immunodeficiency. Mol. Cell *8*, 1175-1185.
287. O'Driscoll,M., Gennery,A.R., Seidel,J., Concannon,P., and Jeggo,P.A. (2004). An overview of three new disorders associated with genetic instability: LIG4 syndrome, RS-SCID and ATR-Seckel syndrome. DNA Repair (Amst) *3*, 1227-1235.
288. Oda,E., Ohki,R., Murasawa,H., Nemoto,J., Shibue,T., Yamashita,T., Tokino,T., Taniguchi,T., and Tanaka,N. (2000a). Noxa, a BH3-only member of the Bcl-2 family and candidate mediator of p53-induced apoptosis. Science *288*, 1053-1058.
289. Oda,K., Arakawa,H., Tanaka,T., Matsuda,K., Tanikawa,C., Mori,T., Nishimori,H., Tamai,K., Tokino,T., Nakamura,Y., and Taya,Y. (2000b). p53AIP1, a potential mediator of p53-dependent apoptosis, and its regulation by Ser-46-phosphorylated p53. Cell *102*, 849-862.
290. Ogawara,Y., Kishishita,S., Obata,T., Isazawa,Y., Suzuki,T., Tanaka,K., Masuyama,N., and Gotoh,Y. (2002). Akt enhances Mdm2-mediated ubiquitination and degradation of p53. J. Biol. Chem. *277* , 21843-21850.
291. Oh,C.W., Bump,E.A., Kim,J.S., Janigro,D., and Mayberg,M.R. (2001). Induction of a senescence-like phenotype in bovine aortic endothelial cells by ionizing radiation. Radiat. Res. *156*, 232-240.
292. Okamura,S., Arakawa,H., Tanaka,T., Nakanishi,H., Ng,C.C., Taya,Y., Monden,M., and Nakamura,Y. (2001). p53DINP1, a p53-inducible gene, regulates p53-dependent apoptosis. Mol. Cell *8*, 85-94.
293. Owen-Schaub,L.B., Zhang,W., Cusack,J.C., Angelo,L.S., Santee,S.M., Fujiwara,T., Roth,J.A., Deisseroth,A.B., Zhang,W.W., Kruzel,E., and . (1995). Wild-type human p53 and a temperature-sensitive mutant induce Fas/APO-1 expression. Mol. Cell Biol. *15*, 3032-3040.
294. Painter,R.B. and Young,B.R. (1980). Radiosensitivity in ataxia-telangiectasia: a new explanation. Proc. Natl. Acad. Sci. U. S. A *77*, 7315-7317.
295. Pan,Q., Petit-Frere,C., Lahdesmaki,A., Gregorek,H., Chrzanowska,K.H., and Hammarstrom,L. (2002). Alternative end joining during switch recombination in patients with ataxia-telangiectasia. Eur. J. Immunol. *32*, 1300-1308.
296. Pandita,T.K., Lieberman,H.B., Lim,D.S., Dhar,S., Zheng,W., Taya,Y., and Kastan,M.B. (2000). Ionizing radiation activates the ATM kinase throughout the cell cycle. Oncogene *19*, 1386-1391.
297. Pannicke,U., Ma,Y., Hopfner,K.P., Niewolik,D., Lieber,M.R., and Schwarz,K. (2004). Functional and biochemical dissection of the structure-specific nuclease ARTEMIS. EMBO J. *23*, 1987-1997.
298. Panta,G.R., Kaur,S., Cavin,L.G., Cortes,M.L., Mercurio,F., Lothstein,L., Sweatman,T.W., Israel,M., and Arsura,M. (2004). ATM and the catalytic subunit of DNA-dependent protein kinase activate NF-kappaB through a common MEK/extracellular signal-regulated kinase/p90(rsk) signaling pathway in response to distinct forms of DNA damage. Mol. Cell Biol. *24*, 1823-1835.

299. Parsons,C.A., Baumann,P., Van Dyck,E., and West,S.C. (2000). Precise binding of single-stranded DNA termini by human RAD52 protein. EMBO J. *19*, 4175-4181.
300. Passalaris,T.M., Benanti,J.A., Gewin,L., Kiyono,T., and Galloway,D.A. (1999). The G(2) checkpoint is maintained by redundant pathways. Mol. Cell Biol. *19*, 5872-5881.
301. Paull,T.T., Rogakou,E.P., Yamazaki,V., Kirchgessner,C.U., Gellert,M., and Bonner,W.M. (2000). A critical role for histone H2AX in recruitment of repair factors to nuclear foci after DNA damage. Curr. Biol. *10*, 886-895.
302. Peake,J., Waugh,A., Le Deist,F., Priestley,A., Rieux-Laucat,F., Foray,N., Capulas,E., Singleton,B.K., De Villartay,J.P., Cant,A., Malaise,E.P., Fischer,A., Hivroz,C., and Jeggo,P.A. (1999). Combined immunodeficiency associated with increased apoptosis of lymphocytes and radiosensitivity fibroblasts. Cancer Res. *59*, 3454-3460.
303. Peng,C.Y., Graves,P.R., Thoma,R.S., Wu,Z., Shaw,A.S., and Piwnica-Worms,H. (1997). Mitotic and G2 checkpoint control: regulation of 14-3-3 protein binding by phosphorylation of Cdc25C on serine-216. Science *277*, 1501-1505.
304. Perkins,E.J., Nair,A., Cowley,D.O., Van Dyke,T., Chang,Y., and Ramsden,D.A. (2002). Sensing of intermediates in V(D)J recombination by ATM. Genes Dev. *16*, 159-164.
305. Petrini,J.H. and Stracker,T.H. (2003). The cellular response to DNA double-strand breaks: defining the sensors and mediators. Trends Cell Biol. *13*, 458-462.
306. Petukhova,G., Stratton,S., and Sung,P. (1998). Catalysis of homologous DNA pairing by yeast Rad51 and Rad54 proteins. Nature *393*, 91-94.
307. Pfeiffer,P., Goedecke,W., and Obe,G. (2000). Mechanisms of DNA double-strand break repair and their potential to induce chromosomal aberrations. Mutagenesis *15*, 289-302.
308. Pierce,A.J., Hu,P., Han,M., Ellis,N., and Jasin,M. (2001). Ku DNA end-binding protein modulates homologous repair of double-strand breaks in mammalian cells. Genes Dev. *15*, 3237-3242.
309. Pim,D. and Banks,L. (2004). p53 polymorphic variants at codon 72 exert different effects on cell cycle progression. Int. J. Cancer *108*, 196-199.
310. Piret,B., Schoonbroodt,S., and Piette,J. (1999). The ATM protein is required for sustained activation of NF-kappaB following DNA damage. Oncogene *18*, 2261-2271.
311. Poinsignon,C., Moshous,D., Callebaut,I., de Chasseval,R., Villey,I., and De Villartay,J.P. (2004). The metallo-beta-lactamase/beta-CASP domain of Artemis constitutes the catalytic core for V(D)J recombination. J. Exp. Med. *199*, 315-321.
312. Polyak,K., Xia,Y., Zweier,J.L., Kinzler,K.W., and Vogelstein,B. (1997). A model for p53-induced apoptosis. Nature *389*, 300-305.
313. Prise,K.M., Davies,S., and Michael,B.D. (1989). Cell killing and DNA damage in Chinese hamster V79 cells treated with hydrogen peroxide. Int. J. Radiat. Biol. *55*, 583-592.
314. Purugganan,M.M., Shah,S., Kearney,J.F., and Roth,D.B. (2001). Ku80 is required for addition of N nucleotides to V(D)J recombination junctions by terminal deoxynucleotidyl transferase. Nucleic Acids Res. *29*, 1638-1646.
315. Qiu,J.X., Kale,S.B., Yarnell,S.H., and Roth,D.B. (2001). Separation-of-function mutants reveal critical roles for RAG2 in both the cleavage and joining steps of V(D)J recombination. Mol. Cell *7*, 77-87.
316. Ramsden,D.A. and Gellert,M. (1998). Ku protein stimulates DNA end joining by mammalian DNA ligases: a direct role for Ku in repair of DNA double-strand breaks. EMBO J. *17*, 609-614.
317. Reddy,Y.V., Ding,Q., Lees-Miller,S.P., Meek,K., and Ramsden,D.A. (2004). Nonhomologous end-joining requires that the DNA-PK complex undergo an autophosphorylation-dependent rearrangement at DNA ends. J. Biol. Chem.
318. Riballo,E., Critchlow,S.E., Teo,S.H., Doherty,A.J., Priestley,A., Broughton,B., Kysela,B., Beamish,H., Plowman,N., Arlett,C.F., Lehmann,A.R., Jackson,S.P., and Jeggo,P.A. (1999). Identification of a defect in DNA ligase IV in a radiosensitive leukaemia patient. Curr. Biol. *9*, 699-702.
319. Riballo,E., Doherty,A.J., Dai,Y., Stiff,T., Oettinger,M.A., Jeggo,P.A., and Kysela,B. (2001). Cellular and biochemical impact of a mutation in DNA ligase IV conferring clinical radiosensitivity. J. Biol. Chem. *276*, 31124-31132.
320. Riballo,E., Kuhne,M., Rief,N., Doherty,A., Smith,G.C., Recio,M.J., Reis,C., Dahm,K., Fricke,A., Krempler,A., Parker,A.R., Jackson,S.P., Gennery,A., Jeggo,P.A., and Lobrich,M. (2004). A Pathway of Double-Strand Break Rejoining Dependent upon ATM, Artemis, and Proteins Locating to gamma-H2AX Foci. Mol. Cell *16*, 715-724.
321. Rich,T., Allen,R.L., and Wyllie,A.H. (2000). Defying death after DNA damage. Nature *407*, 777-783.
322. Richardson,C. and Jasin,M. (2000). Frequent chromosomal translocations induced by DNA double-strand breaks. Nature *405*, 697-700.

323. Robles,S.J. and Adami,G.R. (1998). Agents that cause DNA double strand breaks lead to p16INK4a enrichment and the premature senescence of normal fibroblasts. Oncogene *16*, 1113-1123.
324. Rogakou,E.P., Boon,C., Redon,C., and Bonner,W.M. (1999). Megabase chromatin domains involved in DNA double-strand breaks in vivo. J. Cell Biol. *146*, 905-916.
325. Rooney,S., Sekiguchi,J., Zhu,C., Cheng,H.L., Manis,J., Whitlow,S., DeVido,J., Foy,D., Chaudhuri,J., Lombard,D., and Alt,F.W. (2002). Leaky Scid phenotype associated with defective V(D)J coding end processing in Artemis-deficient mice. Mol. Cell *10*, 1379-1390.
326. Rooney,S., Alt,F.W., Lombard,D., Whitlow,S., Eckersdorff,M., Fleming,J., Fugmann,S., Ferguson,D.O., Schatz,D.G., and Sekiguchi,J. (2003). Defective DNA repair and increased genomic instability in Artemis-deficient murine cells. J. Exp. Med. *197*, 553-565.
327. Rosenthal,A.N., Ryan,A., Al Jehani,R.M., Storey,A., Harwood,C.A., and Jacobs,I.J. (1998). p53 codon 72 polymorphism and risk of cervical cancer in UK. Lancet *352*, 871-872.
328. Rothkamm,K. and Lobrich,M. (2003). Evidence for a lack of DNA double-strand break repair in human cells exposed to very low x-ray doses. Proc. Natl. Acad. Sci. U. S. A *100*, 5057-5062.
329. Rothkamm,K., Kruger,I., Thompson,L.H., and Lobrich,M. (2003). Pathways of DNA double-strand break repair during the mammalian cell cycle. Mol. Cell Biol. *23*, 5706-5715.
330. Rotman,G. and Shiloh,Y. (1998). ATM: from gene to function. Hum. Mol. Genet. *7*, 1555-1563.
331. Roy,K., Kodama,S., Suzuki,K., and Watanabe,M. (1999). Delayed cell death, giant cell formation and chromosome instability induced by X-irradiation in human embryo cells. J. Radiat. Res. (Tokyo) *40*, 311-322.
332. Rugo,R.E., Secretan,M.B., and Schiestl,R.H. (2002). X radiation causes a persistent induction of reactive oxygen species and a delayed reinduction of TP53 in normal human diploid fibroblasts. Radiat. Res. *158*, 210-219.
333. Sablina,A.A., Ilyinskaya,G.V., Rubtsova,S.N., Agapova,L.S., Chumakov,P.M., and Kopnin,B.P. (1998). Activation of p53-mediated cell cycle checkpoint in response to micronuclei formation. J. Cell Sci. *111 (Pt 7)*, 977-984.
334. Sakaguchi,K., Herrera,J.E., Saito,S., Miki,T., Bustin,M., Vassilev,A., Anderson,C.W., and Appella,E. (1998). DNA damage activates p53 through a phosphorylation-acetylation cascade. Genes Dev. *12*, 2831-2841.
335. Samuels-Lev,Y., O'Connor,D.J., Bergamaschi,D., Trigiante,G., Hsieh,J.K., Zhong,S., Campargue,I., Naumovski,L., Crook,T., and Lu,X. (2001). ASPP proteins specifically stimulate the apoptotic function of p53. Mol. Cell *8*, 781-794.
336. Sandor,Z., Calicchio,M.L., Sargent,R.G., Roth,D.B., and Wilson,J.H. (2004). Distinct requirements for Ku in N nucleotide addition at V(D)J- and non-V(D)J-generated double-strand breaks. Nucleic Acids Res. *32*, 1866-1873.
337. Sarkaria,J.N., Bush,C., Eady,J.J., Peacock,J.H., Steel,G.G., and Yarnold,J.R. (1998). Comparison between pulsed-field gel electrophoresis and the comet assay as predictive assays for radiosensitivity in fibroblasts. Radiat. Res. *150*, 17-22.
338. Sasai,K., Evans,J.W., Kovacs,M.S., and Brown,J.M. (1994). Prediction of human cell radiosensitivity: comparison of clonogenic assay with chromosome aberrations scored using premature chromosome condensation with fluorescence in situ hybridization. Int. J. Radiat. Oncol. Biol. Phys. *30*, 1127-1132.
339. Savage,J.R. (1989). Acentric chromosomal fragments and micronuclei: the time-displacement factor. Mutat. Res. *225*, 171-173.
340. Savitsky,K., Bar-Shira,A., Gilad,S., Rotman,G., Ziv,Y., Vanagaite,L., Tagle,D.A., Smith,S., Uziel,T., Sfez,S., and . (1995). A single ataxia telangiectasia gene with a product similar to PI-3 kinase. Science *268*, 1749-1753.
341. Sax,J.K., Fei,P., Murphy,M.E., Bernhard,E., Korsmeyer,S.J., and El Deiry,W.S. (2002). BID regulation by p53 contributes to chemosensitivity. Nat. Cell Biol. *4*, 842-849.
342. Schmitz,A., Bayer,J., Dechamps,N., and Thomas,G. (2003). Intrinsic susceptibility to radiation-induced apoptosis of human lymphocyte subpopulations. Int. J. Radiat. Oncol. Biol. Phys. *57*, 769-778.
343. Schultz,L.B., Chehab,N.H., Malikzay,A., and Halazonetis,T.D. (2000). p53 binding protein 1 (53BP1) is an early participant in the cellular response to DNA double-strand breaks. J. Cell Biol. *151*, 1381-1390.
344. Scott,D., Barber,J.B., Spreadborough,A.R., Burrill,W., and Roberts,S.A. (1999). Increased chromosomal radiosensitivity in breast cancer patients: a comparison of two assays. Int. J. Radiat. Biol. *75*, 1-10.
345. Scully,R., Chen,J., Plug,A., Xiao,Y., Weaver,D., Feunteun,J., Ashley,T., and Livingston,D.M. (1997). Association of BRCA1 with Rad51 in mitotic and meiotic cells. Cell *88*, 265-275.
346. Scully,R. and Livingston,D.M. (2000). In search of the tumour-suppressor functions of BRCA1 and BRCA2. Nature *408*, 429-432.

347. Sedelnikova,O.A., Rogakou,E.P., Panyutin,I.G., and Bonner,W.M. (2002). Quantitative detection of (125)IdU-induced DNA double-strand breaks with gamma-H2AX antibody. Radiat. Res. *158*, 486-492.
348. Shafman,T., Khanna,K.K., Kedar,P., Spring,K., Kozlov,S., Yen,T., Hobson,K., Gatei,M., Zhang,N., Watters,D., Egerton,M., Shiloh,Y., Kharbanda,S., Kufe,D., and Lavin,M.F. (1997). Interaction between ATM protein and c-Abl in response to DNA damage. Nature *387*, 520-523.
349. Shaham,M., Becker,Y., Lerer,I., and Voss,R. (1983). Increased level of bleomycin-induced chromosome breakage in ataxia telangiectasia skin fibroblasts. Cancer Res. *43*, 4244-4247.
350. Shay,J.W. and Wright,W.E. (2001). Aging. When do telomeres matter? Science *291*, 839-840.
351. Shieh,S.Y., Ahn,J., Tamai,K., Taya,Y., and Prives,C. (2000). The human homologs of checkpoint kinases Chk1 and Cds1 (Chk2) phosphorylate p53 at multiple DNA damage-inducible sites. Genes Dev. *14*, 289-300.
352. Shikama,N., Lee,C.W., France,S., Delavaine,L., Lyon,J., Krstic-Demonacos,M., and La Thangue,N.B. (1999). A novel cofactor for p300 that regulates the p53 response. Mol. Cell *4*, 365-376.
353. Shiloh,Y. (1997). Ataxia-telangiectasia and the Nijmegen breakage syndrome: related disorders but genes apart. Annu. Rev. Genet. *31*, 635-662.
354. Shiloh,Y. (2001). ATM and ATR: networking cellular responses to DNA damage. Curr. Opin. Genet. Dev. *11*, 71-77.
355. Sibanda,B.L., Critchlow,S.E., Begun,J., Pei,X.Y., Jackson,S.P., Blundell,T.L., and Pellegrini,L. (2001). Crystal structure of an Xrcc4-DNA ligase IV complex. Nat. Struct. Biol. *8*, 1015-1019.
356. Simon,A.K., Williams,O., Mongkolsapaya,J., Jin,B., Xu,X.N., Walczak,H., and Screaton,G.R. (2001). Tumor necrosis factor-related apoptosis-inducing ligand in T cell development: sensitivity of human thymocytes. Proc. Natl. Acad. Sci. U. S. A *98*, 5158-5163.
357. Slichenmyer,W.J., Nelson,W.G., Slebos,R.J., and Kastan,M.B. (1993). Loss of a p53-associated G1 checkpoint does not decrease cell survival following DNA damage. Cancer Res. *53*, 4164-4168.
358. Smith,G.C., Cary,R.B., Lakin,N.D., Hann,B.C., Teo,S.H., Chen,D.J., and Jackson,S.P. (1999). Purification and DNA binding properties of the ataxia-telangiectasia gene product ATM. Proc. Natl. Acad. Sci. U. S. A *96*, 11134-11139.
359. Smith,G.C. and Jackson,S.P. (1999). The DNA-dependent protein kinase. Genes Dev. *13*, 916-934.
360. Snouwaert,J.N., Gowen,L.C., Latour,A.M., Mohn,A.R., Xiao,A., DiBiase,L., and Koller,B.H. (1999). BRCA1 deficient embryonic stem cells display a decreased homologous recombination frequency and an increased frequency of non-homologous recombination that is corrected by expression of a brca1 transgene. Oncogene *18*, 7900-7907.
361. Sproston,A.R., West,C.M., and Hendry,J.H. (1997). Cellular radiosensitivity in human severe-combined-immunodeficiency (SCID) syndromes. Radiother. Oncol. *42*, 53-57.
362. Stankovic,T., Hubank,M., Cronin,D., Stewart,G.S., Fletcher,D., Bignell,C.R., Alvi,A.J., Austen,B., Weston,V.J., Fegan,C., Byrd,P.J., Moss,P.A., and Taylor,A.M. (2004). Microarray analysis reveals that TP53- and ATM-mutant B-CLLs share a defect in activating proapoptotic responses after DNA damage but are distinguished by major differences in activating prosurvival responses. Blood *103*, 291-300.
363. Stewart,G.S., Maser,R.S., Stankovic,T., Bressan,D.A., Kaplan,M.I., Jaspers,N.G., Raams,A., Byrd,P.J., Petrini,J.H., and Taylor,A.M. (1999). The DNA double-strand break repair gene hMRE11 is mutated in individuals with an ataxia-telangiectasia-like disorder. Cell *99*, 577-587.
364. Stewart,G.S., Wang,B., Bignell,C.R., Taylor,A.M., and Elledge,S.J. (2003). MDC1 is a mediator of the mammalian DNA damage checkpoint. Nature *421*, 961-966.
365. Stiff,T., O'Driscoll,M., Rief,N., Iwabuchi,K., Lobrich,M., and Jeggo,P.A. (2004a). ATM and DNA-PK function redundantly to phosphorylate H2AX after exposure to ionizing radiation. Cancer Res. *64*, 2390-2396.
366. Stiff,T., Shtivelman,E., Jeggo,P., and Kysela,B. (2004b). AHNAK interacts with the DNA ligase IV-XRCC4 complex and stimulates DNA ligase IV-mediated double-stranded ligation. DNA Repair (Amst) *3*, 245-256.
367. Stucki,M. and Jackson,S.P. (2004). MDC1/NFBD1: a key regulator of the DNA damage response in higher eukaryotes. DNA Repair (Amst) *3*, 953-957.
368. Sugiyama,T., Zaitseva,E.M., and Kowalczykowski,S.C. (1997). A single-stranded DNA-binding protein is needed for efficient presynaptic complex formation by the Saccharomyces cerevisiae Rad51 protein. J. Biol. Chem. *272*, 7940-7945.
369. Sung,P. (1997). Function of yeast Rad52 protein as a mediator between replication protein A and the Rad51 recombinase. J. Biol. Chem. *272*, 28194-28197.
370. Sung,P., Krejci,L., Van Komen,S., and Sehorn,M.G. (2003). Rad51 recombinase and recombination mediators. J. Biol. Chem. *278*, 42729-42732.

371. Suzuki,K., Takahara,R., Kodama,S., and Watanabe,M. (1998). In situ detection of chromosome bridge formation and delayed reproductive death in normal human embryonic cells surviving X irradiation. Radiat. Res. *150*, 375-381.
372. Suzuki,K., Kodama,S., and Watanabe,M. (1999). Recruitment of ATM protein to double strand DNA irradiated with ionizing radiation. J. Biol. Chem. *274*, 25571-25575.
373. Suzuki,K., Ojima,M., Kodama,S., and Watanabe,M. (2003a). Radiation-induced DNA damage and delayed induced genomic instability. Oncogene *22*, 6988-6993.
374. Suzuki,K., Yokoyama,S., Waseda,S., Kodama,S., and Watanabe,M. (2003b). Delayed reactivation of p53 in the progeny of cells surviving ionizing radiation. Cancer Res. *63*, 936-941.
375. Symington,L.S. (2002). Role of RAD52 epistasis group genes in homologous recombination and double-strand break repair. Microbiol. Mol. Biol. Rev. *66*, 630-70, table.
376. Szak,S.T., Mays,D., and Pietenpol,J.A. (2001). Kinetics of p53 binding to promoter sites in vivo. Mol. Cell Biol. *21*, 3375-3386.
377. Taccioli,G.E., Amatucci,A.G., Beamish,H.J., Gell,D., Xiang,X.H., Torres Arzayus,M.I., Priestley,A., Jackson,S.P., Marshak,R.A., Jeggo,P.A., and Herrera,V.L. (1998). Targeted disruption of the catalytic subunit of the DNA-PK gene in mice confers severe combined immunodeficiency and radiosensitivity. Immunity. *9*, 355-366.
378. Takata,M., Sasaki,M.S., Sonoda,E., Morrison,C., Hashimoto,M., Utsumi,H., Yamaguchi-Iwai,Y., Shinohara,A., and Takeda,S. (1998). Homologous recombination and non-homologous end-joining pathways of DNA double-strand break repair have overlapping roles in the maintenance of chromosomal integrity in vertebrate cells. EMBO J. *17*, 5497-5508.
379. Takimoto,R. and El Deiry,W.S. (2000). Wild-type p53 transactivates the KILLER/DR5 gene through an intronic sequence-specific DNA-binding site. Oncogene *19*, 1735-1743.
380. Tan,T. and Chu,G. (2002). p53 Binds and activates the xeroderma pigmentosum DDB2 gene in humans but not mice. Mol. Cell Biol. *22*, 3247-3254.
381. Tauchi,H., Kobayashi,J., Morishima,K., van Gent,D.C., Shiraishi,T., Verkaik,N.S., vanHeems,D., Ito,E., Nakamura,A., Sonoda,E., Takata,M., Takeda,S., Matsuura,S., and Komatsu,K. (2002). Nbs1 is essential for DNA repair by homologous recombination in higher vertebrate cells. Nature *420*, 93-98.
382. Taylor,A.M., Harnden,D.G., Arlett,C.F., Harcourt,S.A., Lehmann,A.R., Stevens,S., and Bridges,B.A. (1975). Ataxia telangiectasia: a human mutation with abnormal radiation sensitivity. Nature *258*, 427-429.
383. Taylor,A.M., Metcalfe,J.A., Oxford,J.M., and Harnden,D.G. (1976). Is chromatid-type damage in ataxia telangiectasia after irradiation at G0 a consequence of defective repair? Nature *260*, 441-443.
384. Taylor,A.M., Metcalfe,J.A., Thick,J., and Mak,Y.F. (1996). Leukemia and lymphoma in ataxia telangiectasia. Blood *87*, 423-438.
385. Taylor,A.M., Groom,A., and Byrd,P.J. (2004). Ataxia-telangiectasia-like disorder (ATLD)-its clinical presentation and molecular basis. DNA Repair (Amst) *3*, 1219-1225.
386. Teo,S.H. and Jackson,S.P. (2000). Lif1p targets the DNA ligase Lig4p to sites of DNA double-strand breaks. Curr. Biol. *10*, 165-168.
387. Thacker,J. (1994). Cellular radiosensitivity in ataxia-telangiectasia. Int. J. Radiat. Biol. *66*, S87-S96.
388. Thomas,M., Kalita,A., Labrecque,S., Pim,D., Banks,L., and Matlashewski,G. (1999). Two polymorphic variants of wild-type p53 differ biochemically and biologically. Mol. Cell Biol. *19*, 1092-1100.
389. Tibbetts,R.S., Brumbaugh,K.M., Williams,J.M., Sarkaria,J.N., Cliby,W.A., Shieh,S.Y., Taya,Y., Prives,C., and Abraham,R.T. (1999). A role for ATR in the DNA damage-induced phosphorylation of p53. Genes Dev. *13*, 152-157.
390. Toussaint,O., Medrano,E.E., and von Zglinicki,T. (2000). Cellular and molecular mechanisms of stress-induced premature senescence (SIPS) of human diploid fibroblasts and melanocytes. Exp. Gerontol. *35*, 927-945.
391. Tsai,C.L., Drejer,A.H., and Schatz,D.G. (2002). Evidence of a critical architectural function for the RAG proteins in end processing, protection, and joining in V(D)J recombination. Genes Dev. *16*, 1934-1949.
392. Unger,T., Juven-Gershon,T., Moallem,E., Berger,M., Vogt,S.R., Lozano,G., Oren,M., and Haupt,Y. (1999). Critical role for Ser20 of human p53 in the negative regulation of p53 by Mdm2. EMBO J. *18*, 1805-1814.
393. Uziel,T., Lerenthal,Y., Moyal,L., Andegeko,Y., Mittelman,L., and Shiloh,Y. (2003). Requirement of the MRN complex for ATM activation by DNA damage. EMBO J. *22*, 5612-5621.
394. Valerie,K. and Povirk,L.F. (2003). Regulation and mechanisms of mammalian double-strand break repair. Oncogene *22*, 5792-5812.

395. Vamvakas,S., Vock,E.H., and Lutz,W.K. (1997). On the role of DNA double-strand breaks in toxicity and carcinogenesis. Crit Rev. Toxicol. *27*, 155-174.
396. Van Dyck,E., Stasiak,A.Z., Stasiak,A., and West,S.C. (1999). Binding of double-strand breaks in DNA by human Rad52 protein. Nature *398*, 728-731.
397. van Engelen,B.G., Hiel,J.A., Gabreels,F.J., van den Heuvel,L.P., van Gent,D.C., and Weemaes,C.M. (2001). Decreased immunoglobulin class switching in Nijmegen Breakage syndrome due to the DNA repair defect. Hum. Immunol. *62*, 1324-1327.
398. van Gent,D.C., McBlane,J.F., Ramsden,D.A., Sadofsky,M.J., Hesse,J.E., and Gellert,M. (1995). Initiation of V(D)J recombination in a cell-free system. Cell *81*, 925-934.
399. Van Komen,S., Petukhova,G., Sigurdsson,S., Stratton,S., and Sung,P. (2000). Superhelicity-driven homologous DNA pairing by yeast recombination factors Rad51 and Rad54. Mol. Cell *6*, 563-572.
400. Varon,R., Vissinga,C., Platzer,M., Cerosaletti,K.M., Chrzanowska,K.H., Saar,K., Beckmann,G., Seemanova,E., Cooper,P.R., Nowak,N.J., Stumm,M., Weemaes,C.M., Gatti,R.A., Wilson,R.K., Digweed,M., Rosenthal,A., Sperling,K., Concannon,P., and Reis,A. (1998). Nibrin, a novel DNA double-strand break repair protein, is mutated in Nijmegen breakage syndrome. Cell *93*, 467-476.
401. Velasco-Miguel,S., Buckbinder,L., Jean,P., Gelbert,L., Talbott,R., Laidlaw,J., Seizinger,B., and Kley,N. (1999). PA26, a novel target of the p53 tumor suppressor and member of the GADD family of DNA damage and growth arrest inducible genes. Oncogene *18*, 127-137.
402. Virsik-Kopp,P., Rave-Frank,M., Hofman-Huther,H., and Schmidberger,H. (2004). Role of DNA-dependent protein kinase in the process of radiation-induced aberration formation. Int. J. Radiat. Biol. *80*, 125-133.
403. Vogelstein,B., Lane,D., and Levine,A.J. (2000). Surfing the p53 network. Nature *408*, 307-310.
404. Vousden,K.H. and Lu,X. (2002). Live or let die: the cell's response to p53. Nat. Rev. Cancer *2*, 594-604.
405. Wachsberger,P.R., Li,W.H., Guo,M., Chen,D., Cheong,N., Ling,C.C., Li,G., and Iliakis,G. (1999). Rejoining of DNA double-strand breaks in Ku80-deficient mouse fibroblasts. Radiat. Res. *151*, 398-407.
406. Walczak,H. and Krammer,P.H. (2000). The CD95 (APO-1/Fas) and the TRAIL (APO-2L) apoptosis systems. Exp. Cell Res. *256*, 58-66.
407. Waldman,T., Kinzler,K.W., and Vogelstein,B. (1995). p21 is necessary for the p53-mediated G1 arrest in human cancer cells. Cancer Res. *55*, 5187-5190.
408. Walker,J.R., Corpina,R.A., and Goldberg,J. (2001). Structure of the Ku heterodimer bound to DNA and its implications for double-strand break repair. Nature *412*, 607-614.
409. Wang,Y., Cortez,D., Yazdi,P., Neff,N., Elledge,S.J., and Qin,J. (2000). BASC, a super complex of BRCA1-associated proteins involved in the recognition and repair of aberrant DNA structures. Genes Dev. *14*, 927-939.
410. Wang,Z., Fast,W., Valentine,A.M., and Benkovic,S.J. (1999). Metallo-beta-lactamase: structure and mechanism. Curr. Opin. Chem. Biol. *3*, 614-622.
411. West,S.C. (1996). The RuvABC proteins and Holliday junction processing in Escherichia coli. J. Bacteriol. *178* , 1237-1241.
412. Wilkins,R.C., Kutzner,B.C., Truong,M., and McLean,J.R. (2002). The effect of the ratio of CD4+ to CD8+ T-cells on radiation-induced apoptosis in human lymphocyte subpopulations. Int. J. Radiat. Biol. *78*, 681-688.
413. Williams,K.J., Boyle,J.M., Birch,J.M., Norton,J.D., and Scott,D. (1997). Cell cycle arrest defect in Li-Fraumeni Syndrome: a mechanism of cancer predisposition? Oncogene *14*, 277-282.
414. Wu,G.S., Burns,T.F., McDonald,E.R., III, Meng,R.D., Kao,G., Muschel,R., Yen,T., and El Deiry,W.S. (1999). Induction of the TRAIL receptor KILLER/DR5 in p53-dependent apoptosis but not growth arrest. Oncogene *18*, 6411-6418.
415. Wu,G.S., Kim,K., and El Deiry,W.S. (2000). KILLER/DR5, a novel DNA-damage inducible death receptor gene, links the p53-tumor suppressor to caspase activation and apoptotic death. Adv. Exp. Med. Biol. *465*, 143-151.
416. Wurm,R., Burnet,N.G., Duggal,N., Yarnold,J.R., and Peacock,J.H. (1994). Cellular radiosensitivity and DNA damage in primary human fibroblasts. Int. J. Radiat. Oncol. Biol. Phys. *30*, 625-633.
417. Wyman,C., Ristic,D., and Kanaar,R. (2004). Homologous recombination-mediated double-strand break repair. DNA Repair (Amst) *3*, 827-833.
418. Xia,F., Taghian,D.G., DeFrank,J.S., Zeng,Z.C., Willers,H., Iliakis,G., and Powell,S.N. (2001). Deficiency of human BRCA2 leads to impaired homologous recombination but maintains normal nonhomologous end joining. Proc. Natl. Acad. Sci. U. S. A *98*, 8644-8649.
419. Xu,B., Kim,S.T., Lim,D.S., and Kastan,M.B. (2002). Two molecularly distinct G(2)/M checkpoints are induced by ionizing irradiation. Mol. Cell Biol. *22*, 1049-1059.

420. Yamaguchi-Iwai,Y., Sonoda,E., Sasaki,M.S., Morrison,C., Haraguchi,T., Hiraoka,Y., Yamashita,Y.M., Yagi,T., Takata,M., Price,C., Kakazu,N., and Takeda,S. (1999). Mre11 is essential for the maintenance of chromosomal DNA in vertebrate cells. EMBO J. *18*, 6619-6629.
421. Yaneva,M., Kowalewski,T., and Lieber,M.R. (1997). Interaction of DNA-dependent protein kinase with DNA and with Ku: biochemical and atomic-force microscopy studies. EMBO J. *16*, 5098-5112.
422. Yarnell Schultz,H., Landree,M.A., Qiu,J.X., Kale,S.B., and Roth,D.B. (2001). Joining-deficient RAG1 mutants block V(D)J recombination in vivo and hairpin opening in vitro. Mol. Cell *7*, 65-75.
423. Yeo,T.C., Xia,D., Hassouneh,S., Yang,X.O., Sabath,D.E., Sperling,K., Gatti,R.A., Concannon,P., and Willerford,D.M. (2000). V(D)J rearrangement in Nijmegen breakage syndrome. Mol. Immunol. *37*, 1131-1139.
424. Yount,G.L., Haas-Kogan,D.A., Vidair,C.A., Haas,M., Dewey,W.C., and Israel,M.A. (1996). Cell cycle synchrony unmasks the influence of p53 function on radiosensitivity of human glioblastoma cells. Cancer Res. *56*, 500-506.
425. Yu,J., Zhang,L., Hwang,P.M., Kinzler,K.W., and Vogelstein,B. (2001). PUMA induces the rapid apoptosis of colorectal cancer cells. Mol. Cell *7*, 673-682.
426. Yu,X., Chini,C.C., He,M., Mer,G., and Chen,J. (2003). The BRCT domain is a phospho-protein binding domain. Science *302*, 639-642.
427. Yuan,S.S., Lee,S.Y., Chen,G., Song,M., Tomlinson,G.E., and Lee,E.Y. (1999). BRCA2 is required for ionizing radiation-induced assembly of Rad51 complex in vivo. Cancer Res. *59*, 3547-3551.
428. Zhan,Q., Antinore,M.J., Wang,X.W., Carrier,F., Smith,M.L., Harris,C.C., and Fornace,A.J., Jr. (1999). Association with Cdc2 and inhibition of Cdc2/Cyclin B1 kinase activity by the p53-regulated protein Gadd45. Oncogene *18*, 2892-2900.
429. Zhang,X., Succi,J., Feng,Z., Prithivirajsingh,S., Story,M.D., and Legerski,R.J. (2004). Artemis Is a Phosphorylation Target of ATM and ATR and Is Involved in the G2/M DNA Damage Checkpoint Response. Mol. Cell Biol. *24*, 9207-9220.
430. Zhang,Y., Dimtchev,A., Dritschilo,A., and Jung,M. (2001a). Ionizing radiation-induced apoptosis in ataxia-telangiectasia fibroblasts. Roles of caspase-9 and cellular inhibitor of apoptosis protein-1. J. Biol. Chem. *276*, 28842-28848.
431. Zhang,Y. and Xiong,Y. (2001b). A p53 amino-terminal nuclear export signal inhibited by DNA damage-induced phosphorylation. Science *292*, 1910-1915.
432. Zhao,H., Watkins,J.L., and Piwnica-Worms,H. (2002). Disruption of the checkpoint kinase 1/cell division cycle 25A pathway abrogates ionizing radiation-induced S and G2 checkpoints. Proc. Natl. Acad. Sci. U. S. A *99*, 14795-14800.
433. Zhong,Q., Chen,C.F., Li,S., Chen,Y., Wang,C.C., Xiao,J., Chen,P.L., Sharp,Z.D., and Lee,W.H. (1999). Association of BRCA1 with the hRad50-hMre11-p95 complex and the DNA damage response. Science *285*, 747-750.
434. Zhou,P.K., Sproston,A.R., Marples,B., West,C.M., Margison,G.P., and Hendry,J.H. (1998). The radiosensitivity of human fibroblast cell lines correlates with residual levels of DNA double-strand breaks. Radiother. Oncol. *47*, 271-276.
435. Zhu,C., Mills,K.D., Ferguson,D.O., Lee,C., Manis,J., Fleming,J., Gao,Y., Morton,C.C., and Alt,F.W. (2002). Unrepaired DNA breaks in p53-deficient cells lead to oncogenic gene amplification subsequent to translocations. Cell *109*, 811-821.